

https://dspace.org/

Middle Permian diversity of large herbivores: taxonomic revision of the titanosuchidae (therapsida, dinocephalia) of the Karoo basin, South Africa

Jirah, Sifelani

2022

https://hdl.handle.net/10539/34567

Downloaded from a DSpace repository. https://dspace.org/



MIDDLE PERMIAN DIVERSITY OF LARGE HERBIVORES: TAXONOMIC REVISION OF THE TITANOSUCHIDAE (THERAPSIDA, DINOCEPHALIA) OF THE KAROO BASIN, SOUTH AFRICA.

by

Sifelani Jirah

(226706)

Dissertation

Submitted in fulfilment of the requirements for the degree

Doctor of Philosophy

in

Palaeontology

in the Faculty of Science, University of the Witwatersrand, Johannesburg, South Africa

Supervisor: Professor Bruce Rubidge

Co-supervisor: Professor Fernando Abdala

May 2022

DECLARATION

I declare that this thesis is my own, unaided work. It is being submitted for the Degree of Doctor of Philosophy at the University of the Witwatersrand, Johannesburg, South Africa. It has not been submitted before for any degree or examination at any other University.



On this 5th day of May 2022 in Johannesburg.

ABSTRACT

Titanosuchidae are a goup of derived herbivorous long snouted dinocephalians currently only known from the South African Karoo Supergroup. Taxonomic revision of the titanosuchids, for the first time accompanied by detailed anatomical descriptions and illustrations of representative cranial and postcranial material, enabled recognition of only two genera each represented by a single species out of nine previously recognized species. These are *Titanosuchus ferox* and *Jonkeria truculenta*. *Jonkeria vanderbyli, Jonkeria ingens, Jonkeria haughtoni, Jonkeria parva, Jonkeria rossouwi* and *Jonkeria boonstrai* are here, synonymized with *Jonkeria truculenta.* The species *Jonkeria koupensis* is a *nomen dubium* only identified as Titanosuchid indet.
Cranial characters, which modify during ontogenetic development, were, recognized for *Jonkeria,* and for the first time an ontogenetic growth series is, presented for this species. This research has for the first time produced a phylogenetic analysis of the two titanosuchid taxa with their deuterosaurid, estemmenosuchid, anteosaurid, styracocephalid and tapinocephalid counterparts confirming the sister group relationship between Styracocephalidae, Estemmenosuchidae, Titanosuchidae and Tapinocephalidae. This phylogenetic analysis manifests a long ghost lineage extending over most of the Guadalupian.

The first extensive stratigraphic analysis of the Titanosuchidae shows that the South African Karoo Supergroup hosts both genera in the upper levels of the Abrahamskraal Formation (Moordenaars Member) with a single specimen (Titanosuchid indet) recovered in the lower levels of the overlying Poortjie Member of the Teekloof Formation. The absence of titanosuchids in the Karelskraal Member of the Abrahamskraal Formation and their reappearance in the lower Poortjie could be a case of a “Lazarus taxon”. This gap in the stratigraphic range of this taxon

(range gap), as well as the long ghost lineage, will hopefully be filled in future by intensive targeted collecting in the relevant stratigraphic intervals.

ACKNOWLEDGEMENTS

I am indebted to my supervisors, Prof. Bruce S. Rubidge and Prof. Fernando Abdala for their patience, guidance and support throughout this project. The African Origins Platform of the National Research Foundation (NRF), DSI (Department of Science and Innovation) /NRF Centre of Excellence in Palaeosciences (CoE), and the Palaeontological Scientific Trust (PAST) are acknowledged for financial support, without which this research would not have been possible. For access to the fossil material for my research, I would like to thank the following museum staff members for enabling me to examine specimens under their curatorship: Prof. Roger Smith, Ms Claire Browning and Ms Zaituna Skosan (Iziko Museum, Cape Town, South Africa), Dr. Heidi Fourie (Ditsong Museum, Pretoria, South Africa), Ms Sandra Chapman and Prof. Paul Barett (Natural History Museum, London), Dr Mark Norell and Mr Carl Mehling (American Museum of Natural History, New York) and Dr Daniela Schwarz (Museum fuer Naturkunde Berlin, Germany).

I thank Dr. Marco Romano, for sharing part of his dataset of synapsid postcranial measurements as well as his knowledge on principal component analysis. Special acknowledgment to Mr. Pepson Mukanela of the Evolutionary Studies Institute for his help in the preperation of some of the titanosuchid specimens. I also would like to acknowledge Dr. Christian Kammerer, Dr. Michael Day and Dr. J. Benoit, for sharing their knowledge about dinocephalians and other palaeontological matters.

Last but not least, I am grateful for the enduring support and patience of my family. I would like to dedicate this Thesis to my late mother Mrs Egfah Jirah Sibanda and my dad, Mr Timothy Jirah Sibanda for instilling a love for education since I was a kid and to my son Sean Mayibongwe Jirah for his never-ending curiosity and encouragement.

TABLE OF CONTENTS **Page**
ABSTRACT iii

ACKNOWLEDGEMENTS v

TABLE OF CONTENTS vi

LIST OF FIGURES ix

LIST OF TABLES xix

INSTITUTIONAL ABBREVIATIONS xix

ANATOMICAL ABBREVIATIONS xx

1 **INTRODUCTION** 1

1.2 Literature review 5

1. 2.1 Taxonomic history of titanosuchid dinocephalians 5

1. 2.2 Stratigraphic ranges of Titanosuchid dinocephalians 15

2 **MATERIAL AND METHODS** 20

2.1 Specimens 20

2.2 Preparation 20

2.3 Suture Identification 20

2.4 Microfocus X-Ray Computed Tomography (CT) Scanning 21

2.5 Allometric growth 22

2.6 Principal component analysis 24

2.7 Phylogenetic analysis 25

2.8 Interpretative drawings 26

3 **CRANIAL DESCRIPTION OF *TITANOSUCHUS FEROX* AND *JONKERIA TRUCULENTA*** 27

3.1 Introduction 27

3.2 Systematic Palaeontology 27

3. 2.1 Family Titanosuchidae 29

3. 2.2 Valid Titanosuchid taxa 30

3. 2.3 Junior synonyms 36

3.3 Cranial description of *T. ferox* 41

3.4 Decription of the cranial morphology of *Jonkeria* 43

3. 4.1 Skull roof 47

3. 4.2 Palate 56

3. 4.3 Occiput and Basicranium 60

3. 4.4 Lower jaw 63

3. 4.5 Dentition 69

3.5 Allometry 77

3.6 Discussion 81

3.7 Conclusion 88

4 **DESCRIPTION OF *TITANOSUCHUS FEROX* AND *JONKERIA TRUCULENTA* LIMB ELEMENTS** 90

4.1 Introduction 90

4.2 Revised J*onkeria* taxonomy 92

4.3 Morphological description 96

4. 3.1 Humerus of Titanosuchidae 98

4. 3.1.1 *Titanosuchus ferox* humerus 98

4. 3.1.2 *Jonkeria truculenta* humerus 102

4.3.2 Ulna 106

4.3.3 Radius 111

4.3.4 Femur 113

4.3.5 Tibia 116

4.3.6 Fibula 118

4.4 Principal component analysis 122

4.5 Discusion 131

4.6 Conclusion 134

5 **PHYLOGENETIC ANALYSIS** 137

5.1 Introduction 137

5.2 Methods 139

5.2.1 Specimens used in the analysis 140

5.3 Results 141

5.4 Discusion 143

6 **STRATIGRAPHIC DISTRIBUTION OF TITANOSUCHIDS** 146

6.1 Stratigraphic range of *Titanosuchus ferox* 147

6.1.1 Range in the Beaufort West sector (most easterly occurrence) 147

6.1.2 Occurrence in the Laingsburg sector 147

6.1.3 Range in the Leeu-Gamka sector 148

6.1.4 Range in the Merweville sector 148

6.1.5 Overall stratigraphic range 148

6.2 Stratigraphic range of *Jonkeria* 149

6.2.1 Range in the Beaufort West sector 149

6. 2.2 Occurrence in the Laingsburg sector 149

6. 2.3 Range in the Leu-Gamka sector 149

6. 2.4 Range in the Merweville sector 150

6. 2.5 Overall stratigraphic range 150

7 **DISCUSSION & CONCLUSION** 154

7.1 Karoo middle Permian biostratigraphy 154

7.2 Middle Permian Tetrapod Taxonomy 156

7.3 Conclusion & perspectives 162

8 **REFERENCES** 166

Appendix A Fossils used in this study 192

Appendix B Cranial measurements (mm) used for allometric analysis 194

Appendix C Limb bone dataset for Principal component analysis 195

Appendix D Morphological character list for phylogenetic analysis 198

Appendix E Data matrix used in the phylogenetic analysis 205

Appendix F All the observed and identified Titanosuchid specimens and their stratigraphic positions. 206

LIST OF FIGURES

Figure 1.1. The cranial fragments of the holotype of *Titanosuchus ferox* (NHMUK 49367), as illustrated in Owen (1879, Plate XI, figs. 1-9): showing a. Inner side view of a portion of the left maxillary. b. Horizontal or transverse section of the alveolar border and implanted roots of the postcanine teeth of the same maxillary. c. Transverse section of the root of the first upper incisor. d. Longitudinal section of the root of the same tooth. e. Longitudinal section of the root of the eleventh molar of the left maxillary. f. Symphysial end of left mandibular ramus, with the

alveolar border in horizontal section. g. Horizontal section of the alveolar border and roots of the postcanines of the same mandibular ramus. h. Vertical or longitudinal section of the implanted root of the canine of the same ramus. i. Longitudinal section of the root of the third postcanine of the same ramus 7

Figure 1.2. Postcranial elements of *Titanosuchus ferox*. Humerus (NMHUK49369) a. ventral view. b. lateral view. Femur (NMHUK49368) c. anterior view. d. posterior view, as illustrated in Seeley (1889) 8

Figure 1.3. Stratigraphic ranges of the Titanosuchids *Titanosuchus ferox* and *Jonkeria truculenta* alongside other *Tapinocephalus* Assemblage Zone taxa occurring in the Diictodon – Styracocephalus Subzone. Kk=Karelskraal; Kp= Koornplaats; Mo=Moordenaars; Po=Poortjie; Sk=Swaerskraal. (Day & Rubidge 2020) 18

Figure 2. 1. Illustration of the skull of *Jonkeria* showing the cranial measurements taken for comparison between different skulls. After Boonstra (1969) 23

Figure 2. 2. Limb bone measurements for PCA analysis: PW, proximal width; DW, distal width; SW, width at mid-shaft; TL, total length. a, humerus; b, ulna; c, radius; d, femur; e, tibia; f, fibula. 25

Figure 3.1. *Titanosuchus ferox* holotype NHMUK 49370. a. medial side of a portion of the left maxilla which includes the trace of the socket of the canine, s, with part of the base or root of that tooth, c. b. left mandibular ramus with the alveolar border and roots of incisors, canine and postacanines in cross section. Scale bar is 5cm 31

Figure 3.2. Lateral view of *Jonkeria truculenta* holotype (TM 212). Skull lacks left squamosal and quadratojugal. Pterygoids are damaged and all teeth lost, reconstructed by plaster of Paris 33

Figure 3. 3. Lateral view of the *Jonkeria vanderbyli* holotype (AMNH 5620). Skull mostly covered in plaster of Paris. Scale bar represents 10cm 36

Figure 3.4. Lateral view of the *Jonkeria ingens* holotype (AMNH 5634) with less than 50% of the skull preserved. Scale bar represents 10cm 37

Figure 3.5. Lateral view of *Jonkeria haughtoni* holotype (SAM-PK- 4343). The skull is dorsoventrally crushed. Scale bar represents 10cm 39

Figure 3.6. Lateral view of the skull of *Jonkeria boonstrai* holotype (MB. R.983). The skull is distorted, with two thirds of the ventral surface and teeth missing (plaster of Paris reconstruction). Scale bar represents 10cm 40

Figure 3.7. Holotype of *Titanosuchus ferox* (NHMUK 49370) a. Medial view and b. Longitudinal section of the alveolar border and implanted roots of the postcanine teeth of a portion of the left maxilla of the. Scale is 10cm 41

Figure 3.8. *Titanosuchus ferox* holotype (NHMUK 49370) a. left dentary and b. left maxilla showing the cross-section of post-canine teeth. Scale represents 5cm 42

Figure 3.9. Illustrations of the dorsal (a) and lateral (b) views of *Jonkeria truculenta* holotype (TM 212) taken from Broom (1929: pages 12-13: Fig.1 & Fig. 2). Broom managed to trace only a few sutures owing to the similarity between bone and matrix. ang, angular; la, lacrimal; mx, maxilla; na, nasal; pmx, premaxilla; s.ang, surangualr; smx, septomaxilla; sq, squamosal. The illustrations are 1/6 of the natural size 43

Figure 3.10. Lateral view of *Jonkeria truculenta* skulls. **a.** SAM-PK-11884; **b.** TM212; **c.** SAM-PK-4343; **d.** AMNH 5620. TM212 is the left side flipped for

comparison. Scale bars represent 10cm. 45-46

Figure 3.11. Dorsal view of *Jonkeria truculenta* skulls. **a.** SAM-PK-11884; **b.** TM 212; **c.** SAM-PK-4343; **d.** AMNH 5620. Scale bars represent 10cm. 49-50

Figure 3.12. Ventral view of *Jonkeria truculenta* skulls. **a.** SAM-PK-11884; **b.** TM212; **c.** SAM-PK- 4343; **d.** FMNHUC 1511. Scale bars represent 10cm. **e.** MB.R. 983; **f.** AMNH 5634; g. AMNH 5608; **h.** AMNH 5620. 57-58

Figure 3.13. Occipital view of *Jonkeria truculenta* skulls. **a.** FMNHUC 1511; **b.** SAM-PK- 4343; **c.** SAM-PK- 11884; **d.** TM 212; **e.** AMNH 5620; **f.** MB.R. 983. Scale bars represent 10cm. 61

Figure 3.14. Lateral view of *Jonkeria truculenta* mandibles. a. SAM-PK-12030. b. AMNH 5633. Scale bars represent 10cm. 64

Figure 3.15. Medial view of *Jonkeria truculenta* mandibles. **a.** SAM-PK- 12030.**b.** AMNH 5633. Scale bars represent 10cm. Scale bars represent 10cm. 66

Figure 3.16. Dorsal view of *Jonkeria truculenta* mandible SAM-PK-11884 showing the position of the coronoid bones on the right and left ramii of this mandible. Scale bars represent 10cm 67

Figure 3.17. Close-up of the ventral view of anterior snout (right premaxilla) of SAM-PK - 4343 showing the morphology of the canine tooth and the incisor teeth I4 and I5 and tooth replacement. Scale bars represent 10cm 71

Figure 3.18. Medial view of the left anterior mandible (a), lateral view of left maxilla (b), ventral view of premaxilla (c) for ROZ. B96 and (d) ventral view of the right anterior snout of SAM-PK-12030. Scale bars represent 10cm 73

Figure 3.19. *Jonkeria truculenta* SAM-PK-12030 showing arrangement of teeth in occlusion. The upper postcanines are at the edge of the maxilla and they rest on the ledge on the dentary. The lower postcanines lie lingual to the upper postcanines. Upper canine rests on a hollow in the outer face of the dentary. There is a diastema between i5 and the upper canine to accommodate the outward pointing lower canine in occlusion. Scale bar represents 10cm 75

Figure 3.20. Dentary of specimen MB. R. 983 showing the postcanine tooth crowns (2 - 4). (b) Maxilla of specimen SAM-PK-4343 showing replacement postcanines (PC^1). (c) Left maxilla of specimen SAM-PK-12030 showing a row of postcanine teeth with tooth size decreasing in an anterior – posterior direction. Lingual to the 6th postcanine is a replacement (PC^1). Scale for a represents 1cm and for b and c represents 10cm 76

Figure 3.21. Regression of length of the total skull length (log Variable 1) on a. the antero-posterior orbital diameter (log Variable 3). b_1= 1.96; b. the width of the snout at the level of canines (log Variable 8). b_1= 1.92; c. the greatest width of the skull at the level of squamosals (log Variable 9). b_1= 1.71 and d. the distance from posterior margin of pineal foramen to the edge of occipital condyle (log Variable 16). b_1= 3.10 80

Figure 3.22. Ontogenetic variation within Jonkeria truculenta skulls. The arrow

indicates size increase. As this species grows older it has a relatively longer snout, and more cranial pachyostosis around the prefrontal, frontal, postorbital and parietal bones.Total skull length of each skull is provided. Scale bar represents 10cm 87

Figure 4.1. Ventral view of the right humerus of Jonkeria parva holotype (SAM-PK- 9149). Scale bar represents 10cm. 93

Figure 4.2. Limb elements of the *Jonkeria rossoouwi* holotype (SAM-PK- 5014). From left to right: humerus, ulna, radius, femur, fibula and tibia. Scale bars represent 10cm. 94

Figure 4. 3. a. *Jonkeria koupensis* pelvis in lateral view (holotype SAM-PK-9004). b. isolated ilium of *Jonkeria koupensis* (SAM-PK-11983) in lateral view. c. comparative ilium of *Jonkeria haughtoni* (holotype SAM-PK-4343) and d. ilium of *Jonkeria rossouwi* (holotype SAM-PK-5014). Abbreviations. Ac- acetabulum; A.pr- anterior iliac process; Ifr- ilio-fibularis ridge; PF- pubic foramen; P.pr- posterior iliac process; PT- tuberculum pubis; Sab- supra-acetabular buttress; San- supra-acetabular notch. Scale bars represent 10cm 95

Figure 4.4. *Jonkeria truculenta* right humerus (SAM-PK-4343) in dorsal (a) and ventral (b) views to illustrate morphological features of a titanosuchid humerus 97

Figure 4.5. Photographs and illustrative drawings of *Titanosuchus ferox* humeri in ventral view. a. NHMUK49369, left humerus; b. BP/1/7380, left humerus; c. SAM-PK- 773, left humerus; d. SAM-PK-5001, right humerus; e. SAM-PK- 11881, right humerus (both d and e flipped 180°. Scale bars represent 10cm 99

Figure 4. 6. Photographs and illustrative drawings of humeri of *Titanosuchus ferox* in dorsal view; a. NHMUK 49369; b. BP/I/ 7380 ; c. SAM-PK- 773 (proximal part missing); d. SAM-PK-11578 (proximal part missing); e. SAM-PK-11881. a, b and d are left humeri; c and e are right humeri that were flipped 180° for comparison with the left humeri. Scale bars represents 10cm 101

Figure 4. 7. Photographs and illustrative drawings of *Jonkeria truculenta* humeri in ventral view. a. SAM-PK- 4343; b SAM-PK-9149;. a, and b are right humeri which were flipped for comparison with the rest. Scale bars represent 10cm 103-104

Figure 4.8. Humeri of *Jonkeria truculenta* in dorsal view. a. SAM-PK- 4343; b. SAM-PK- 9149; c. AMNH 5577; d. SAM-PK- 3433. a and b are right humeri flipped for comparison with c and d which are left humeri. Scale bars represent 10cm 105-106

Figure 4.9. Lateral view of titanosuchid left ulnae. a. SAM-PK- 4343 (*J. truculenta*); b. AMNH 5577 (*J. truculenta*); c. SAM-PK- 5014 (*J. truculenta*); d. SAM-PK- 9002 (*J. truculenta*); e. SAM-PK- 9163 (*T. ferox*). Scale bars represent 10cm 109

Figure 4.10. Medial view of the titanousuchid left ulnae. a. SAM-PK- 4343 (*J. truculenta*); b. AMNH 5577 (*J. truculenta*); c. SAM-PK- 5014 (*J. truculenta*); d. SAM-PK- 9002 (*J. truculenta*); e. SAM-PK- 9163 (*T. ferox*). Ridge (il) = ridge for the insertion of the interosseous ligament Scale bars represent 10cm 110

Figure 4.11. Titanosuchid radii in anterior and posterior view; a. T. ferox:

SAM-PK-11299 (anterior view); b. *T. ferox*; SAM-PK- 11299 (posterior view); c. *J. truculenta*: SAM-PK- 5014 (anterior view); d. *J. truculenta*; SAM-PK- 5014 (posterior view). SAM-PK- 11299 is the right radius and SAM-PK- 5014, the left radius, has been flipped for comparison. Scale bars represent 10cm 112

Figure 4.12. Titanosuchid femora in anterior view. a. *T. ferox*: NHMUK 49368 (holotype); b. *T. ferox*: SAM-PK- 11491; c. *T. ferox*: SAM-PK- 5001; d. *T. ferox*: SAM-PK- 9127; e. *J. truculenta*: SAM-PK- 5014.All are left femora except b which was flipped for comparison. Scale bars represent 10cm 114

Figure 4.13. Titanosuchid femora in posterior view; a. *T. ferox*: NHMUK 49368 (holotype); b. *T. ferox*: SAM-PK- 11491; c. *T. ferox*: SAM-PK- 5001; d. *T. ferox*: SAM-PK- 9127; e. *J. truculenta*: SAM-PK- 5014; a, b, d and e are left femora and b, was flipped 180° for comparison. Scale bars represent 10cm 116

Figure 4.14. Titanosuchid tibia in anterior view. a.TM 212 (*J. truculenta*); b. SAM-PK-5014 (*J. truculenta*); c. SAM-PK- 11299 (*T. ferox*) d. SAM-PK- 11488 (*T. ferox*). All are right tibia except SAM-PK- 5014, which is a left tibia flipped for comparison. Scale bars represent 10cm 117

Figure 4.15. Titanosuchid tibia in posterior view. a.TM 212 (*J. truculenta*); b. SAM-PK-5014 (*J. truculenta*); c. SAM-PK-11299 (*T. ferox*); d. SAM-PK- 11488 (*T. ferox*). All are right tibia except SAM-PK- 5014, which is a left tibia flipped for comparison. Scale bars represent 10cm 118

Figure 4.16. Titanosuchid fibula in anterior view: a. *T ferox*: SAM-PK-9127;

b. *T ferox*: SAM-PK-9163; c. *T. ferox*: SAM-PK- 11989;
d. *T. ferox*: SAM-PK- 11488; e. *J. truculenta*: SAM-PK- 5014;
f. *J. truculenta*: SAM-PK- 4343 Scale bars represent 10cm 120

Figure 4.17. Titanosuchid fibula in posterior view: a. *T ferox*: SAM-PK-9127;
b. *T ferox*: SAM-PK-9163; c. *T. ferox*: SAM-PK- 11989; d.
T. ferox: SAM-PK- 11488; e. *J. truculenta*: SAM-PK- 5014;
f. *J. truculenta*: SAM-PK- 4343. dist art = distal articulation
surface; prox art = proximal aarticualtion surface.
Scale bars represent 10cm 121

Figure 4. 18. Scatter plot and loadings of first and second principal components
for the sample of humerus bones of *Titanosuchus* and *Jonkeria*
compared to the tapinocephalids and the basal synapsid *Dimetrodon*.
TL, bone total length; PW, bone proximal width; DW, bone distal
width; SW, bone maximal narrowing at mid shaft. Grey =
Dimetrodon; Red = Titanosuchus; Blue = Jonkeria;
Green = tapinocephalids 124

Figure 4. 19. Scatter plot and loadings of principal component 1 and component
2 for the ulna of *Titanosuchus* (red) and *Jonkeria* (blue) and selected
tapinocephalids (*Moschops*, *Struthiocephalus* and *Tapinocaninus*;
green) and the basal synapsid *Dimetrodon* (grey). TL,
bone total length; PW, bone proximal width, DW, bone distal
width; SW, bone maximal narrowing at mid shaft 126

Figure 4. 20. Scatter plot and loading of principal component 1 and component 2
for the radius of *Titanosuchus* (red) and *Jonkeria* (blue) and the basal
synapsid *Dimetro*don (grey). TL, bone total length; PW, bone
proximal width; DW, bone distal width; SW, bone maximal
narrowing at mid shaft 127

Figure 4. 21. Scatter plot and loading of first and second principal components for the femur of *Titanosuchus* (red) and *Jonkeria* (blue) and selected Tapinocephalids (*Moschops*, *Riebeeckosaurus* and *Tapinocaninus*: green) and the basal synapsid *Dimetrodon* (grey). TL, bone total length; PW, bone proximal width; DW, bone distal width; SW, bone maximal narrowing at mid shaft 128

Figure 4. 22. Scatter plot of first and second principal components in tibia for *Titanosuchus* (red) and *Jonkeria* (blue) and selected Tapinocephalids (*Moschops* and *Tapinocaninus*: green) and the basal synapsid *Dimetrodon* (grey). TL, bone total length; PW, bone proximal width; DW, bone distal width; SW, bone maximal narrowing at mid shaft 129

Figure 4. 23. Scatter plot of first and second principal components in fibula for *Titanosuchus* (red) and *Jonkeria* (blue) and selected Tapinocephalids (*Moschops* and *Tapinocaninus* (green)) and the basal synapsid *Dimetrodon* (grey). TL, bone total length; PW, bone proximal width; DW, bone distal width; SW, bone maximal narrowing at mid shaft 130

Figure 5. Results of the phylogenetic analysis. A. Strict consensus (equal weight) tree of six most parsimonious trees. B. Majority rule consensus of three most parsimonious trees with implied weights (K=3). Number of the nodes indicates proportion of fundamental trees where the group is represented (66 indicate that the group is recovered in two of the three most parsimonious trees) 142

Figure 6.1. Map showing the sectors used in the calculation of specimen stratigraphic positions. 1 = Victoria West, 2 = Fraserburg,3 = Sutherland, 4 =Laingsburg, 5 = Merweville, 6 = Leeu-Gamka,7 =

Beaufort West, 8 = Jansenville, 9 = Grahamstown. (Day, 2013) 146

Figure 6.2. Composite stratigraphic ranges of Titanosuchid genera in the middle Permian Beaufort Group. TK Fm = Teekloof Formation. 151

Figure 6.3. Fragmentary titanosuchid indet skull from the Poortjie Member on farm Ou Tuin, Sutherland disrtrict, South Africa**,** showing the following titanosuchid characters: **a**. dorsal view of the skull fragment (with a dispalced heeled incisor in the right orbit; **b.** maxillary fragment with a large canine and a series of postcanines 153

LIST OF TABLES

Table 3.1**.** Summary of the regressions on the total skull length from the tip of the snout to the occipital condyle (variable 1) of *Jonkeria truculenta*. Abbreviations: b_1, coefficient of allometry calculated via reduced major axis method; P(iso), isometry; n, sample size; pos, positive allometry; R^2, adjusted coefficient of determination. Variables with allometric trends indicated in bold 77-78

INSTITUTIONAL ABBREVIATIONS

AMNH: American Museum of Natural History, New York, USA; **NHMUK**: Natural History Museum, London, UK; **BPI (ESI)**: Evolutionary Studies Institute (formerly Bernard Price Institute for Palaeontological research), University of the Witwatersrand, Johannesburg, South Africa; **FMNHUC**: Field Museum of Natural History, University of Chicago, Illinois, USA; **SAM**: Iziko South African Museum, Cape Town, South Africa; **TM (DMNH)**: Ditsong Museum

of Natural History, Pretoria, South Africa (formerly Transvaal Museum, Pretoria, South Africa); **MB (MfN):** Museum für Naturkunde, Berlin, Germany. **ROZ:** Roy Ousthuizeni collection, Prince Albert Museum (specimen currently curated at Iziko South African Museum)

ANATOMICAL ABBREVIATIONS

ac- acetabulum; **advl**- anterior dorso-ventral line; **ang-** angular**; a.pr-** anterior iliac process; **art-** articular; **arf-** articular fossa; **bf**- biccipital fossa; **bo-** basioccipital; **bs-** basisphenoid; **C**- upper canine; **c-** lower canine**; cap-** caput humeralis (humeral head); **cn.b-** cnemial boss; **cn.g-** cnemial groove; **cn.r-** cnemial ridge; **cor-** coronoid; **cor.em**- coronoid eminence; **cp**- coronoid process; **dent-** dentary; **dis art**- distal articulation; **dpc**- delto-pectoral crest; **ect.c-** facet for the lateral femoral condyle; **ectepic**- ectepicondyle; **ect.f**- ectepicondylar foramen; **ect.p-** ectopterygoid; **ent.c-** facet for the medial femoral condyle; **entepic**- entepicondyle; **ent.f**- entepicondylar foramen; **ex.o-**exoccipital; **ex. tr**- external trochanter; **fem h**- femoral head; **fm**- foramen magnum; **fr-** frontal; **f.ra**- facet for radiale; **f.in**- facet for the ulnare; **ft**- origin of the femoro-tibialis; **i-** incisor; **ic**- inner elliptical cavity of the articular; **ifr-** ilio-fibularis ridge; **int fos**- intertrochantic fossa; **int. tr**- internal trochanter; **int.sulc**- intercondylar sulcus; **ipa**- inperparietal; **ipv-** interpterygoidal vacuity; **jf**- jugular foramen **ju-** lugal; **la-** lacrimal; **lat cond**- lateral condyle; **lml**- latero-medial line; **lsf**- lip to sigmoid fossa; **med cond**- medial condyle; **mx-** maxilla; **na**- nasal; **oc**- outer cavity of the articular; **olec**- olecranon; **olec.f**- olecranon fossa; **or-** orbit; **p-** parietal; **pa**- parietal; **pal-**palatine; **pc-** postcanine**; pf-** pubic foramen; **p.f-** pineal foramen; **p.lat**- processus lateralis; **p.med**- processus medialis; **p.pr-** posterior iliac process; **pr.art-** prearticular**; pmx-** premaxilla; **po**- paraoccipital; **p.orb-** postorbital**; pof;** postfrontal;

ppt- palatine ramus of the pterygoid; **pr.fr-** prefrontal**; prox.art-** proximal articulation; **pt**- tuberculum pubis; **q-** quadrate; **qj-** quadratojugal; **qpt-** quadrate ramus of pterigoid; **ra**- radial condyle; **rad art**- radius articulation; **ref.lam.ang-** reflected lamina; **sab-** supra-acetabular buttress; **san-** supra-acetabular notch; **s.ang-** surangular; **smx-** septomaxilla; **so**- supraoccipital; **splen-** splenial; **sq-** squamosal; **st-** stapes; **sty**- styloid flange; **ta-** tabular; **ul**- ulnar condyle;

CHAPTER ONE: INTRODUCTION & LITERATURE REVIEW

1.1 Introduction

Dinocephalians, which lived during the Guadalupian of the Permian period, are a group of mainly large therapsids characterized by intermeshing heeled incisors, reduction in the size of postcanine teeth, forward shift in the jaw articulation, grooved or excavated vomers and non-terminal nostrils (Boonstra, 1969; King, 1988; Kemp, 1982). They constitute a significant part of the middle Permian tetrapod biodiversity and are found in Kazakhstan (Tchudinov, 1968), Russia (Ivakhnenko, 1995; 2000), South Africa (Boonstra, 1963; Rubidge, 1991; 1994; 2005), China (Li and Cheng, 1995; Cheng and Li, 1997; Simon *et al*., 2010), Zimbabwe (Boonstra, 1946; Lepper *et al*. 2000; Munyikwa, 2001; Simon *et al*., 2010), Tanzania (Simon *et al*. 2010), Brazil (Langer, 2000; Simon *et al*. 2010 Cisneros *et al*. 2012; Boos *et al*. 2015) and Zambia (Sidor *et al.* 2014). The taxon comprises six families after the synonymisation of the seventh family (Brithopidae) with Anteosauridae by Kammerer (2011). Four (Anteosauridae, Titanosuchidae, Tapinocephalidae and Styracocephalidae) of these six families occur in South Africa (Boonstra, 1969; King, 1988; Angielczyk and Kammerer, 2018).

Following the taxonomic subdivision of the dinocephalians by Broom (1923), titanosuchids and carnivorous anteosaurs were considered, within the Titanosuchia. Nopcsa (1928b) placed Dinocephalia in two suborders: Titanosuchoidea and Tapinocephaloidea. Titanosuchoids included dinocephalians with an elongated snout and frontal contribution to the orbits; while Tapinocephaloids were characterized by a relatively shortened snout, no frontal contribution to the orbit, dorsally oriented temporal fenestra, and a relatively short quadrate lacking a foramen.

According to Nopcsa (1928b), the Titanosuchoidea comprised four families: a) Moschosauridae (*Moschosaurus*) with no pachyostosis, and a moderate size canine; b) Deuterosauridae (*Deuterosaurus*) with no contact between postorbital-squamosal, laterally inclined temporal fenestra, a relatively shorter skull and the quadrate exhibiting a foramen; c) Titanosuchidae (*Titanosuchus* and *Burnetia*) with elongated snout; 4) Lamiasauridae (*Lamiasaurus*) only known from a single jaw fragment.

Boonstra (1954a) erected the family Anteosauridae for the carnivorous dinocephalians, and they are the most widespread dinocephalian family across Pangea, with representatives from South Africa, Brazil, Russia, Kazakhstan and China (Cisneros *et al.* 2012; Rubidge, 2005; Tchudinov, 1968). Anteosauridae is considered the most basal dinocephalian family (Hopson and Barghusen, 1986; Rubidge and Sidor, 2001; Kammerer, 2011), although King (1988) conversely attributed this position to the Russian estemmenosuchids.

Watson and Romer's (1956) revised classification for Therapsida differed considerably from previous proposals by using the terms Theriodontia and Anomodontia for carnivorous and herbivorous therapsids respectively. They split the Dinocephalia, grouping the carnivorous dinocephalians as infraorder Titanosuchia under Theriodontia and the herbivorous forms as infraorder Dinocephalia under Anomodontia. According to this revised scheme, Titanosuchia comprised the families Brithopodidae, Anteosauridae and Jonkeriidae. They suggested that jonkerids differ from anteosaurids in having a smaller temporal fenestra and more anteriorly positioned quadratojugal.

Olson (1962) excluded dinocephalians from Anomodontia and placed Brithopodidae under the

infraorder Eotheriodonta. He recognized the Suborder Dinocephalia (designated as "Deinocephalia") which included two infraorders namely Eodeinocephalia (which includes Deuterosauridae) and Eudeinocephalia. This infraorder comprised two superfamilies namely tapinocephaloids (Moschopidae and Tapinocephalidae) and titanosuchoids (Titanosuchidae). Olson (1962) further concluded that the tapinocephaloids originated from deuterosaurids and concurred with Watson and Romer (1956) in regarding similarities between the brithopids and deuterosaurids as a result of convergent evolution.

Boonstra (1969) grouped South African Dinocephalia into four families: a) Anteosauridae as primitive carnivorous dinocephalians with long pointed intermeshing incisors, more derived than the Russian brithopids; b) Titanosuchidae as primitive herbivorous dinocephalians with a slightly pachyostosed, canine bearing skull, intermeshing incisors with a talon and heel morphology, and spatulated postcanines with a serrated edges; c) Tapinocephalidae which comprises derived herbivorous dinocephalians with moderate to very thick cranial bones, lacking a canine and dentition exhibiting a talon and heel morphology with the upper and lower jaws fully intermeshed; d) Styracocephalidae as advanced herbivores with a canine, palatal teeth and tabular bosses.

Most recent taxonomic schemes relating to the Dinocephalia recognize two subclades: Anteosauria, which comprises the carnivorous taxa of the family Anteosauridae; and Tapinocephalia, which includes herbivorous forms in the families Titanosuchidae, Tapinocephalidae, Styracocephalidae and Estemmenosuchidae (Hopson and Barghusen, 1986; Rubidge and van den Heever, 1997; Rubidge and Sidor, 2001; Kammerer, 2011). The

Tapinocephalia comprises individuals of large body size, which were herbivorous, and most developed thick cranial pachyostosis (Rubidge and Sidor, 2001; Modesto *et al*., 2001).
The carnivorous anteosaurids and the herbivorous styracocephalids and tapinocephalids are currently the best understood dinocephalian families, having recently undergone a comprehensive taxonomic revision (Kammerer, 2011; Fraser-King *et al*. 2019; Neumann, 2020).
Styracocephalidae historically was one of the most enigmatic dinocephalian families, largely because of the paucity of well-preserved specimens (Rubidge and van den Heever, 1997), but the recent description of a relatively complete additional specimen (Fraser-King *et al.* 2019) has solidified the vailidity of the taxon.
These recent taxonomic revisions reduced the valid anteosaurid species from twenty-one to ten (six from Russia, two from South Africa, one from China, and one from Brazil (Cisneros *et al*. 2012).

Tapinocephalidae is the most diverse of the dinocephalian families with at least nine genera currently considered valid (Neumann, 2020). They are also the most derived dinocephalian family (Rubidge and Sidor, 2001; Sidor, 2000; Neumann, 2020), are known from Russia, Brazil, Zimbabwe, Tanzania and Zambia (Rubidge, 2005; Simon *et al.* 2010; Sidor, 2014; Boos *et al*. 2015), and are by far most abundant in South Africa.
Research on the remaining South African dinocephalian family, the Titanosuchidae, has been long neglected, with the last significant taxonomic contributions by Boonstra (1969) and King (1988). However, there has been important recent contributions to the study of titanosuchid palaeobiology such as by Rey *et al*. 2021 and Bhat *et al*. 2021. This is a family of herbivorous dinocephalians known only from South Africa in which the canine has been retained as a large

element, the incisors have a piercing talon and crushing heel, the postcanines have serrated spatulated crowns (Boonstra, 1969), and the pineal foramen is positioned relatively far anterior to the occipital border (Sidor, 2000).

This project is a contribution to a larger project of the Evolutionary Studies Institute at the University of the Witwatersrand aimed at documenting middle Permian biodiversity in the Karoo Supergoup of South Africa and understanding biodiversity change during the middle Permian leading to the end Guadalupian extinction event (Boonstra, 1971; Pearson *et al.* 2013; Day *et al.* 2015). Understanding the nature of this extinction event in the terrestrial realm is dependent on reliable taxonomic assessment of middle Permian tetrapods which included a range of temnospondyl amphibians, parareptiles, basal synapsids (pelycosaurs), as well as a wide diversity of therapsids (anomodonts, biarmosuchians, dinocephalians, gorgonopsians and therocephalians) of which the most abundant, in terms of both taxonomic diversity and number of individuals, were the herbivorous anomodonts and dinocephalians (Boonstra, 1969; Smith *et al.* 2012; Day, 2013). Titanosuchid dinocephalians, owing to their large size, formed an integral component of terrestrial tetrapod biomass during the middle Permian and this work contributes to the refining biostratigraphic ranges of titanosuchid dinocephalians in the Beaufort Group of the South African Karoo Basin.

1.2 Literature Review

1.2.1 Taxonomic history of Titanosuchid dinocephalians

Dinocephalian taxonomy was, initiated with the recognition that they are “reptiles” with mammalian affinities (mammal-like reptiles) and the subsequent naming of the orders Synapsida

and Therapsida, which includes the Dinocephalia (Kutorga, 1838; Owen, 1876; Osborn, 1903; Broom, 1905a).

Cope (1878, 1880) recognized relationships between the South African, Russian and North American Palaeozoic-Triassic reptile faunas and coined the term Theromorpha to include Pelycosauria and Anomodontia. Following Cope's (1880) proposal of Theromorpha, Lydekker (1889, p.1051, 1053) used the term "Theromorous Branch" to include only the order Anomodontia (as an equivalent to Cope's (1880) Theromorpha) and established the family Tapinocephalidae for *Tapinocephalus* and *Titanosuchus* under Anomodontia. Broom (1905a) was the first to include in Therapsida the Dinocephalia, Therocephalia, Anomodontia (for *Dicynodon* and its allies), and Cynodontia (=Theriodontia). At that stage, Broom (1905) considered Dinocephalia to comprise the holotypes of *Delphinognathus* and *Titanosuchus* but not *Tapinocephalus*. Broom (1910) considered the dinocephalians to be primitive therapsids and argued that the South African and North American Permian faunas had a common ancestor, which most probably inhabited the northern part of South America (Broom 1910, p. 233). This early work was, followed by the description of a large number of dinocephalian species and the recognition of subgroups (*e.g.* Broom, 1911, 1915; Haughton, 1915a, b; Watson, 1914). The past five decades have seen the refinement of dinocephalian taxonomy by way of synonymizing of taxa together with a quest to understand phylogenetic relationships of the different species (*e.g.* Boonstra, 1936a, 1936b, 1969; Hopson and Barghusen, 1986; Kammerer, 2011; King, 1988; Kruger, 2017; Neumann, 2020).

The first description of a titanosuchid was by Richard Owen (1879) who described, under the name *Titanosuchus ferox*, portions of a skull housed in The Natural History Museum, London. This specimen comprises an extremely weathered maxilla, dentary with some poorly preserved tooth roots, and postcranial material and is from "Gouph Tract", Beaufort West, South Africa (Fig. 1.1).

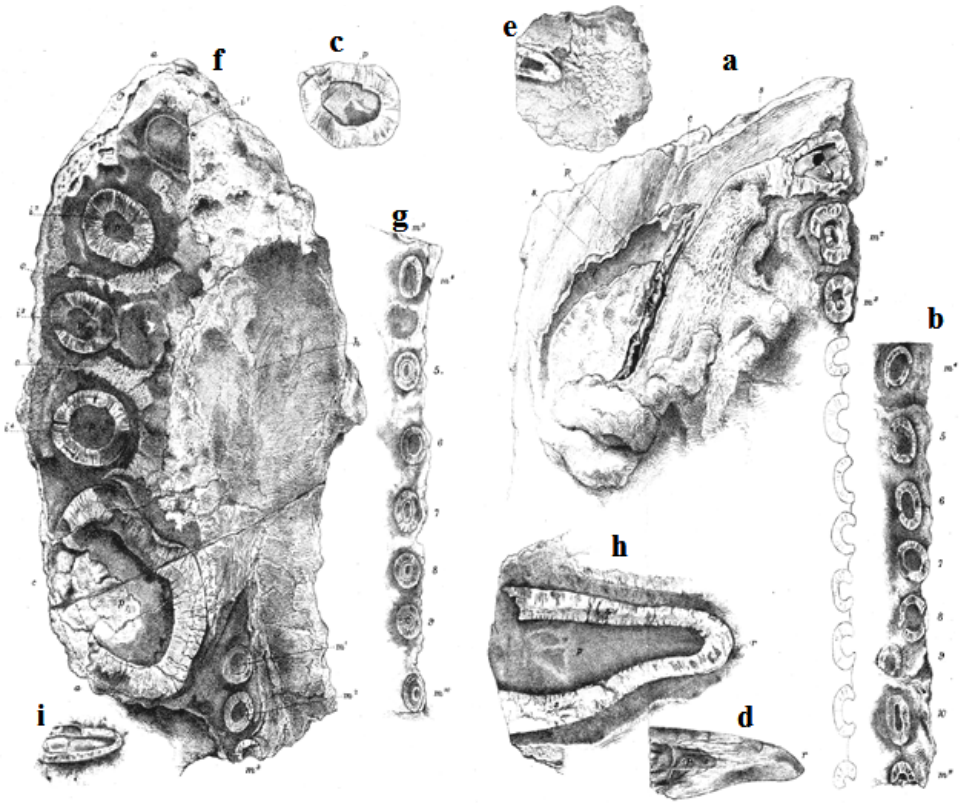

Fig. 1.1: The cranial fragments of the holotype of *Titanosuchus ferox* (NHMUK 49367), as illustrated in Owen (1879, Plate XI, figs. 1-9): showing **a**. Inner side view of a portion of the left maxillary. **b**. Horizontal or transverse section of the alveolar border and implanted roots of the postcanine teeth of the same maxillary. **c**. Transverse section of the root of the first upper incisor. **d**. Longitudinal section of the root of the same tooth. **e**. Longitudinal section of the root of the eleventh molar of the left maxillary. **f**. Symphysial end of left mandibular ramus, with the alveolar border in horizontal section. **g**. Horizontal section of the alveolar border and roots of the postcanines of the same mandibular ramus. **h**. Vertical or longitudinal section of the implanted root of the canine of the same ramus. **i**. Longitudinal section of the root of the third postcanine of the same ramus.

In 1889, Seeley described and figured the postcranial elements (limb bones) associated with the *Titanosuchus ferox* holotype. He observed that the femoral shaft is most constricted in its lower third and that the proximal end is more transversely expanded than the distal end. The humerus has both the proximal and distal ends greatly expanded with concave lateral outlines (Fig. 1.2). Broom later (1929) disputed the possibility of the postcrania belonging to the jaw fragments on the basis of there being two left humeri of the same morphology in the collection, a manifestation of the fact that the bones did not belong to one skeleton.

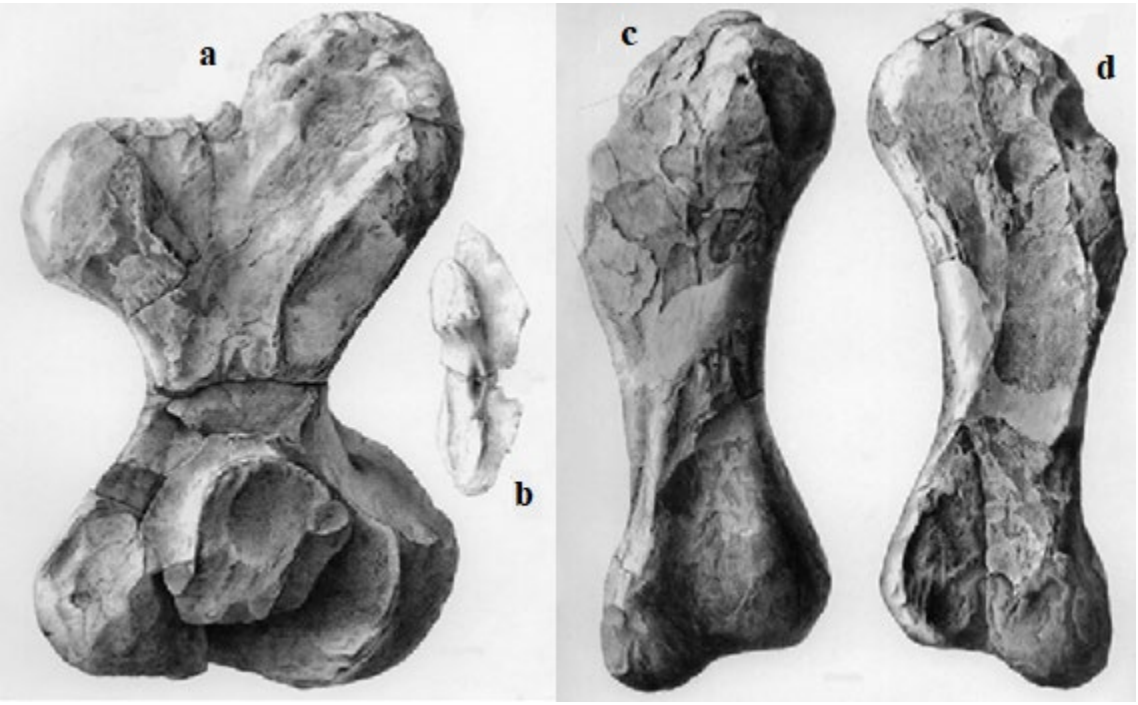

Fig. 1.2: Postcranial elements of Titanosuchus ferox. Humerus (NMHUK49369) **a.** ventral view. **b.** lateral view. Femur (NMHUK49368) **c**. anterior view. **d**. posterior view, as illustrated in Seeley (1889).

Broom (1903) described the anterior portion of a lower jaw (SAM-PK-731) which he referred to a new species, *Titanosuchus cloetei*. Broom (1904) described a fragmentary jaw and a humerus (SAM-PK-769), under the name *Scapanodon duplessisi* from the lower Karoo beds of Prince

Albert, South Africa. Watson (1914) examined all dinocephalian remains in the British Museum, and described a new type of snout under the name *Lamiasaurus newtoni*. However, Boonstra (1969) observed that this jaw fragment could not even be identified to family and could be either titanosuchid or anteosaurid. Haughton (1915) described the front half of a mandible from Platfontein, Prince Albert which he ascribed to a new species and named it *Titanosuchus dubius*. Broom (1929) placed this specimen in a new genus *Dinocynodon* because he noticed a flattening of the canine, which was not due to crushing and was quite unlike any of the other titanosuchids. Boonstra (1962) transferred the specimen to *Jonkeria* but later (Boonstra, 1969) decided that the specimen was poorly preserved, and it was determinable only to family level.

Haughton (1919) pointed out the similarity between Dinocephalia and Pelycosauria and placed the dinocephalians in two families, namely a) Tapinocephalidae for short snouted skulls and b) Titanosuchidae with elongated skulls and carnivorous dentition. This included *Titanosuchus*. Haughton (1919) emphasized that the difference between the two dinocephalian branches was not only the snout length, but also their diet emanating from the differences in dentition.

The genus *Titanosuchus* is characterized by a dentigerous border of the premaxilla, which curves, antero-dorsally with an associated step-up of the anterior part of the alveolar border of the dentary and the incisors long with no lingual crushing surface (Haughton and Brink, 1954; Tchudinov, 1983; King, 1988). The humerus is very large with a short and wide shaft; the delto-pectoral crest is fairly short with a knoblike extremity; processus medialis is situated well proximally and the capitellum is strong and extends far proximally along the ventral face of the bone and the ectepicondyle is developed as a fairly thin sheet of bone whose foramen is situated

well away from the edge of the bone (Boonstra, 1955a). The femur is a very long bone with a fairly narrow shaft and the fibula is large and massive (Boonstra, 1955a).

The genus *Jonkeria* was erected by Van Hoepen (1916) as *Jonkeria truculenta* for a specimen TM 212 from the farm Abrahamskraal in the Prince Albert district. Van Hoepen (1916) provided a preliminary description of *Jonkeria truculenta* and Broom (1929) gave a full description of the skeleton.

Broom (1923) described cranial fragments under the name *Dinartamus vanderbyli*. These fragments were, considered by Boonstra (1969) to have features too indefinite for a generic diagnosis and could, only be considered as titanosuchian indeterminate as to genus.

Broom (1923) reviewed the titanosuchians and divided them into the herbivorous suborder Tapinocephalia and carnivorous suborder Titanosuchia. He also suggested that the holotype of *Moschosaurus longiceps* was an immature titanosuchid. Broom further proposed that the holotype of *Lamiasaurus newtoni*, comprising only the snout, be placed in Titanosuchia.

In 1923, a description of two skulls representing a new type was undertaken by Broom and he named the species *Dinophoneus ingens*. Broom later (1929) removed the topotype specimen from *Dinophoneus* and placed it in the genus *Jonkeria,* forming a new species *J. pugnax*. Boonstra (1936a) considered that Broom's original diagnosis was correct and that the two skulls belong to the same species referable to the genus *Jonkeria*. Hence, *Dinophoneus* was, synonymized with *Jonkeria*, and *Jonkeria pugnax* was, synonymized with *Jonkeria ingens* (King, 1988). Broom (1923) also described a new genus and species, *Enobius strubeni*, from two dentaries found on the farm Abrahamskraal, Prince Albert, South Africa. Boonstra (1953b)

lumped this genus with *Titanosuchus* since he could not find any distinguishing features in the poorly preserved holotypes and later decided that the holotype of *Enobius* could be identified only as an indeterminate titanosuchid (Boonstra, 1969). Broom (1929) described a new species, *Jonkeria vanderbyli* on a skull from Jan Willemsfontein, Prince Albert. He conceded that the skull agrees closely with that of *Jonkeria truculenta*; so much so that it was only after some hesitation that he decided to ascribe it to a new species and not the adult of *J. truculenta*. Broom noted a few differences between the two species, with *Jonkeria vanderbyli* featuring a much shorter internasal process of the premaxillaries in, a groove in the frontal region and a much flattened snout.

In the same year Broom (1929) re-evaluated the taxonomy of *Titanosuchus cloetei* noting that, it closely resembled *Jonkeria* (with similarities in the splenial and articular bones) and thus transferred this species to the genus *Jonkeria cloetei*. He did not transfer it to the existing *Jonkeria* species since *J. vanderbyli* did not have a lower jaw for comparison and the jaw of *J. truculenta* was of an immature specimen. Boonstra (1969) considered that the fragmentary lower jaw of *J. cloetei* permitted it to be identifiable only to family level.

Scylla gigas was erected by Broom in 1929 from a poorly preserved snout which shows no definite titanosuchian characters. Boonstra (1969) suggested that the possible presence of teeth on the palatine may be an anteosaurid character and hence the specimen must be considered indeterminable.

The new taxon, *Dinosphageus haughtoni* was described by Broom (1929) based on a skull, humerus and ilium found at Welgemoed (Kruidfontein 33), near Fraserburg Road Station.

Boonstra (1969) noted that this specimen shows no features that distinguish it from *Jonkeria* and named it *J. haughtoni*. Broom (1929) also described a new species based on some skeletal remains consisting of both dentaries, a scapula, a humerus, partial ulna and a few imperfect vertebrae found near Kruidfontein Station. He named this species *Jonkeria crassus*. However, Boonstra (1969) observed that the humerus cannot be distinguished from that of *J. haughtoni* and, as such, it should be considered a synonym of this species. In addition, Broom (1929) described the titanosuchid *Phoneosuchus angusticeps* based on a jaw fragment from Abrahamskraal, Prince Albert. Boonstra (1969) synonymized this species with *J. truculenta*. Broom (1936) described *Dinopolus atrox* from a snout. Boonstra (1969) considered that features exhibited in this snout are those known as characters of the genus *Jonkeria* and cannot be used for a specific diagnosis and suggested that *Dinopolus atrox* is thus an indeterminable species of the genus *Jonkeria*.

Boonstra (1936) produced composite drawings of titanosuchids in the American Museum of Natural History showing most of the sutures and he was even able to describe the brain case of the *Jonkeria ingens.* He then concluded that, compared with other dinocephalians, titanosuchids show less bone thickening, no reduction in the antero-posterior diameter of the temporal fossa, no widening of the intertemporal region, long snout, quadrate posteriorly situated, concave occiput and narrow across the squamosals.

Boonstra (1955) described three new species *Jonkeria koupensis*, *J. parva* and *J. rossouwi*. From Klein Koedeoskop, Beaufort West, he described *Jonkeria koupensis*, which comprises a pelvis lacking ischia, and distal two thirds of an ulna. A referred specimen of this species comprising

only an ilium (SAM-PK-011983) comes from Abrahamskraal, Prince Albert. *Jonkeria parva* from Saairivier (Jan Willemsfontein 32), Prince Albert, is represented by a well preserved right humerus, whereas *J. rossouwi* also described after postcranial elements (pectoral girdle, scapula, interclavicle, deformed left humerus, deformed left ulna, and left radius, pelvis, left femur, left tibia and left fibula) comes from Abrahamskraal.

Boonstra (1955) described several additional specimens from the Beaufort West and Prince Albert districts. A femur from Mynhardtskraal, Beaufort West, and humeri from Seeikoeigat, were assigned to *Scapanodon duplessisi* and some postcranial bones from Sewefontein, Prince Albert, and Aasvoelbos, Beaufort West to *Scapanodon septemfontis*. Cranial and postcranial remains from various farms in the Beaufort West and Prince Albert districts were assigned to *Parascapanodon avifontis*. Boonstra (1969) synonymized the *Scapanodon* and *Parascapanodon* species with *Titanosuchus ferox*.

Janensch (1959) described a skull and lower jaw, from Springfontein near Letjiesbosch, Beaufort West, as *Jonkeria boonstrai*.

Boonstra (1962) undertook an analysis of the dentition of the titanosuchian dinocephalians based on 37 specimens housed at Iziko South African Museum. His focus was dental formulae, tooth morphology and tooth replacement patterns. He pointed out the importance of the intermeshing incisors of Dinocephalia as a unique phenomenon that separated it from the rest of the therapsid groups and the significance of the variation of this character amongst Dinocephalia. Boonstra (1969) pointed out that even well-preserved batteries of teeth exhibit much variation between the left and right hand sides of the same specimen.

According to Boonstra (1969), the genera *Titanosuchus* and *Jonkeria* can only be distinguished because in *Titanosuchus* the limb bones are long whereas in all the species of *Jonkeria* they are short and squat. The current state of affairs is that the Family Titanosuchidae comprises two genera (*Titanosuchus* and *Jonkeria*) and nine species (*T. ferox*, *J. boonstrai*, *J. haughtoni*, *J.ingens*, *J. koupensis*, *J. parva*, *J. rossouwi*, *J. truculenta* and *J. vanderbyli*) (Boonstra, 1969, King, 1988).

Kammerer (2009) agreed with Boonstra (1955a, 1969) that two morphotypes of titanosuchid postcrania can be recognized, corresponding to the genera *Jonkeria* and *Titanosuchus*. He observed that *Jonkeria* is characterized by extremely short, robust appendicular elements even by dinocephalian standards, with a diagnostic "dumb-bell" shaped humerus while on the other hand the humerus of *Titanosuchus* is more elongate, with a relatively narrow shaft compared to the short, broad condition in *Jonkeria.* Another important contribution by Kammerer (2009) was his observation that *Jonkeria truculenta, Jonkeria ingens, Jonkeria vanderbyli, Jonkeria haughtoni and Jonkeria boonstrai* are conspecific but he never presented evidence to support this argument. Kammerer (2009) stated that cranial proportions (especially height of the pineal region and width of the snout tip) vary between titanosuchid skulls, and that these characters had been used by earlier authors to differentiate a number of species known only from skulls. He concluded that these proportional characters vary continuously between specimens and more likely reflect individual variation than species distinction. As such, he concluded that titanosuchid crania are non-diagnostic to genus, echoing Boonstra's (1969) observation.

Species based solely on craniodental material and only on postcranial elements were considered *nomina dubia* by Kammerer (2009) with the hope that future discoveries of associated titanosuchid crania and postcrania will allow these taxa to be properly identified. Morphometric analyses in Kammerer's PhD thesis treated titanosuchid crania as representing a single taxon, labelled *Jonkeria truculenta*.

1.2.2 Stratigraphic ranges of Titanosuchid dinocephalians

Since dinocephalians are an important component of middle Permian tetrapods, the taxonomic revision of dinocephalian families is crucial in elucidating the stratigraphic ranges of these middle Permian taxa to help understand biodiversity changes leading to the end Gaudalupian extinction event.

The first formal recognition of a biostratigraphic division that is today known as the *Tapinocephalus* Assemblage Zone was presented by Seeley (1892). The first fossils collected from this zone were mostly large bones attributable to dinocephalians and pareiasaurs, though therocephalians and dicynodonts were also part of the fauna in this zone (Day and Rubidge, 2020). Broom (1906) noted that dicynodonts were common to all the zones of the lower Beaufort Group but that *Tapinocephalus* and *Titanosuchus* were confined to the oldest Beaufort strata, which he named *Pareiasaurus* Beds. Watson (1914) proposed that the name *Pareiasaurus* Beds be replaced by *Tapinocephalus* Zone. It was Rossouw and de Villiers (1953) who first proposed a subdivision of the *Tapinocephalus* Zone, in which they recognised two main zones separated by a third intermediate zone (Day and Rubidge, 2020). The three zones were essentially characterised by an incrementally decreasing abundance of pareiasaurs and (to a lesser degree) of dinocephalians, with an associated and 'phenomenal' increase in the abundance of dicynodonts

(Rossouw and de Villiers, 1953:59). This three-fold division was also supported and advanced by Boonstra (1969), who proposed that the uppermost subdivision contained a lower abundance of dicynodonts than the middle zone and practically no dinocephalians or pareiasaurs. This impoverished fauna in the upper *Tapinocephalus* Zone was, later interpreted as the result of the Capitanian extinction event (Day *et al*. 2015a; Day *et al*. 2018). Keyser and Smith (1978) named the uppermost part of the original *Tapinocephalus* Zone, corresponding to the same stratigraphic interval identified by Rossouw and de Villiers (1953), the *Pristerognathus-Diictodon* Assemblage Zone. In a revision of the Beaufort Group biozones, the *Tapinocephalus* Assemblage Zone was recently subdivided into two subzones, the lower *Eosimops - Glanosuchus* Subzone and the upper *Diictodon - Styracocephalus* Subzone based primarily on the presence or absence of the dicynodont *Diictodon feliceps* (Day and Rubidge, 2020). Substantial progress has been made on the determination of dinocephalian biodiversity in the middle Permian of South Africa due to the work of various researchers such as Rubidge (1994); Kammerer (2011) for anteosaurian dinocephalians; Rubidge and van den Heever 1997, Fraser-King *et al*. (2019) for *Styracocephalus*; Boonstra (1969), Rubidge (1991); Kammerer (2009), Guven *et al*. (2013), and Neumann (2020) for tapinocephalid dinocephalians; Boonstra (1969) and Kammerer (2009) addressed the Titanosuchidae.

Over the years numerous studies have been conducted at the Evolutionary Studies Institute, University of the Witwatersrand, using the Beaufort Group vertebrate fossil database from the Karoo Basin of South Africa, (Rubidge 2005, Nicolas 2007, Van der Walt *et al.* 2011, Smith *et al*. 2012; Day 2013b, Day *et al.* 2015a) and has culminated in the production of refined stratigraphic ranges of most of the major tetrapod groups.

These biostratigraphic studies over almost two decades have provided evidence for an extinction event, correlated with the end-Guadalupian extinction recognised in the marine realm from China (Day 2013b, Day *et al.* 2015a, Day and Rubidge 2021) at the end of the *Tapinocephalus* Assemblage Zone. On land, the end-Guadalupian extinction event, manifests as a faunal changeover when the large basal taxa give way to more derived, medium- to small-sized taxa and the dinocephalian therapsids and the large basal pareiasaurs (e.g. *Bradysaurus*, *Embrithosaurus*) become extinct (Nicolas 2007, Van der Walt *et al.* 2011, Day 2013b, Day *et al.* 2015a; Day and Rubidge 2021, van den Brandt *et al*. 2020).

Stratigraphic ranges of middle Permian South African titanosuchid dinocephalians have been produced by Keyser and Smith (1995a) and Day (2013b). Day and Rubidge (2020) used the combination of taxonomy of Boonstra (1969) and data from Keyser and Smith (1995a) to generate stratigraphic ranges for South African middle Permian titanosuchid genera (Figure 1.3). My research will add to the refinement of the biostratigraphic work by Day and Rubidge (2020) through the re-examination of all the holotypes and referred specimens of titanosuchid dinocephalians including new and nearly all previously known material.

This thesis therefore addresses two important research aims:

- Determine the number of valid species of titanosuchid dinocephalians from the middle Permian *Tapinocephalus* Assemblage Zone of the Beaufort Group through performing a detailed taxonomic reassessment, based on new detailed cranial and postcranial descriptions of taxa, updated species level diagnoses, and updated phylogenetic analysis.

- Contribute towards understanding middle Permian tetrapod biodiversity and the terrestrial occurrence of the end-Guadalupian extinction event, through determining the stratigraphic ranges of valid titanosuchid dinocephalian species.

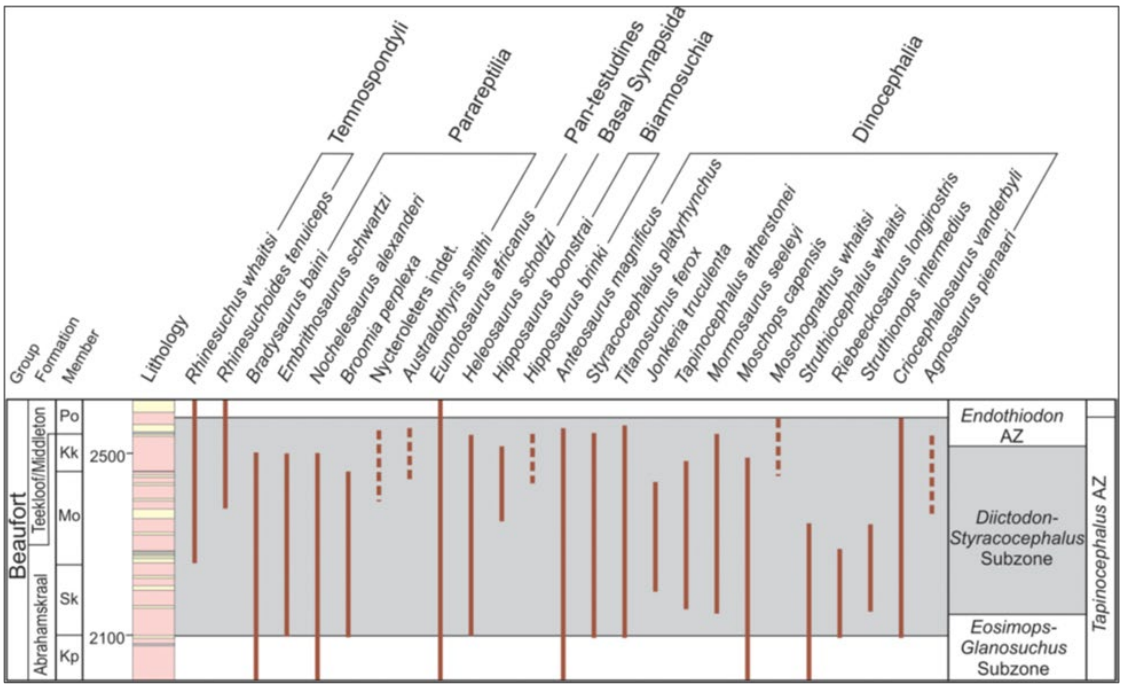

Fig. 1.3: Stratigraphic ranges of the Titanosuchids *Titanosuchus ferox* and *Jonkeria truculenta* alongside other *Tapinocephalus* Assemblage Zone taxa occurring in the *Diictodon – Styracocephalus* Subzone. Kk=Karelskraal; Kp= Koornplaats; Mo=Moordenaars; Po=Poortjie; Sk=Swaerskraal. (Day and Rubidge 2020).

The manuscript has been structured to address these aims as follows.

- The crania of titanosuchid dinocephalians are described in detail in Chapter 3, based on the holotypes, important referred specimens and some unpublished material. The accuracy

of the descriptions has been facilitated and improved by inclusion of specimens FMNHUC 1511 and ROZ.B96, and the additional preparation using modern techniques on some of these specimens and high-resolution photography.

- Chapter 4 provides the detailed re-description of the limb postcrania of *Titanosuchus* and *Jonkeria* using the holotype and important referred specimens, including the new, unpublished specimen BP/1/7380.
- An updated phylogenetic analysis for these middle Permian herbivores is provided in chapter 5, based on updated character scores.
- Production of updated stratigraphic ranges and geographic locations of all valid middle Permian *Titanosuchus* and *Jonkeria* specimens (chapter 6) resulting from re-examination of all curated material of middle Permian titanosuchids in collections world-wide.

CHAPTER TWO: MATERIALS AND METHODS

2.1 Specimens

For this project, it was necessary to, personally examine, all titanosuchid specimens housed in museum collections around the world. The study concentrated on holotype and referred specimens but also included other published and undescribed specimens and includes both cranial and appendicular postcranial material. All specimens used for this study are, presented in Appendix A and come from the middle Permian *Tapinocephalus* Assemblage Zone, Abrahamskraal Formation, Beaufort Group of the South African Karoo Basin, except for BP/I/7168, which is from the Poortjie Member, Teekloof Formation, Beaufort Group.

2.2 Preparation

Preparation of the specimens SAM-PK-11884 and SAM-PK-12030 was, undertaken at the ESI. Specimen TM 212 was prepared/altered at the DMNH where most of the plaster that held the skull and lower jaw together was, removed. All preparation at the ESI was mechanical and was undertaken by using a Desoutter VP2-X air scribe fitted with tips of tungsten carbide under a stereoscopic microscope whose magnification varies from 4X to 40X. Paraloid B-72 glue (paraloid pellets dissolved in acetone), was used as an adhesive.

2.3 Suture Identification

A combination of several methods was, used to identify cranial sutures.

1) Use of a stereoscopic microscope and magnifying glasses.
2) Use of alcohol/water to wet the specimen, which momentarily reveals matrix, sutures and cracks on the bone.

3) SAM-PK-11884 and SAM-PK-12030 were, chemically stained using the dye "Alizarin Red S" using the reversible technique as described by Rubidge and van den Heever (1997). A 10% solution of hydrochloric acid (HCI) was, brushed on the bones and immediately rinsed off with tap water. A small amount of the biological staining agent Alizarin Red S was, mixed with 4% solution of potassium hydroxide (KOH). This mixture was then, brushed onto the bones, staining them with a deep purple color. This procedure helped reveal sutures and any cracks in the bone. To remove the stain, the 10% solution of HCI was, again brushed on the bones and immediately rinsed off with tap water.
4) Use of previous workers "drawn on" sutures directly on the bone in black or white ink, when deemed to be reliable.

2.4 Microfocus X-Ray Computed Tomography (CT) Scanning

Microfocus X-Ray Computed Tomography (CT) Scanning has over the years proved to be invaluable tool to palaeontologists for the non-destructive application and analysis of fossilized material with excellent results. CT scans were, done of titanosuchid dinocephalian jaws for non-invasive analysis and reconstruction.

SAM-PK-11884 and SAM-PK-12030 jaws were scanned using Microfocus X-ray computed tomography (CT) with a Nikon Metrology XTH 225/320 LC dual source industrial CT system at the Evolutionary Studies Institute, University of the Witwatersrand, Johannesburg, South Africa (ESI). Elements to be scanned were packed into specially constructed Perspex tubes, supported by polyethylene foam blocks. Due to its large size the lower jaw of specimen SAM-PK-11884

was separated into two pieces by dissolving, with acetone, the paraloid B72 adhesive which had been used previously to glue the pieces together. Each scan was completed at 190KV and 105μA. Three thousand projections were taken at an average of two frames per second. A 2.4mm copper filter was used during the scanning process.

Data from each scan was uploaded to the Virtual Imaging Processing (VIP) Laboratory at the ESI, for analysis. The resultant scans were reconstructed using VSG's Avizo® Fire. Each reconstructed scan was segmented using the same software. Due to metallic inclusions in the scanned specimen, the resolution was too poor to obtain any useful results.

2.5 Allometric growth

The following cranial measurements were taken for allometric growth analysis (Fig. 2.1) and are recorded in Appendix B.

1. Total skull length (tip of the snout to occipital condyle)
2. Snout length
3. Antero-posterior orbital length
4. Inter-orbital width
5. Inter-temporal width (at level of pineal foramen)
6. Width of the post-orbital bar
7. Width of the snout (at level of canine roots)
8. Greatest width of the skull (at level of squamosals)
9. Antero-posterior temporal opening width
10. Pterygoid process width
11. Width of jugal below orbit
12. Inter-nostril width

13. Occiput height

14. Distance from anterior margin of pineal foramen to tip of snout

15. Distance from posterior margin of pineal foramen to edge of occipital condyle

16. Distance from lateral flanges of pterygoid to tip of snout

17. Length of the lower jaw from articular to anterior tip of mandible

18. Height of the dentary on the symphysis

19. Height of the lower jaw on the coronoid eminence

20. Width of occiput between squamosals

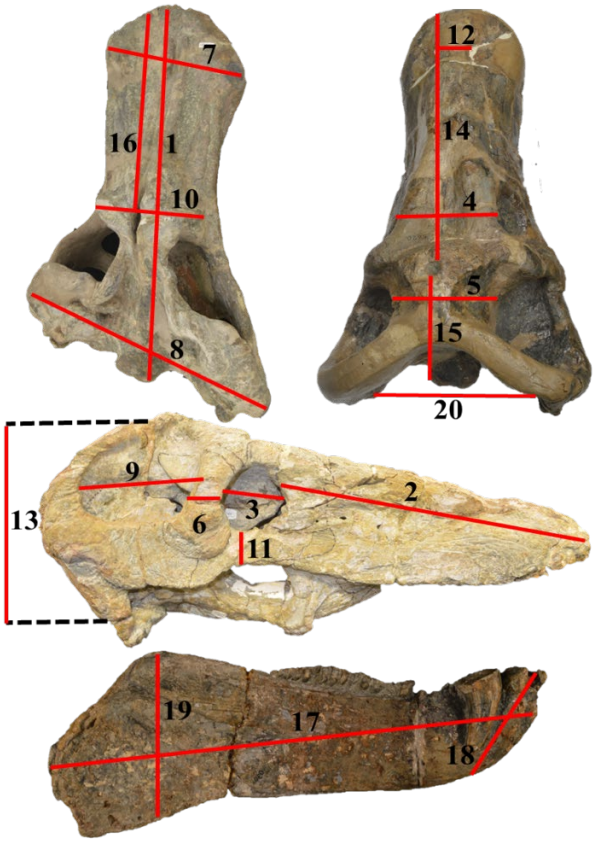

Fig. 2.1: Illustration of the skull of *Jonkeria* showing the cranial measurements taken for comparison between different skulls. FMNH UC 1511 skull (top left, ventral view), AMNH 5620 skull (top right, dorsal view), SAM-PK-11884 skull (middle, lateral view), and SAM-PK-12030 lower jaw (bottom, lateral view).

2.6 Principal Component Analysis

Appropriate titanosuchid specimens were directly analyzed and measured and are reported in Appendix B. For each limb bone, four measurements (see below) were taken using a sliding digital vernier caliper and taking as reference the same homologous points (in the sense of topographical identity). In Fig. 2.2, the homologous points are reported for each considered osteological limb element. Using the acquired dataset a principal component analysis (PCA) was performed for the limb bones using the software PAST 3.10 (Hammer *et al.* 2001). For these computations the raw data were log-transformed for the correspondence of the log-transform to an isometric null hypothesis and to fit linear models (Chinnery 2004; Cheng *et al*. 2009; Romano & Citton 2015; 2016). Specimens which did not afford sufficient data were removed from the analysis. For PCA plots, the basal synapsid *Dimetrodon* and tapinocephalids (*Moschops*, *Riebeeckosaurus*, *Struthiocephalus* and *Tapinocaninus*) were used for comparative purposes.

The following four measurements were taken for limb elements (Fig. 2.2):

- Total length
- proximal width
- distal width
- width at mid shaft.

Measurements for each specimen are recorded in Appendix C.

Wherever possible, the specimens were directly analyzed and measured but there are a few instances where data was taken from the literature (for comparative material).

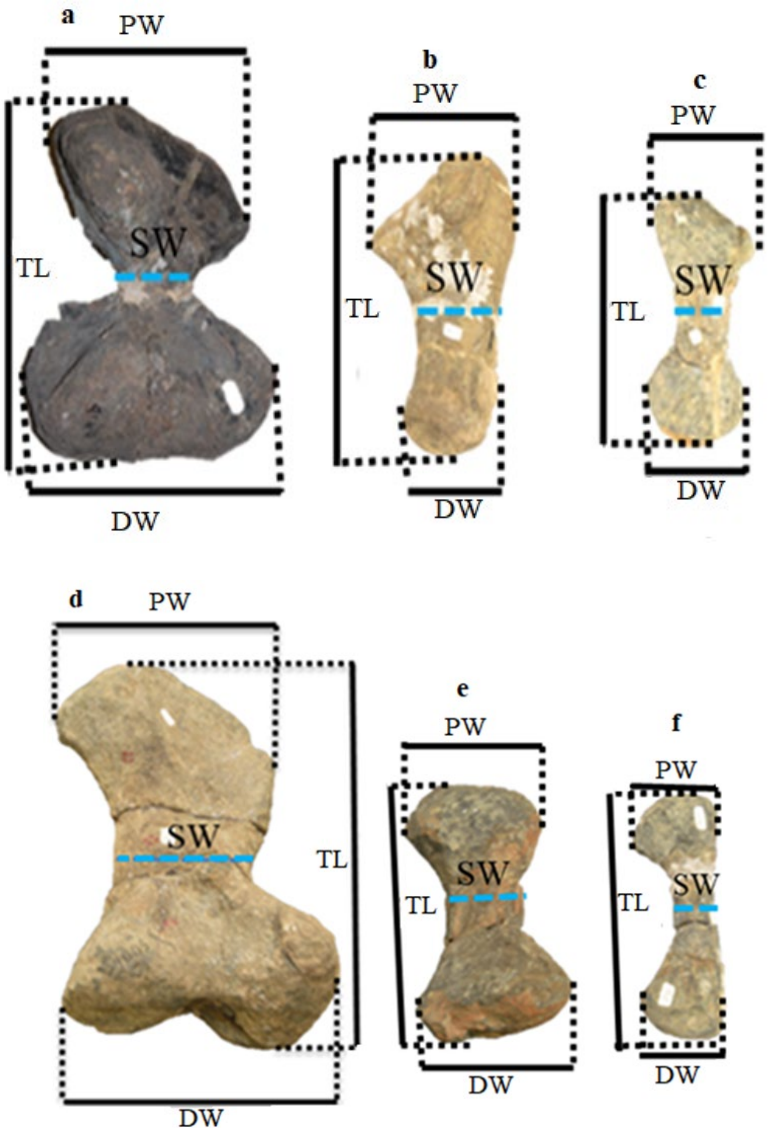

Fig. 2.2. Limb bone measurements for PCA analysis: **PW**, proximal width; **DW**, distal width; **SW**, width at mid-shaft; **TL**, total length. **a**, humerus (SAM-PK- 9149); **b**, ulna (SAM-PK- 4343); **c**, radius (SAM-PK- 5014); **d**, femur (SAM-PK- 5001); **e**, tibia (SAM-PK- 5014); **f**, fibula (SAM-PK-5014).

2.7 Phylogenetic analysis

The character matrix was prepared in Mesquite version 3.51 (Maddison and Maddison, 2017). Characters used in previous analyses, some of them with modifications as well as new proposed characters, were considered (Appendix D). The data matrix (Appendix E) was treated under the

assumption of parsimony, using TNT version 1.5. A first round was the search of the most parsimonious trees using equal weight for characters (treated as unordered), using implicit enumeration in TNT, an option that guarantees finding all the shortest trees from the data-matrix. A second analysis used implied weighting, with K set at three (default in TNT). *Biarmosuchus* was the root taxon and the dinocephalian taxa coded include members of Anteosauridae, *Deuterosaurus*, *Estemmenosuchus*, members of Titanosuchidae and Tapinocephalidae. The aim was to show the relationship of the Titanosuchidae to other dinocephalian taxa.

2.8 Interpretative Drawings

For most photographed osteological elements, interpretative drawings were produced using the GNU Image Manipulation Programs (GIMP 2.8) and Inkscape 0.91. GIMP is a raster graphics editor used for image retouching and editing, free-form drawing, converting between different image formats, and more specialized tasks, (Peck, 2006). Inkscape is a multi-platform, open-source vector graphics editor that uses SVG as its native file format.

CHAPTER 3: CRANIAL DESCRIPTION OF *TITANOSUCHUS FEROX* AND *JONKERIA TRUCULENTA*

3.1 Introduction

From chapters one and two it is evident that since 1879, when the first titanosuchid dinocephalian was described, 24 titanosuchid species have been proposed, but most of these are based on fragmentary and undiagnostic material. Boonstra (1969) followed by King (1988), synonymized most of the genera and concluded that only one species of *Titanosuchus* and eight species of *Jonkeria* were valid. Boonstra, (1969) also pointed out that the skulls of the two genera are morphologically indistinguishable, but they differ in the morphology of some limb bones. This chapter presents an updated cranial description of the Titanosuchidae taxa. Of the nine currently recognized titanosuchid species, three are based on and known from cranial remains, three on both cranial and postcranial remains and the other three on postcranial material.

3.2 SYSTEMATIC PALAEONTOLOGY

Family Titanosuchidae Broom 1903
Subfamily Titanosuchinae Broom 1903c
Jonkeria van Hoepen 1916b
Genotype: *Jonkeria truculenta* van Hoepen 1916b

Synonyms: *Jonkeria angusticeps* (Broom 1929) Boonstra 1969 = *Phoneosuchus angusticeps* Broom 1929
Jonkeria vanderbyli Broom 1929
Jonkeria haughtoni (Broom 1929) Boonstra 1969 = *Dinosphageus haughtoni* Broom 1929
Jonkeria ingens (Broom 1923) Boonstra 1936a = *Dinophoneus ingens* Broom 1923
Jonkeria parva Boonstra 1955a
Jonkeria rossouwi Boonstra 1955a
Jonkeria boonstrai Janensch 1959

Holotype: TM212: skull with an incomplete right mandible; vertebrae; right shoulder girdle, lacking the top of the scapula; right clavicle; portion of the right cleithrum; interclavicle; part of the left clavicle; right tibia; a few portions of ribs.

Referred specimens: SAM-PK-12030: incomplete skull with right mandibular ramus; AMNH 5633: ischium and lower jaw; AMNH 5620: skull without lower jaw; SAM-PK- 11884: skull and lower jaw; SAM-PK-4343: skull without lower jaw, humeri, ilia, scapula, cleithrum, ulna, ischium, incomplete femur, fibula, coracoids and vertebrae; AMNH 5577: scapula, humerus part of ulna and ilium associated with dentaries; AMNH 5634: incomplete skull without mandible; AMNH 5608: incomplete skull with right mandibular ramus ; SAM-PK- 738: isolated humerus; SAM-PK- 3433 isolated humerus; SAM-PK-9149: right humerus; SAM-PK- 12005: isolated humerus; SAM-PK-5014: left scapula, incomplete precoracoid and coracoid, incomplete interclavicle, left humerus, left ulna, left radius, right ilium, left femur, left tibia and left fibula; MB.R. 983: incomplete skull and partial lower jaw; FMNHUC 1511: skull, lower jaw, and fragmentary postcranial elements.

Titanosuchus Owen 1879a
Genotype: *Titanosuchus ferox* Owen 1879a
Synonyms: *Scapanodon duplessisi* Broom 1904g
Scapanodon septemfontis Boonstra 1955a
Parascapanodon avifontis Boonstra 1955a

Holotype: NHMUK 49370 (fragmentary jaws: maxilla and mandible); NHMUK 49367-69 (post-crania that includes two left humeri, femur and two phalanges).

Referred specimens: SAM 739: femur; SAM 11491: femur, SAM-PK- 772: humerus, SAM-PK- 773: humerus, SAM 5001: pelvic girdle, humerus and femur; SAM 11578: part of scapula

and part of humerus; SAM 9127: precoracoid, clavicle, femur, fibula associated with skull fragments; SAM 11881: humerus

Titanosuchidae *incertae sedis*

Titanosuchus cloetei Broom 1903d

Titanosuchus dubius Haughton 1915b

Dinartimus vanderbyli Broom 1923

Enobius strubeni Broom 1923

Dinocynodon dubius Broom 1929.

Jonkeria koupensis Boonstra 1955a

Age and stratigraphy: All specimens are Guadalupian (middle Permian) and occur high in the *Tapinocephalus* Assemblage Zone, in the Moordenaars Member towards the top of the Abrahamskraal Formation of the Beaufort Group. A titanosuchid indet specimen from the lower Poortjie Member of the Teekloof Formation is identified as the youngest record of the group. (see chapter 6).

3.2.1 Family Titanosuchidae

Previous diagnosis of the family Titanosuchidae. Dinocephalians with an enlarged heel on the incisor teeth, a reduced but distinct canine, a jaw hinge positioned relatively far anteriorly, and many leaf-shaped and denticulated postcanine teeth (Broom, 1903c; Boonstra, 1972, King, 1988; Kemp, 2005). Boonstra (1962) observed that on the dentary the postcanines are positioned

medially relative to the canine and that the anterior-most postcanines are placed on the medial side of the canine. The diagnosis of the family was later summarized by Boonstra (1969:35) as "retention of the canine, very strong incisors with a piercing talon and a crushing heel and the long series of postcanines with serrated spatulated crowns, and very little pachyostosis of the skull" .

Emended diagnosis of Titanosuchidae. Long snouted dinocephalians with the following suit of characters: a distinct canine of which the longer upper canine curves moderately to strongly backwards and the lower is shorter, less pointed and directed outwards; incisors exhibit a talon and heel morphology, the lingual edge of the heel forming a sharp ridge with coarse denticles in unworn teeth; many leaf shaped, denticulated postcanines with the anteriormost being larger and positioned medial to the canine on the mandible; the skull is less pachyostosed than tapinocephalids and anteosaurines among anteosaurs but there is considerable pachyostosis on the prefrontals, postfrontals, postorbitals, and especially the parietals; parietal is laterally bayed; round pineal foramen on the raised parietals; flat, elongate, strap-like vomers extending nearly two-thirds of the length of the palate with a shallow midline trough and bifurcated anterior end; near horizontal dorsal skull roof profile; a craniomandibular articulation positioned further anteriorly than anteosaurids; mandible with a sloping mentum, with the angle of slope varying from 45° to almost 80°.

3.2.2 Valid Titanosuchid taxa

Boonstra (1969) and King (1988) recognized the following titanosuchid taxa.

***Titanosuchus ferox* Owen 1879[a] (Fig. 3.1)**



Fig. 3. 1. *Titanosuchus ferox* holotype NHMUK 49370. **a**. medial side of a portion of the left maxilla which includes the trace of the socket of the canine, s, with part of the base or root of that tooth, c. **b.** left mandibular ramus with the alveolar border and roots of incisors, canine and postacanines in cross section. Scale bar is 5cm.

Previous diagnosis of Titanosuchus ferox. No diagnosis

Remarks. Owen (1879a) summarized the characters for *Titanosuchus ferox* (Fig. 3.1) as "a very strong and massive dentary with a fairly upright mentum and the mandible being thick in proportion to its depth at its symphysial end. Cross section through incisors more nearly elliptical, with the long axis transverse to the jaw, canine in section less regular oblong shape and the anterior postcanines largest in size and size decreasing in the posterior direction of the jaw and roots of anterior postcanines elliptical in section with long axis parallel to that of the jaw and those of the posterior postcanines circular in section. Dental formula: i5/4, c1/1, pc11/10-11" (Owen 1879a:189-199). Haughton and Brink (1954:45) and King (1988:23) summarized the characters as follows: "Skull possibly large and massive, bosses probably present, no evidence of pachyostosis, dentigerous border of the premaxilla curves antero-dorsally with an associated step-up of the anterior part of the alveolar border of the dentary, incisors apparently long with no lingual crushing surface and strong and massive dentary with a slanted and upright mentum."

Dental formula (Boonstra 1953b): i4-5/4, c1/1, pc11-15+/7-12+

The suit of cranial characters above are non-diagnostic and they do not enable a distinction of *Titanosuchus* from *Jonkeria*. Of the postcranial elements, the humerus shows a clear distinction between *Titanosuchus* and *Jonkeria.*

The humerus of *Titanosuchus* is more elongate, with a relatively narrow shaft compared to the short, broad condition in *Jonkeria*; proximal end is greatly expanded while the distal end is slightly less expanded and the lateral outlines of the shaft of the *Titanosuchus* humerus are only slightly concave (relative to those of the *Jonkeria*); both the proximal and distal portions of the *Titanosuchus ferox* humerus are less lateromedially expanded than those of *Jonkeria truculenta*; in dorsal view, the twist on the humerus shaft is extensive (about 40 degrees) compared to 15 - 30º in *Jonkeria*; massive capitellum that nearly reaches the level of the entepicondylar foramen in *Titanosuchus* and extends beyond this level in *Jonkeria.* A full description of the limb elements is presented in chapter 4

***Jonkeria truculenta* van Hoepen 1916 (Fig. 3.2**



Fig. 3. 2. Lateral view of *Jonkeria truculenta* holotype (TM 212). Skull lacks left squamosal and quadratojugal. Pterygoids are damaged and all teeth missing, reconstructed by plaster of Paris.

Previous diagnosis for Jonkeria truculenta. van Hoepen **(**1916b: 1) summarized the diagnostic characters of *Jonkeria truculenta* (Fig.3.2) as "skull long and narrow broadening considerably below and behind the orbits; large orbits almost the same size as the temporal vacuities; no pachyostosis of the upper and hinder rim of the orbit; nostrils far in front and lateral; pineal foramen situated at the extreme end of the upper surface of the skull onto of a broad and high boss; large incisors with a high sharp-edged anterior cusp and a broad flat posterior cusp; a row of small postcanines on the maxilla, the crowns of which are flattened and serrated in front and behind".

The *Jonkeria truculenta* characters were later summarized by Broom (1932: 20), Boonstra (1953b: 23) and Haughton & Brink (1954: 43), as "skull medium to large and not massive, no prominent bosses, parietals forming a prominent ridge thickened around the pineal foramen but with no well demarcated boss, no palatine boss but palatine possibly dentigerous, the dentigerous

border of premaxilla does not curve upwards with no corresponding upward sweep of the dentary, incisors teeth of medium length with labial talon and with a well-developed crushing surface, pineal foramen some distance from the occipital border, relatively long, broader an high snout with frontals slightly swollen and premaxilla fairly flat, squamosal does not extend far ventrally and does not sweep far posteriorly, posterior to the interparietal and also very little lateral sweep of the squamosal, fairly large temporal fossa, small to moderate intertemporal width with laterally pinched parietals forming a high narrow crest, strong dentary with a sloping mentum and dental formula i4-5/4, c1/1, pc14-19/13-15+.

King (1988: 21) proposed the following suit of characters for *Jonkeria truculenta*, "skull medium to large with no prominent bosses, parietals forming a prominent ridge, thickened round pineal foramen, but not forming a distinct boss, dentigerous border of premaxilla not curving upwards, dentary with no upward sweep, incisors of medium length with a labial pointed talon and a well-developed lingual crushing surface, pineal foramen some distance in front of occipital border, snout relatively long, broader than high, frontals slightly swollen, premaxilla fairly flat, squamosal not extending far ventrally and not passing far behind plane of inter-parietal, fairly large temporal fossa and intertemporal width small to moderate".

These characters are similar to what is currently known of the fragmentary *Titanosuchus* cranial elements and as such, *Jonkeria truculenta* and *Titanosuchus ferox* cannot be distinguished based on cranial characters.

Revised diagnosis for Jonkeria truculenta. The defining combination of characters for *Jonkeria truculenta* are: large skulls with a length ranging from 500 to 680mm with a long and narrow

snout (length of snout on average about 60% of total skull length); skull broadens considerably behind the orbit; no pronounced thickening of the dorsal and hind rim of the orbit; external nares situated far anteriorly and laterally; swelling around the pineal foramen due to the pachyostosis of the parietal; This thickened parietal mound is pierced by a prominent circular pineal foramen, situated on a chimney. The intertemporal width is slightly wider than the interorbital width, but at the level of the pineal foramen because the parietal is raised and is laterally bayed it appears narrower. The temporal opening is relatively large, and its anteroposterior diameter is not reduced to a transverse slit as in the tapinocephalids. The lateral surface of the snout has a moderate concavity between the orbit and posterior margin of the septomaxilla. In lateral view the jaw articulation is positioned far anteriorly almost ventral to the postorbital bar. Dental formula: i5/4, c1/1, pc19/18-21 with large incisors with a high sharp-edged anterior cusp and a broad flat posterior cusp; robust canines with the maxillary canines having a large conical crown which lacks serrations and which curves backwards, moderately flattened from side to side. Lower canine smaller than the upper, shorter, less pointed and curved and its blunt point directed outwards. Canine has a large and long root, which causes the maxilla to bulge both internally and externally. Presence of a diastema between the last upper incisor and the canine to enable the lower canine to pass between these two teeth in occlusion. Posterior to the canine is a row of small postcanines on the maxilla, the crowns of which are flattened and denticulated on the anterior and posterior surfaces. Palatines without any prominent bosses or teeth but slightly raised towards their posterior extremity where they contact the vomers.

The humerus shaft is very short and greatly constricted in the central portion when compared to that of *Titanosuchus*; twist of the shaft varies from 15 – 30 degrees compared to 40 degrees in

Titanosuchus and the massive capitellum extends beyond the level of the entepicondylar foramen in *Jonkeria* but only extends to this level in *Titanosuchus.*

3.2.3 Junior synonyms

Following omparison of all *Jonkeria* cranial material the following species are synonomised with *Jonkeria truculenta*.

***Jonkeria vanderbyli* Broom 1929 (Fig. 3.3)**



Fig. 3. 3. Lateral view of the *Jonkeria vanderbyli* holotype (AMNH 5620).

Skull mostly covered in plaster of Paris. Scale bar represents 10cm.

Previous diagnosis for Jonkeria vanderbyli. Broom (1929) noted that *Jonkeria vanderbyli* (Fig. 3.3) agrees morphologically with that of *Jonkeria truculenta* with only minor dissimilarities namely: “premaxilla larger and flatter in *Jonkeria vanderbyli*, but more abruptly turned down in front, a shorter inter-nasal region of the premaxillars, and skull with a groove down the middle of the frontal region” (Broom, 1929: 23-25). In lateral view, Broom (1932) mentioned the “considerably flatter snout and presence of a deep notch at the posterior end of the jugal and the position of the quadrate under the postorbital” (Broom, 1932: 24). Broom (1929) remarked “..the

skull agrees closely with that of *Jonkeria truculenta*, so much so that it has only been after some hesitation that I have decided that it is a new species and not the adult of the species described by van Hoepen" (Broom, 1929: 24).

Remarks. The dorsal and anterior skull profile of this species is not a diagnostic feature since this region is deformed. The internasal region extends posteriorly as far as the anterior edge of the frontals. The notch at the posterior end of the jugal and the positon of the quadrate are pliable features easily distorted by post depositional taphonomic factors.

***Jonkeria ingens* (Broom 1923) Boonstra 1936 (Fig. 3.4)**



Fig.3. 4. Lateral view of the *Jonkeria ingens* holotype (AMNH 5634) with less than 50% of the skull preserved. Scale bar represents 10cm.

Previous diagnosis for Jonkeria ingens. Broom (1923) described two skulls AMNH 5608 and AMNH 5634 (Fig. 3.4) under the name *Dinophoneus ingens* and later removed his topotype

specimen (AMNH 5608) and placed it in the new species *Jonkeria pugnax*. Broom (1923) presented a cursory description of *Dinophoneus ingens* with no diagnosis or comparison with *Jonkeria truculenta*. Boonstra (1936) synonymized *Dinophoneus* with *Jonkeria and J. pugnax* with *J. ingens.* Boonstra gave a detailed description of *J. ingens* but he compared this species with gorgonopsians, therocephalians, cynodonts and bauriomorphs but not with *Jonkeria truculenta* and his description was centered more on the braincase. Most of the characters he described were later covered in plaster of Paris. Broom (1932: 27) attempted a comparison of *J. ingens* with *J. truculenta* and *J. vanderbyli* where he pointed out that "the parietals in *Jonkeria ingens* are much wider than in *J. truculenta* or *J. vanderbyli* and though the postorbitals are large they do not meet the squamosals". Boonstra (1936: 111) mentioned that "in palatal view the essential structural details in *J. vanderbyli* are as described for *J. ingens* but differing in detailed proportions such as the quadrate rami of the pterygoids being not so divergent in posterior direction, slender vomers, the median pterygoid keel posterior to the interpterygoid vacuity being much deeper and the bassioccipital being situated relatively farther posteriorly in *J. vanderbyli*".

Remarks. Contra Broom (1932), the parietals are of similar size in the holotypes of *J. ingens* and *J. vanderbyli* (83mm) and both wider than those of *J. truculenta* (juvenile skull). The postorbitals in the holotype of *J. ingens,* as in all *Jonkeria* specimens, do not meet the squamosals. The divergence of the quadrate rami of the pterygoids are interpreted here as taphonomic distortion and/or a consequence of ontogenetic development. The greatest width of the skull at the level of squamosals shows positive allometry (Table 3.1; Fig. 3.19) hence larger skulls will show more divergent quadrate rami of pterygoids than smaller skulls.

***Jonkeria haughtoni* Broom 1929 (Fig. 3.5)**



Fig. 3. 5. Lateral view of *Jonkeria haughtoni* holotype (SAM-PK- 4343).

The skull is dorsoventrally crushed. Scale bar represents 10cm.

Previous diagnosis for Jonkeria haughtoni. According to Broom (1929: 31) in *Jonkeria haughtoni* (Fig. 3. 5) "vomers form a marked median ridge on their posterior two-thirds and the pterygoids project much less downwards than in other species of *Jonkeria*"

Remarks. This species was the first described which has a better preserved skull with an associated humerus (SAM-PK- 4343), hence its importance. There are no diagnostic features of the skull to separate it from the other *Jonkeria* species except for "pterygoids which project much less downwards than in other *Jonkeria* specimens" (Broom, 1929: 31). It is apparent that the downward projection of pterygoids is not a diagnostic character for this specimen (SAM-PK-4343 holotype) and is the result of dorso-ventral deformation of this skull.

***Jonkeria boonstrai* Janensch 1959 (Fig.3.6)**

Previous diagnosis for Jonkeria boonstrai. According to Janensch (1959) for the *Jonkeria boonstrai* skull (Fig. 3. 6) the ratio of the occiput height to the total skull length is approximately

57% compared to 50% for *J. truculenta, J. vanderbyli* and *J. haughtoni*, and a bit more for *J. ingens*.



Fig. 3. 6. Lateral view of the skull of *Jonkeria boonstrai* holotype (MB. R.983). The skull is distorted with two thirds of the ventral surface and teeth missing (plaster of Paris reconstruction). Scale bar represents 10cm.

The difference in the ratio of the width of the snout to the total skull length is about 41% for the *J. boonstrai* while it is only 30% in the other species of *Jonkeria* and the angled outline of the *J. boonstrai* holotype skull not seen in other species of *Jonkeria* and a very steep mandibular mentum (Janensch, 1959).

Remarks. MB.R. 983 suffered lateral compression in the posterior region (Fig. 3.6) resulting in a higher occiput to total skull length ratio. The ratio of the snout width to the total skull length is also higher for MB.R.983 compared with other *Jonkeria* specimens. This specimen suffered both lateral and anteroposterior compression and this, together with ontogenetic factors (positive allometry for snout width versus total skull length (Table 3.1; Fig. 3.18), is responsible for the difference between specimen MB.R.983 from other *Jonkeria* specimens. It is noteworthy that the

symphysis of the mandible of MB.R.983 is more inclined (with the mentum slope almost 60°) compared to that of other *Jonkeria* mandibles where the mentum slope is almost 30° (Fig. 3.23). This is interpreted as a result of antero-posterior compression of the lower jaw.

3.3 Cranial description of *Titanosuchus ferox*

The medial side of the left maxilla of the *Titanosuchus ferox* holotype (NHMUK 49370) (Fig. 3.7.a) shows the trace of the socket of the canine, with part of the base or root of that canine tooth and of its pulp-cavity. The first postcanine seems to have been implanted close to the canine. The bases of three of the postcanines, are visible in what remains of their sockets, and a section along the rest of the alveolar border (Fig.3.7.b) shows eight additional postcanine teeth of similar size and shape, making a total of 11?.

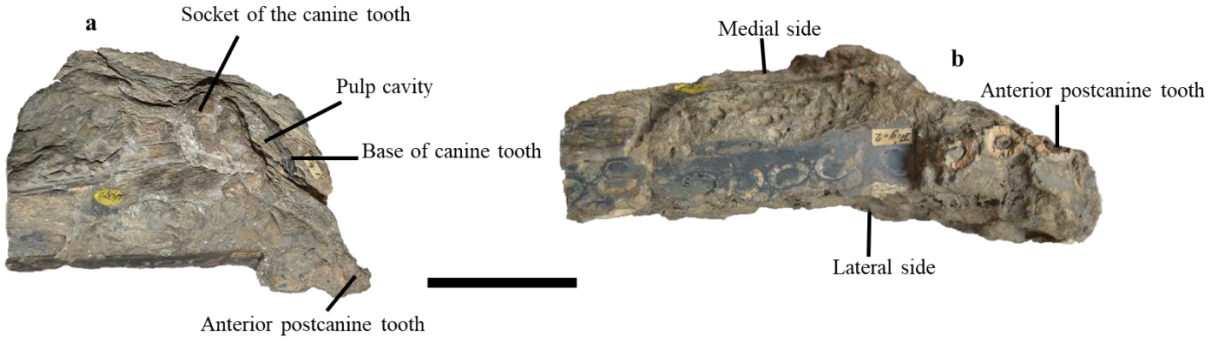

Fig.3.7. Holotype of *Titanosuchus ferox* (NHMUK 49370) **a.** Medial view and **b**. Longitudinal section of the alveolar border and implanted roots of the postcanine teeth of a portion of the left maxilla of the. Scale is 10cm.

Anteriorly the mandible fragment is a fairly massive bone to support the powerful incisors and canine (Fig. 3.8) and has a large sloping mentum. The anterior lower postcanines are positioned medial to the canine while the posterior ones are almost in line with the canine (Fig. 3.8.a). No

crowns are preserved; in cross section, i2 and i3 are ellipsoid while i4 is circular with no diastema between it and the canine (Fig. 3.8.a).

The dentary bears a single canine, which has a long and thick root causing the dentary to bulge laterally and medially. The canine cross section is antero-posteriorly longer than laterally wide. The maxilla and dentary have been filed down by previous researchers and present cross sections of 11 postcanines (Fig. 3.8. a, c). The roots of the anterior four postcanines are elliptical, with an anteroposterior long axis, the posterior roots are almost circular. On the dentary, all the postcanine teeth are situated close to the medial border of the jaw, leaving a ledge lateral to the teeth (Fig. 3.8.a). On the maxilla, the postcanine teeth are situated on the lateral border.

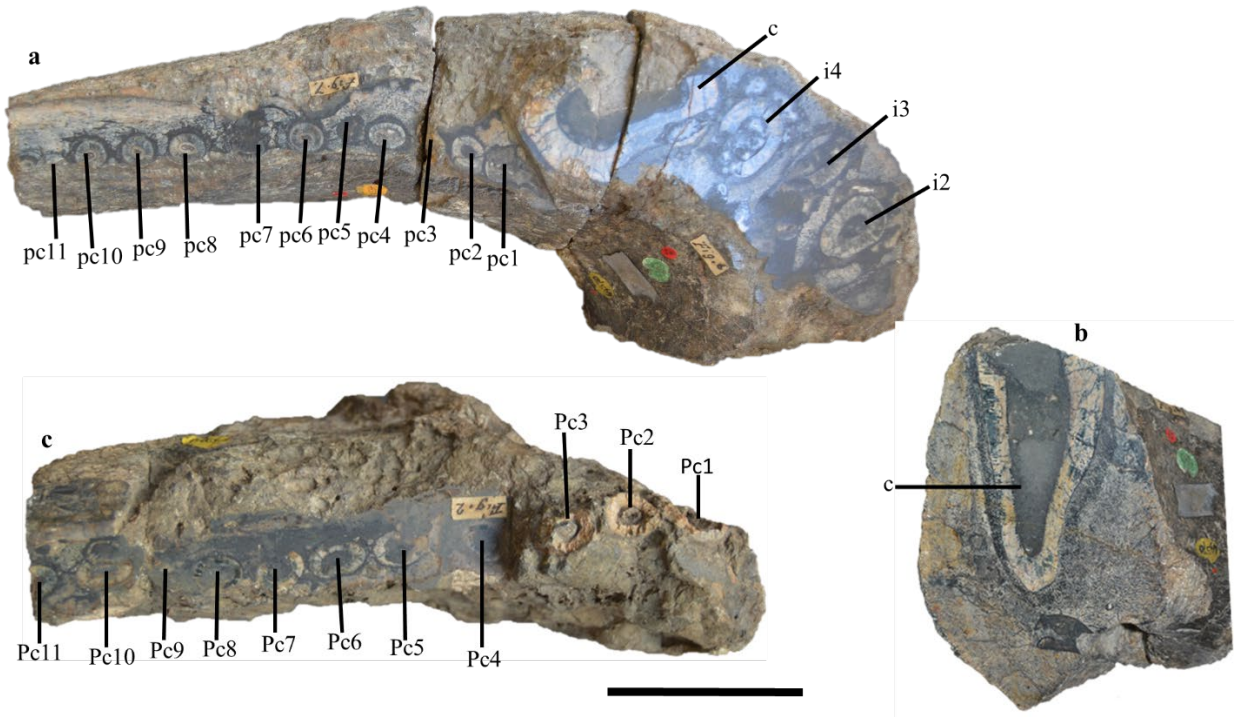

Fig. 3.8. *Titanosuchus ferox* holotype (NHMUK 49370) **a.** left dentary, **b.** vertical section of the implanted root of the dentary canine (c). and **c.** left maxilla showing the cross-section of post-canine teeth. Scale bar represents 5cm.

The first postcanine of both the maxilla and dentary is the largest and the rest of the postcanines decrease posteriorly.

3.4 Description of the cranial morphology of *Jonkeria*

Van Hoepen (1916 b) provided a preliminary description of the skull of the holotype but did not figure or give a diagnosis for the genus. Broom (1929) gave a full description of the specimen with figures accompanying his description (Fig. 3.9).

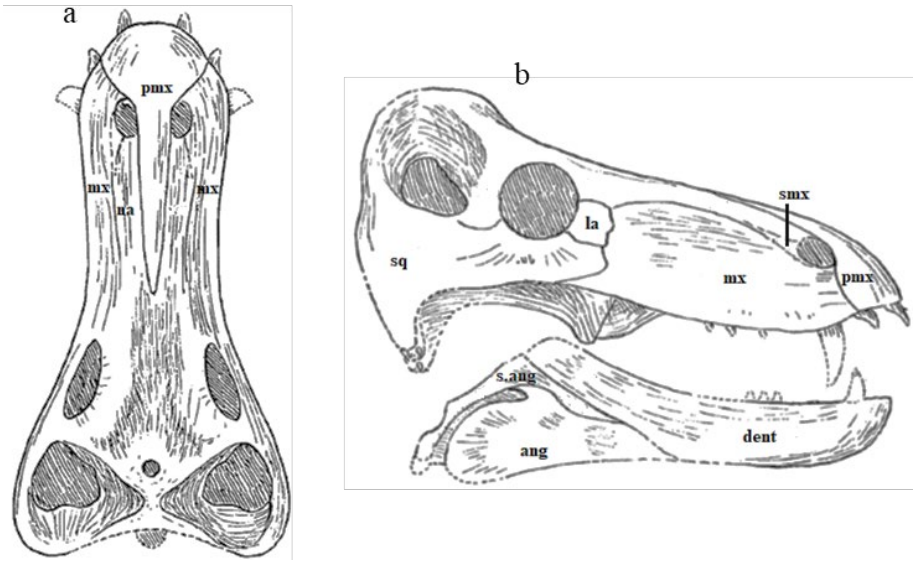

Fig. 3.9. Illustrations of the dorsal (a) and lateral (b) views of *Jonkeria truculenta* holotype (TM 212) taken from Broom (1929: pages 12-13: Fig.1 & Fig. 2). Broom managed to trace only a few sutures owing to the similarity between bone and matrix. **ang**, angular; **la**, lacrimal; **mx**, maxilla; **na**, nasal; **pmx**, premaxilla; **s.ang**, surangualr; **smx**, septomaxilla; **sq**, squamosal. The illustrations are 1/6 of the natural size.

Boonstra (1969) and King (1988) recognized the following *Jonkeria* species (*J. truculenta*, *J. ingens*, *J. vanderbyli*, *J. haughtoni*, *J. boonstrai*, *J. parva*, *J. rossouwi and J. koupensis*) the first

five are represented by cranial material. This Chapter seeks to show the similarity of these five cranially recognized *Jonkeria* species hence the decision to symonymize all of them with *Jonkeria truculenta*. The following section provides a full cranial description of *Jonkeria* based on all available material in museum collections.

Jonkeria specimens have large skulls with a length ranging from 500 – 680mm; a long and narrow snout (length on average about 60% of total skull length); skull broadens considerably behind the orbit. No pronounced thickening of the dorsal and hind rim of the orbit, and the nares are situated far anteriorly and laterally. The most conspicuous feature is the swelling around the pineal foramen formed by pachyostosis of the parietal. This thickened parietal mound is pierced by a prominent circular pineal foramen, situated on a chimney. The intertemporal width is slightly wider than the interorbital width, but at the level of the pineal foramen because the parietal is raised and is laterally bayed, it appears narrower. The temporal opening is relatively large, and its anteroposterior diameter is not reduced to a transverse slit as in the tapinocephalids. The lateral surface of the snout has a moderate concavity between the orbit and posterior margin of the septomaxilla. In lateral view, the jaw articulation is positioned far anteriorly, almost ventral to the postorbital bar.

Boonstra (1936) provided a comprehensive description of the cranial morphology of some *Jonkeria* skulls and lower jaws curated at the American Museum of Natural History emphasizing the differences between them. Here the first detailed cranial description of *Jonkeria* is presented, based on all available material ascribed to *Jonkeria*.

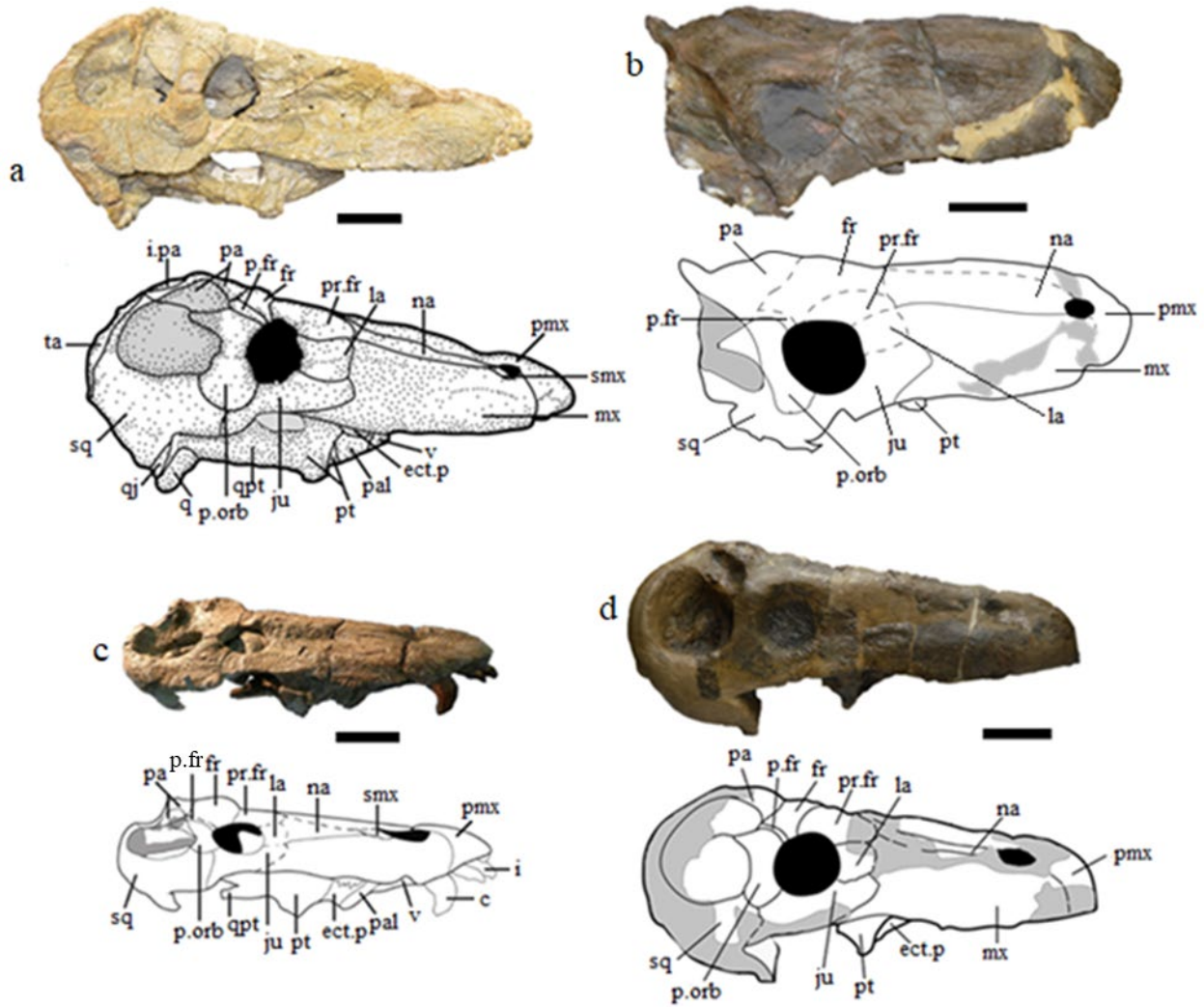

Fig.3.10. Lateral view of *Jonkeria truculenta* skulls. **a.** SAM-PK-11884; **b.** TM212; **c.** SAM-PK-4343; **d.** AMNH 5620. TM212 is the left side flipped for comparison. Scale bars represent 10cm.

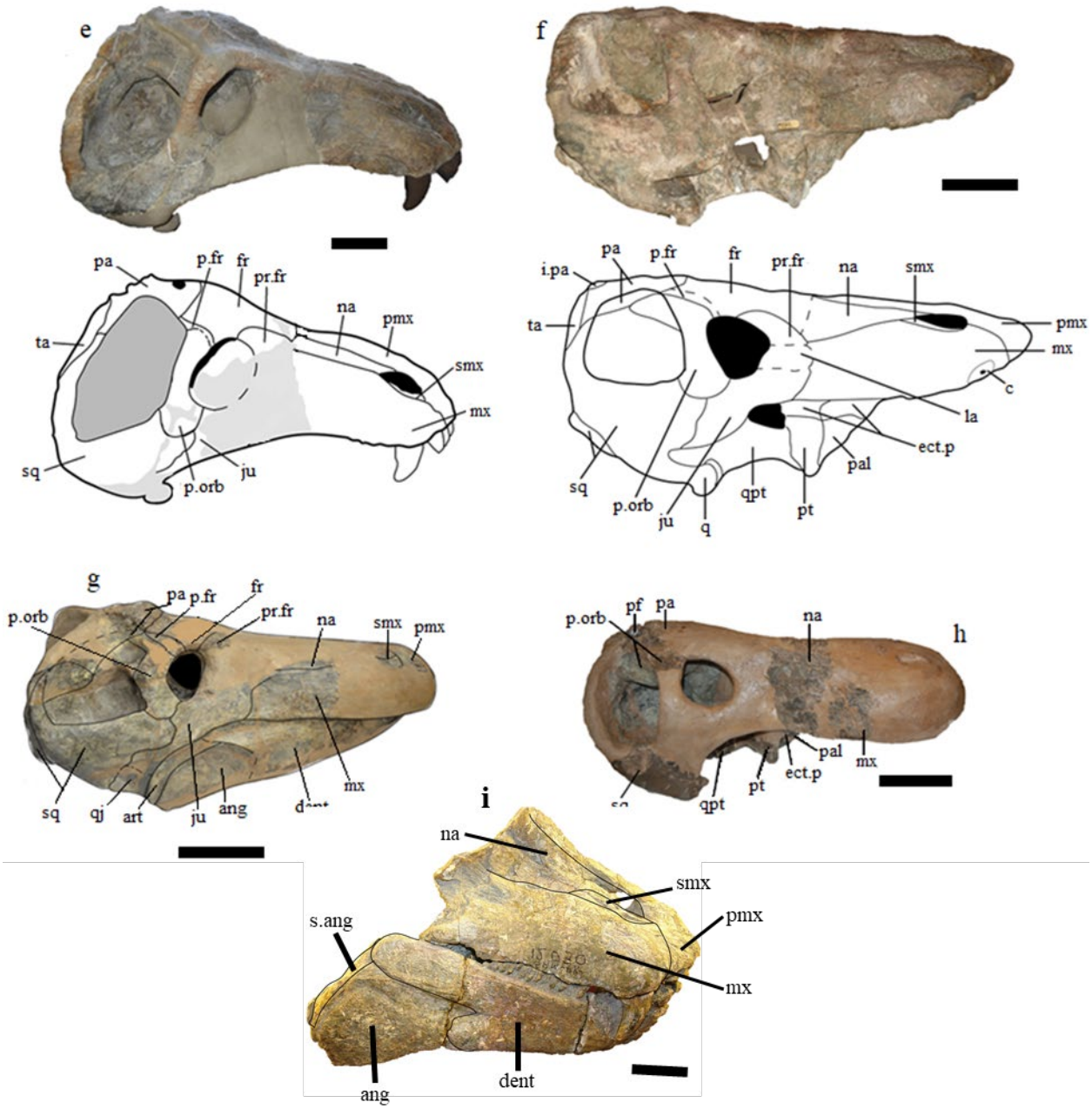

Fig.3.10. continued. Lateral view of *Jonkeria truculenta* skulls **e.** MB.R.983; **f.** FMNHUC 1511; **g.** AMNH 5608; **h.** AMNH 5634; **i.** SAM-PK-12030. Skulls in parts e, h and I are flipped for comparison Scale bars represent 10cm.

3.4.1 Skull roof

The following description is based largely on specimen SAM-PK-11884, referred specimen of *Jonkeria vanderbyli*, as it is the best-preserved and one of very few complete *Jonkeria* skulls, but additional information is included from other specimens. As the right lateral side of this specimen is better preserved than the left, the right lateral view will be preferentially used in this description.

Jonkeria skulls have an almost horizontal dorsal profile, the parietal being the highest point of the skull. The best-preserved skulls are illustrated with annotated photographs or line drawings and the figures of SAM-PK-11884 (the best-preserved skull) are shaded.

3.4.1.1 *Premaxilla*

The premaxilla is a fairly large bone located at the anterior tip of the snout, with a midline sutural contact with its contralateral element, forming part of the anterior and dorsal margin of the external naris (Fig. 3 .10; Fig. 3.11). In dorsal view, the anterior part of the roughly triangular premaxilla makes up a large portion of the snout anterior to the external nares, from this anterior portion a long and broad inter-nasal process tapers posteriorly to form a pointed posterior contact with the frontals and is flanked by the nasals on either side (Fig. 3.11).

Laterally, the anterior end of the premaxilla is larger than visually apparent as it is overlapped by the maxilla (Broom, 1929). In specimens SAM-PK-11884, SAM-PK-4343 and FMNHUC 1511 (Fig. 3.10.a, c, f) the premaxilla is less abruptly downturned anteriorly unlike the condition in specimens TM 212, AMNH 5620 and MB.R.983 (Fig. 3.10.b, d, e).

In ventral view, the premaxilla has an oblique sutural contact with the maxilla laterally and meets the vomer postero-medially where the anterior bifurcated end of the paired vomers forms a V shaped contact (Fig. 3.12). The premaxilla bears five incisor teeth. Ventrally, the premaxilla overlies the antero-medial surface of the maxilla and extends posteriorly beyond the canine teeth but does not contact the palatine. However, the morphology is slightly different in SAM-PK- 4343, where the premaxilla sutures with the palatine and extends into the trough formed at the palatine-vomer junction thereby forming the lateral border of the internal naris to the exclusion of the maxilla (Fig. 3.12.c).

3.4.1.2 *Septomaxilla*

Facial expression of the septomaxilla is relatively small and triangular where it produces a tapering posterior projection on the skull roof behind the external naris. For some specimens this bone extends ventrally to the anterior rim of the external naris (Fig. 3.10.c, e, f, i) while for specimen SAM-PK- 11884 (Fig. 3.10a) the septomaxilla is close to the posterior rim of the external naris. SAM-PK-12030 presents a well-preserved septomaxilla, which extends into, and forms the floor of, the external naris (Fig. 3.10.i).

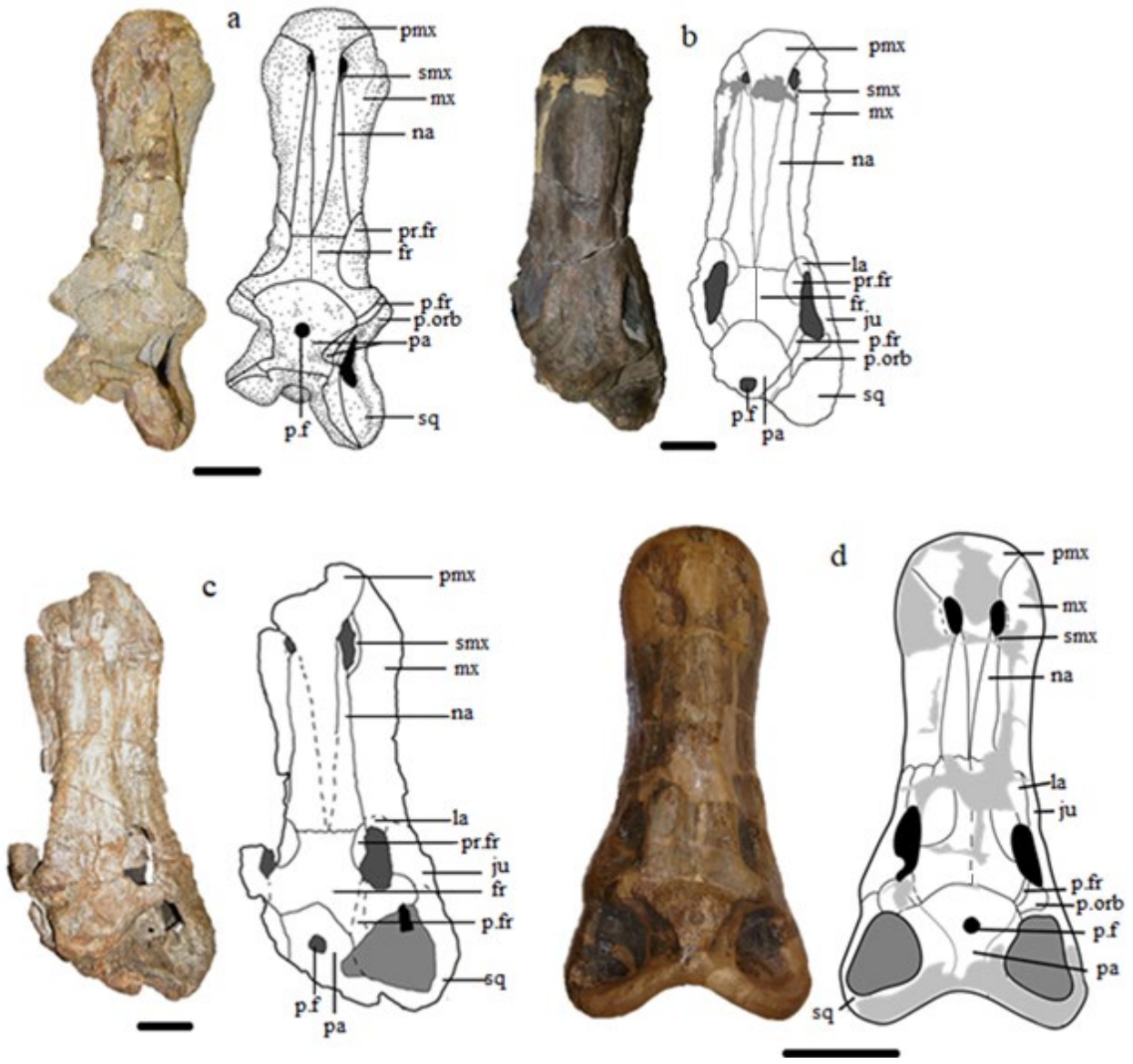

Fig. 3.11..Dorsal view of *Jonkeria truculenta* skulls. **a.** SAM-PK-11884; **b.** TM 212; **c.** SAM-PK-4343; **d.** AMNH 5620. Scale bars represent 10cm.

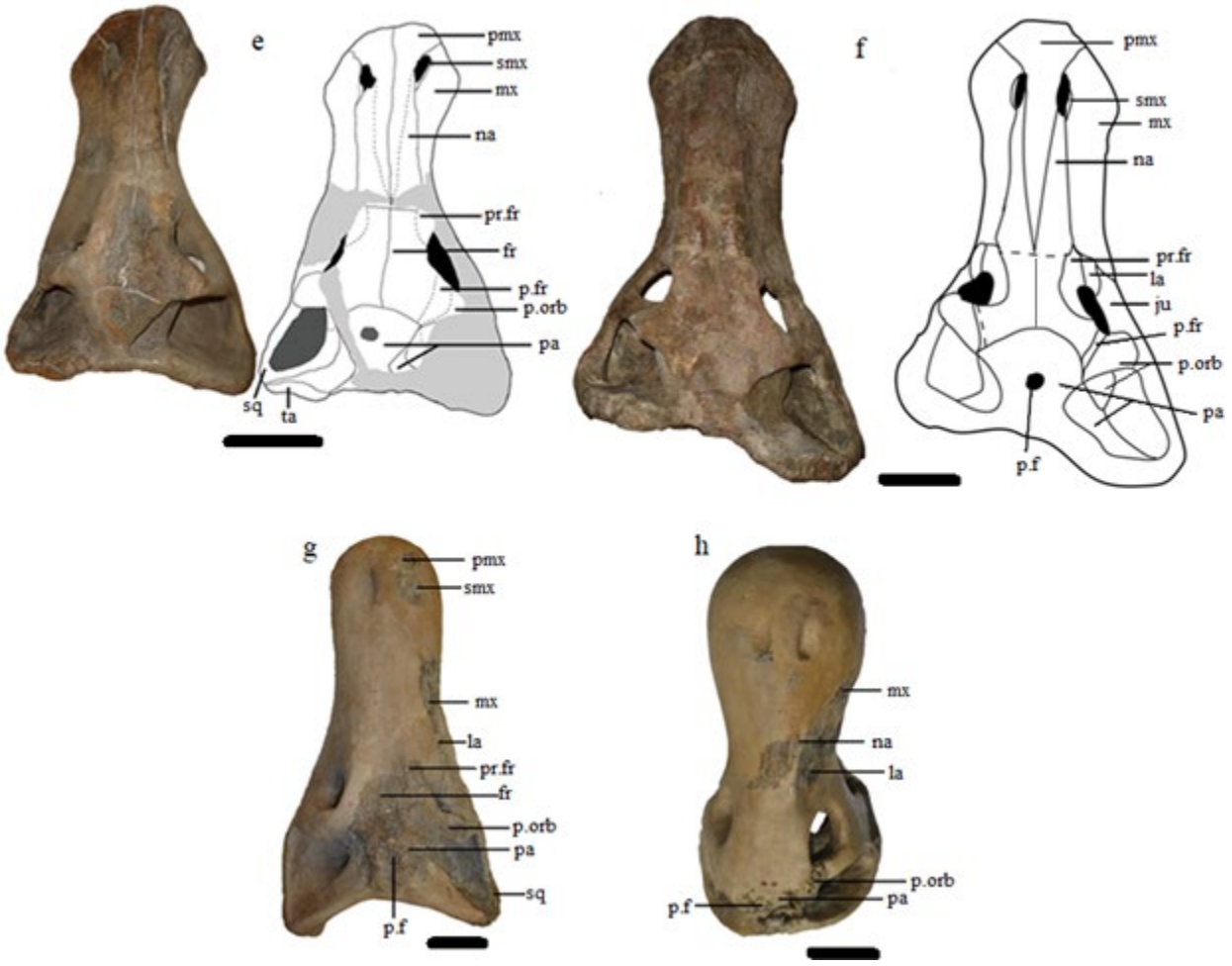

Fig. 3.11. continued. e. MB.R.983; **f.** FMNHUC1511; **g.** AMNH 5608; **h.** AMNH 5634. Scale bars represent 10cm.

3.4.1.3 *Maxilla*

In lateral view, the maxilla is a long and rather flat bone, which covers most of the lateral side of the snout. It bears a single canine anteriorly and behind this canine are small postcanines varying in number (19 – 21) according to the size of the skulls. Smaller skulls have a lesser number of postcanines than larger skulls. The maxilla (in lateral view) is a vertically oriented bone with an oblique to slightly crescent shaped sutural contact with the premaxilla anteriorly, anterior to the

external naris. Below and slightly posterior to the external naris it contacts the septomaxilla and posterior to the septomaxilla has a long horizontal dorsal sutural contact with the nasals (Fig. 3.10. a, b, c, d, e, g). For specimen FMNHUC 1511 this dorsal maxilla/nasal suture is slightly oblique posteriorly (Fig. 3.10.f). Posteriorly the maxilla is in sutural contact with the prefrontal, lacrimal and jugal where it has an almost vertical contact with the lacrimal and a posterior oblique sutural contact with the jugal. There is a notable lateral expansion in the anterior portion of the maxilla to accommodate the root of the large canine. The right maxilla of SAM-PK-11884 (Fig. 3.10.a, 3.11.a) is well preserved compared to the weathered left side, but appears to be slightly displaced dorsally and in an unnatural position when compared with the left. In this skull, a postero-ventral spur of the maxilla extends along the ventral border of the skull of SAM-PK-11884 up to a point halfway along the orbit, a condition also found in AMNH 5620 (Fig. 3.10.a, d). However, in TM 212 and AMNH 5608, this posterior extension of the maxilla ends anterior to the orbit (Fig. 3.10.b, g).

In ventral view, the maxilla has a curved anteromedial sutural contact with the premaxilla and is ventrally overlain by the palatine posteriorly (Fig. 3.12. a- d). On the medial side it contacts the lateral margin of the vomers (Fig. 3.12. a, b, d, e) and for specimen SAM-PK- 4343 the maxilla does not make any contact with the vomers (Fig. 3.12.c) The anterior maxilla-palatine contact is posterior to the canine and almost in line with the second postcanine (Fig. 3.12.a) and for specimen SAM-PK-4343 this contact is at the level of the first postcanine (Fig. 3.12.c).

3.4.1.4 *Nasals*

These are long, narrow, and anteriorly tapering bones positioned between the posterior end of the external nares and the frontal. For their entire length, the inter-nasal processes of the premaxillae is medially positioned making the nasals look as if they are separated. Anteriorly and laterally, the nasal has sutural contact with the maxilla, a short postero-ventral contact with the prefrontal, and transverse posterior contact with the frontal (Fig. 3.10, 3.11)

3.4.1.5 *Lacrimal*

The lacrimal is a relatively small quadrangular bone in lateral view, forming the anterior margin of the orbit (Fig. 3.10.a, b, c, d, f). It contacts the jugal ventrally, the maxilla anteriorly, and the prefrontal dorsally. The lacrimal has an almost horizontal ventral contact with the jugal and a horizontal to slightly oblique contact with the prefrontal, which occurs along a small ridge. The lacrimal has a slightly vertical anterior contact with the maxilla and forms the ant-orbital depression in lateral view (Fig. 3.10a, b, c, d, f).

3.4.1.6 *Jugal*

This is a large bone, which forms most of the suborbital arch, part of the temporal arch, and a considerable part of the pre-orbital portion of the face (Fig.3.10a). The jugal makes up the entire ventral border of the orbit and extends anteriorly as far as the anterior end of the lacrimal to form an anterior and antero-ventral contact with the maxilla. Posteriorly, it forms a curved suture with the ventral part of the postorbital bar. The posterior extension of the jugal and its contact with the squamosal is preserved only in SAM-PK- 4343, SAM- PK- 11884 and FMNHUC 1511 (Fig. 3.10.a, f). In these three specimens, the anterior projection of the squamosal forms a notch where

the posterior end of the jugal and the quadratojugal meet. This notch is lost in all the other specimens. For specimen SAM-PK- 11884, the ventral part of the jugal is weathered more so in the posterior end (Fig. 3.10a) such that the jugal and qudratojugal appear as if they separated.

3.4.1.7 *Prefrontal*

The ovoid prefrontal, which is slightly pachyostosed on the dorsal surface, has both dorsal and lateral exposure on the skull roof (Fig.3.10, 3.11). It is a prominent bone, twice as long as it is wide, forming the anterior and dorsal borders of the orbit, articulating with the maxilla anteriorly, lacrimal ventrally, and the nasal antero-medially and frontal on the medial side.

3.4.1.8 *Frontal*

This paired bone comprises most of the interorbital region on the dorsal surface of the skull and is relatively short and broad. On its dorsal surface, the frontal is flat anteriorly but bends upwards posteriorly to articulate with the elevated parietal (Fig. 3.10. a-f, 3.11. a-g). Anteriorly the frontal has a straight, transverse suture with the nasals and antero-laterally a curved suture with the prefrontal. Between the prefrontal and postfrontal, it forms a small part of the supraorbital border and postero-laterally has a short and almost straight suture with the postfrontal. Postero-laterally, it forms a small part of the anteromedial border of the temporal fenestra (Fig. 3.11.a-f) and has a slightly curved sutural contact posteriorly with the parietal. There is no visible pachyostosis on the dorsal surface of the frontals except a slight thickening at its contact with the postfrontal as well as at its contribution to the dorsal orbital rim. There is a dorsal ridge that runs on the frontal midline from the frontal-parietal suture and terminates almost in line with the anterior border of

the orbits. This is more prominent on TM 212 and MB.R.983 (Fig. 3.11. b, e) and to a lesser extent on AMNH 5620 (Fig. 3.11.d).

3.4.1.9 *Postfrontal*

The postfrontal is a small almost rectangular bone in dorsal view and is positioned between the frontal and the postorbital where it forms the dorsal part of the postorbital bar and has a small contribution to the postero-dorsal orbital border, and the antero-dorsal border of the temporal opening (Fig. 3.10. a-g, 3.11. a-f).

3.4.1.10 *Postorbital*

This is a large bone, which forms the anterior border of the postorbital bar. It forms the anterior border of the temporal fenestra and the posterior border of the orbit. Dorsally it meets the postfrontal and postero-medially, it has a long sutural contact with the parietal, and also meets the squamosal above the temporal fenestra. Its ventral margin contacts the jugal antero-ventrally (Fig. 3.10. a-g) and postero-ventrally has an extensive rounded contact with the squamosal. In the middle of the orbit, this bone is 34mm wide for the smallest specimen TM 212 and 42mm in the larger AMNH 5620 skull.

3.4.1.11 *Parietal*

This bone is laterally bayed but because it is pachyostosed, the midline suture is not visible. Posteriorly it forms a high and fairly narrow “parietal crest” (Fig. 3.11. a-f). The anterior end of the parietal forms a transverse sutural contact with the frontal and laterally it is in contact with both the postorbital and the squamosal within the temporal fenestra. Posteriorly it contacts both

the interparietal and tabular bones. A circular pineal foramen is located central or slightly on the posterior surface of the parietal (Fig. 3.11).

3.4.1.12 *Squamosal*

The squamosal is a large element forming the subtemporal and most of the posttemporal bars and making up the entire ventral and posterior borders of the temporal fenestra. At the posterior end of the temporal fenestra, the squamosal is a very large bone with an ascending, a descending, and an anterior process, which forms much of the sub-temporal arch. The ascending process of the squamosal forms the back of the temporal fenestra and sutures with the parietal dorsally and the tabular posteriorly. The descending process passes ventrally and turns slightly forwards as the anterior process, which meets the jugal antero-ventrally (Fig. 3.10). Anterodorsally, the squamosal has sutural contact with the postorbital. The squamosal is in contact with the quadratojugal on the ventrolateral side of the external auditory meatus and on the ventral side, it contacts the ascending quadrate ramus of the pterygoid. The squamosal forms the lateral side of the occiput where is in contact with the tabular, supraoccipital and paroccipital process of the opisthotic.

3.4.1.13 *Quadratojugal*

The quadratojugal (Fig. 3.10) is a relatively small wedge-shaped bone, which is partially obscured from lateral view by the squamosal. This small bone is situated on the postero-ventral corner of the zygoma, having a laterally exposed portion positioned under the postero-ventral portion of the squamosal while medially it contacts the lateral condyle of the quadrate.

3.4.1.14 *Quadrate*

This is a fairly large bone extending dorsally on the anterior side of the squamosal (Fig.3.10) and comprises a flattened dorsal process and two large ventral condyles with a sulcus between them. The medial condyle contacts the posterior end of the quadrate ramus of the pterygoid. The anterior facing surface of the dorsal process of the quadrate is smooth and featureless and is positioned anterior to the ventral process of the squamosal. A stapedial groove is situated between the dorsal process and the medial condyle of the quadrate to receive the distal end of the stapes.

3.4.2 Palate

The palate comprises the vomer, palatine, ectopterygoid, pterygoid (anterior, transverse and posterior processes), as well as the palatal sections of the premaxilla and maxilla. The titanosuchid palate forms an internal, flat, horizontally oriented shelf anteriorly and extends ventrally toward the posterior end from the posterior third of the vomers until the pterygoid process. This palatal description is based on SAM-PK- 11884, unless otherwise stated.

3.4.2.1 *Vomer*

The paired vomer comprises flat elongate strap like bones extending as stout rods nearly two-thirds of the length of the ventral side of the skull. The vomers have a shallow midline trough. In well-preserved specimens, the anterior end of the paired vomers is bifurcated (Fig. 3.12.a-e). Posteriorly, the vomers are slightly ventrally elevated where they meet the pterygoids and

posterolaterally they are overlain by the palatines. They form the medial border of the elongated internal naris.

3.5.2.2 *Palatine*

The palatine (Fig.3.12) is a complex bone with a broad posterior portion with sutural contacts with the vomers medially, the ectopterygoid laterally, and the pterygoids posteriorly and postero-laterally.

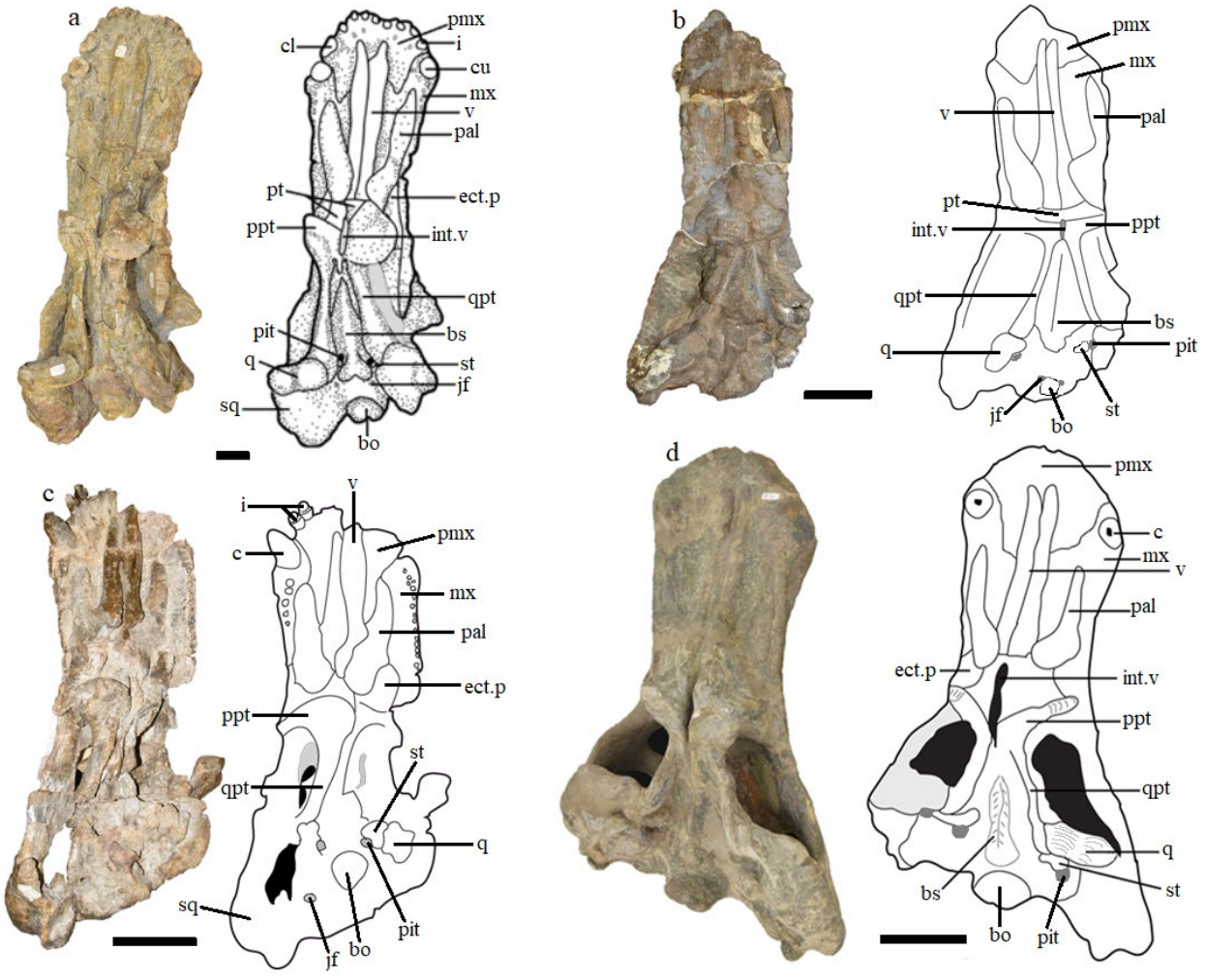

Fig. 3.12. Ventral view of *Jonkeria truculenta* skulls. **a.** SAM-PK-11884; **b.** TM212; **c.** SAM-PK- 4343; **d.** FMNHUC 1511. Scale bars represent 10cm. **e.** MB.R.983; **f.** AMNH 5634; g. AMNH 5608; **h.** AMNH 5620.

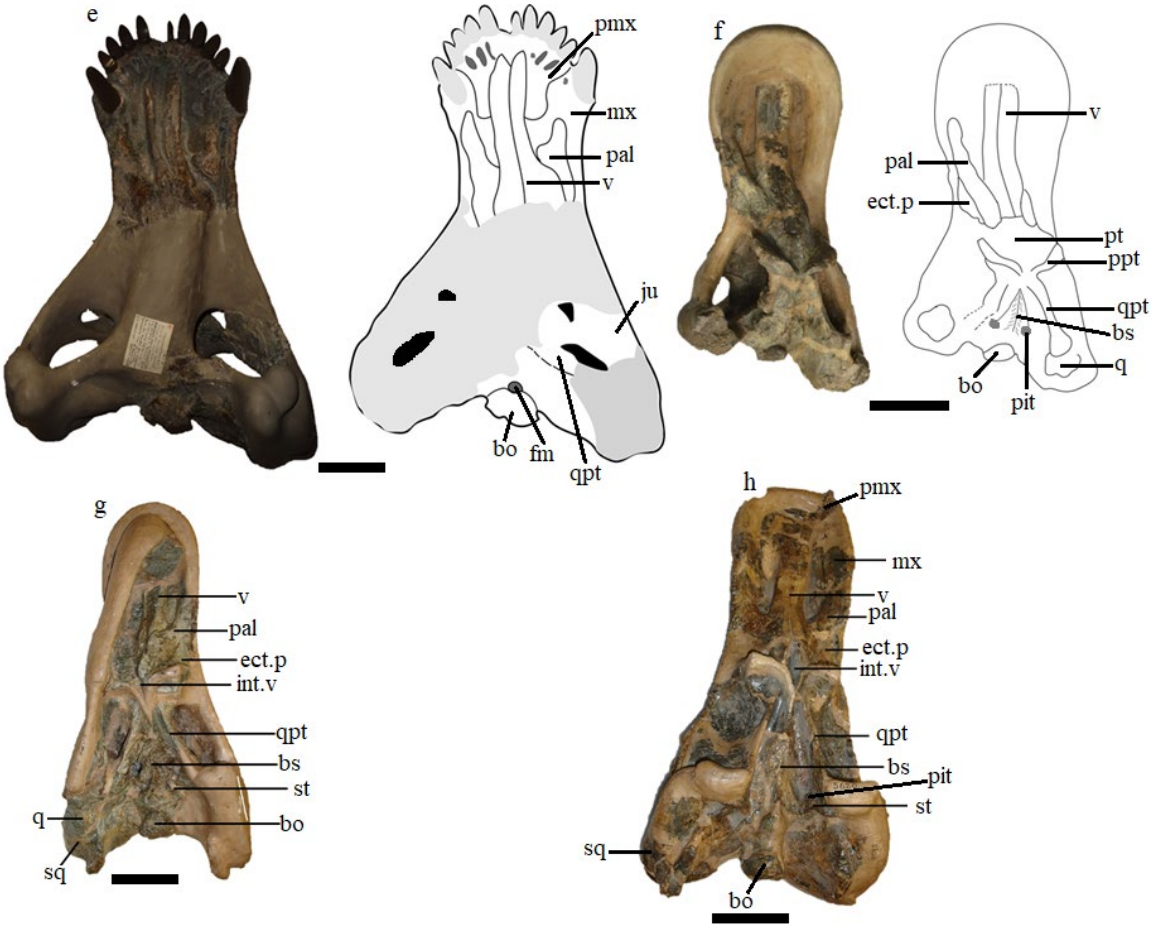

Fig. 3.12. continued. Ventral view of *Jonkeria truculenta* skulls **e.** MB.R.983; **f.** AMNH 5634; g. AMNH 5608; **h.** AMNH 5620. Scale bars represent 10cm.

The anterolateral process extends anteriorly almost as far as the canine tooth, forming most of the posterior and lateral borders of the internal nares. There are no palatine bosses in *Jonkeria* but the palatines are ventrally elevated at their point of contact with the vomers.

3.5.2.3 *Ectopterygoid*

The ectopterygoid is a small triangular bone positioned between the palatine anteriorly, the jugal posterolaterally and the lateral process of the pterygoid on the posterior side it descends halfway down the anterior face of the lateral pterygoid ramus and abuts against the posterior end of the maxilla. Just like the palatines, the ectopterygoid is also exposed in lateral view in some specimens (Fig. 3.10. a, c, f, h) and is morphologically similar in all the specimens where it is preserved (Fig. 3.12. a, c, d, f, g, h).

3.5.2.4 *Pterygoid*

The pterygoid is one of the largest bones of the palate and accounts for about a third of the length of the palate. This bone comprises three rami namely the anterior, transverse and posterior. The anterior ramus is a very short anteromedial projection, which has a curved sutural contact with the palatine and a transverse sutural contact with the vomers. The transverse ramus comprises the prominent lateral flange of the pterygoid, which is weathered in all the specimens. Its ventral surface is a broad rugose ridge, which narrows as it curves postero-medially toward the interpterygoid vacuity. The slit shaped interpterygoid vacuity extends posteriorly from behind the level of vomer-pterygoid contact to the posterior side of the lateral flanges of the pterygoid (Fig. 3.12). The posterior ramus of the pterygoid extends postero-medially to meet the basisphenoid and postero-laterally to contact the medial condyle of the quadrate as the quadrate ramus of the pterygoid (Fig. 3.12. a, c, d, f, g, h). The quadrate ramus of the pterygoid sweeps backwards as a thin sheet of bone in ventral view but is quite broad in lateral view (Fig.3.12. a, b, c, d, f, g, h).

3.4.3 Occiput and Basicranium

The occiput is best preserved in FMNHUC 1511, and is also preserved, though weathered, in AMNH 5620, SAM-PK-4343, SAM-PK-11884 and TM212. In occipital view, the titanosuchid skull is broadly ovoid and almost vertically oriented with a slight antero-ventral incline.

3.4.3.1 *Interparietal*

The interparietal is positioned dorsally on the occipital plate (Fig. 3.13) and it also enters the dorsal surface of the skull where has a slightly curved sutural contact with parietal. Laterally the inter-parietal contacts the tabular and ventrally it has a long horizontal sutural contact with the supraoccipital. It is wider dorsally where it contacts the parietal and tapers ventrally where it contacts the supraoccipital.

3.4.3.1 *Tabular*

The tabular is a relatively large, semilunate bone with a long ventral projection extending between the squamosal and the supraoccipital (Fig. 3.13) and forming the postero-dorsal margin of the post temporal fenestra (Fig. 3.10. a, e, f). Laterally the tabular has extensive contact with the squamosal, dorso-medially with the inter-parietal where the suture is on a ridge, and ventrally meets the supraoccipital and paraoccipital process of the opisthotic (Fig. 3.10).

3.4.3.2 *Supraoccipital*

This relatively large transversely positioned unpaired bone occupies most of the central part of the occiput. Dorsally it is in sutural contact with the interparietal, laterally with the tabulars and

ventrally it forms the dorsal border of the foramen magnum and is in contact with the exoccipital and the paroccipital process of the opisthotic (Fig. 3.13).

3.4.3.3. *Basioccipital*

This bone forms a large occipital condyle (Fig.3.13), and in ventral view, it contacts the parabasisphenoid anteriorly. The occipital condyle is well preserved and protrudes relatively far posteriorly in specimens FMNHUC 1511, SAM-PK-4343, SAM-PK-11884 and AMNH 5620 (Fig.3.13. a, b, c, e).

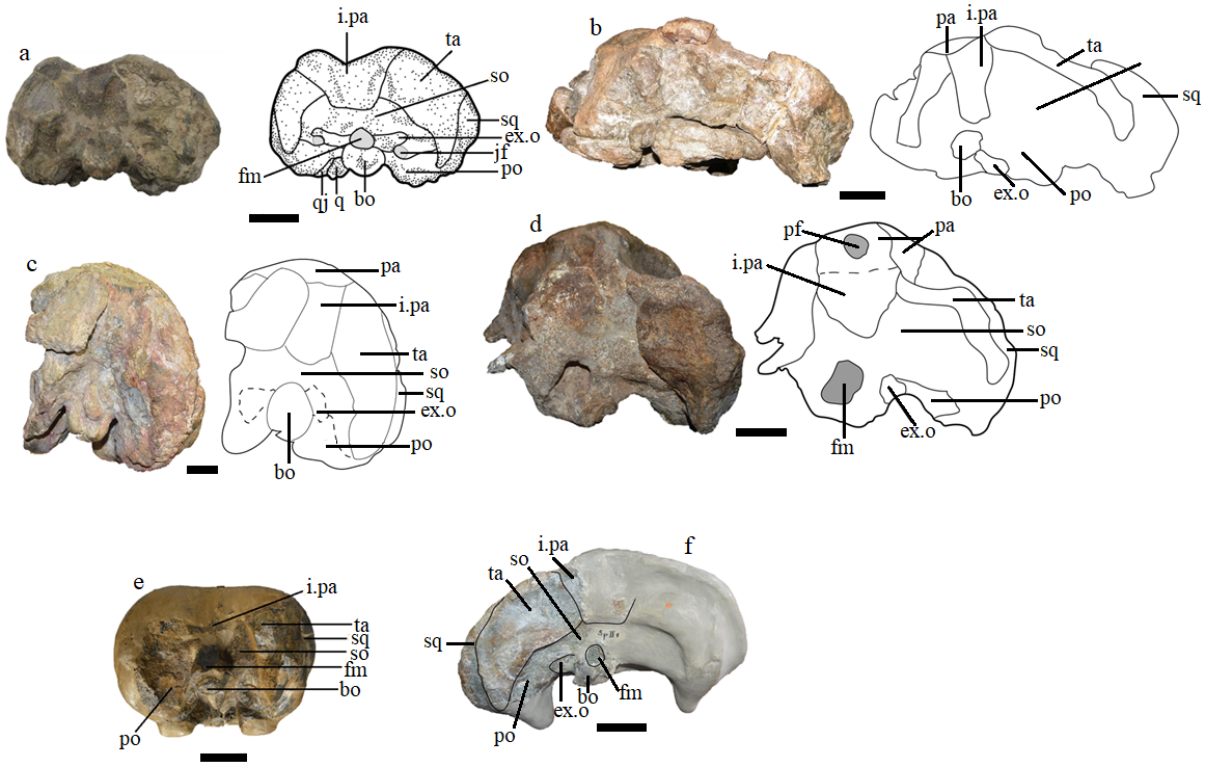

Fig.3.13. Occipital view of *Jonkeria truculenta* skulls. **a.** FMNHUC 1511; **b.** SAM-PK- 4343; **c.** SAM-PK- 11884; **d.** TM 212; **e.** AMNH 5620; **f.** MB.R. 983. Scale bars represent 10cm.

3.4.3.4 *Opisthotic*

This bone makes up a large part of the occiput with the robust paraoccipital process, which is preserved in FMNHUC 1511, SAM-PK-4343, SAM-PK-11884 (Fig. 3.13). In occipital view the paroccipital process is medially narrow where it borders on the ventral side of the jugular foramen (Fig.3.13. a) and expands laterally where it has a sutural contact with the squamosal and ventrally with the dorsal process of the quadrate. Dorsally the opisthotic is in contact with the supraoccipital and the tabular. Ventro-medially, the opisthotic meets the basioccipital.

3.4.3.5 *Exoccipital*

The paired exoccipitals (Fig. 3.13) are small sub-triangular bones positioned lateral to the foramen magnum, overlie the paroccipital process of the opisthotic, and abut against the basioccipital. These bones are situated lateroventrally relative to the foramen magnum (Fig. 3.13. a, c, f) and contact the basioccipital ventromedially and the foramen magnum ventrolaterally.

3.4.3.6 *Parabasisphenoid*

This is a relatively small triangular bone, which forms a pointed contact anteriorly with the postero-medial portion of the pterygoid and widens posteriorly where it meets the basioccipital. The parabasisphenoid has a low midline ridge, which bifurcates posteriorly (Fig. 3.12). Laterally, towards its posterior end, the parabasisphenoid has two notches, the anterior one is the lateral opening leading into the pituitary fossa and the posterior one is the large fenestra ovalis. Posteriorly, the parabasisphenoid and basioccipital are indistinguishably fused.

3.4.3.7 *Stapes*

In AMNH 5620, SAM-PK- 11884 and FMNHUC 1511 the stapes is preserved in situ and in SAM-PK- 4343 the left stapes is preserved out of position, oriented antero-posteriorly instead of medio-laterally (Fig. 3.12). The stapes is a rod like structure with expanded ends. It extends medially from the medial face of the quadrate, immediately posterior to the quadrate ramus of the pterygoid, to the fenestra ovalis. The rounded proximal end is positioned in the fenestra ovalis and the slender posterodorsal projection lacks a stapedial foramen. The distal end articulates with the medial condyle of the quadrate.

3.4.4 Lower jaw

The lower jaw of *Jonkeria,* as is ancestral for therapsids, comprises the dentary, coronoid, splenial, angular, surangular, prearticular and articular bones. Only seven skulls (AMNH 5608; SAM-PK-11884; SAM-PK-12030; MB.R. 983; TM 212, ROZ. B96 and FMNHUC 1511) have the lower jaw preserved in association and the lower jaw of AMNH 5633 has no accompanying cranial material. The lower jaw of FMNHUC 1511 is well preserved but is mostly covered in matrix while that of MB.R. 983 consists mostly of plaster.

3.4.4.1 *Dentary*

The dentary (Fig.3.14 and 3.15) forms more than half of the lateral side of the jaw, but only about a third of the medial side. Anteriorly the bone is fairly massive to support the four large incisors and canine, and in the symphysial region forms a large posteriorly sloping mentum.

On the lateral surface, the dentary is in contact posteriorly with the angular, and with the sur-angular postero-dorsally by means of an inclined suture extending antero-ventrally from the coronoid eminence (Fig. 3.14). The ventral margin of the dentary, behind the symphysial region, is mostly sub-horizontal but curves postero-dorsally at the contact with the angular and has a posterior facing inverted sigmoid shaped sutural contact with the angular (Fig. 3.14). Posterolateral to the symphysis, the dentary forms a slight convexity, which extends from the canine and extends for about a third of the length of the mandible. A concavity extends from this point up to the coronoid eminence and the anterior portion of the reflected lamina of the angular. The ventral margin of the dentary is straight.

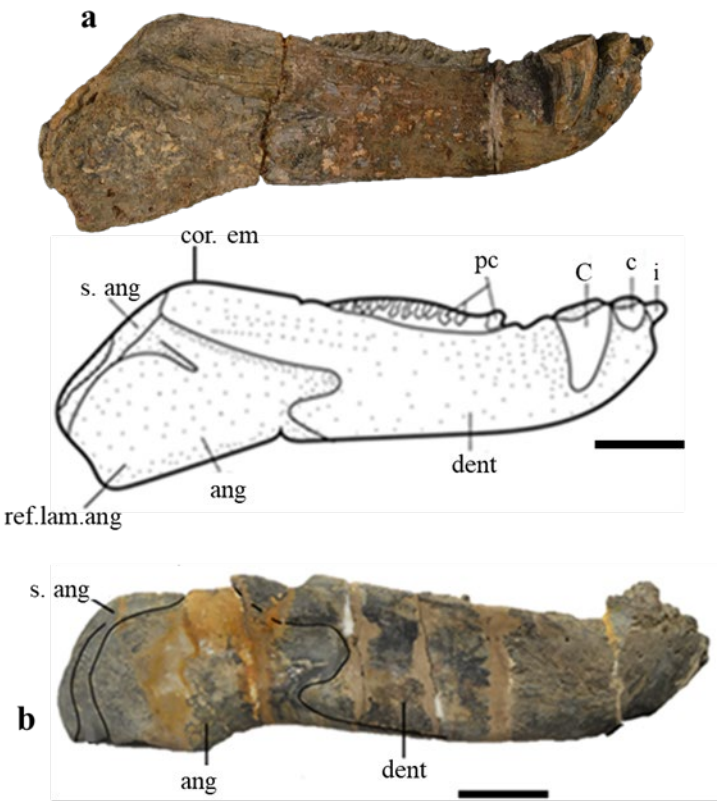

Fig. 3.14. Lateral view of *Jonkeria truculenta* mandibles. **a.** SAM-PK-12030. **b.** AMNH 5633. Scale bars represent 10cm.

In medial view (Fig. 3. 15), the dentary is exposed over a shorter distance than the lateral view and makes up a little more than half of the length of the jaw. It tapers posterodorsally and in this region, it contacts the anterior portion of the surangular. Dorso-medially, the dentary is overlain by the coronoid (Grine, 1997). Anteromedially the dentary widens on either side of the symphysis to form a dorsal shelf and a ventral depression, which accommodates the symphyseal portion of the splenial. On the medial side, the dentary has a long horizontal ventral sutural contact with the splenial and is overlain by the pre-articular postero-medially.

3.4.4.2 *Surangular*

The surangular is a relatively large bone forming the posterodorsal part of the mandible in lateral view (Fig. 3.14). It has contact with the dentary, coronoid, prearticular and angular. In lateral view, the surangular forms a laterally projecting ridge on the dorsolateral face of the mandible that separates this bone from the angular. In medial view, the surangular forms the posterior end of the lower jaw from the coronoid eminence to the posterior end of the jaw positioned on the dorsal side of the prearticular. Here it is in contact with the posterior portion of the prearticular anteroventrally and meets the articular posteroventrally (Fig. 3.15). On the medial side, the anterodorsal surface of the surangular forms a slight trough, which accommodates the posterior end of the coronoid (Fig.3.15).

3.4.4.3 *Prearticular*

The prearticular, which extends more than half the length of the mandible, is exposed only on the medial side of the jaw and has an open inverted “V” shape (Fig.3.15). It is triangular and higher in the middle region and ventrally directed in both the anterior and posterior directions. It is in

contact with the dentary anterodorsally, the splenial antero-ventrally and the angular postero-ventrally. On its dorsal surface, it contacts the coronoid.

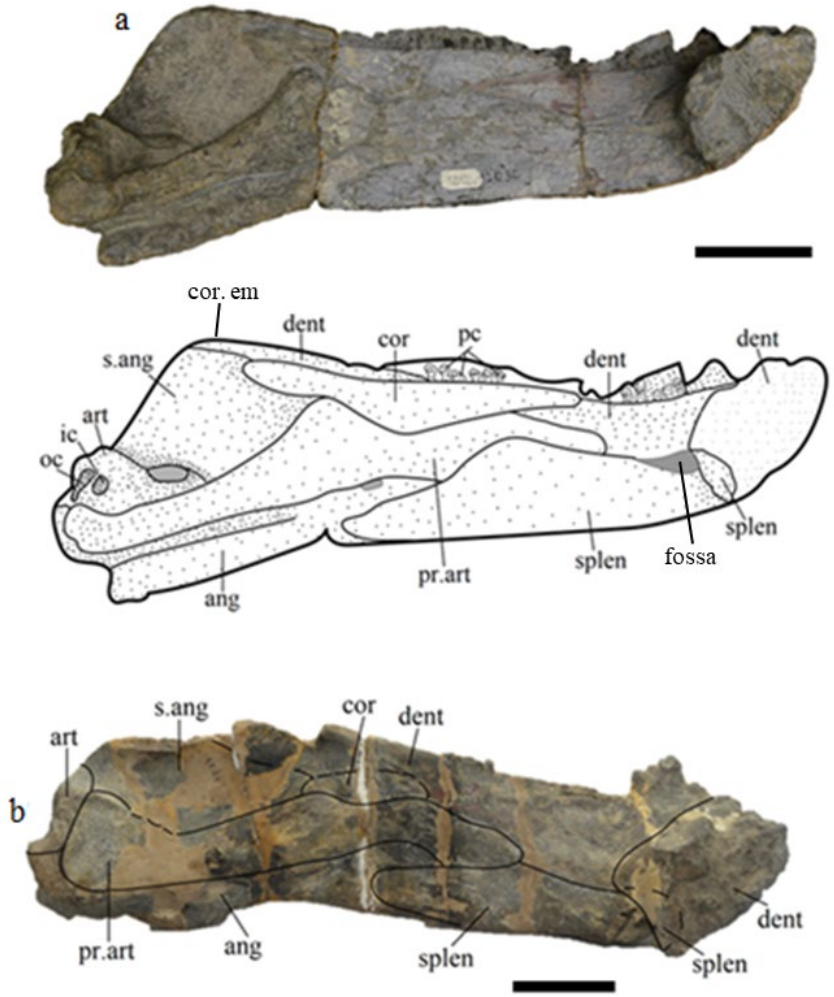

Fig. 3.15. Medial view of *Jonkeria truculenta* mandibles. **a.** SAM-PK- 12030.**b.** AMNH 5633. Scale bars represent 10cm.

3.4.4.4 *Articular*

The articular is positioned on the posteromedial side of the surangular and angular bones and contacts the prearticular anteriorly. The articular is medio-laterally robust. The dorsally positioned articulation surface comprises a small, anteriorly positioned elliptical cavity with the

long axis oriented dorsoventrally, and a larger, posteriorly positioned outer cavity with its long axis oriented medio-laterally and which extends dorsally (Fig. 3.15. a).

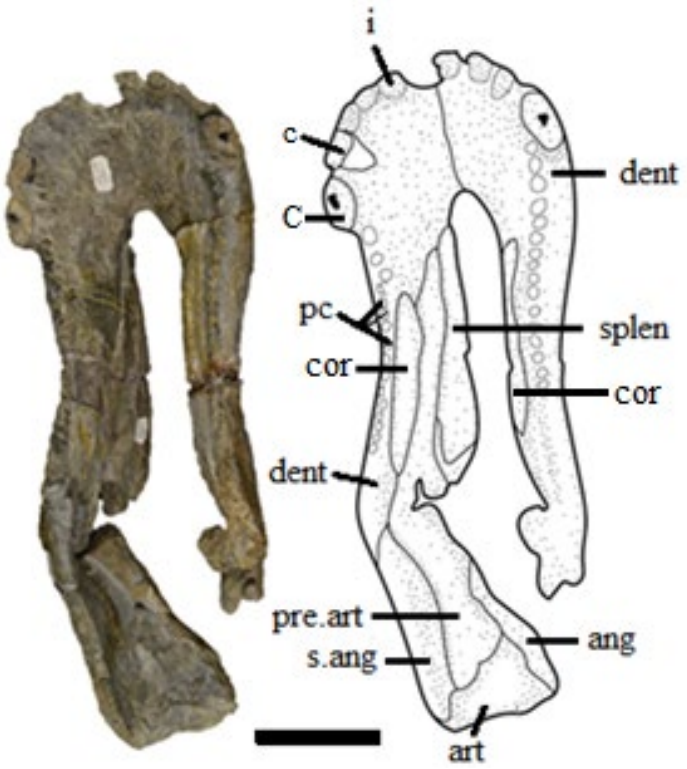

Fig. 3.16. Dorsal view of *Jonkeria truculenta* mandible SAM-PK-11884 showing the position of the coronoid bones on the right and left ramii of this mandible. Scale bar represents 10cm.

3.4.4.5 *Angular*

The angular bone (Fig. 3.15) forms most of the posterior portion of the lower jaw. The anterior thinner end of the angular is wedged between the splenial and the dentary. In lateral view, the angular becomes higher towards the back and forms most of the posterolateral surface of the jaw. Laterally a prominent reflected lamina is present below the coronoid eminence, which extends to the ventral margin of the lower jaw. The reflected lamina has a flat lateral surface with no ridges. There is a groove that runs from the posterior end of the angular in a dorso-ventral direction then

downturns into the angular just below the coronoid eminence (Fig. 3.14. a). On the medial side, exposure of the angular is relatively small and is largely obscured by the pre-articular.

3.4.4.6 *Splenial*

This bone is exposed only on the medial side of the jaw and attains its greatest height half way along its length where it contacts the prearticular postero-dorsally and the angular postero-ventrally (Fig. 3.15). The splenial is an exceptionally long splint of bone extending over the anterior half of the lower jaw forming the lower half of the medial surface and also forms a small part of the mandibular symphysis (Fig. 3.15). A fossa on the dorsomedial surface of the splenial, close to the symphysis (Fig. 3.15), was possibly for insertion of the anterior end of the genioglossus muscle (Smith, 1992).

3.4.4.7 *Coronoid*

The coronoid is a loose bone and becomes easily dislodged (lost or displaced) postmortem (Grine, 1997) with the result that its position varies in different specimens. This is a long bone positioned posterodorsally on the medial side of the dentary. It extends from the first third of the postcanine series to halfway along the coronoid eminence. In SAM-PK-12030, the coronoid is positioned at the base of the postcanine tooth series while in SAM-PK-11884 the position of this bone is different on the right and left sides of the jaw (Fig. 3.16). According to Grine (1997), the position of the right coronoid bone on SAM-PK-11884 (Fig. 3.16), situated along the superior aspect of the dentary adjacent to the tooth row, is in the correct anatomical position. In TM 212 and NHMUK 49730, the coronoid is not visible as this part of the mandible is weathered and in AMNH 5633, the dorsal extent of the coronoid is not clear.

3.4.5. Dentition

As in most therapsids, *Jonkeria* is characterized by a heterodont dentition comprising incisors, canines and postcanines with a dental formula of i5/4, c1/1, pc19/18-21 (Boonstra 1962). A problem in describing the teeth of *Jonkeria* is that no jaws have all the teeth preserved, so it is difficult to fully describe the dentition of the genus.

3.4.5.1. *Incisors*

Incisor morphology

There are five upper and four lower incisors. SAM-PK-4343 has two complete premaxillary incisors preserved while in SAM-PK-11884 and SAM-PK-12030 only cross-sections through the roots remain (Fig. 3.17, Fig. 3.18.d). Specimen ROZ. B96 has well preserved incisors on the dentary (Fig. 3.18.a). The incisors have a strong long curved conical root, which is oval in section with an equally long curved claw-like pointed talon. These teeth have a convex labial face and a more flattened lingual face with a prominent heel on the lingual side at the junction of the crown and root (Boonstra, 1962).

The incisor heel forms an oblique ledge where the inner (lingual) side of the incisor heel is lower than the outer (labial side) (Boonstra, 1962). The opposite is true for the lower incisors. In unworn teeth, the lingual portion of the heel forms a sharp ridge with coarse serrations as is the case for the well-preserved dentary incisor teeth for specimen ROZ. B96 (Fig. 3.18a), but as a result of wear the edge loses the serrations and the sharp edge becomes rounded.The crown of the first incisor is wider than longer and the width increases towards the fourth.

In the right premaxilla of specimen SAM-PK- 4343, the crowns of I4 and I5 are well preserved, whereas the other three are broken off at the alveolar border (Fig. 3.17). As preserved, the incisors are directed far anteriorly in this specimen, but this orientation is due to post-mortem dorso-ventral crushing of the skull. For I4 the inner face of the talon runs obliquely from the heel to the tip without the usual distinctive face on the heel itself. As for I5, this sloping inner face is also evident, but in this tooth, it is bipartite — the outer and greater part is for the reception of the lower canine. The morphology of the crowns of I4 and 15 (SAM-PK- 4343) seem to be similar and the cross sections though the maxillary incisors of ROZ. B96 and SAM-PK- 12030 (Fig. 3.18. c, d) shows that I1 is smaller than the rest of the incisors and I2-I5 are almost of the same size. The dentary incisors of ROZ. B96 seem to be of the same size from I1-14 (Fig. 3.18.a).

Incisor replacement

Because the teeth are not completely preserved in any specimens of *Jonkeria*, coupled with poor resolution obtained for CT scans, it is difficult to accurately determine the mode of tooth replacement in *Jonkeria.* In the premaxilla of specimens ROZ B96, SAM-PK- 4343 and SAM-PK- 12030, it appears that (Fig. 3.17, 3.18.a, c, d) a cavity develops in the bone lingual to the alveolus housing the functional incisor. This cavity houses the germ from which the replacing incisor develops. The talon of the young replacement tooth, when just emerging, is flattened antero-posteriorly and is roughly triangular in outline (Fig. 3.18.a, c).

ROZ B96 (Fig. 3.18c) and SAM-PK- 12030 (Fig. 3.18.d) show cross sections through five upper incisors. Replacement incisors 2^1 is still an empty pit and 1^1, 4^1, 3^1 and 5^1 show erupting crowns in replacement pits. The emerging cusps of replacing teeth can be seen, each lying lingual to a

functional tooth. For both these right maxilla (Fig. 3.18. c, d), the replacing order for both specimens seems to be 1, 4, 3, 5, 2, in agreement with the observation by Boonstra (1962) for specimen SAM-PK-12030.

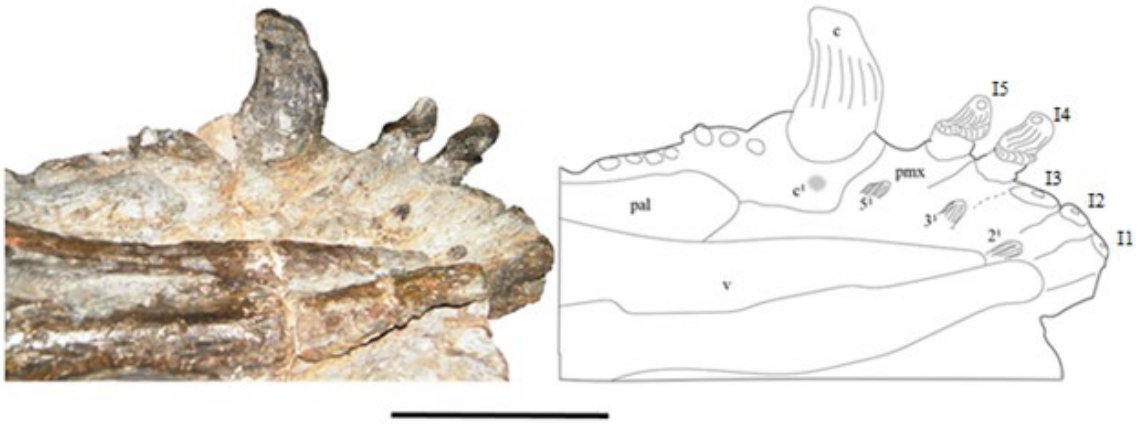

Fig. 3.17. Close-up of the ventral view of anterior snout (right premaxilla) of SAM-PK - 4343 showing the morphology of the canine tooth and the incisor teeth I4 and I5 and tooth replacement. Scale bars represent 10cm.

3.4.5.2 *Canines*

Canine morphology

The maxilla and dentary each bear a single curved canine. The upper canine has a large conical crown which curves backwards and is slightly laterally flattened (Fig. 3.17, 3.18. a, b). The lower canine is smaller, less curved than the upper, and is outwardly directed, which is a diagnostic feature of titanosuchids (Boonstra, 1962). The canine is preserved on the maxilla of specimens SAM-PK- 4343, SAM-PK- 11884, SAM-PK-12030 and ROZ. B 96 and the dentary of ROZ. B 96.

The maxillary canine has a long and large root, which causes the maxilla to have a swelling on the lateral side. In cross-section the canine roots are longer antero-posteriorly than wide (Fig. 3.18.d). A diastema (Fig.3.17, 3.18.d, 3.19) is present between the upper canine and the last upper incisor to allow the lower canine to fit between these two teeth in occlusion and the upper canine passes behind the lower canine to fit in a hollow in the outer face of the dentary (Fig.3.19). In all the specimens, where the crown is preserved, the canine is rounded in cross section. In SAM-PK- 4343 the right maxillary canine has its crown very well preserved. This is rather short and greatly recurved and directed outwards, this outward projection of the canine may be taphonomic and possibly due to the dorso-ventral crushing the skull has undergone.

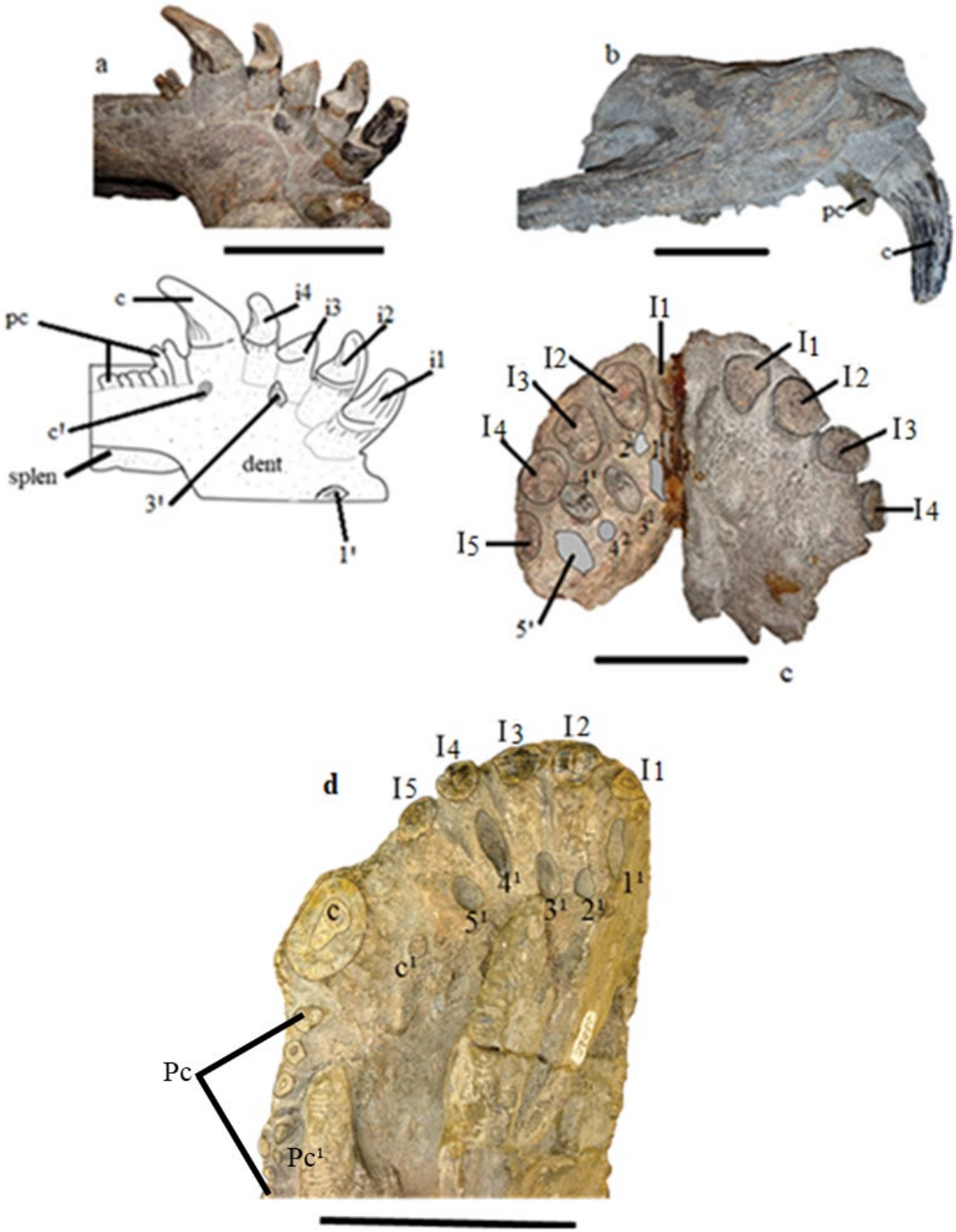

Fig. 3.18. Medial view of the left anterior mandible (a)**,** lateral view of left maxilla (b), ventral view of premaxilla (c) for ROZ. B96 and ventral view of the right anterior snout of SAM-PK-12030 (d). Scale bars represent 10cm.

In SAM-PK-11884, the upper canines are large, pointed and curve backwards. The length of the crown is 90 mm. and the basal diameters (anteroposterior length x labio-lingual width) are right 49 x 36 mm, and left 45 x 34 mm. Specimen ROZ B96 has both the lower and upper canines presered and the lower canine is smaller, shorter and less pointed than the upper (Fig. 3.18.a, b).

Canine replacement

In both the maxilla (SAM-PK- 4343, SAM-PK- 12030) and dentary (ROZ.B96) there is a small pit in the lingual wall just above the inner alveolar edge of the functional canine (Fig. 3.14, 3.18.a, d). Judging by the position of this pit on specimen SAM-PK-12030 (Fig. 3.18.d), these pits are interpreted here as representing the points of eruption of the replacing canine.

3. 4.5.3 *Postcanines*

Postcanine morphology

In specimen SAM-PK- 11884 the upper postcanines are very poorly preserved, most have fallen out (possibly after death) and their alveoli are difficult to determine. However, on both sides the first postcanine is much larger than those further back. In the dentaries the postcanines are well preserved. On the right side, 18 postcanine teeth are preserved while the left side has 19 teeth with p18 and p19 represented by empty alveoli.

In the left dentary of MB.R.983 (Fig. 3.20), a good set of crowns has been exposed from the lingual side. The functional lower postcanines show, on their lingual faces, a moderately developed heel forming a cingulum at the junction of crown and root and above this the inner face of the crown is concave. The spatulate crowns are roughly triangular in outline with the

outer face moderately convex while the inner face is slightly concave (Boonstra, 1962). The crowns lie obliquely to the long axis of the jaw at an angle of approximately 40º, the anterior end directed inwards while the posterior edge is directed outwards (Boonstra, 1962).



Fig. 3.19. *Jonkeria truculenta* SAM-PK-12030 showing arrangement of teeth in occlusion. The upper postcanines are at the edge of the maxilla and they rest on the ledge on the dentary. The lower postcanines lie lingual to the upper postcanines. Upper canine rests on a hollow in the outer face of the dentary. There is a diastema between i5 and the upper canine to accommodate the outward pointing lower canine in occlusion. Scale bar represents 10cm

Unlike the incisors and canines, the postcanine teeth of the lower and upper jaws do not intermesh and the lower set lies lingual to the upper set, in occlusion (Fig. 3.19).

The upper postcanines are implanted closer to the lateral edge of the maxilla while those of the lower jaw are closer to the medial edge almost 20mm from the edge of the dentary. The resulting dentary ledge receives the maxillary teeth in occlusion. In both the upper and lower jaws, the

crowns lie obliquely to the long axis (almost 40º) with the anterior edge directed inwards and the posterior edge directed outwards (Boonstra, 1962) (Fig. 3.20).

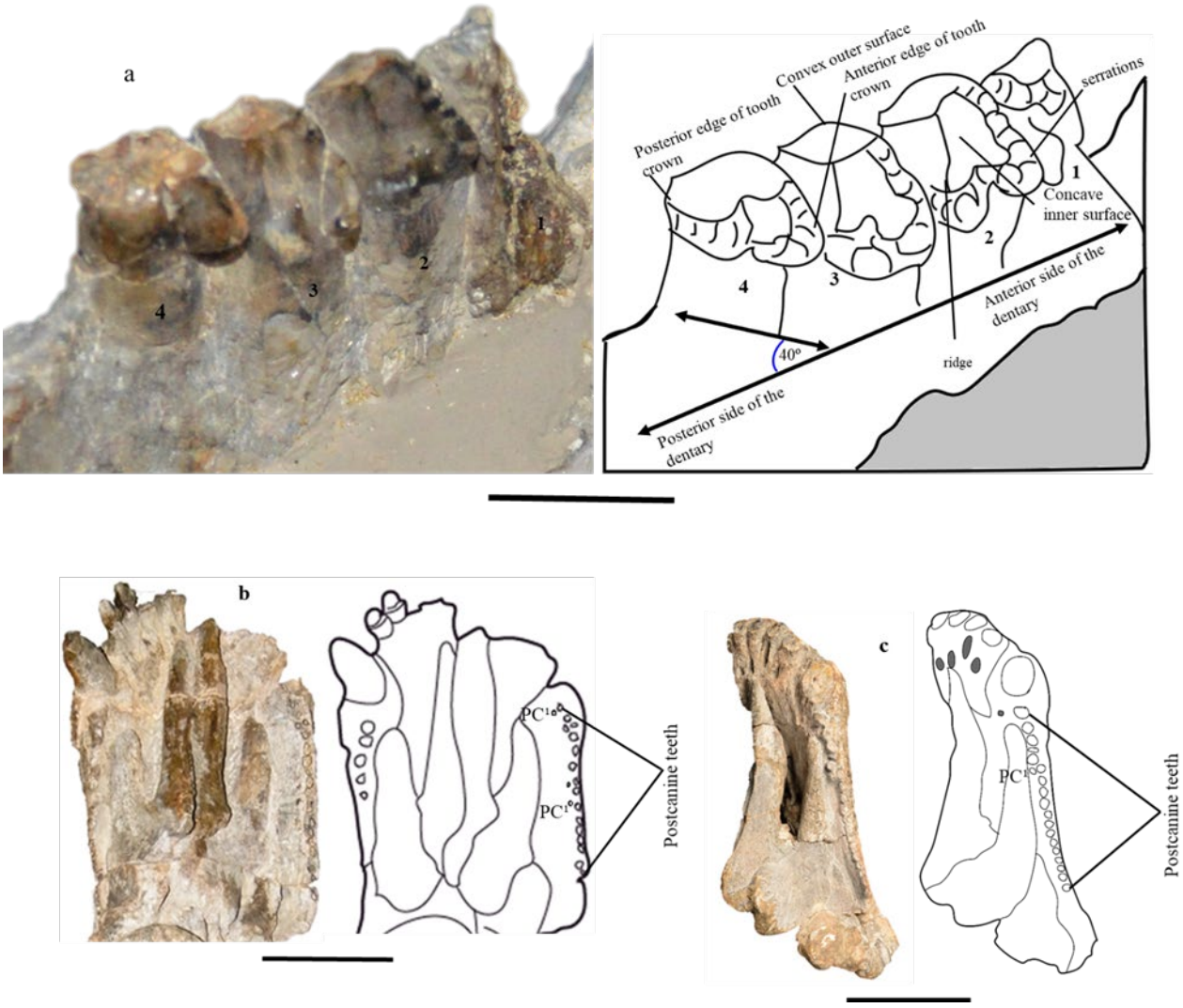

Fig. 3.20. (a) Dentary of specimen MB. R. 983 showing the postcanine tooth crowns (2 - 4). (b) Maxilla of specimen SAM-PK-4343 showing replacement teeth (PC^1) for the first and 13th postcanines. (c) Left maxilla of specimen SAM-PK-12030 showing a row of postcanine teeth with tooth size decreasing in an anterior – posterior direction. Lingual to the 6th postcanine is a pit for a replacement tooth (PC^1). Scale for **a** represents 1cm and for **b** and **c** represents 10cm.

The first postcanine is the largest and the size decreases posteriorly. Each postcanine tooth is oval in section and has a spatulate crown that is almost triangular in outline. Unworn postcanine teeth are flattened and serrated on both the mesial and distal margins including anterior and posterior sides (Fig. 3. 20). The number of postcanines in fully-grown individuals is 19 for the upper jaw and varies from 18 to 21 for the lower jaw (smaller skulls with 18 and the largest skulls with 21).

Because of the paucity of fossils it is not possible to explain tooth replacement of the postcanines but there is evidence of replacement pits lingual to some postcanine teeth on the left maxillae of specimens SAM-PK- 4343 and SAM-PK- 12030 (Fig. 3.20. b, c).

3.5. Allometry

Considering the different sizes of the cranial specimens of *Jonkeria* an analysis of allometry of a selected variables is presented to demonstrate a growth model for the taxon. Fourteen measurements of the skull were used in the analysis of allometry (Table 3.1). The skull measurements are presented in chapter 2 (Materials and Methods, Fig. 2.1).

Table 3.1. Summary of the regressions on the total skull length from the tip of the snout to the occipital condyle (variable 1) of *Jonkeria truculenta*. Abbreviations: b_1, coefficient of allometry calculated via reduced major axis method; P(iso), isometry; n, sample size; pos, positive allometry; R^2, adjusted coefficient of determination. Variables with allometric trends indicated in bold.

Variables	n	R^2	b_1	P(iso)	Trend
2. Snout length	7	0.44	0.97	0.10	no correlation
3. Orbital length (antero-posterior)	6	**0.74**	1.96	**0.02**	**pos**
4. Orbital height (dorso-ventral)	7	0.12	2.08	0.44	no correlation
5. Interorbital width	7	0.25	1.65	0.25	no correlation
6. Intertemporal width (at level of pineal foramen)	7	0.16	-2.94	0.37	no correlation

7. Width of postorbital bar	6	0.19	0.94	0.38	No correlation
8. Width of snout (at level of canine)	7	**0.76**	1.92	**0.01**	**pos**
9. Greatest width of the skull (at level of squamosals)	6	**0.69**	1.71	**0.03**	**pos**
12. Pterygoid process width	7	0.04	0.62	0.65	no correlation
13. Width of jugal below eye orbit	6	0.42	3.12	0.15	no correlation
14. Inter-nostril width	8	0.005	-2.13	0.86	no correlation
15. Occiput height	8	0.04	1.58	0.61	no correlation
17. Distance from lateral flanges of pterygoid to tip of snout	7	0.04	0.62	0.65	no correlation
18. Width of occiput (between squamosals)	5	**0.82**	1.13	**0.03**	**pos**

A digital vernier caliper and Tailor's Tape measure were used to take cranial mesasurements and the measurements were recorded to the nearest millimeter. Because of the paucity of well preserved and complete skulls of *Jonkeria*, if there is deformation in the skull the measurement was approximated as closely as possible. If a reasonable approximation was impossible the measurement was discarded.

The relation of each cranial variable with overall size was studied through the equation of allometry Log $y = \log b_0 + b_1 \log x$ (Abdala and Giannini, 2000) which derives from the exponential growth equation $y = b_0 \times b_1$ (Alexander, 1985) where b_0 represents the y-intercept and b_1 is the slope of the line which denotes the coefficient of allometry. A t-test was applied to assess the significance of slope values and deviations from isometry assessed by comparing the allometry coefficient with the one expected under geometric similarity (Alexander, 1985). My estimator of overall size was the total skull length (Simpson *et al*. 1960; Emerson and Bramble, 1993; Radinsky, 1981a, b). The expected coefficient under isometry is 1.0 for all the variables measured in this study and t-tests were used with the null coefficient set equal to 1.0 to assess significant deviations from isometry (Abdala and Giannini, 2000). If a coefficient is significantly

less than expected by isometry this is referred to as 'negative' allometry while one significantly higher than expected is referred to as 'positive' (Emerson and Bramble 1993).

Of the fourteen variables, only five variables have statistical significance with a 95% confidence, indicating that they are different from 1 (isometry) and these variables have positive allometry. The five statistically significant variables include; antero-posterior orbital length (Variable 3; Fig. 3.21. a); width of snout (Variable 8; Fig. 3.21. b); greatest width of the skull at the level of squamosals (Variable 9; Fig. 3.21. c); and width of occiput (Variable 18; Figure 3.21. d).

Despite the reduced sample size as most *Jonkeria truculenta* skulls are incompletely preserved (n between 5 and 7) it is possible to demonstrate allometric growth for characters that show extreme differences between the smallest and largest specimens of the sample.

When b = 1 there is isometry (the maintenance of the geometric similarity with the increase of the length of the skull -- the shape is maintained with increasing size). When b < 1 (negative allometry), the ratio variable ***x*** / total skull length decreases with the absolute magnitude increase of total skull length. When b > 1 (positive allometry), there is a differential increase of variable ***x*** relative to total skull length.

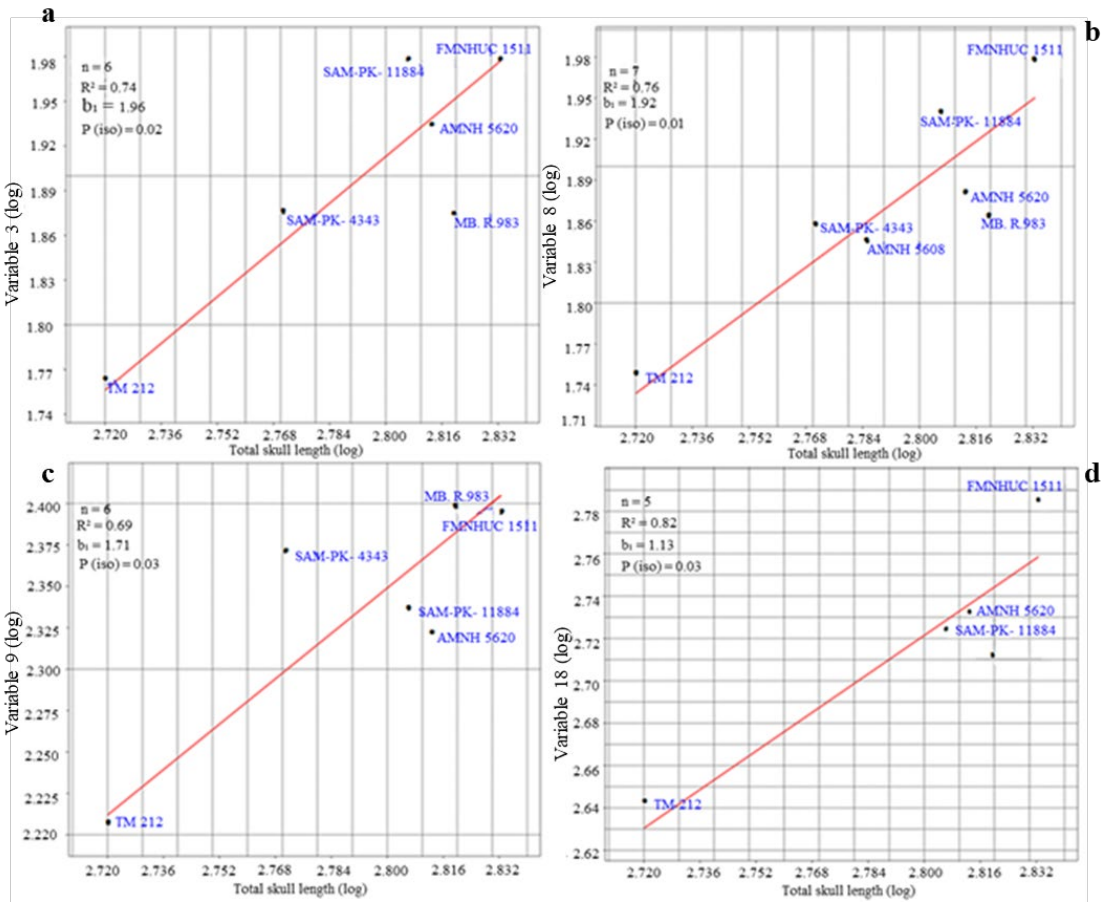

Fig. 3. 21. Regression of length of the total skull length (log Variable 1) on **a.** the antero-posterior orbital diameter (log Variable 3). b_1= 1.96; **b.** the width of the snout at the level of canines (log Variable 8). b_1= 1.92; **c.** the greatest width of the skull at the level of squamosals (log Variable 9). b_1= 1.71 and **d.** the width of occiput between squamosals (log Variable 18). b_1= 1.13.

This regression analysis suggests that specimen TM 212 is a juvenile specimen, and AMNH 5608, SAM-PK- 4343, SAM-PK- 11884, AMNH 5620, MB. R. 983 and FMNHUC 1511 represent adults (Fig. 3.22).

3.6. Discussion

The family Titanosuchidae is currently known to comprise only the genera *Titanosuchus* and *Jonkeria*, *Titanosuchus* comprises only one species, *Titanosuchus ferox,* while *Jonkeria* on the other hand has eight species namely *Jonkeria truculenta*, J. *vanderbyli*, J. *ingens*, J. *haughtoni*, J. *koupensis*, J. *parva*, J. *rossouwi*, and J. *boonstrai* (Boonstra 1969, King 1988). Five of the eight *Jonkeria* holotypes are known from cranial material (*J. truculenta*, *J. vanderbyli*, *J. ingens*, *J. haughtoni* and *J. boonstrai*). This chapter sought to undertake a cranial diagnosis of members of the family Titanosuchidae on the basis of holotypes described from cranial material. Diagnosis of *Jonkeria koupensis*, *J. parva* and *J. rossouwi*, which are described on the basis of only postcranial material, shall be dealt with in chapter four.

As is evident from the description of the holotype of *Titanosuchus ferox*, the cranial material of this species is very incomplete, comprising only a maxillary and mandibular fragment. Because these fragments are so small and undiagnostic, it is not possible to determine the cranial morphology of *Titanosuchus* and to differentiate *Titanosuchus* and *Jonkeria* on the basis of cranial or cranio-dental characters as was previously noted by Boonstra (1969).
Based on cranial characters, *Jonkeria* is currently considered to comprise five species. This study however, demonstrates that there is only a single *Jonkeria* species (*Jonkeria truculenta*). The idea that *J. truculenta, J. ingens, J. vanderbyli, J. haughtoni and J. boonstrai* are conspecific was first suggested by Kammerer (2009) but he did not document detail to support this argument.

The skull roof bones (prefrontal, frontal, postfrontal, parietal, and squamosal) are well preserved in holotype specimens TM 212, MB. R. 983, AMNH 5620, SAM-PK- 4343 and SAM-PK-

11884 and have the same morphology in all specimens. Prefrontal, frontal and postfrontal are slightly pachyostosed and the parietal is the most pachyostosed cranial bone (less pachyostosed in specimen TM 212 and more pachyostosed in the rest of the specimes). There is a gentle transition from the skull roof to the snout on the top of the skull giving all the skulls an almost horizontal dorsal profile. All the skulls have a narrow interorbital region, which ranges in width from 100 mm for the smallest specimen (TM 212) to 125 mm for the largest specimen (FMNHUC 1511). Cranial characters such as dorsal profile of the skull and divergence of the quadrate rami of pterygoids) vary between skulls largely because of allometric size differences and because of deformation.

Taxonomy

Broom (1929) in his description of *Jonkeria vanderbyli* (AMNH 5620) conceded that the skull agrees closely with that of the genotype *Jonkeria truculenta* so much so that it was only after some hesitation that he decided to recognize it as a new species. Broom (1929) documents that the dorsal views of the two holotypes (AMNH 5620 and TM 212) are similar, with the main points of difference being that the internasal process of the premaxilla is much shorter in *Jonkeria truculenta* than in *Jonkeria vanderbyli.* However, contra Broom (1929), the internasal process extends all the way to the frontal bone. Contra Broom (1929, 1932) and Boonstra (1936), who both agreed that the flatter snout and anteriorly directed squamosal below the temporal fenestra were sufficiently diagnostic to distinguish between *Jonkeria truculenta* and *Jonkeria vanderbyli*, the dorsal skull profile of individual *Jonkeria* specimens is so variable that even between specimens ascribed to the same species (eg. *Jonkeria vanderbyli*: holotype AMNH 5620 and referred specimen SAM-PK-11884 and *Jonkeria truculenta*: holotype TM 212 and referred

specimen SAM-PK-12030) their dorsal snout profiles are different (Fig. 3.10) owing to the degree of deformation.

As is the case in tapinocephalids, the occipital plate is more anteroventrally tilted in the larger specimens, shifting the jaw joint further anteriorly. (Neumann, 2020) and this together with deformation is the reason the squamosal is anteriorly directed in specimen AMNH 5620 and more so in FMNHUC 1511 compared to the juvenile specimen TM212. As such this feature is not a valid diagnostic feature to distinguish between TM212 and AMNH 5620 and *Jonkeria vanderbyli* is thus a junior synonym of *Jonkeria truculenta*.

Broom (1929) presented a deformed skull SAM-PK-4343 as the holotype of *Jonkeria haughtoni* but gave no distinct diagnostic characters to differentiate it from *Jonkeria truculenta* (TM 212) apart from the vomers which were said to form a marked median ridge on their posterior two-thirds and the pterygoids projecting much less downwards than in other species of *Jonkeria*. The vomers in SAM-PK-4343 have the same morphology (median ridge on their posterior two thirds in specimens AMNH 5620, MB.R. 983, SAM-PK-12030 and FMNHUC 1511). The median ridge is slightly visible in specimen TM 212 since this part of the ventral part of the skull is slightly weathered. The downward projection of the pterygoids for specimen SAM-PK-4343 is less than the other *Jonkeria* specimens where it is well preserved, which is the result of dorsoventral compression (deformation) of the skull SAM-PK-4343 and the pterygoids have been crushed. There is no justification to taxonomically differentiate SAM-PK- 4343 from other *Jonkeria* skulls hence *Jonkeria haughtoni* is considered an adult of *Jonkeria truculenta* (TM 212).

Boonstra (1936) stated that *Jonkeria vanderbyli* and *Jonkeria ingens* are similar in palatal view differing only in that the quadrate rami of the pterygoids of *J. vanderbyli* are less divergent posteriorly than those of *J. ingens* and also *J. vanderbyli* has very slender vomers compared to those of *J. ingens.* This project has demonstrated that the less divergence of the quadrate rami of the pterygoids in *J. vanderbyli* is the result of deformation. In all *Jonkeria* specimens the vomers appear as stout rods with birfucated anterior ends. The slight differences in sizes of the vomers are attributed to ontogenetic and intraspecific differences. As a result, *Jonkeria ingens* is a junior synonym of *Jonkeria truculenta*.

According to Janensch (1959), the skull of *Jonkeria boonstrai* (MB.R. 983) differs in that the occiput height to the total skull length ratio of *Jonkeria boonstrai* is 57% compared to 50% for *J. truculenta, J. vanderbyli* and *J. haughtoni*, and 54% for *J. ingens* (54%). Janensch (1959) also noted the difference in the ratio of the width of the snout to the total skull length at about 41% for the *J. boonstrai* while it is only 30% in the other species of *Jonkeria,* and a very steep mandibular mentum for *J. boonstrai* compared to other *Jonkeria* species. The holotype skull of *Jonkeria boonstrai* (MB.R. 983) suffered lateral compression in the posterior region (Fig. 3.6) resulting in a higher occiput to total skull length ratio. Janensch (1959: 41) also considered the "angled outline of the MB. R 983 skull as being different to other species of *Jonkeria"*. However, all *Jonkeria* specimens have a similar outline with a roughly triangular tip of the snout, a concavity from the canine bulge on the maxilla until the anterior end of the lacrimal then widening of the skull from this point until the occiput (Fig. 3.11). Janensch (1959) noted that in the lower jaw of *Jonkeria boonstrai* differs from that of other species in that the contour of the

anterior edge recedes towards the symphysis suture. This feature, however, is also present in *Jonkeria truculenta* referred specimen AMNH 5633.

Allometric growth

Ten of the fourteen variables analyzed for allometry do not show correlation with the skull length, which is likely related to taphonomic deformation. The remaining four variables however feature positive allometry. These are (3) antero posterior orbital length, (8) width of the snout at the level of the canines, (9) greatest width of the skull (at the level of the squamosal), and (18) width of the occiput between squamosals. Variation in the width of the snout is mostly likely due to an increase in the size of canines, as the snout needs to expand to accommodate the enlarged canine roots. The variable width of skull, and width, of occiput between squamosals, point to a faster growth of the temporal region, which is related to an increase in volume of the occlusal musculature in the larger skulls.

From the description of the best preserved *Jonkeria* cranial material size variation is evident. TM 212 is the smallest skull with a cranial length of 520 mm, SAM-PK- 4343 and AMNH 5608 are intermediate with estimated skull lengths of 590-610 mm respectively and SAM-PK- 11884, MB.R.983, AMNH 5620 and UC 1511, with skull lengths ranging from 640 mm to 680mm, are the largest. In all these specimens, the snout length constitutes about 60% of the total skull length from juveniles to adults.

The occiput (best preserved in FMNHUC 1511 and partially preserved in SAM- PK- 4343 and SAM-PK- 11884) slopes anteroventrally and thus the jaw joint is positioned further anteriorly. TM

212 (the smallest specimen) has only a slight antero-ventral slant of the occiput and the angle of inclination increases in larger skulls with the occiput of FMNHUC 1511 (the largest skull) having the greatest angle of inclination. This antero-ventral inclination of the occiput means that the jaw joint of the juvenile (TM 212) is positioned below the temporal fenestrae while that of larger specimens (adults) is positioned further forward, almost below the post-orbital bar (Fig. 3.22).

The smallest skull (TM 212) has relatively large orbits relative to the size of the temporal fenestra in comparison with the other skulls. This feature is commonly considered a juvenile characteristic in therapsids (Abdala *et al*. 2001; Giannini *et al.* 2010; Jasinoski and Chinsamy-Turan, 2012; Kruger *et al*. 2015; Kruger *et al*. 2017). In the therapsid *Biarmosuchus*, the orbit remains similar in absolute size during growth from the juvenile to adult and therefore, reduces its size relative to skull length (Ivakhnenko, 1999, 2008).

Within the growth series of *Jonkeria truculenta* the following morphological changes in the different skulls were noted and are considered to be related to ontogenetic development: thickening of the prefrontal postorbital bar, postfrontal and parietal, anterior placement of the jaw joint in the skull; an increase in intertemporal breadth and a decrease of orbit size in relation to the temporal fenestra. Similar changes in the skull roof have been noted in the ontogeny of *Anteosaurus* (Kruger *et al.* 2017). With ontogenetic development, the temporal fenestra enlarges diagonally (antero-dorsal – postero-ventral direction) and there is an increase of the thickness of the post-orbital bar to accommodate the increase in size of the occlusal musculature.



Fig.3.22. Ontogenetic variation within *Jonkeria truculenta* skulls. The arrow indicates size increase of the different skulls. As this species grows older it acquires a relatively longer snout, and more cranial pachyostosis around the prefrontal, frontal, postorbital and parietal bones.Total skull length of each skull is provided. Scale bar represents 10cm.

A low development of cranial ornamentation and pachyostosis have been linked to an early ontogenetic stage in various groups of therapsids (Estes, 1961; Van Heerden, 1972; Ivakhnenko, 2008; Cassini *et al*. 2015 Kammerer, 2011; Liu, 2013; Kruger *et al*. 2017; Kulik and Sidor, 2019). Ivakhnenko (2008) and Kruger *et al*. (2017) showed that in the anteosaurid dinocephalians *Titanophoneus potens* and *Anteosaurus magnificus* the fronto-nasal ridge,

supraorbital bosses, and pachyostosis developed between the juvenile and the adult conditions. The formation of cranial bosses in the anteosaurian genus *Sinophoneus* was also noted as a postnatal development (Liu, 2013) and a similar ontogenetic development has been observed for the bosses of *Estemmenosuchus uralensis* (Ivakhnenko, 2008). In tapinocephalids, the extent of cranial pachyostosis increases while the relative size of the orbit and temporal fenestra shrinks during ontogenetic growth (Gregory and Broom, 1926; Boonstra and Broom, 1936; Boos *et al*. 2015; Neumann, 2020). In burnetiamorphs, a low degree of pachyostosis has also been linked to juvenility, with greater pachyostosis occurring in more mature individuals (Duhamel *et al*. 2021). However the degree of pachyostosis and cranial boss development has also been shown to increase with phylogentic development in biarmosuchians with basal forms displaying a lower degree of cranial pachyostosis and smaller cranial bosses than derived burnetiamorphs (Sidor and Rubidge, 2006; Day *et al*. 2018). Sexual dimorphism may also result in differences in pachyostotic development (Lande, 1980; Kraaijeveld *et al*. 2007; Benoit *et al*. 2016; Gates *et al*. 2016) but this is yet to be demonstrated in titanosuchid dinocephalians and will require a larger sample of well-preserved specimens than is currently avialable.

3.7. Conclusion

This detailed study of the cranial morphology of all titanosuchid cranial material has demonstrated that it is not possible to distinguish *Titanosuchus* from *Jonkeria* solely on cranial characters, largely because the preserved cranial remains of *Titanosuchus* are too poorly preserved for comparison. The cranial description and the allometric study undertaken for this study strongly indicates that all cranial specimens of *Jonkeria* can be accommodated within the species *Jonkeria truculenta.* The morphology of the cranial bones is similar in all the *Jonkeria*

specimens, and the characters used to differentiate between the different species in the past have been shown to be manifestations of a combination of taphonomic deformation, ontogenetic variation, and possibly sexual dimorphism as well. It is thus concluded that, on cranial material, the genus *Jonkeria* comprises a single species *Jonkeria truculenta* van Hoepen 1916b and that the species *J. ingens, J. vanderbyli, J. haughtoni and J. boonstrai* are junior synonyms of *Jonkeria truculenta*.

Allometric studies have shown that there is positive allometry for some variables of the skull such as orbital length, width of snout and of the skull at the level of squamosals, length of the skull from the posterior margin of pineal foramen until the occipital condyle and the width of the occiput between squamosals. TM 212, the smallest specimen represents the juvenile form of *Jonkeria truculenta* (77% of the skull length of the largest specimen, FMNHUC 1511) and has larger orbits relative to the size of the temporal fenestra, lesser angle of the frontal and the posterior position of jaw joint.

Subadult and adult *Jonkeria* show a higher degree of pachyostosis in the prefrontal, frontal, postfrontal, postorbital and parietal regions.

CHAPTER 4: DESCRIPTION OF *TITANOSUCHUS FEROX* AND *JONKERIA TRUCULENTA* LIMB ELEMENTS

4.1 Introduction

As stated in Chapter 3, the two recognized titanosuchid genera cannot be distinguished based on cranio-dental morphology, but past research suggests that they can be differentiated on the basis of humeral morphology (Kammerer, 2009). Boonstra (1955a, 1969) indicated that *Titanosuchus* has longer limbs compared to the extremely short, robust appendicular elements of *Jonkeria*.

Apart from the *Jonkeria truculenta* holotype (TM 212), very little titanosuchid appendicular skeletal material is preserved in association with the skulls. The present study aims to understand the differences in the appendicular elements of *Titanosuchus ferox* and *Jonkeria truculenta* and excludes vertebrae and ribs because there are not many preserved in titanosuchids. These reasons, coupled with Boonstra's (1955a, 1969; King, 1988) observation that the two genera differ only in the size of limb bones and Kammerer's (2009) observation that the morphology of the humeri differs between these two genera, is why of the appendicular elements, only the limb bones were considered for this study.

The first dinocephalian humerus to be figured was one from Varsfontein, which Owen (1879) in error referred to *Pareiasaurus*, and Lydekker (1890) later provisionally referred to *Tapinocephalus*. Seeley (1899) figured a humerus from Koedoeskop as that of *Titanosuchus ferox*, since this humerus was considered to have been associated with the holotype skull fragments. Broom (1904), in his description of *Scapanodon duplessisi* (*Titanosuchus ferox*), mentioned three humeri as possibly associated with jaw fragments, but did not figure them.

Broom (1914) figured the humerus of *Moschops* and also published a photograph of the forelimb of a Titanosuchian, which he erroneously referred to *Tapinocephalus atherstonei*. This humerus was subsequently figured by Gregory (1926) without the indication of an ectepicondylar foramen which Boonstra (1936) later demonstrated to be present, thus proving it to be titanosuchid and not tapinocephalid.

When reviewing the dinocephalian material in the Natural History Museum of London, Watson (1914) recognized an ent - and ect- epicondylar foramen in the *Titanosuchus* humerus described by Seeley. Broom (1928) figured a humerus that he regarded as that of *Tapinocephalus atherstonei* by virtue of it having two epicondylar foramina, Boonstra (1936) however considered this specimen to be of a titanosuchian. Broom (1929a) figured and described the pectoral girdle of *Jonkeria truculenta*. The same year Broom (1929b) figured the humerus of *Jonkeria crassus* (*haughtoni*). He also briefly described, a humerus identified as *Jonkeria* sp. and provided photographs of the humerus of *Dinosphageus* (*Jonkeria*) *haughtoni* and stated that there was a humerus associated with the holotype skull of *Jonkeria pugnax* (*J. ingens*).

Boonstra (1955) undertook a comprehensive description of limbs and girdles of dinocephalians from the Iziko South African Museum where he noted some similarities and differences between the limbs of different dinocephalian taxa. Boonstra (1955a) observed the following differences between *Titanosuchus* and *Jonkeria* limb bones; *Titanosuchus* humeri are very large with a short and wide shaft whereas those of *Jonkeria* are short and small to fairly large. The processus medialis is situated well proximally in *Titanosuchus* humeri and distally in J*onkeria*; *Titanosuchus* femora are massive and long whereas they are smaller for *Jonkeria*; fibula are large

and massive for *Titanosuchus* and large and fairly slender for *Jonkeria* and tibia are almost of the same proportions in both genera.

According to Kammerer (2009), titanosuchid humeri comprise two distinct morphotypes, corresponding to the genera *Titanosuchus* and *Jonkeria*. Kammerer (2009) further recognized that *Jonkeria* has a diagnostic "dumb-bell" shaped humerus whereas that of *Titanosuchus* is more elongate, with a relatively narrow shaft. Both *Jonkeria* and *Titanosuchus* humeri exhibit an extremely long deltopectoral crest relative to the length of the humerus and a massive capitellum (radial condyle) that nearly reaches the level of the entepicondylar foramen in *Titanosuchus* but extends slightly beyond this level in *Jonkeria.* However, Kammerer (2009) did not provide full descriptions of the limb bone elements.

To understand the morphological similarities and differences between *Titanosuchus* and *Jonkeria*, a detailed descriptive morphological analysis of each bone of the appendicular skeleton was undertaken as well as principal component analysis. Wherever possible, the specimens were directly analyzed and measured, but in some cases, data was taken from the literature. All specimens considered in this postcranial section are presented in Appendix C.

4.2 Revised *Jonkeria* taxonomy

Boonstra (1969) and King (1988) recognized eight valid *Jonkeria* species, five of which are known from cranial elements, and three from postcranial remains (*J. parva* Boonstra, 1955a (SAM-PK- 9149), *J. rossouwi* Boonstra 1955a (SAM-PK- 5014) and *J. koupensis* Boonstra 1955a (SAM-PK-9004).

***Jonkeria parva* Boonstra 1955a (= *Jonkeria truculenta*)**



Figure 4.1. Ventral view of the right humerus of *Jonkeria parva* holotype (SAM-PK- 9149).

Scale bar represents 10cm.

This species was described from an isolated well preserved right humerus (SAM-PK- 9149, Fig. 4.1). Boonstra (1955a, Fig. 89, pages 302-303) described the humerus briefly but did not present a diagnosis.

Remarks: The humerus can be positively identified as titanosuchid owing to the presence of both the entepicondylar and ectepicondylar foramen (Watson, 1914; Boonstra, 1936). The morphology is typical of the *Jonkeria* morph (see section 4.2.1.2 below) hence in agreement with Kammerer (2009) *Jonkeria parva* should be considered as an invalid junior synonym of *Jonkeria truculenta*.

***Jonkeria rossouwi* Boonstra 1955a** (= *Jonkeria truculenta*)



Fig. 4.2. Limb elements of the *Jonkeria rossouwi* holotype (SAM-PK- 5014). From left to right: humerus, ulna, radius, femur, fibula and tibia. Scale bars represent 10cm.

Holotype: (SAM-PK- 5014). Left scapula and incomplete precoracoid and coracoid, imperfect interclavicle, deformed left humerus, deformed left ulna and left radius, right ilium, left femur, left tibia and left fibula (Fig. 4.2).

Diagnosis: Boonstra (1955a) gives a description of the osteological elements but no diagnosis except for the ulna which he says "suffered pathological deformation so that the olecranon is proximally prolonged as a thick outgrowth, and the normal ulna would appear to have a more slender shaft and a weaker coronoid process than the other known species of *Jonkeria*" (Boonstra, 1955a, page 305).

Remarks: The *Jonkeria rossouwi* holotype has the left humerus preserved, and even though it is deformed, it manifests both the ect and entepicondylar foramina and falls within the *Jonkeria* humeral morph hence the species *Jonkeria rossouwi,* in agreement with Kammerer (2009), should be considered an invalid junior synonym of *Jonkeria truculenta.*

***Jonkeria koupensis* Boonstra 1955a**

Holotype: (SAM-PK- 9004). Fragmentary pelvis, lacking ischia (Fig. 4.3.a) and distal two-thirds of an ulna.

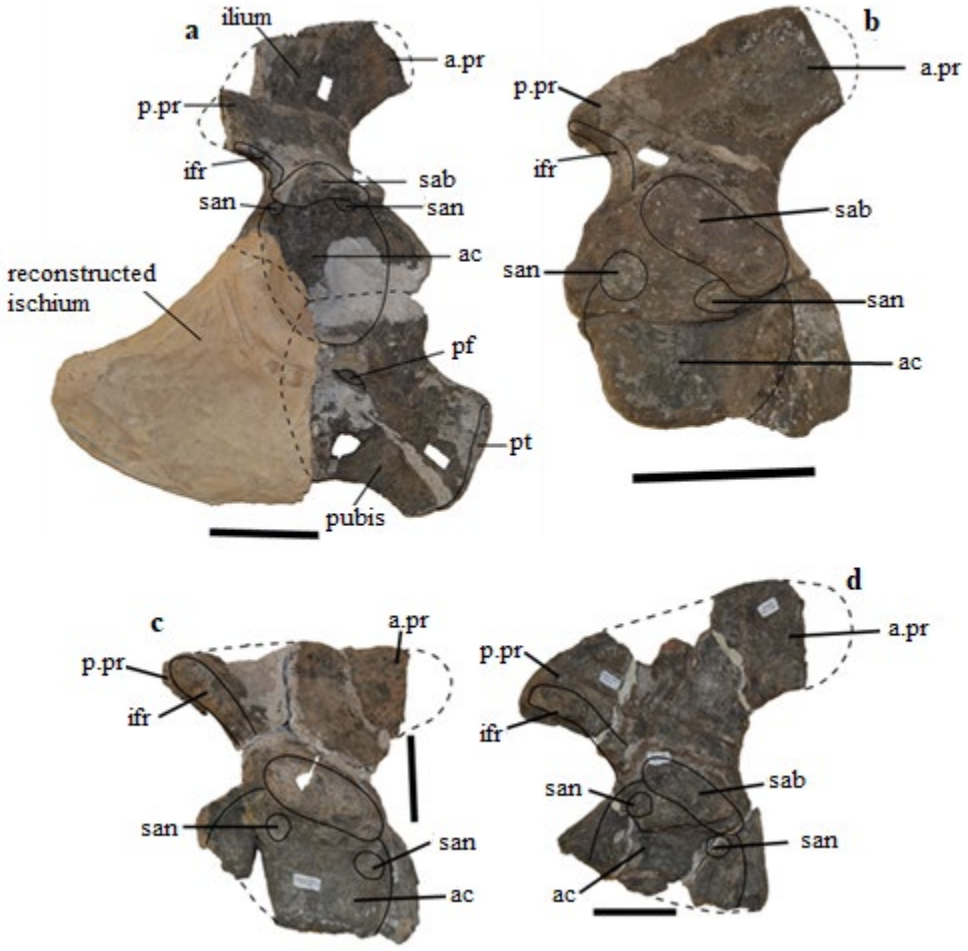

Fig. 4.3. a. *Jonkeria koupensis* pelvis in lateral view (holotype SAM-PK-9004). **b**. isolated ilium of *Jonkeria koupensis* (SAM-PK-11983) in lateral view. **c.** comparative ilium of *Jonkeria haughtoni* (holotype SAM-PK-4343) and **d.** ilium of *Jonkeria rossouwi* (holotype SAM-PK-5014). Scale bars represent 10cm.

Remarks. The pelvic characters used by Boonstra (1955a) to distinguish titanosuchid species (e.g., angulation and length of the puboischiadic plate and iliac blade) are highly subject to

taphonomic distortion (Kammerer, 2009), and these regions are broken in many titanosuchid pelves (Fig. 4.1). Since specimen SAM-PK-9004 presents an outward facing acetabulum it is not an anteosaurian where this feature is directed ventrally (Boonstra, 1955a), therefore, making it either a tapinocephalian or titanosuchian. The presence of a high supra-acetabular part of the ilium, as well as a very strong supra-acetabular buttress strongly suggest a titanosuchid affinity (Boonstra, 1955a). Therefore, specimen SAM-PK-9004 is a *nomen dubium* and can only be identified as a Titanosuchid indet for now until the range of variation in titanosuchid pelves is better understood.

4.3 Morphological description

4.3.1 Humerus of Titanosuchidae

The titanosuchid humerus is a massive bone, varying in size from small, short and squat to large, and long (Boonstra, 1955a). Its radial condyle (capitellum) is strong, thick, extends far proximally along the ventral face, reaching the plane of the entepicondylar foramen in some specimens, and lies well distal of the base of the delto-pectoral crest. According to Boonstra (1955a), the processus medialis always lies far proximally, nearly in the same plane as the caput humeralis and the ventral side of the humerus, pierced by an oval entepicondylar foramen while the ectepicondylar foramen is small and circular.

Because of the very obvious differences in humeral morphology in the holotype specimen of *Ttianosuchus ferox* (NHMUK 49369) and *Jonkeria truculenta* (SAM-PK- 4343) detailed anatomical comparison was undertaken of the bones of the fore-and hind- limbs of all available titanosuchid specimens.

In dorsal view, the humerus is divided into two parts by the anterior dorso-ventral line (advl). Anterior to this line is the proximal face, formed by the strong development of the delto-pectoral crest (dpc) (Fig. 4.4). Posterior to the anterior dorso-ventral line is the diagonally oriented ridge, the latero-medial line (lml) (Fig. 4.4.a). The ulnar condyle (Fig. 4.4.a) hand is relatively weak and not distinctly demarcated from the radial condyle, which is only visible in ventral view (Fig. 4.4.b). The proximal and distal expansion of this bone, including the length and width of the shaft, differs significantly between *Titanosuchus* and *Jonkeria*.

All titanosuchid specimens, which have the humerus preserved, were divided into two groups (either the *Titanosuchus* or *Jonkeria* group) based on the shape of the humerus of the holotype specimens to determine whether there were additional differences between the two genera in the different limb elements.

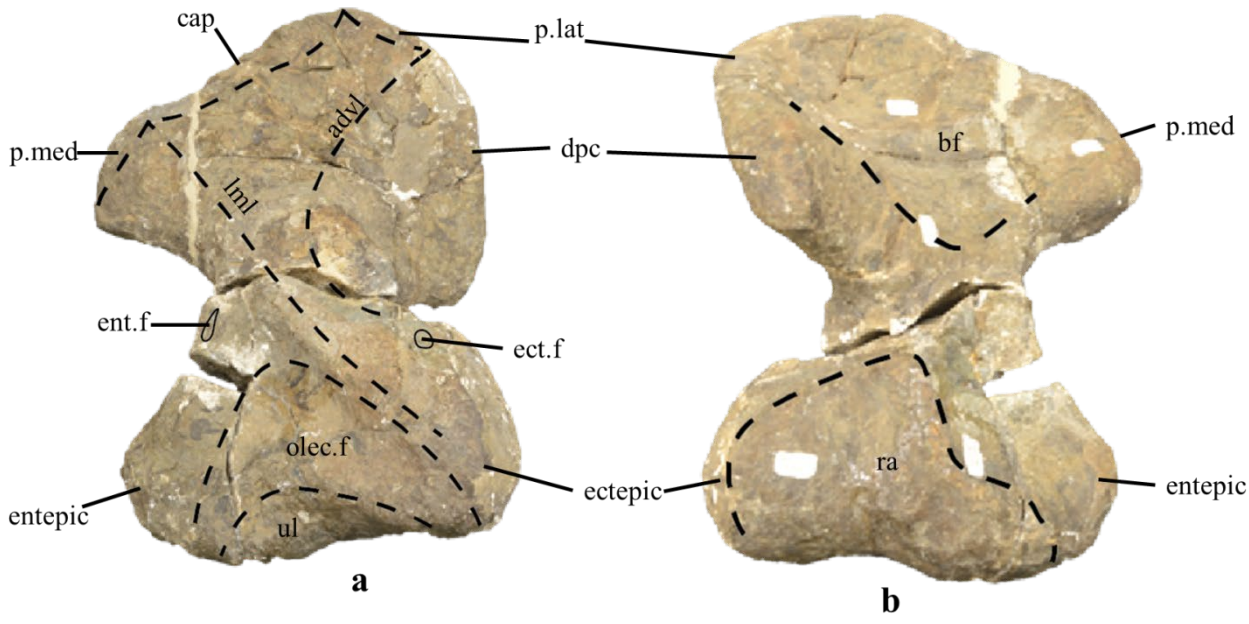

Fig. 4.4. *Jonkeria truculenta* right humerus (SAM-PK-4343) in dorsal (a) and ventral (b) views to illustrate morphological features of a titanosuchid humerus.

4.3.1.1 *Titanosuchus ferox* humerus

The humerus of the holotype of *Titanosuchus ferox* (NHMUK 49369) is a robust bone with a relatively long shaft. The proximal end is greatly expanded while the distal end is slightly less expanded (Fig. 4.5) and the lateral outlines of the shaft are only slightly concave (relative to those of the *Jonkeria*). This humeral morph is present in several specimens and all these considered in the *Titanosuchus ferox* group. The humerus for this group is represented by NHMUK 49369, BP/1/7380, SAM-PK- 773, SAM-PK- 5001, SAM-PK- 11578 and SAM-PK-11881.

In ventral view the proximal end of the bone, which represents part of the humeral head (caput humeralis), is well rounded and directed inward, and defined from the distal side of the bone by a deep triangular concavity (bicipital fossa) which extends to the middle of the shaft (Fig. 4.5). The wide proximal expansion forms the base of this triangular fossa and the apex of the triangle merges into the shaft (Fig. 4.5. a, b). The delto-pectoral crest is long with its knob-like extremity extending almost as far as the ectepicondylar foramen (Fig. 4.5). The length of the delto-pectoral crest in *Titanosuchus ferox* ranges from 320mm for the smallest specimen (BP/1/7380) to about 450*mm (asterisk is indicative of incomplete part of the bone) for the largest specimen (SAM-PK- 11881). The distal end of the ventral surface of the *Titanosuchus ferox* humerus consists of a large and massive capitellum (radial condyle) whose distal height ranges from 127mm (BP/1/7380) to about 190*mm for NHMUK 49369. The radial condyle is triangular, with the base formed by the distal-most part of the humerus and the apex at the plane of the ect- and entepicondylar foramina.

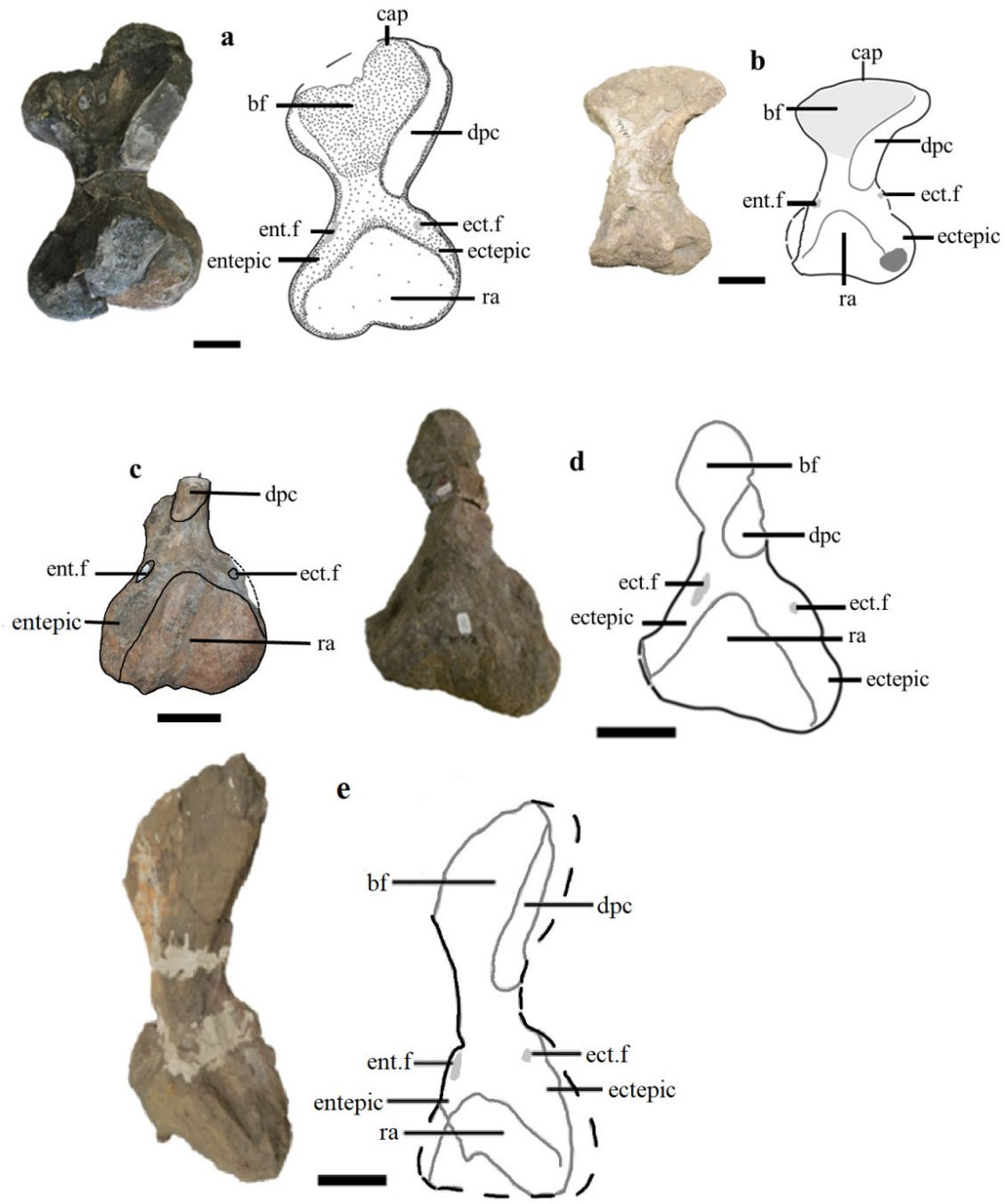

Fig.4.5. Photographs and illustrative drawings of *Titanosuchus ferox* humeri in ventral view. **a.** NHMUK49369, left humerus; **b.** BP/1/7380, left humerus; **c.** SAM-PK- 773, left humerus; **d.** SAM-PK-5001, right humerus; **e.** SAM-PK- 11881, right humerus (both d and e flipped 180°). Scale bars represent 10cm

In dorsal view, the twist on the shaft is extensive (about 40 degrees) and the latero-medial line (lml) which extends diagonally on both the proximal and distal dorsal surfaces of the humerus is strong, forming a pronounced bulge on the dorsal surface of the shaft. A strong and sharp anterior dorso-ventral line (advl) divides the proximo-dorsal surface of the humerus into two parts (Fig. 4.6). Anterior to the advl is the triangular upper face formed by the delto-pectoral crest.

The distal end of the dorsal surface of the humerus has a triangular depression with its base at the distal-most end of the humerus and the apex directed proximally, toward the middle of the shaft. The distal portion of the bone is laterally expanded because of the widened ectepicondyle and entepicondylar flanges. The entepicondyle is developed as a moderately thick, but not greatly flaring flange of bone, with a ventral slit-like opening (entepicondylar foramen) close to the edge of the bone. The ectepicondyle is a greatly flaring thin sheet of bone pierced by the ectepicondylar foramen lying well removed from the edge of the bone. In contrast, the entepicondylar foramen perforates the entepicondylar flange obliquely such that its ventral exit is positioned further distally. The distal part of the humerus has a deep oblique depression (olecranon fossa) facing laterally, with the latero-medial line forming the posterior (postaxial) border of this fossa (Fig. 4.6). The ulnar condyle is well rounded on the distal surface, and is positioned within the olecranon fossa (Fig. 4.6).

Both the proximal and distal portions of the *Titanosuchus ferox* humerus are less lateromedially expanded than those of the *Jonkeria truculenta* humerus (see later) and is one of the diagnostic features separating these humerus morphs.

From the sample available in museum collections, the *Titanosuchus ferox* humerus ranges in length from a subadult individual (BP/I/7380: 400mm long) to an adult (SAM-PK-11881:

620mm long). The smallest humerus (BP/1/7380) has a short and wide shaft (125 x 120mm) and has a relatively long deltopectoral crest (320mm) for a humerus that size. Although the distal end of the humerus is weathered and broken, it terminates as a knoblike extremity (Fig. 4.6. b). The same morphology is observed for the holotype specimen (NHMUK 49369) (Fig. 4.6.a).

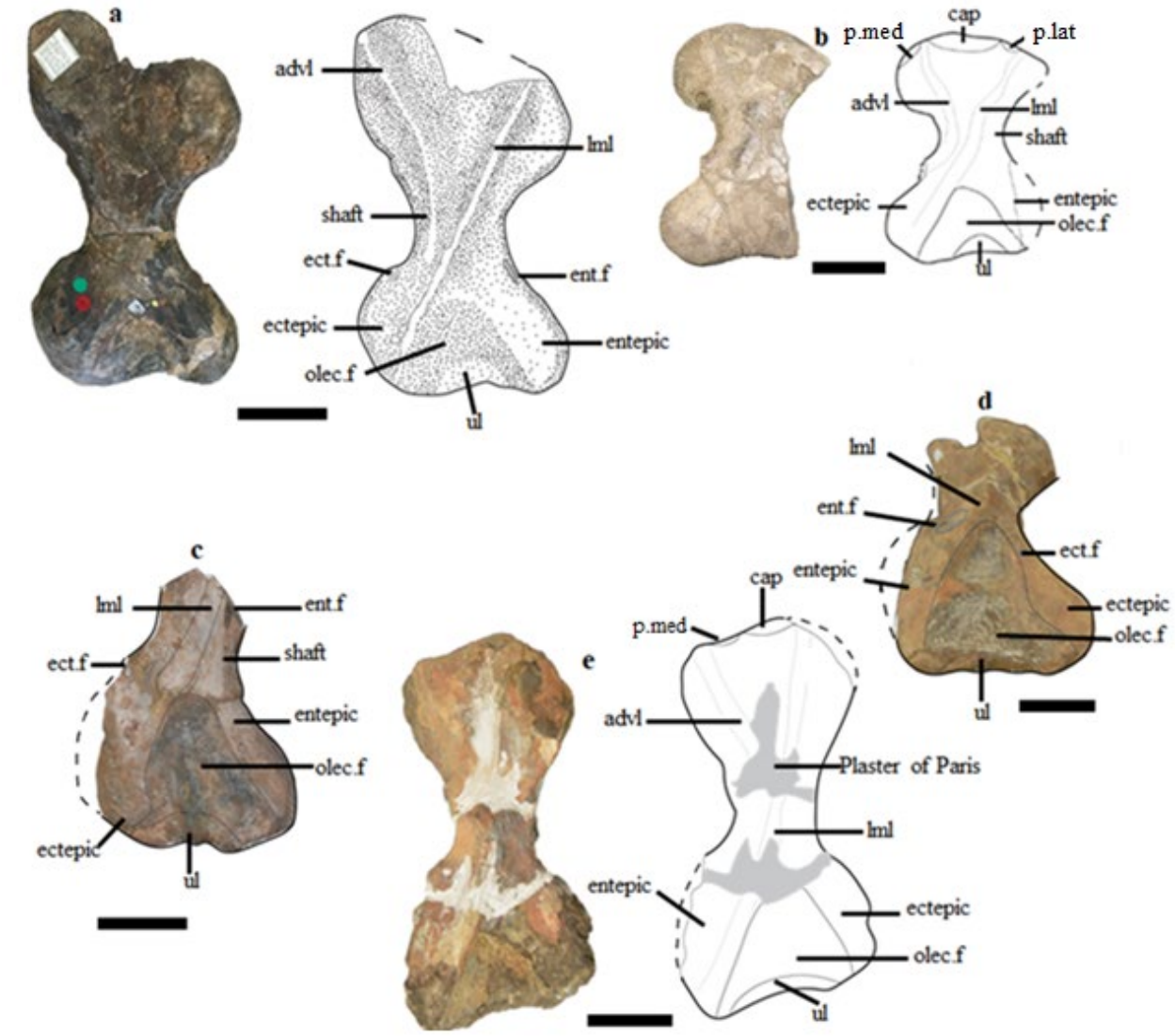

Fig. 4.6. Photographs and illustrative drawings of humeri of *Titanosuchus ferox* in dorsal view; **a.** NHMUK 49369; **b.** BP/I/ 7380; **c.** SAM-PK- 773 (proximal part missing); d. SAM-PK-11578 (proximal part missing); e. SAM-PK-11881. **a**, **b** and **d** are left humeri; **c** and **e** are right humeri that were flipped 180° for comparison with the left humeri. Scale bars represents 10cm.

4.3.1.2 *Jonkeria truculenta* humerus

The available sample of *Jonkeria* humeri comprises elements of different sizes, with the smallest (SAM-PK- 9149) being 312mm long and the largest (SAM-PK- 3433) estimated to be 506*mm long (asterisk represents incomplete bone). The *Jonkeria truculenta* humerus is a dump-bell shaped massive bone with greatly expanded proximal and distal ends and the proximal width being much greater than the distal width in dorsal view. The shaft is very short and broad. In ventral view, the caput of the *Jonkeria* humerus is oval in outline. It is thick, and extends into the deltopectoral crest, which reaches far proximally along the ventral face reaching the plane of the entepicondylar foramen (Fig. 4.7). The proximal half of the humerus comprises a large and relatively deep triangular biccipital fossa that extends to the middle of the shaft (Fig. 4.7).

The shaft is very short and greatly constricted in the central portion when compared to that of *Titanosuchus* (Fig. 4.7) and the twist of the shaft varies from 15 – 30 degrees and is less than that of *Titanosuchus*. The distal end of the ventral surface has a large and massive radial condyle with a height ranging from 108mm in SAM-PK-9149 to 133mm in the larger AMNH 5577. The radial condyle is very strong and extends far proximally along the ventral surface, and in the smallest specimen (SAM-PK-9149), it almost reaches the base of the delto-pectoral crest (Fig. 4.7.b).

In dorsal view, the humeral head (caput) is flanked by the processus medialis and processus lateralis (Fig. 4.8.a). The processus medialis lies very far distally of the plane in which the caput lies for specimen SAM-PK-4343 (Fig. 4.8.a) and less slightly so in specimens SAM-PK- 9149, AMNH 5577, SAM-PK-3433, SAM-PK-5014 and SAM-PK-738 (Figs. 4.8. b, c, d). The antero-dorso ventral line in *Jonkeria truculenta* humeri, as in *Titanosuchus ferox,* is strongly developed

with a strong swelling on the dorsal surface (Fig. 4.8) and terminates closer to the entepicondyle (Fig. 4.8. a, b, c). The latter is a strongly developed thick plate of bone, and the dorsal opening of the entepicondylar foramen is large and slitlike compared to the smaller and rounded ectepicondylar foramen. The ectepicondyle is developed as an outflaring thick sheet of bone pierced obliquely by a small ectepicondylar foramen positioned well away from the edge of the bone (Fig. 4.8).

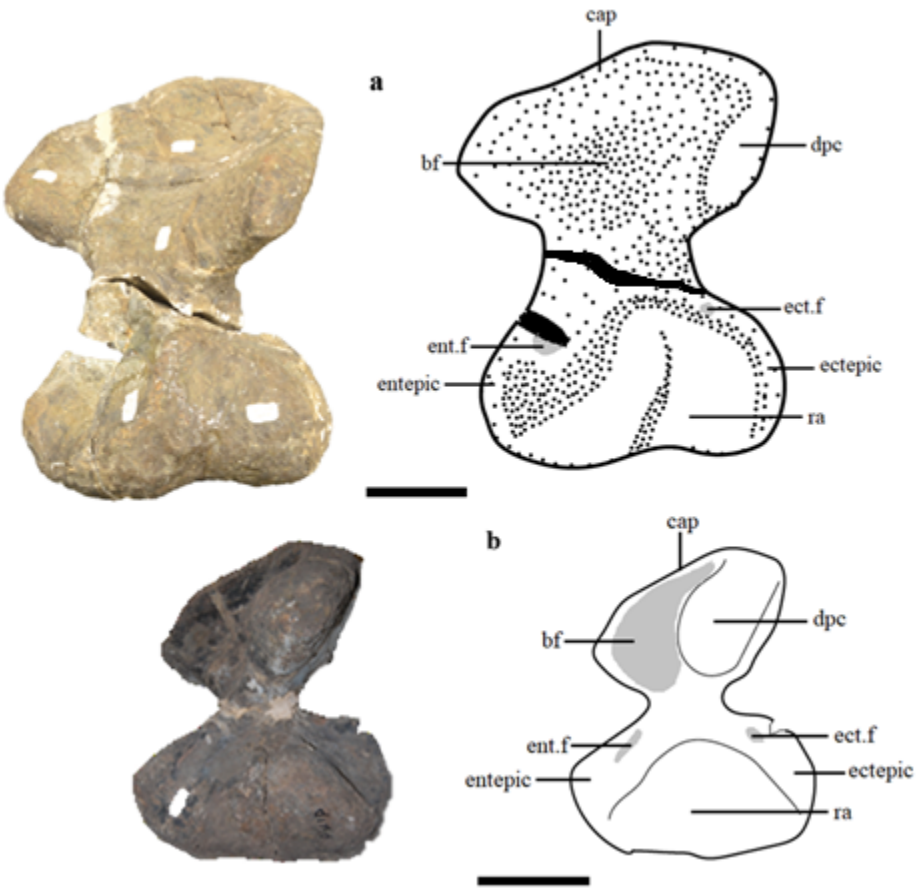

Fig. 4.7. Photographs and illustrative drawings of *Jonkeria truculenta* humeri in ventral view. **a.** SAM-PK- 4343; **b** SAM-PK-9149**;**. **a**, and **b** are right humeri which were flipped for comparison with the rest. Scale bars represent 10cm

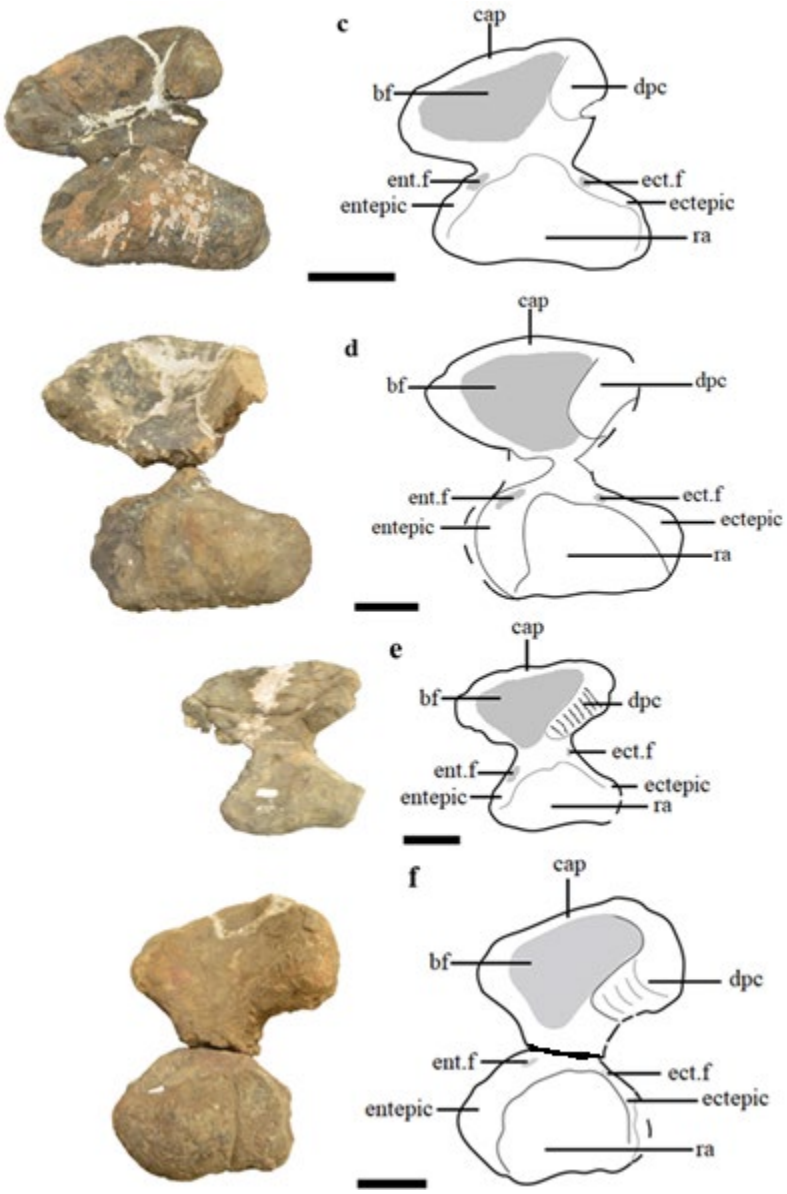

Fig. 4.7. **continued**: Photographs and illustrative drawings of *Jonkeria truculenta* humeri in ventral view. **c.** AMNH 5577; **d.** SAM-PK- 3433; **e**. SAM-PK-5014; **f.** SAM-PK-738. All (c-f) are left humeri humeri. Scale bars represent 10cm.

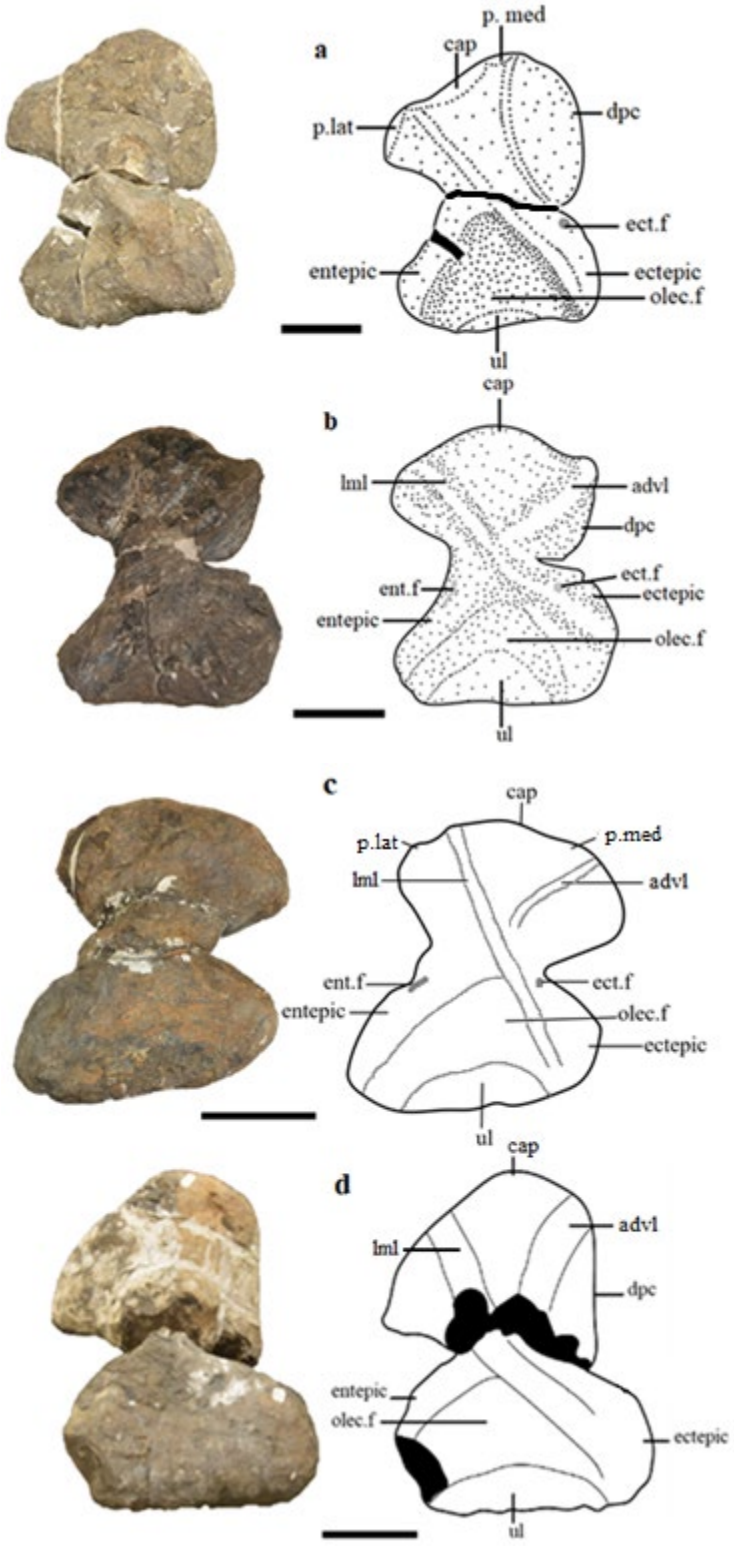

Fig. 4.8. Humeri of *Jonkeria truculenta* in dorsal view. **a**. SAM-PK- 4343; **b.** SAM-PK- 9149; **c.** AMNH 5577; **d.** SAM-PK- 3433. **a** and **b** are right humeri flipped for comparison with **c** and **d** which are left humeri. Scale bars represent 10cm.

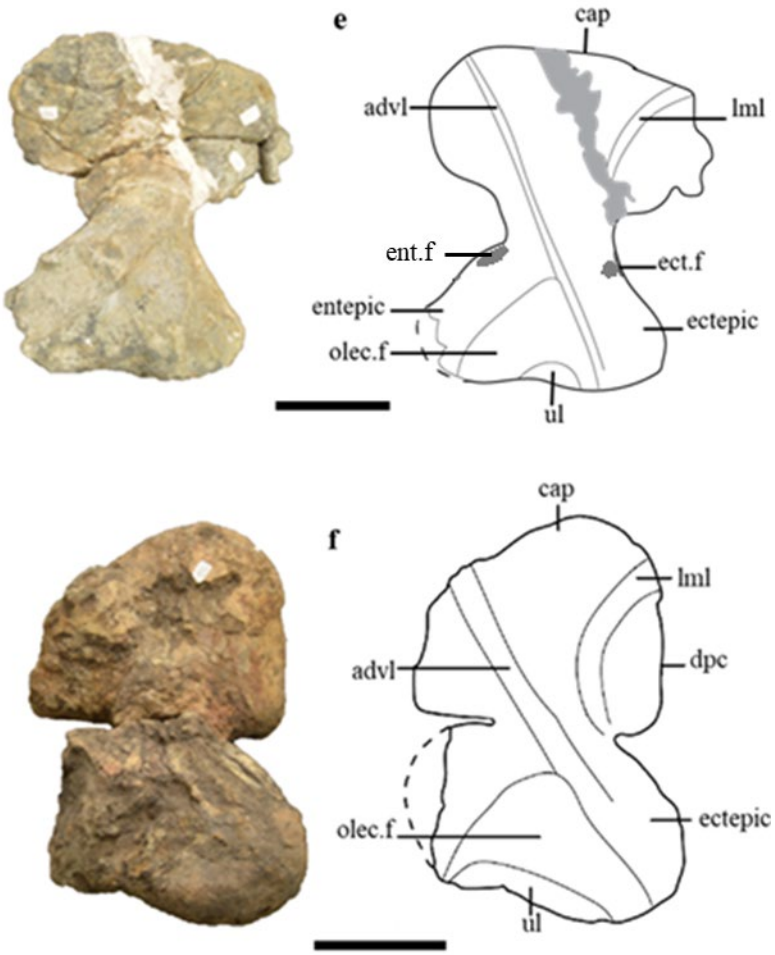

Fig. 4.8. continued: Humeri of *Jonkeria truculenta* in dorsal view. **e.** SAM-PK- 5014; **f.** SAM-PK- 738. Both **e** and **f** are left humeri. Scale bars represent 10cm

The distal end of the humerus bears the articulation surface for the radius and ulna. At this point is the base of the triangular olecranon fossa and its apex is in line with the ect- and ent-epicondylar foramina. The ulnar condyle is present at the base of the olecranon fossa (Fig. 4.8).

4.3.2 Ulna

Only five titanosuchid ulnae were available for study and are preserved in various degrees of completeness (AMNH 5577, SAM-PK- 4343, SAM-PK- 5014, SAM-PK- 9002, and SAM-PK-

9147) (Fig.4.9). Only one ulna is preserved of *Titanosuchus ferox* (SAM-PK- 9163) and it is so similar in morphology to those of *Jonkeria truculenta* that only one morphological description is presented here.

Titanosuchid ulnae are fairly large to very massive bones (length 350 - 402 mm) with a greatly expanded proximal end and a broad and flattened shaft. The radius and ulna proximal facets form one continuous facet for articulation with the humerus. The ulna is more anteroposteriorly flattened and more robust than the radius. The proximal end of the ulna is expanded but the bone tapers distally such that the distal end is narrower than that of the radius as demonstrated in specimen SAM-PK-5014 where both ulna and radius are preserved, the ulna distal width is 109 mm compared to 131 mm for the radius.

In lateral view (Fig. 4.9), the proximal end of the ulna has a large surface for articulation with the humerus on the preaxial surface. In this view, the ulna is widest over the coronoid process. As in the basal tapinocephalid *Tapinocaninus pamelae* (Rubidge *et al*., 2019), in the proximal third of the bone is a prominent tuberosity which tapers ventrally to form a ridge. In front of this tuberosity is a shallow inverted triangular fossa, which is bordered by ridges anteriorly, posteriorly, and dorsally (Fig. 4.9). A concave rim next to the coronoid process serves as the articulation for the radius such that in articulation the sigmoid face of the ulna is continuous with the proximal face of the radius thereby forming a conjoined articulatory surface for the humeral head. The saddle shaped articulatory surface of the distal end is very pronounced in SAM-PK-4343, SAM-PK- 9006 and SAM-PK- 9163 (Fig. 4. 9. a, d, e), but in specimen AMNH 5577 the distal end is more rounded, possibly due to weathering (Fig. 4.9.b). At the distal end of the ulna is another ridge that extends antero-posteriorly and is well developed in specimens SAM-PK-

4343 and SAM-PK-9163 (Fig. 4.9. a, e), but less pronounced in specimens SAM-PK-5014 and SAM-PK-9002 (Fig. 4.9. c, d) and is sheared off in specimen AMNH 5577 (Fig. 4.9. b).

On the surface of the ulna facing the radius there is a ridge (Fig 4.9), possibly for the insertion of the interosseus ligament (Boonstra, 1955a) and the anterior surface bears a long, deep, broad furrow for the hand flexors (Boonstra, 1955a).

In medial view a prominent fossa is present on the posterior half of the ulna and is bordered by prominent ridges anteriorly and posteriorly (Fig. 4.10). The fossa is widest proximally, as it fades into the shaft toward the anterior end. The olecranon, though well ossified proximally, is not well developed except in SAM-PK-5014 where the olecranon is elongated as a thick outgrowth caused as a result of taphonomic deformation. (Fig.4.10.c).

Near the distal end, the posterior surface of the ulna is drawn into a wide, rounded ridge with the facet for the ulnare at the distal end.

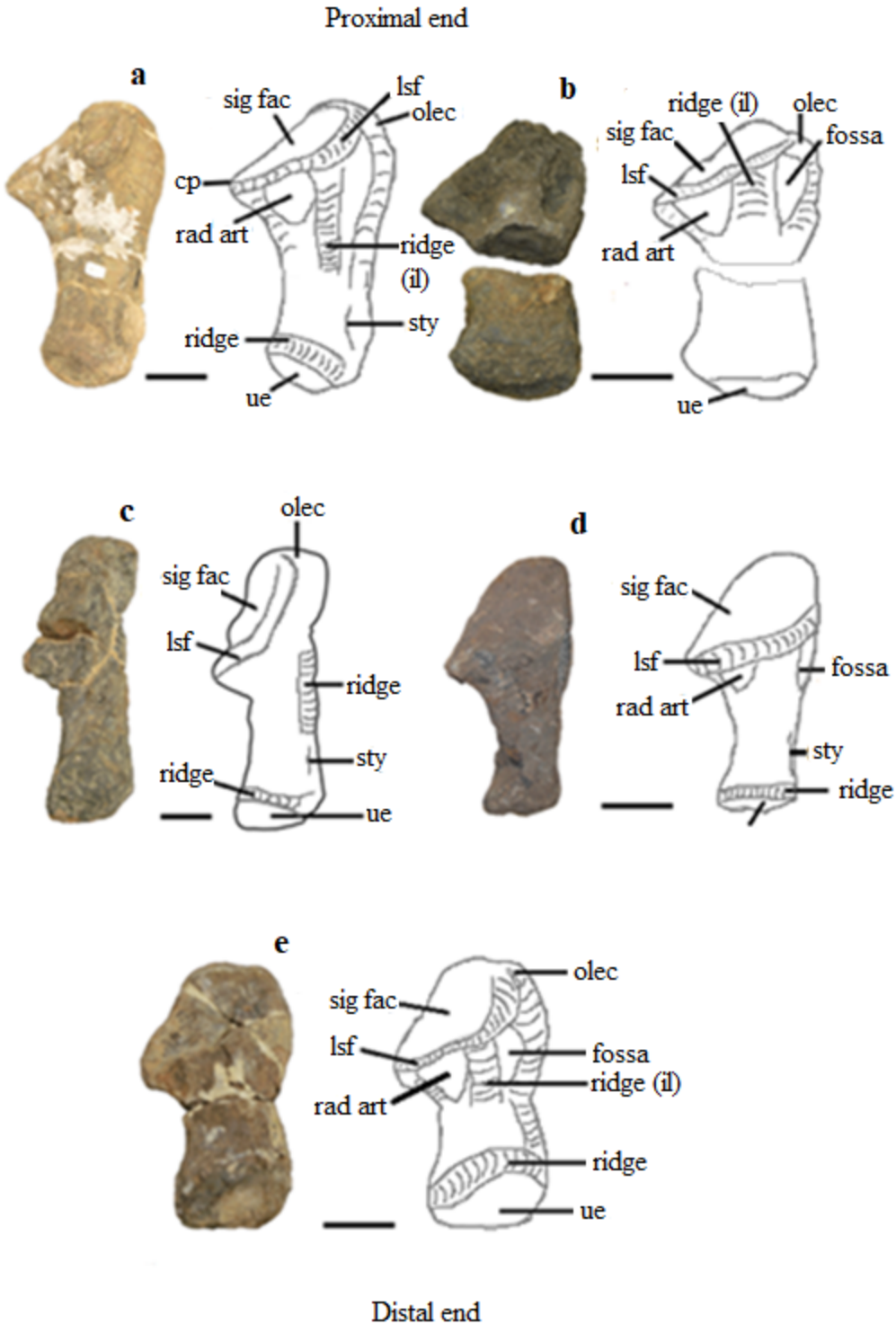

Fig. 4.9. Lateral view of titanosuchid left ulnae. a. SAM-PK- 4343 (*J. truculenta*); b. AMNH 5577 (*J. truculenta*); c. SAM-PK- 5014 (*J. truculenta*); **d.** SAM-PK- 9002 (*J. truculenta*); **e.** SAM-PK- 9163 (*T. ferox*). Ridge (il) = ridge for the insertion of the interosseus ligament. Scale bars represent 10cm.

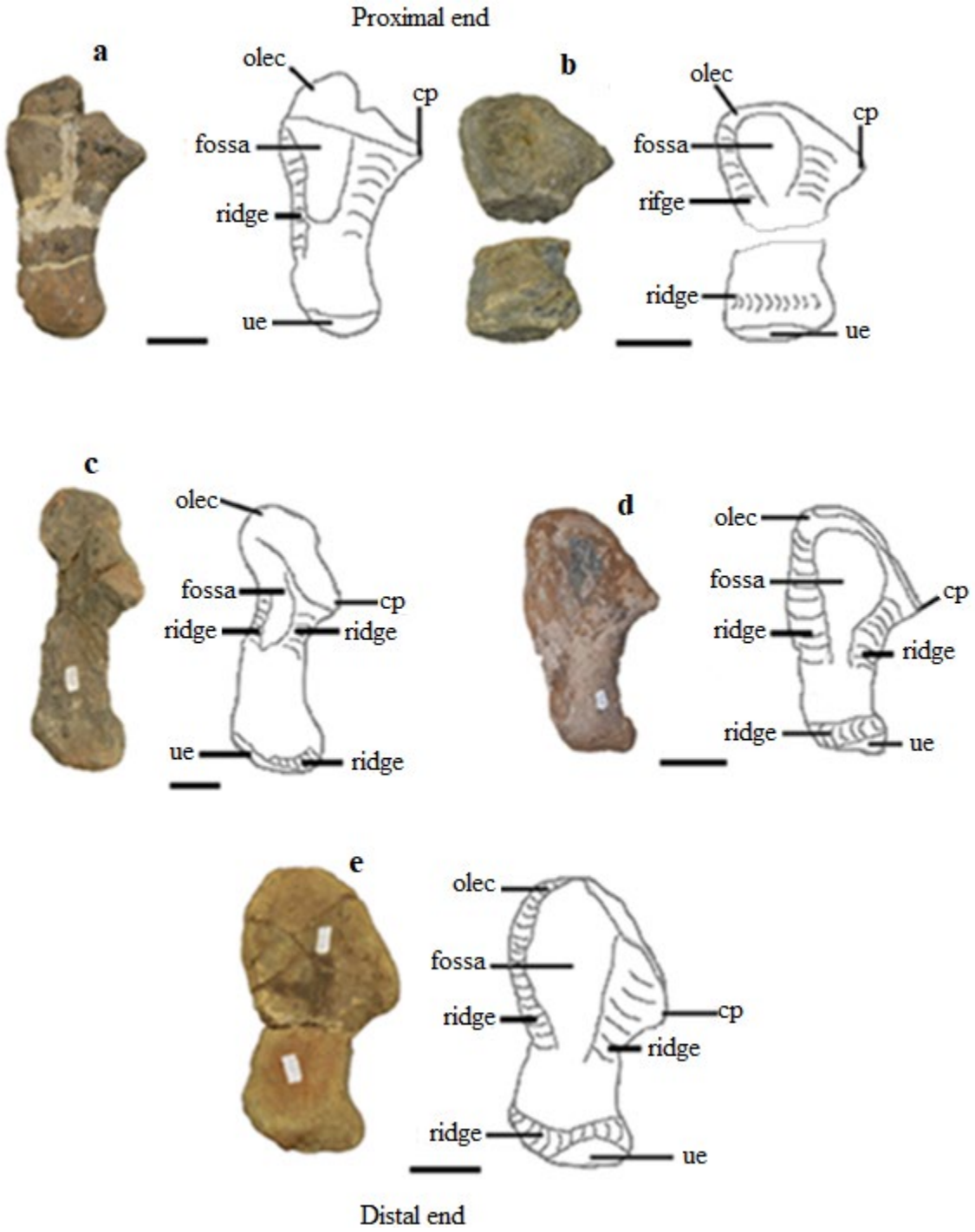

Fig. 4.10. Medial view of the titanousuchid left ulnae. **a.** SAM-PK- 4343 (*J. truculenta*); **b.** AMNH 5577 (*J. truculenta*); **c.** SAM-PK- 5014 (*J. truculenta*); **d.** SAM-PK- 9002 (*J. truculenta*); **e.** SAM-PK- 9163 (*T. ferox*). Scale bars represent 10cm.

4.3.3 Radius

Only two titanosuchid radii, which are roughly the same size, were available for this study (*T. ferox*: SAM-PK- 11299, right radius and *J. truculenta*: SAM-PK- 5014, left radius). These are associated with humeri/cranial elements and can be identified to species level. Both radii display similar morphology with only slight differences and will thus be described together.

The radius is a large robust cylindrical limb bone with expanded ends with the planes of the proximal and distal expansions slightly twisted relative to each other. It is a stout and short bone, significantly shorter than the ulna, and has a robust shaft. The proximal end is more expanded than the distal end (Fig. 4. 11. a, b, c), and both ends and shaft are oval in section. In anterior view, the proximal end has a medial flange for the insertion of the biceps muscle (Boonstra, 1955a). The proximal articulation is concave with a concave lateral edge, which abuts against the ulna. The proximal expansion is wider in the *Titanosuchus* specimen than it is for its *Jonkeria* counterpart and also the shaft outline is more concave (dumpbell shaped) for specimen SAM-PK-11299. The distal articulation facet is also concave and has a small facet for the radiale and a larger one for the intermedium (Fig. 4.11. a, c). From the pitted nature of the bone surface of the articulation facets it appears these were covered with a substantial layer of cartilage in life possibly to cushion the joint from mechanical wear during locomotion (King, 1988).

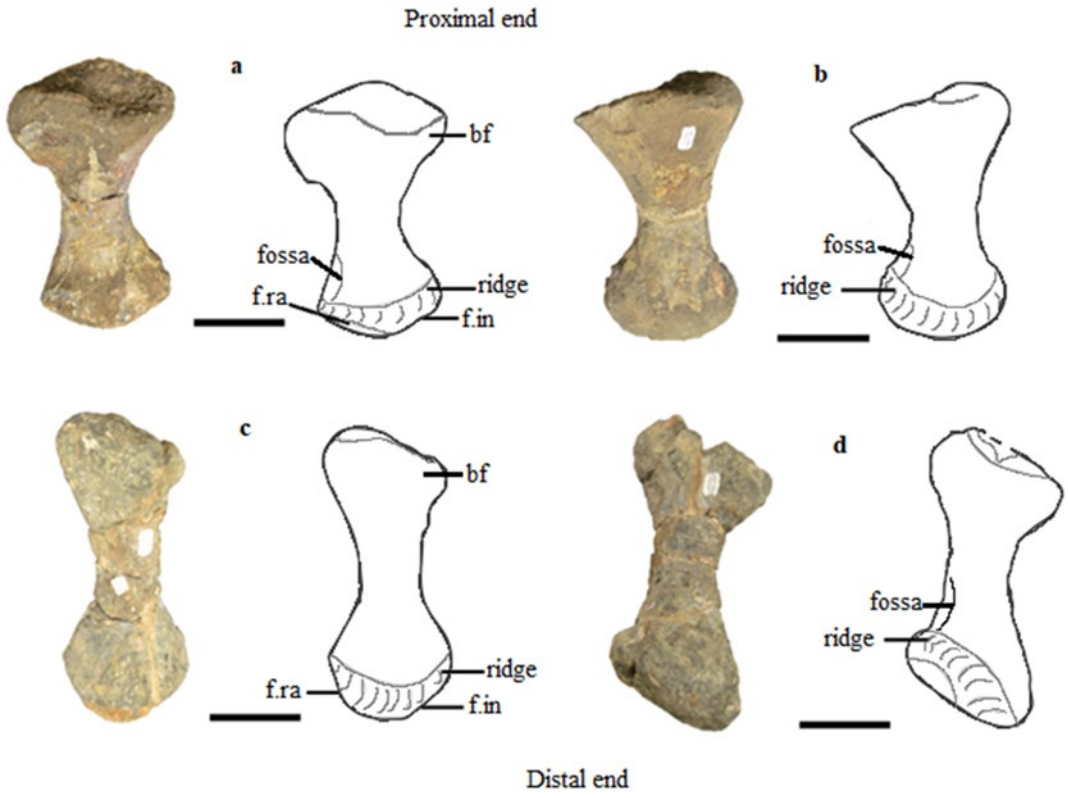

Fig. 4.11. Titanosuchid radii in anterior and posterior view; **a.** *T. ferox:* SAM-PK-11299 (anterior view); **b.** *T. ferox;* SAM-PK- 11299 (posterior view); **c.** *J. truculenta*: SAM-PK- 5014 (anterior view); **d.** *J. truculenta;* SAM-PK- 5014 (posterior view). SAM-PK- 11299 is the right radius and SAM-PK- 5014, the left radius, has been flipped for comparison. Scale bars represent 10cm.

Both radii have a ridge on the lateral side towards the distal end of the bone bordering on a more proximal fossa which is visible on both the anterior and posterior sides of this limb element in *Titanosuchus* (Fig. 4.11. a, b,) but not visible in the anterior view of the *Jonkeria* specimen SAM-PK-5014 (Fig. 4.11. c).

It should be noted that the *Jonkeria* specimen SAM-PK- 5014 suffered taphonomic deformation and has a weak bicipital flange (Fig. 4. 11. c, d). This specimen also has a strong ridge bordering

the distal articulation surface (Fig. 4. 11. c, d) and both the proximal and distal ends of the radius are slightly obliquely slanted.

As each genus is represented by only a single radius specimen and that of *Jonkeria* is deformed it is not possible to determine whether the slight differences in morphology (shape of the proximal and distal ends, slight curvature of the lateral outline for the shaft of SAM- PK- 5014) can be attributed to generic differences or are a consequence of taphonomic distortion.

4.3.4 Femur

The femur, which is longer than the humerus in specimens where both bones are preserved (e. g. NHMUK 49368, SAM-PK- 5001 and SAM-PK- 5014), is a massive bone with a relatively long, broad and flat shaft and expanded proximal and distal ends. The femoral head projects medially and somewhat dorsally, and both an internal and external trochanter are present on the ventral surface. The medial face of the femur is strongly concave with the thickened femoral head directed medially for *Titanosuchus* SM-PK-11491, SAM-PK-9127 and *Jonkeria* SAM-PK-5014 (Fig.4. 12. b, d, e) and less so for *Titanosuchus* NHMUK 49368 and SAM-PK-5001 (Fig. 4. 12. a, c). Except for the holotype specimen, all the *Titanosuchus ferox* femora are robust with a more inflected femoral head posteriorly. The holotype is less robust with a less inflected femoral head (Fig. 4.12.a). The *Jonkeria* femur of SAM-PK-5014 is more gracile than other *Jonkeria* femora and is similar to that of the *Titanosuchus ferox* holotype, but unlike the *T. ferox* holotype femur, its femoral head is more inflected as in the other *Titanosuchus* femora (Fig. 4. 12. b, c, d, e).

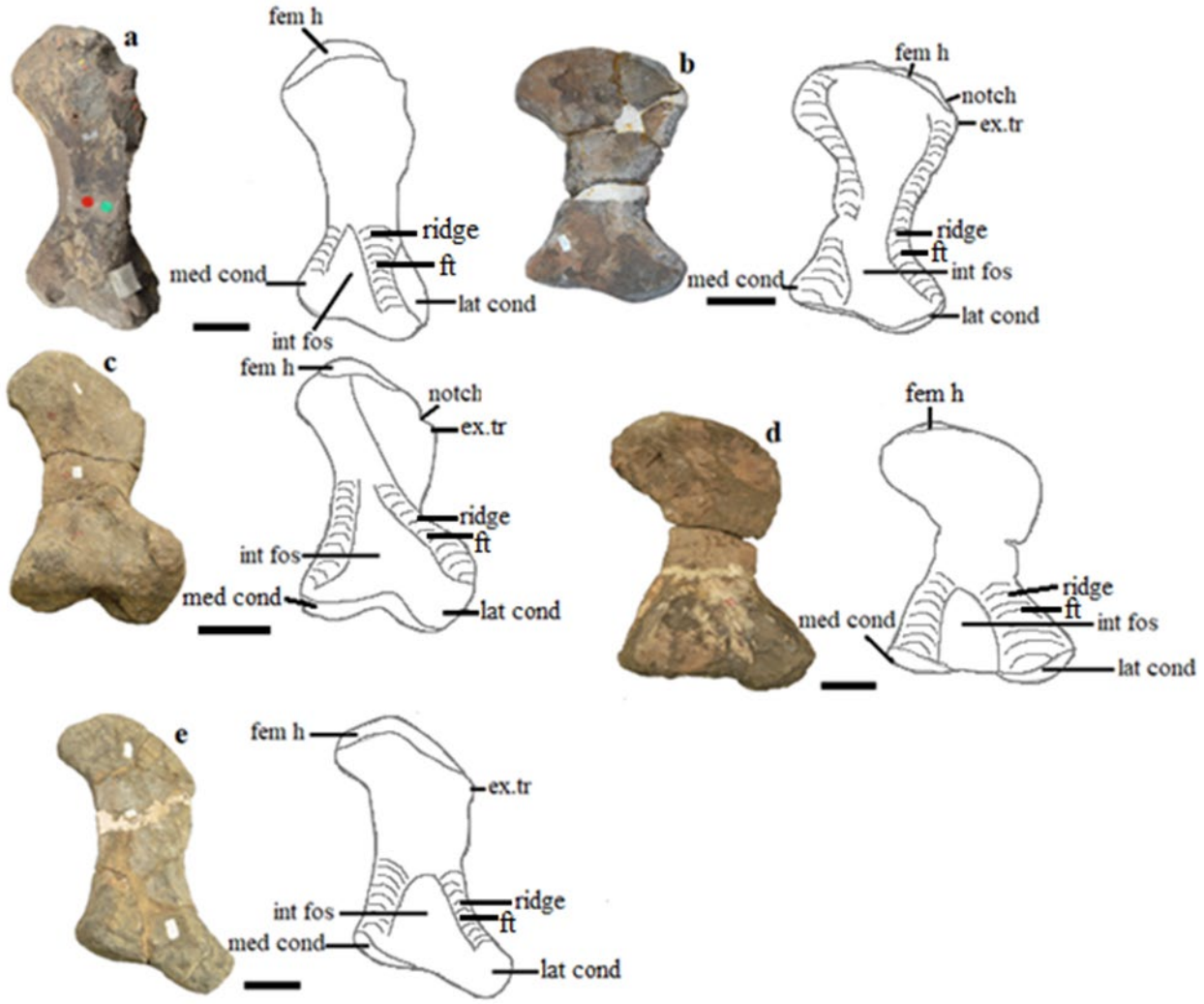

Fig. 4.12. Titanosuchid femora in anterior view. **a.** *T. ferox*: NHMUK 49368 (holotype); **b.** *T. ferox*: SAM-PK-11491; **c.** *T. ferox*: SAM-PK- 5001; **d.** *T. ferox*: SAM-PK- 9127; **e.** *J. truculenta*: SAM-PK- 5014.All are left femora except **b** which was flipped for comparison. Scale bars represent 10cm.

Laterally the femoral head tapers gently towards the external trochanter from which it is separated by a slight notch. This notch is particularly visible in SAM-PK- 5001 and SAM-PK-11491 (Fig. 4.12. b and Fig. 4.12.c). As this part of the femoral head is weathered in specimens NHMUK 49368 and SAM-PK- 9127 (Fig.4.12. a, d and Fig. 4.13. a, d) the notch is not

preserved. On its medial side, the femoral head is convex and fits into the acetabulum of the pelvic girdle.

The external trochanter is positioned far laterally to form the proximo-lateral corner of the femur; from here the postaxial edge of the bone sweeps inwards with a fairly straight edge to the shaft and further distally extends laterally to form the outer border of the lateral condyle (Fig. 4. 12 and Fig.4. 13). The anterior view of the femur shows a very shallow intercondylar fossa and, from the lateral condyle, an oblique ridge extends proximally toward the femoral head (Fig. 4. 12). It has been postulated that the femoro-tibialis muscle (Fig. 4.12) had its origin on the middle part of this ridge (Boonstra, 1955a).

In posterior view, the proximal half of the femur is an ovoid tubercle, with the internal trochanter positioned almost centrally (Fig. 4. 13). A fossa is present posterior to the femoral head and probably served for insertion of the ilio-femoralis muscle (Boonstra, 1955). The medial portion of the proximal end is much more projected (inflected) than the lateral. The shaft is anteroposteriorly flattened. At the distal end of the femur the two articular facets for the tibia are rounded and separated by a deep and wide intercondylar sulcus (Fig. 4. 13). The intercondylar sulcus extends into a trough, which continues proximally and fades almost midway up the shaft (Fig. 4.13). In all the Titanosuchid femora, the lateral condyle is the largest and extends further distally than its medial counter-part with this condition being more pronounced for the *Jonkeria truculenta* specimen SAM-PK-5014 (Fig.4.12.e and Fig.4.13.e).

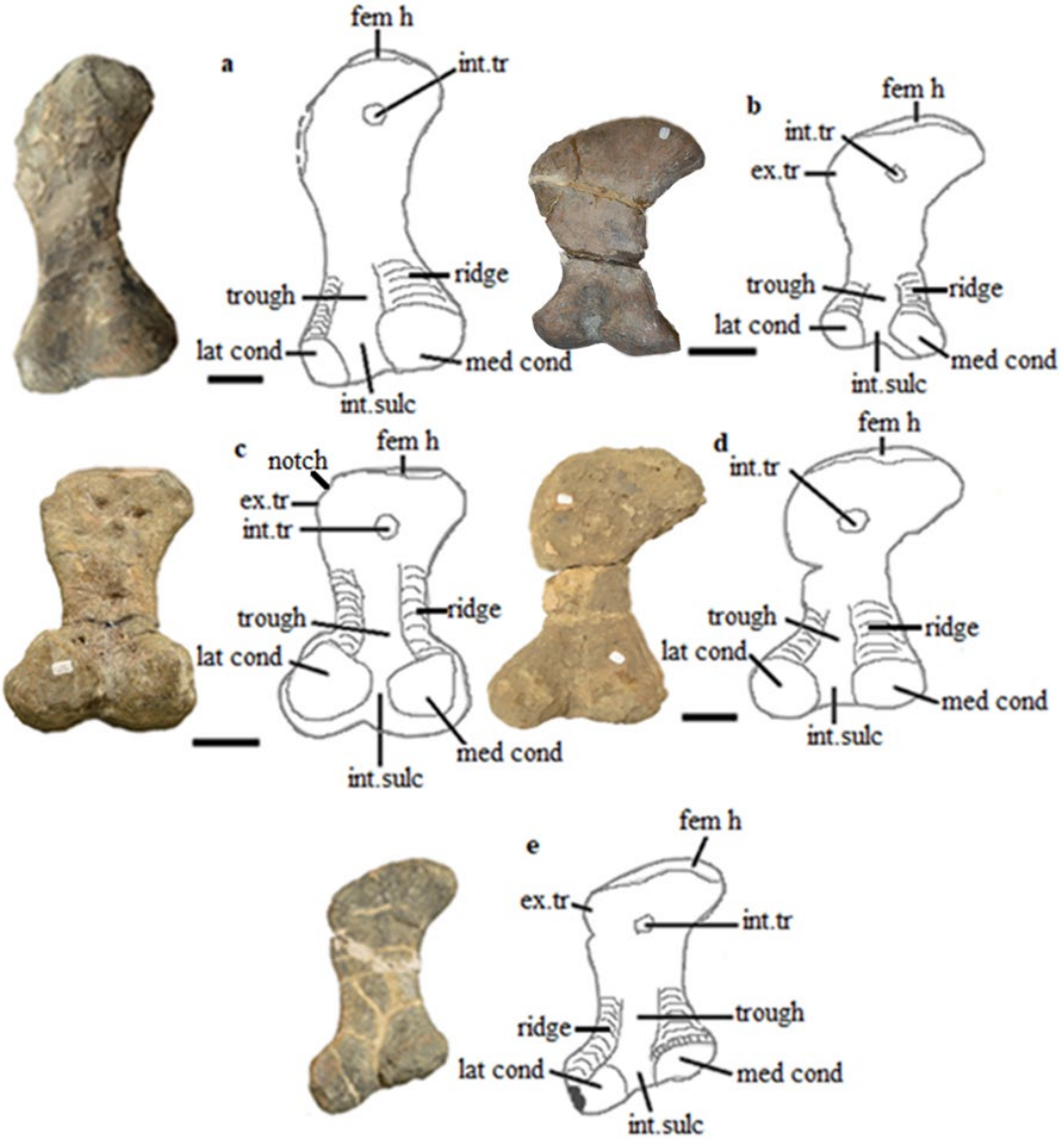

Fig. 4.13. Titanosuchid femora in posterior view; **a.** *T. ferox*: NHMUK 49368 (holotype); **b.** *T. ferox*: SAM-PK-11491; **c.** *T. ferox*: SAM-PK- 5001; **d.** *T. ferox*: SAM-PK- 9127; **e.** *J. truculenta*: SAM-PK- 5014; **a, b**, **d** and **e** are left femora and **b,** was flipped 180° for comparison. Scale bars represent 10cm

4.3.5 Tibia

In general morphology, the titanosuchid tibia resembles those of other dinocephalian taxa, being shorter than the femur. The tibia, represented by specimens SAM-PK- 11299, SAM-PK- 11488,

SAM-PK- 11938 (*T. ferox*) and SAM-PK- 5014, TM 212 (*J. truculenta*), is a massive, latero-medially flattened bone with a greatly enlarged proximal end relative to the distal end, which is more expanded in the *Titanosuchus ferox* specimens than it is in *Jonkeria truculenta*. A small tuberosity is present on the anterior surface and forms a gently sloping crest, the cnemial ridge (Fig. 4. 14) and this longitudinal ridge extends from the proximal end of the tibia towards the distal edge but fades into the shaft (Fig. 4.14.a, c, e, g). A longitudinal groove (cnemial groove), bordered by the cnemial ridge on its medial side, is present on the anterior surface and probably served for insertion of the flexor digitorum muscle (Boonstra, 1955a).

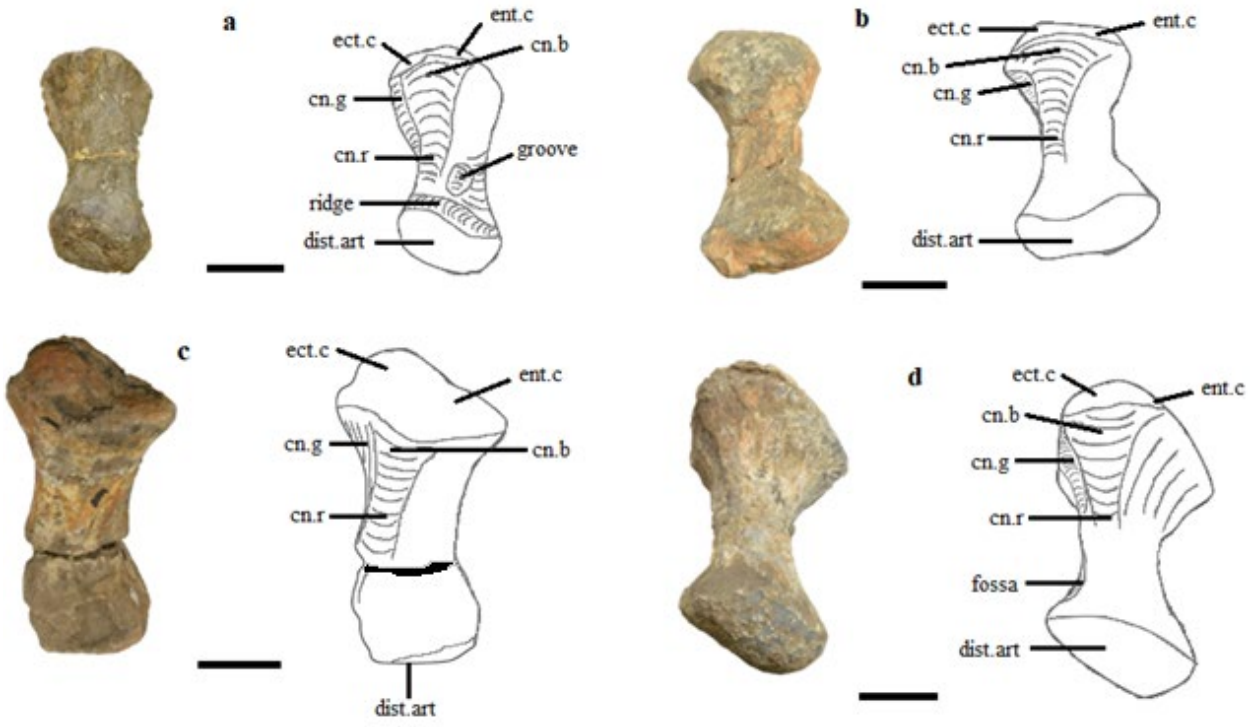

Fig. 4.14. Titanosuchid tibia in anterior view. **a.**TM 212 (*J. truculenta*); **b.** SAM-PK-5014 (*J. truculenta*); **c.** SAM-PK- 11299 (*T. ferox*) **d.** SAM-PK- 11488 (*T. ferox*). All are right tibia except SAM-PK- 5014, which is a left tibia flipped for comparison. Scale bars represent 10cm

On the proximal surface are two articulation sites for the femur, the facets for the lateral femoral condyle and the medial femoral condyle (Fig. 4. 14.c). On the distal end there is a distal articulation surface for the astragalus (Fig. 4.14 and Fig. 4.15).

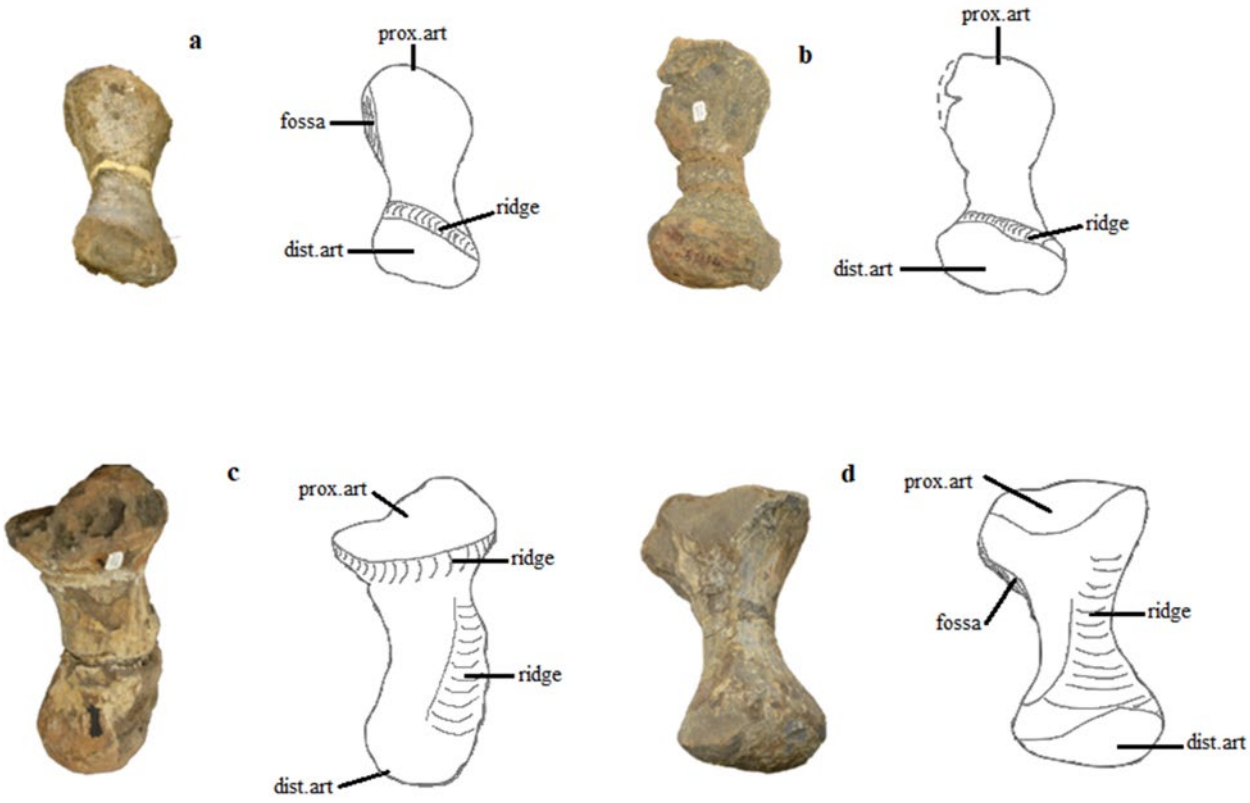

Fig. 4.15. Titanosuchid tibia in posterior view. **a.**TM 212 (*J. truculenta*); **b.** SAM-PK-5014 (*J. truculenta*); **c.** SAM-PK-11299 (*T. ferox*); **d.** SAM-PK- 11488 (*T. ferox*). All are right tibia except SAM-PK- 5014, which is a left tibia flipped for comparison. Scale bars represent 10cm. Abbreviations. dist.art. distal articulation; prox.art. proximal articulation.

4.3.6 Fibula

This hind limb element is represented in four *Titanosuchus* (SAM-PK- 9127, SAM-PK- 9163, SAM-PK- 11488 and SAM-PK-11989) and two *Jonkeria* (SAM-PK- 4343 and SAM-PK- 5014) specimens, and the morphology of the fibulae is the same in both species.

The fibula is characterized by a deeply concave anterior face along the length of the midline and a straight posterior face. In specimen SAM-PK- 11488 the proximal expansion is larger than the distal one (Fig. 4.16. d). In specimens SAM-PK- 9127, SAM-PK- 9163, SAM-PK- 11989, and SAM-PK- 5014 the proximal and distal ends are subequal (Fig. 4.16.a, b, c, e) and in specimen SAM-PK- 4343 (Fig. 4.16.f) the distal end is broken. The fibula shaft is long, fairly wide but flattened, and slightly twisted (Fig.4. 16. a, b, c, e and Fig.4.17. a, b, c, e).

The proximal articulation surface is convex in section (Fig. 4. 16 and 4. 17) with a reniform outline, which is more apparent in specimens SAM-PK- 9127, SAM-PK- 9163, SAM-PK- 11989 and SAM-PK- 5014 (Fig. 4. 16. a, b, c, e). In anterior view, there is a ridge close to the head of this bone (Fig. 4.16. a, b, c, e), which most likely is for the insertion of the iliofibularis muscle (Boonstra, 1955a).

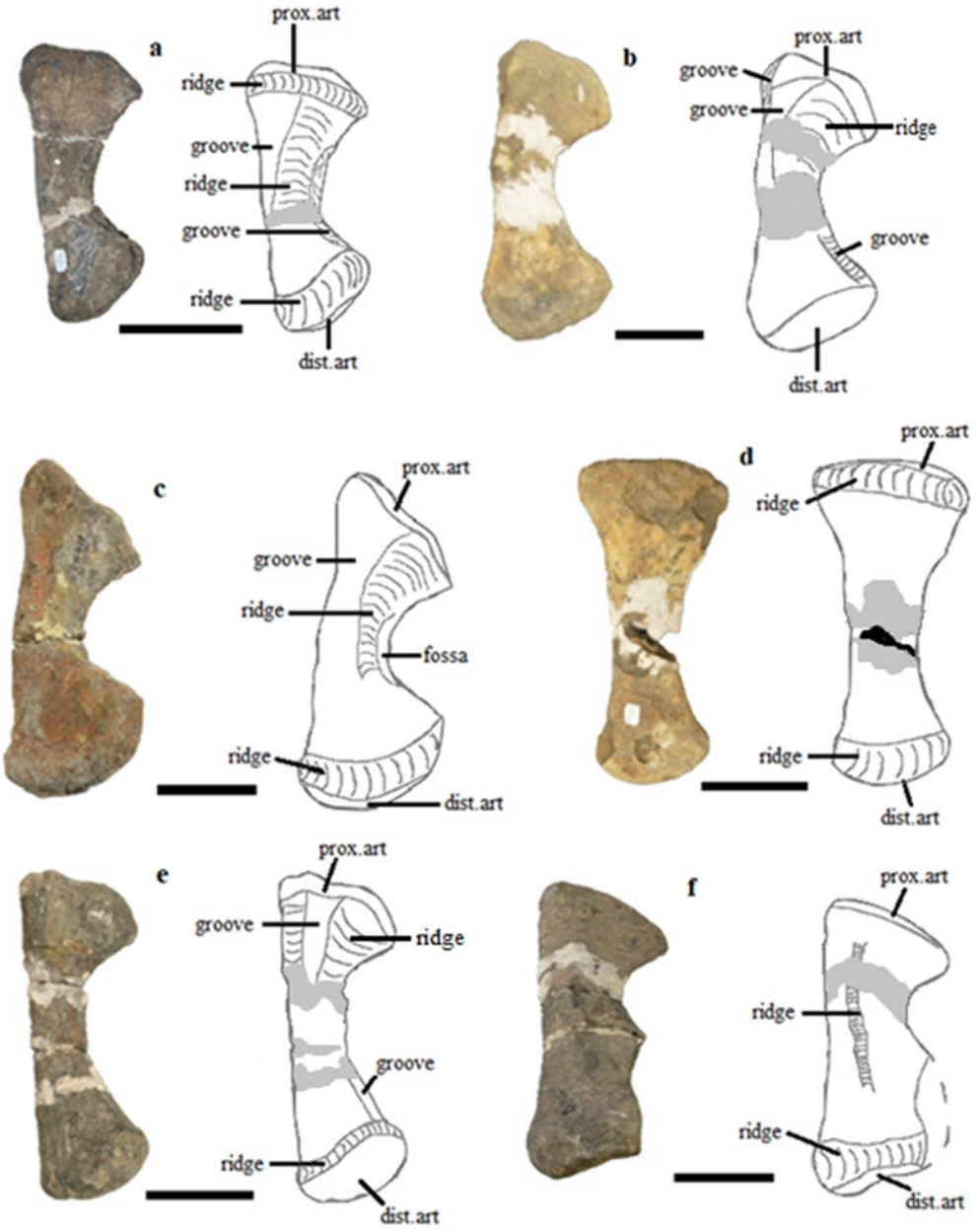

Fig. 4.16. Titanosuchid fibula in anterior view: **a.** *T ferox*: SAM-PK-9127; **b.** *T ferox:* SAM-PK-9163**; c.** *T. ferox*: SAM-PK- 11989; **d.** *T. ferox*: SAM-PK- 11488; **e.** *J. truculenta*: SAM-PK- 5014; **f.** *J. truculenta*: SAM-PK- 4343 Scale bars represent 10cm. Abbreviations. dist.art.= distal articulation surface; prox.art = proximal articulation surface.

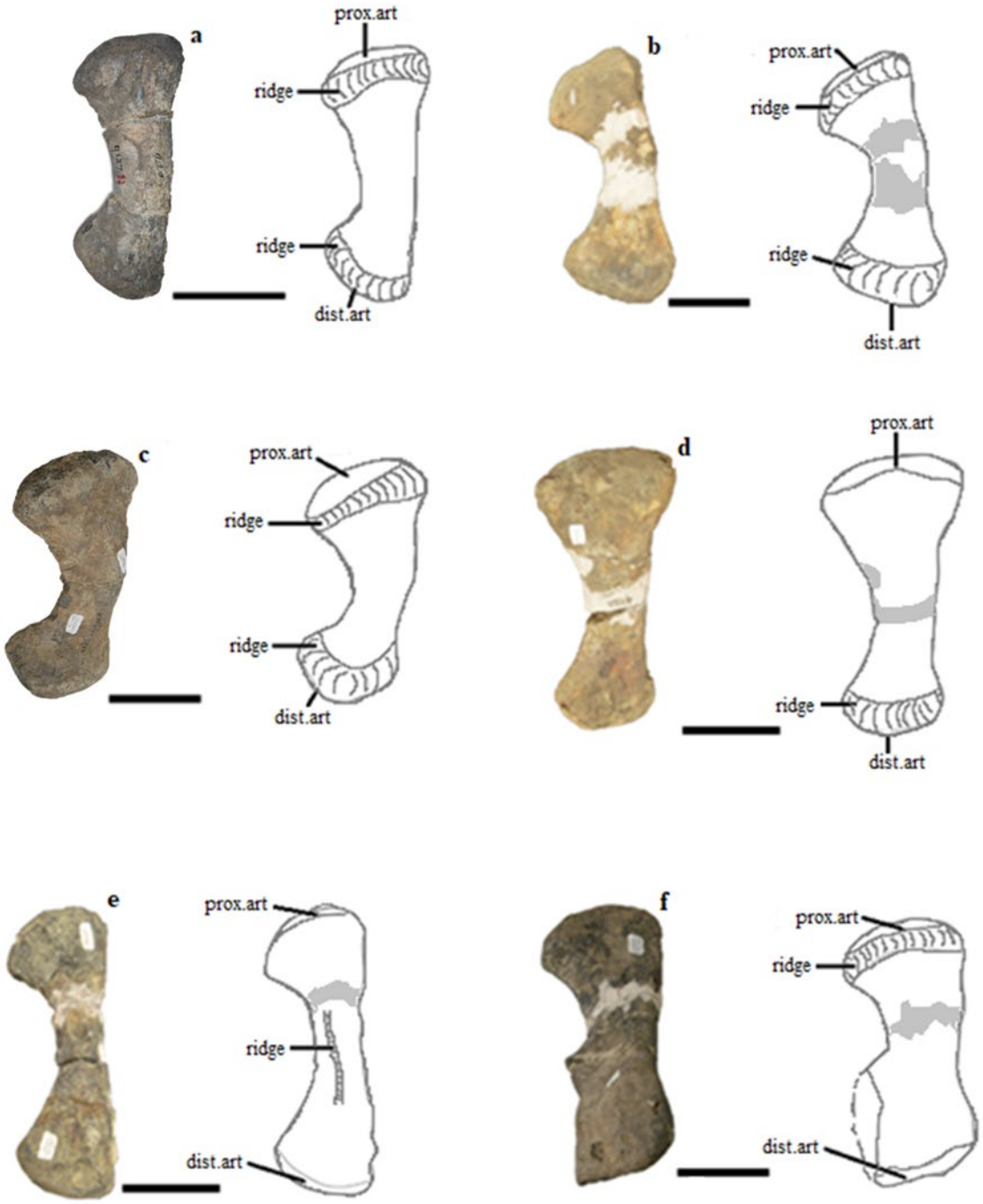

Fig. 4.17. Titanosuchid fibula in posterior view: **a.** *T ferox*: SAM-PK-9127; **b.** *T ferox:* SAM-PK-9163**; c.** *T. ferox*: SAM-PK- 11989; **d.** *T. ferox*: SAM-PK- 11488; **e.** *J. truculenta*: SAM-PK- 5014; **f.** *J. truculenta*: SAM-PK- 4343 Scale bars represent 10cm.

4.4. Principal component analysis

To demonstrate morphological disparity between the limb elements of *Jonkeria* and *Titanosuchus* a Principal Component Analysis (PCA) was undertaken using measurements of all titanosuchid limb bones in museum collections available for this study. Measurements for *Dimetrodon* (basal synapsid) and tapinocephalid postcranial elements were also included for comparison of the clustering of the various dinocephalian taxa relative to those of a basal synapsid. Tapinocephalids were included for comparison because it is the only other South African dinocephalian family where a representative sample of postcranial elements are preserved.

The PCA was conducted on a variance – covariance matrix, with 1000 bootstrap replicas. Only the scatter plots of the first two Principal Components (PC1 and PC2) are reported, because these represent more than 96.7% of the total variance in all cases (femur, 99.7%; fibula, 99.4%; humerus, 98.1%; radius, 99.8%; tibia, 100% and ulna, 99.4%). These first two Principal Components in the PCA summarize the primary sources of variance in the data.

To facilitate reading of bivariate plots, taxa of the same genus were connected by a convex hull (polygon), which provides an immediate estimate of the morphological disparity (i.e. occupied morphospace) and variability for each identified group. By convention, Principal Component loadings are considered significant if they are greater than 0.3 and smaller than -0.3 (Hammer and Harper, 2006) (Figures 4.18 – 4.23). The different clusters delimited by the convex hulls are more separated and distinct between the tapinocephalid and titanosuchid dinocephalian sample in the case of the ulna, femur, tibia and fibula (Fig. 4.19, Fig.4.21, Fig.4.22 and Fig. 4.23).

For the humerus (Fig. 4. 18), the loadings for Component 1 are all positively correlated and greater than 0.3 thus indicating that all the variables (total bone length, proximal, distal and shaft widths) contribute to the variation observed (Hammer and Harper, 2006) and probably indicates the absolute size of the specimens. For principal Component 2, only the proximal width and shaft width are significant and contribute marginally to the identification of variability for this limb bone. Proximal width and shaft width are inversely correlated, therefore, as the proximal width increases, the shaft width decreases proportionally. *Titanosuchus ferox* humeri occupy the same morphospace (pink convex hull polygon) while the *Jonkeria trucuclenta* humeri also cluster together (blue convex hull polygon) Tapinocephalids fall between these two Titanosuchid genera.

The ulna (Fig. 4.19) shows a positive correlation for Component 1 between proximal, distal and shaft widths while total length is insignificant whereas only total length and shaft width contribute to variability for Component 2. The two measurements (total length and shaft width) are inversely correlated hence larger taxa tend to have slender ulnas.

For the morphospace there is a clear separation between tapinocephalid and titanosuchid ulnae but no distinction between *Titanosuchus ferox* and *Jonkeria truculenta* ulnae with the only *Titanosuchus ferox* specimen in the sample (SAM-PK-9163) plotting within the *Jonkeria truculenta* polygon (Fig. 4.19).

For the radius (Fig. 4.20), the proximal, distal and shaft widths are significant for Component 1 and only the proximal width and shaft width contribute to variability for Component 2. The two variables (proximal width and shaft width) are inversely correlated, hence radii with a wider proximal head are more slender. The plot shows no differentiation between the radii of *Titanosuchus ferox* and *Jonkeria truculenta*.

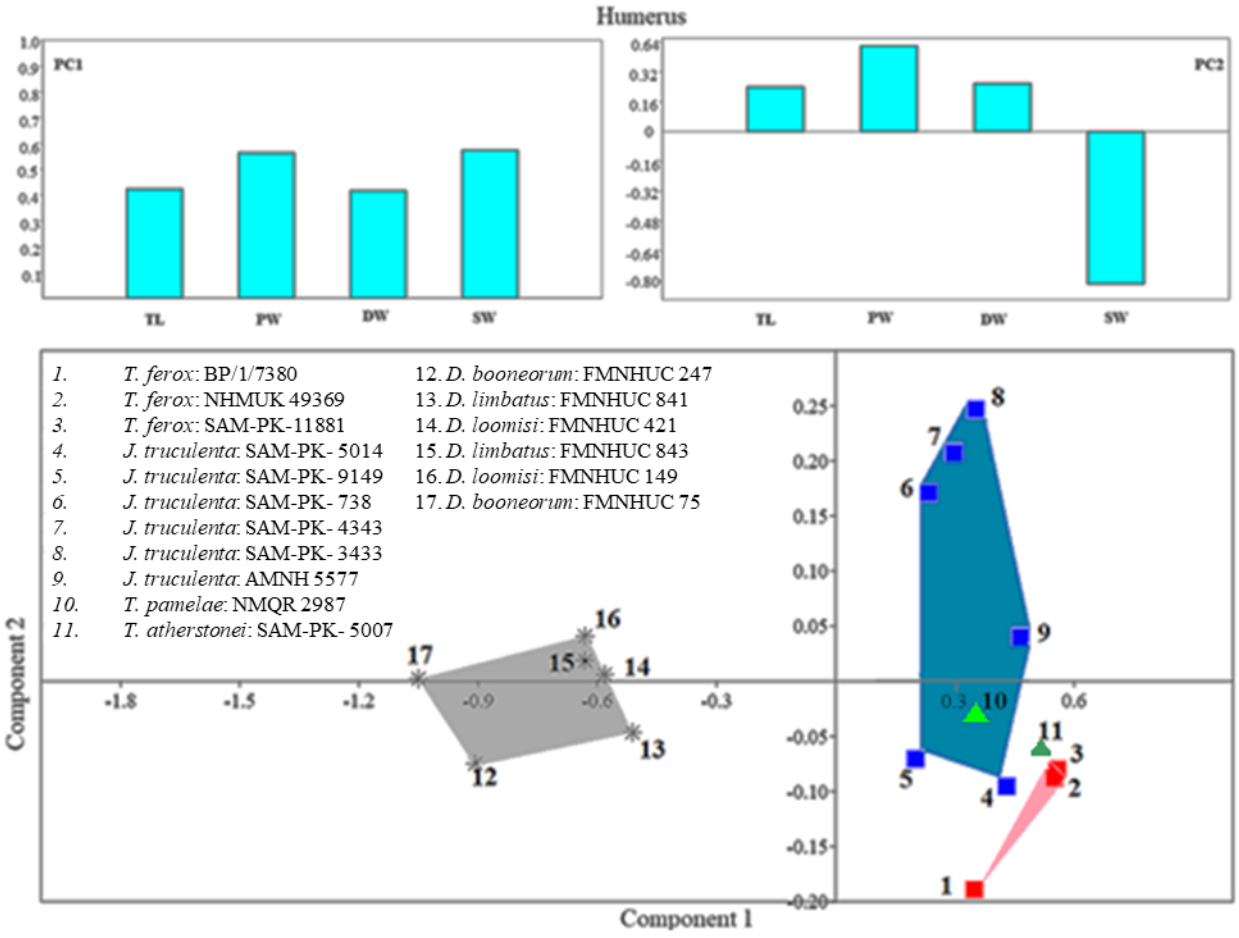

Fig. 4.18. Scatter plot and loadings of first and second principal components for all the studied humerus bones of *Titanosuchus* and *Jonkeria* and for comparison the tapinocephalids *Tapinocaninus* and *Tapinocephalus* and the basal synapsid *Dimetrodon*. TL, bone total length; PW, bone proximal width; DW, bone distal width; SW, bone maximal narrowing at mid shaft. Grey == *Dimetrodon*; Red = *Titanosuchus*; Blue = *Jonkeria*; Green is tapinocephalids.

In the hind limb the femur (Fig.4.21), for principal Component 1, all loadings are significant thus indicating the variation in absolute body size of the considered specimens. For Component 2, total length, proximal width and width of shaft are all significant variables contributing to the intraspecific variation observed within *Titanosuchus ferox*. So with increasing length the femora

become more slender with a less wide proximal head. There is a separation between tapinocephalid and titanosuchid femora and the only *Jonkeria truculenta* specimen represented in the sample (SAM-PK-5014) plots within the *Titanosuchus ferox* polygon. The titanosuchid femora are tightly clustered showing morphological stability except for specimen NHMUK 49368, which plots furthest from the rest of the *Titanosuchus ferox* femora (Fig.4.21).

Loadings for the tibia show that for Component 1 all loadings are significant, positive and directly correlated indicating once again variation in absolute body size whereas for Component 2, only total length and shaft width are significant, and the proximal width does not contribute significantly to variations observed for this limb element (Fig.4.22). It is to be noted also that the distal width is significant being greater than 0.3. The total length and width of the distal head are positively correlated, and are inversely related to the width of the shaft hence with increasing length the tibiae are more slender with a wider distal head. There is a slight distinction between the *Jonkeria truculenta* tibia (SAM-PK- 5014) and *Titanosuchus ferox* tibia and a clear seperation between *J. truculenta* specimen TM 212 with *T. ferox* tibia while there is a clear distinction between titanosuchids and tapinocephalids (expect for *Jonkeria truculenta* specimen TM 212) which plots more closely to the tapinocephalid polygon (Fig. 4.22).

In the fibula (Fig. 4.23) proximal, distal and shaft widths show a positive correlation for component 1 while for Component 2, total bone length, proximal and shaft width are significant. The proximal head length and width are directly correlated, and are inversely related to the shaft width, therefore, longer fibulae are more slender and with a larger proximal head in proportion.

There is differentiation between tapinocephalid and titanosuchid fibulae while there is no differentiation between *Jonkeria truculenta* specimen SAM-PK-4343 and *Titanosuchus ferox* fibulae as these bones appear to present a variation extreme in all the groups in relation to

component 2. (Fig. 4.23). The *Jonkeria truculenta* fibula (SAM-PK-5014) does not only show a differentiation with *Titanosuchus ferox* but also with its compatriot (SAM-PK- 4343). Morphologically, the fibula between the two Titanosuchid species is similar and this is also shown in the PCA plot where there is no differentiation between the *T. ferox* convex hull polygon and the two *J.truculenta* specimens (SAM-PK- 4343 and SAM-PK- 5014 (Fig. 4.23).

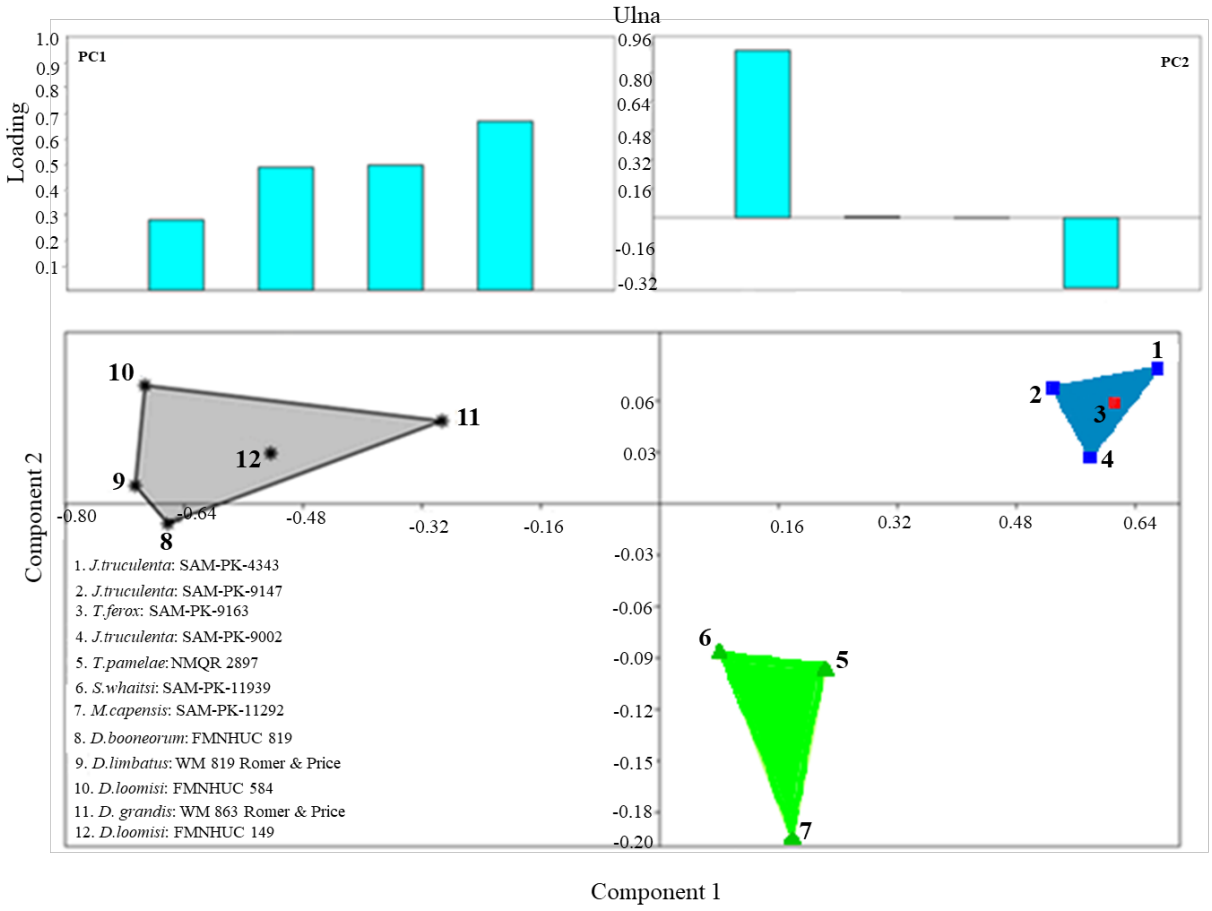

Fig. 4.19. Scatter plot and loadings of principal component 1 and component 2 for the ulna of *Titanosuchus* (red) and *Jonkeria* (blue) and selected tapinocephalids (*Moschops, Struthiocephalus* and *Tapinocaninus;* green) and the basal synapsid *Dimetrodon* (grey). TL, bone total length; PW, bone proximal width; DW, bone distal width; SW, bone maximal narrowing at mid shaft. The ulna is different between titanosuchids and tapinocephalids but no difference between *Titanosuchus* and *Jonkeria*.

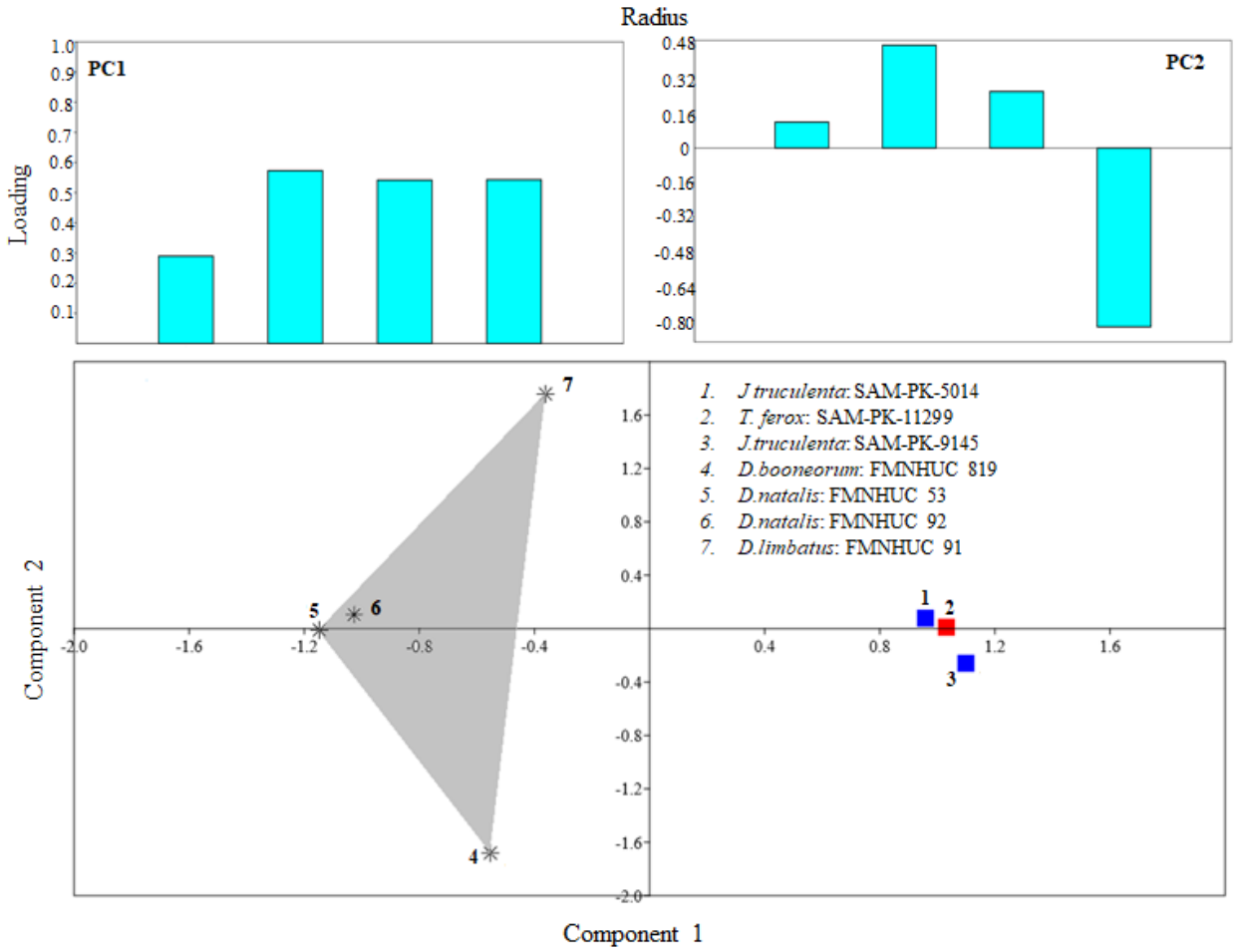

Fig. 4.20. Scatter plot and loading of principal component 1 and component 2 for the radius of *Titanosuchus* (red) and *Jonkeria* (blue) and the basal synapsid *Dimetrodon* (grey). TL, bone total length; PW, bone proximal width; DW, bone distal width; SW, bone maximal narrowing at mid shaft. There is no differentiation between the radius of *Jonkeria* and that of *Titanosuchus*.

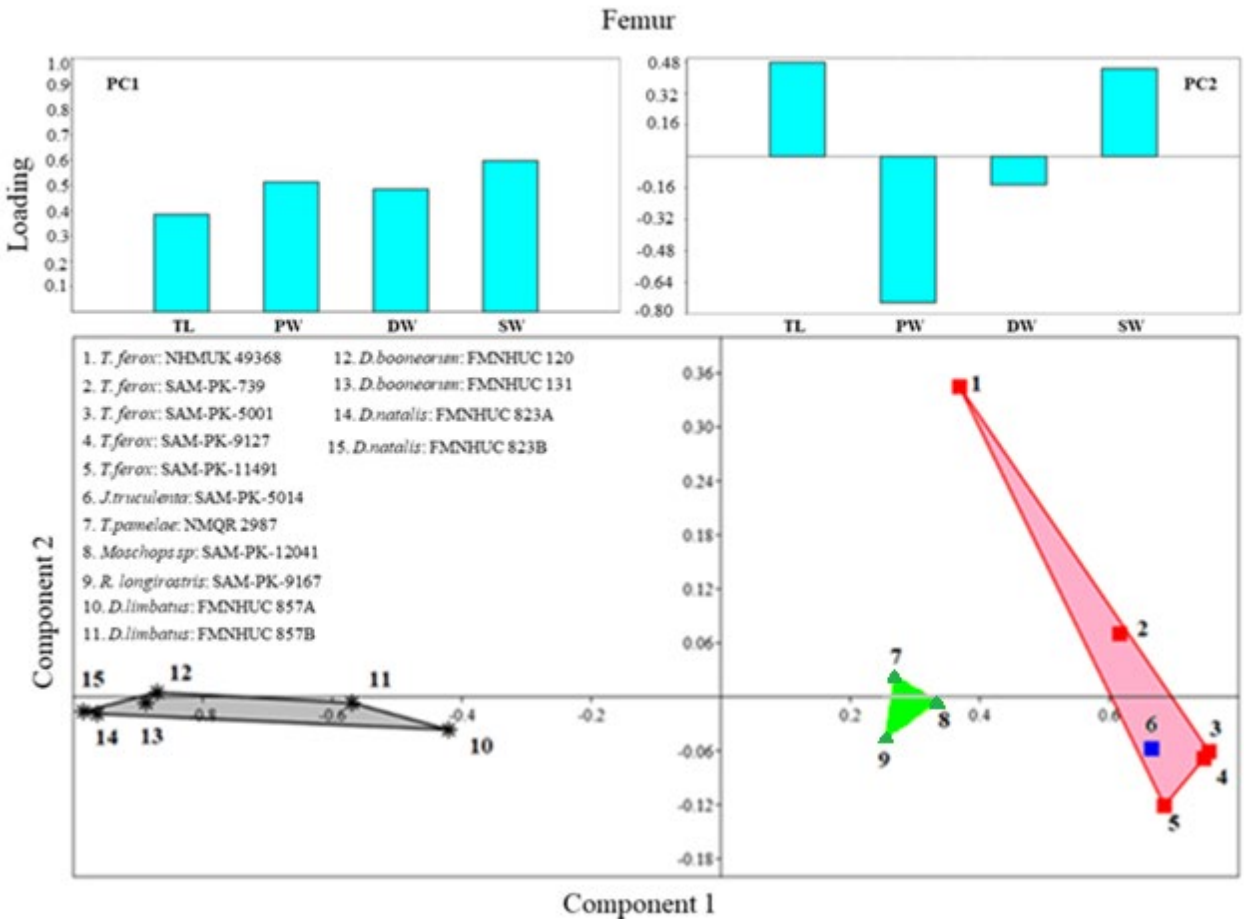

Fig. 4.21. Scatter plot and loading of first and second principal components for the femur of *Titanosuchus* (red) and *Jonkeria* (blue) and selected Tapinocephalids (*Moschops, Riebeeckosaurus* and *Tapinocaninus*: green) and the basal synapsid *Dimetrodon* (grey). TL, bone total length; PW, bone proximal width; DW, bone distal width; SW, bone maximal narrowing at mid shaft. No differentiation between *Titanosuchus* and *Jonkeria*.

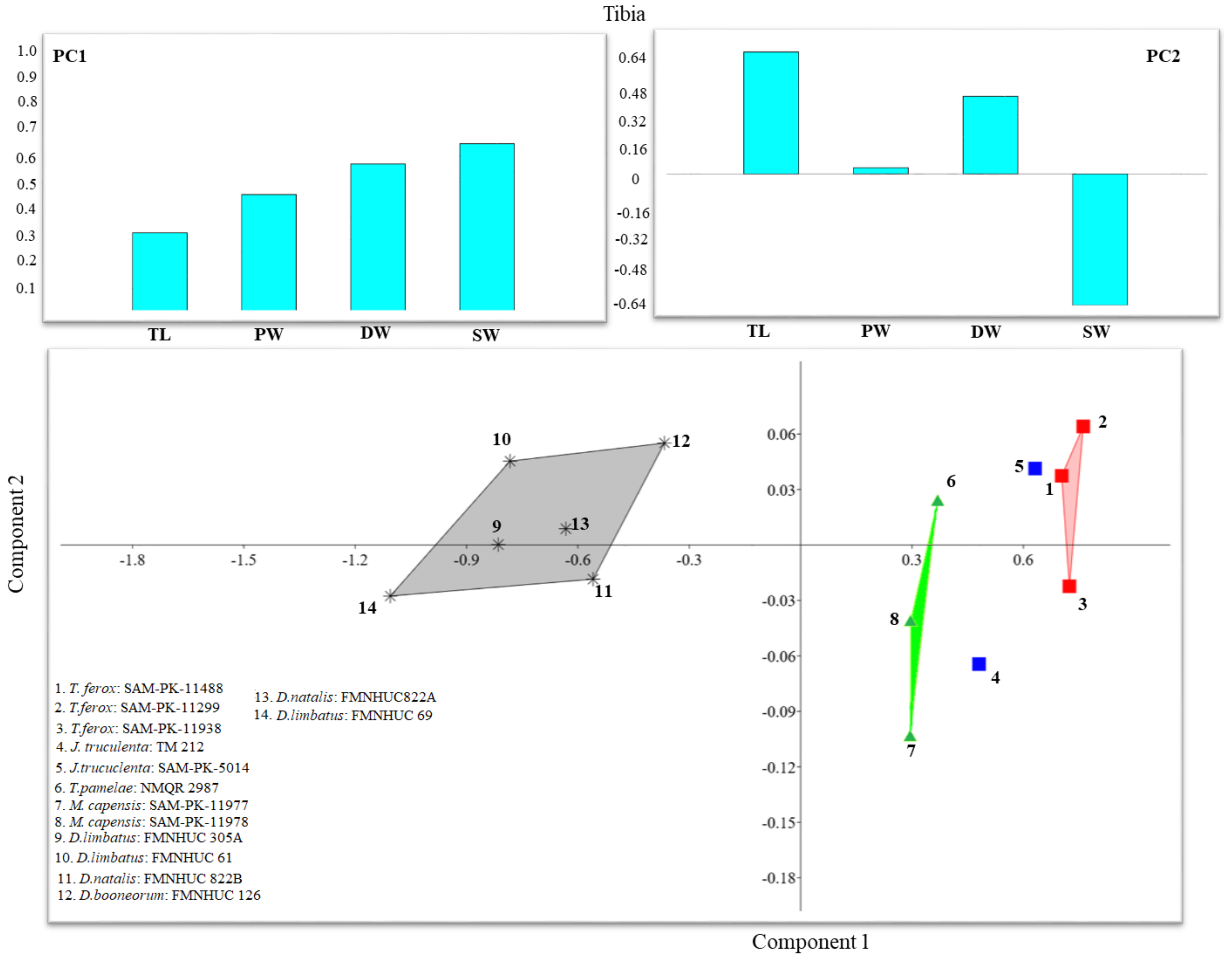

Fig. 4.22. Scatter plot of first and second principal components in tibia for *Titanosuchus* (red) and *Jonkeria* (blue) and selected Tapinocephalids (*Moschops* and *Tapinocaninus*: green) and the basal synapsid *Dimetrodon* (grey). TL, bone total length; PW, bone proximal width; DW, bone distal width; SW, bone maximal narrowing at mid shaft.

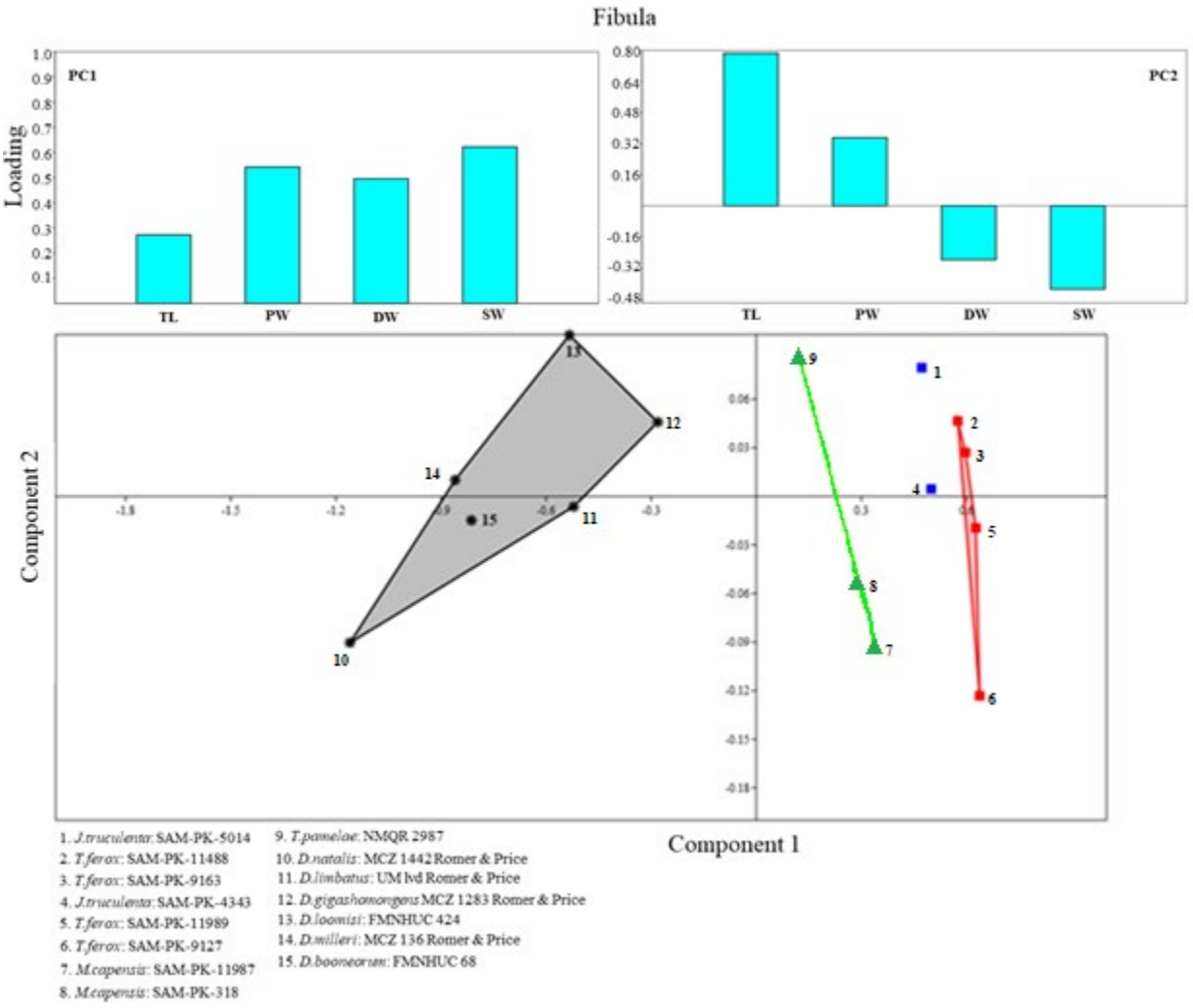

Fig. 4.23. Scatter plot of first and second principal components in fibula for *Titanosuchus* (red) and *Jonkeria* (blue) and selected Tapinocephalids (*Moschops* and *Tapinocaninus* (green)) and the basal synapsid *Dimetrodon* (grey). TL, bone total length; PW, bone proximal width; DW, bone distal width; SW, bone maximal narrowing at mid shaft. This shows a difference in the fibula of *Jonkeria* specimen SAM-PK-5014 and *Titanosuchus* but the fibula of *Jonkeria* specimen SAM-PK- 4343 is similar to the *Titanosuchus* fibulae.

4.5 Discusion

In the hind limb, the femur is more robust and longer in titanosuchids than in the tapinocephalids *Riebeeckosaurus*, *Moschops* and *Tapinocaninus*. The *Titanosuchus ferox* holotype (NHMUK 49368) presents a more gracile femur and a less inflected femoral head compared to other specimens of the same species. This difference between the *T. ferox* holotype femur and other titanosuchid femora also manifests in the Principal Component Analysis plot where this femur (NHMUK 49368) plots far from all the other titanosuchid femora (Fig.4.21). The only *Jonkeria truculenta* femur (SAM-PK-5014) used for this study is morphologically similar to the *Titanosuchus ferox* femora, which are more robust with a slightly thicker shaft width and a more inflected femoral head. This *Jonkeria* femur also has a slightly inflected lateral condyle (more distal relative to the medial condyle) just like the *Titanosuchus* specimens SAM-PK-11491 and NHMUK 49368, which may be due to deformation.

According to Orlov (1958), the femur of the Russian anteosaurian dinocephalian *Titanophoneus adamanteus* is a slender S-shaped bone with enlarged proximal and distal ends with the long axes of the expanded ends making an angle of approximately 45° to each other. The femoral head in these Russian forms, just like in titanosuchids occupies most of the proximal surface and the distal articulations are, turned more forward dorsally.

Only a single well-preserved *Jonkeria truculenta* femur (SAM-PK- 5014) was available for this study compared to five *Titanosuchus ferox* femora, it is, therefore, difficult to attribute the similarities in morphological characters of the femur in these two titanosuchid genera as a product of generic differences or merely a result of a *J. truculenta* reduced sample.

The femur PCA plot shows that the morphospace for *T. ferox* specimens is widely spread along the second component, which is, basically, for the remote placement of NHMUK 49368. This is important because it indicates a variability in the proportions of the bones, and not in the absolute dimensions (component 1). Remaining specimens of titanosuchids (including *Jonkeria truculenta*) have a more compact distribution in the plot, just slightly more spread out than the compact *Dimetrodon* and tapinocephalid morphospaces (Fig. 4.21). This is indicating a more intraspecific variation in the titanosuchid femora, portrayed more particularly by one very different specimen (NHMUK 49368). Cognizant of the fact that the titanosuchid specimens are of differing sizes, it follows that the changes are at least in part due to ontogenetic factors, but sexual dimorphism may be another possibility (Stovall *et al*. 1966; Olson 1968). The tibia of tapinocephalids and titanosuchids is similar but it appears that in *Titanosuchus* this bone has a more expanded proximal end than it is for *Jonkeria*. The plot of these elements in both tapinocephalids and titanosuchids are compact along the first component but quite expanded in relation to the second components, this indicating consistent variation in morphology rather than in body size, whereas the morphospace in *Dimetrodon* is expanded in both axes (Fig. 4.22). Considering titanosuchids, the plot is portraying a slighter robust condition in *Titanosuchus* tibia, whereas the variation of the bone along the second component is larger between the two specimens of *Jonkeria* than between the three of *Titanosuchus*.

The fibula in titanosuchids, as in tapinocephalids, has a deeply concave preaxial face (Boonstra, 1955).The fibula in the Russian form, *Titanophoneus adamanteus,* is a more slender and longer bone with expanded ends, the distal end being more expanded than the proximal (Orlov, 1958). The anterior surface bears a longitudinal ridge (Fig. 4.16. a, b, c, e, f) possibly for the interosseous ligament (Boonstra, 1955a). In *Moschops* (Gregory, 1926) the ends of the fibula are

more expanded but otherwise, this limb bone is comparable with the titanosuchids. As in the case of the tibia, the morphospace for fibulae of tapinocephalids and titanosuchids are again compact along the first component but widespread along the second component and it is spread along both components for *Dimetrodon* (Fig. 4.23). In addition, the fibulae of *Titanosuchus* are slightly more robust that the one of *Jonkeria*. The major variation along the second component is in *Titanosuchus* specimens.

The scatter plots obtained from the Principal Component Analysis indicate a greater morphospace for the titanosuchid femur and humerus compared to those of tapinocephalids, although it should be stressed that the sample of the latter is reduced, especially for the humerus represented by two elements against nine of titanosuchids. Another interesting aspect of the plots is the fact that the humerus is the only bone in which robusticity of the bones of tapinocephalids and titanosuchids are more similar (superposed in the Component 1). This could be related to the presence of very heavy large heads, and therefore a weight decidedly moved forward. In all the other cases (with exception with the radius lacking bones of tapinocephalids) the bones of titanosuchids consistently appear more robust than those of tapinocephalids.

Studies on extant animals have shown shape differences in the humerus and ulna of males and females of the hairy armadillo (*Chaetophractus villosus*) concentrated at the attachment sites for the main muscles involved in digging (Acuña *et al*. 2017). The humerus of females of this species is characterized by a relatively more robust morphology with several features that would increase the in-forces and the related in-levers (Acuña *et al*. 2017). The arrangement at the female shoulder seem to impart structural strength to the use of the limb in a powerful digging stroke while keeping the required stabilization, which could be attained by combining the great development of a spherical humeral head and a medially enlarged lesser tubercle (Acuña *et al*.

2017). Although dinocephalians indeed do not have a fossorial lifestyle, and I ascribe the differences in morphology of the limbs elements to taxonomy. However, the presence of sexual dimorphism in species such as presented by Acuña *et al*. (2017) open the possibility of recognize sexual variation when studying titanosuchid limb bones. Currently, there is no record in the fossil record of animals that exhibit differences in humeral morphology as a result of sexual dimorphism.

4.6 Conclusion

The humerus is the only element in which the size is more or less concordant in tapinocephalids and titanosuchids. It is the only case where the two genera of titanosuchidsare represented by a good sample size and *Jonkeria* is more variable morphologically. There is practically no variation between the radii of *Jonkeria* and *Titanosuchus*, although the sample is quite poor with *Titanosuchus ferox* represented by a single specimen and *Jonkeria* by two. Ulnae are remarkably more robust in titanosuchids than in tapinocephalids and they are also morphologically well-differentiated occupying different morphospace regions along the principal Component 2 (y-axis).

Along the Principal Component 1 (x – axis) of the femur, portraying differences in absolute size rather than in shape, titanosuchids are the largest followed by tapinocephalids. Titanosuchids are much more spread out along the Component 2 than tapinocephalids and *Dimetrodon*, but this is mostly because of specimen NHMUK 49368 that is widely separated from other titanosuchids. *Jonkeria truculenta*, represented by one specimen (SAM-PK-5014), plots close to several specimens of *Titanosuchus ferox*.

Both tibia and fibulae are slightly more robust in titanosuchids and variation along the Principal Component 2 is similar in tapinocephalids and titanosuchids. There are no differences in fibula morphology between *Titanosuchus* and *Jonkeria*. However, there are only two *Jonkeria* fibulae in this study and this cannot provide a conclusive comparison with *Titanosuchus*.

Taking into account the relatively similar and large body sizes of *Titanosuchus* and *Jonkeria* and also between titanosuchids and tapinocephalids it is possible that the structural necessity for the support of a greater body mass has led to the development of robust limb elements with the following limb proportions (humeral length ranging from 378mm – 620mm for titanosuchids, 440mm – 610mm for tapinocephalids and femoral length in titanosuchids, ranging from 500mm – 620mm compared to a range of 375mm – 440mm for tapinocephalids). This suggests that in taxa that are very similar with respect to diet and trophic niche, the appendicular skeleton can respond in a similar way to biomechanical requirements (both in the static rest position and during locomotion) to the change of factors such as the absolute body size and weight (Romano, 2017). Long bones "overbuilt" may be due to the fact that, these taxa were still sprawling or semi-sprawling, therefore, by increasing the body size, the long bones must increase in strength in a non-isomectric way (Romano, 2017)

The results indicate that *Titanosuchus ferox* and *Jonkeria truculenta* differ in the morphology of their limb elements, in particular humerus and tibia, and not in the length of their limb elements contra Boonstra (1969) as this is demonstrated by the overlap in size ranges for the limb bones for the two genera (Appendix C).

Jonkeria parva and *Jonkeria rossouwi* are junior synonyms of *Jonkeria truculenta* by virtue of them having the *Jonkeria* humeral morph and *Jonkeria koupensis* can only be identified to family level by an outward facing acetabulum, presence of a high supra-acetabular part of the

ilium as well as a very strong supra-acetabular buttress. The species *Jonkeria koupensis* is a *nomen dubium* and specimen SAM-PK- 9004 is thus identified as Titanosuchid indet.

CHAPTER 5: PHYLOGENETIC ANALYSIS

5.1 Introduction

Various authors have discussed different classifications within the dinocephalians aiming to reflect phylogenetic relationships. Watson and Romer (1956) placed brithopodines, anteosaurines and jonkeriids in the infraorder Titanosuchia of the suborder Theriodontia and placed "deuterosaurids", "moschopids" and tapinocephalines in the infraorder Dinocephalia of the Anomodontia. They disregarded the link between the herbivorous and carnivorous dinocephalians since they considered that the only characters which the forms have in common, were the clumsy body build and the thickening of the skull bones, both consequences of large size (King, 1988).

Olson (1962) advanced polyphyly of the dinocephalians where he suggested that biarmosuchids and brithopodines were related by characters such as a high, narrow temporal fenestra, a vertical occiput, lack of a distinct maxillary step, and the pineal foramen situated in a collar of bone. He considered the deuterosaurs, titanosuchines and tapinocephalines to be more closely related to the Russian *Estemmenosuchus*.

Boonstra (1963a) discussed the origin of the dinocephalian lineages and families. He included dinocephalians and dicynodonts in the suborder Anomodontia. In his treatment of South African dinocephalian diversity, he traced evolutionary paths between the various families, noting that all divergences had already occurred by the beginning of the *Tapinocephalus* Zone. The characters used to diagnose the infraorder Dinocephalia were, on the whole, a mixture of primitive characters, or characters shared with carnivorous forms, or characters not expressed consistently throughout the group.

Boonstra (1972) placed the Dinocephalia (both herbivorous and carnivorous forms) with the Eotitanosuchia and the Gorgonopsia in the superorder Alphatherapsida. He considered that this lineage was derived from a sphenacodontid such as *Haptodus*. The characters used by Boonstra to define the Alphatherapsida are mostly primitive (carnivorous dentition, lack of secondary palate, narrow epipterygoid). Subsequent authors have not recognized alphatherapsids as a valid group.

Kemp (1982) included a cladogram of the Dinocephalia but did not give specific characters to support the tree topology he presented. Tchudinov (1983) placed Estemmenosuchidae as a family in the order Titanosuchia together with Brithopodidae, Deuterosauridae, Anteosauridae and Titanosuchidae. Contra Boonstra (1963), he considered a closer relationship between the Titanosuchidae and Anteosauridae.

Hopson and Barghusen (1986) presented a cladistic analysis of the therapsids where they produced a comprehensive character list for the different therapsid clades. Regarding dinocephalians they recognized two monophyletic groups, the Anteosauria (Brithopia of Boonstra, 1972), comprising a single family they designated the Anteosauridae and the Tapinocephalia (Titanosuchia of Boonstra, 1972) comprising the families Estemmenosuchidae, Titanosuchidae and Tapinocephalidae.

King (1988) proposed the following suite of characters for the infraorder Dinocephalia: intermeshing incisors, reduction in the size of postcanine teeth, enlarged temporal fenestra, loss of coronoid bones in the lower jaw, vomers grooved or excavated longitudinally and non-terminal nostrils. Estemmenosuchoidea synapomorphies were teeth on the vomers, pachyostosed bone, and horn-like bosses. Anteosauroidea were characterized by having a small heel on incisor

teeth, reduction in the size and number of postcanine teeth, jaw articulation moved slightly further forward and a tendency towards cranial pachyostosis. Brithopidae featured enlarged palatal teeth, usually confined to a reniform cluster on the palatine, and an enlarged canine. Titanosuchidae synapomorphies were enlarged heel on the incisor teeth, reduction in size of the canines, jaw hinge even more anteriorly placed and many leaf-shaped and serrated postcanine teeth. Lastly, Tapinocephalinae proposed synapomorphies were a heel on the incisor teeth, all teeth were interdigitating, and the size of temporal fossa was reduced due to pachyostosis.

Cladistic analysis has also been applied to test phylogenetic placement of different genera within the Dinocephalia (e.g. Rubidge, 1991, 1994, Rubidge and van den Heever, 1997; Cisneros *et al*. 2012, Liu, 2013, Fraser-King *et al*. 2019) and also hypotheses of relationships between taxa in different dinocephalian lineages such as Anteosauridae (Kammerer, 2011) and Tapinocephalidae (Neumann, 2020). Having undertaken a detailed restudy of the cranial and postcranial morphology of the Titanosuchidae, this chapter presents a phylogenetic analysis aimed at exploring the relationships of the titanosuchid taxa recognized in this study.

5.2 Methods

The character matrix, which comprises 13 taxa and 48 characters (44 craniodental characters and 4 postcranial characters, Appendix D and E), was prepared in Mesquite version 3.51 (Maddison and Maddison, 2017). Characters used in previous analyses (Rubidge and van den Heever, 1997; Sidor, 2000; Kammerer, 2011; Cisneros *et al*. 2012; Fraser-King *et al*. 2019; Neumann, 2020), some of them with modifications as well as new proposed characters, were considered.
The data matrix was treated under the assumption of parsimony, using TNT version 1.5 (Goloboff *et al*. 2008; Goloboff and Catalano, 2016). A first round was the search of the most

parsimonious trees using equal weight for characters (treated as unordered), using implicit enumeration in TNT, an option that guarantees finding all the shortest trees from the data-matrix. A second analysis used implied weighting, with K set at three (default in TNT). *Biarmosuchus* was the root taxon and taxa include members of Anteosauridae, *Deuterosaurus*, *Estemmenosuchus*, members of Titanosuchidae and Tapinocephalidae. The aim was to show the relationship of the Titanosuchidae to other dinocephalian taxa. In cases where multiple specimens of different size of a given taxon were present and character codings for this taxon differed based on size class, codings were based on the largest known ('inferred adult') specimens.

5.2.1. Specimens used in the analysis

The following specimens were used for this analysis. *Biarmosuchus tener*: PIN1758/2. Anteosauridae represented by *Archaeosyodon*: PIN1758/3, PIN1758/95, PIN1758/293, PIN1758/294, PIN1758/328; *Syodon*: PIN 157/2 and *Anteosaurus magnificus:* BP/1/1369, SAM-PK-K1683, and SAM-PK-K360. *Deuterosaurus*: PIN1954/1, PIN2629/1. *Estemmenosuchus mirabilis*: PIN 1758/6. (Data for the Russian forms was, obtained from Kammerer, 2011 and Neumann, 2020). Titanosuchidae are represented by *Jonkeria truculenta*: AMNH 5577, SAM-PK- 4343, SAM-PK- 11884, SAM-PK-12030, SAM-PK- 4343, SAM-PK-5014, SAM-PK-9149, and ROZ B96 and *Titanosuchus ferox*: BMNH 49367, BMNH 49369, SAM-PK-5001, BP/1/7380. Tapinocephalidae are represented by *Tapinocaninus pamelae*: NMQR2987, NMQR2986, NMQR2985; *Ulemosaurus*: PIN2207/1, PIN2207/2, PIN 157/4; *Struthiocephalus*: SAM-PK-2678, SAM-PK-272, BP/I/1575 and *Moschops capensis*: SAM-PK-

11582, SAM-PK-319, SAM-PK-12067 and Styracocephalidae are represented by *Styracocephalus*: BP/1/7141 (characters for these tapinocephalids was obtained from Neumann, 2020).

5.3 Results

Six most parsimonious trees of 141 steps were obtained with consistency index (CI) 0.493, retention index (RI) 0.587 and rescaled consistency index (RC) 0.29. The strict consensus result with equal weight is presented in figure 5A.

Jonkeria and *Titanosuchus* form a monophyletic Titanosuchidae clade with the Russian *Estemmenosuchus* recovered as sister-taxon in the majority rule consensus of the three most parsimonious trees with implied weights. This group is the sister clade of Tapinocephalidae (*Tapinocaninus*, *Ulemosaurus*, *Struthiocephalus* and *Moschops*). The base of the cladogram is represented by *Deuterosaurus* and Anteosauridae (*Archaeosyodon*, *Syodon* and *Anteosaurus*), the latter recovered as paraphyletic.

Titanosuchidae synapomorphies are characters 7:1-> 0, moderate canine curvature; 28:0->1, parietal raised and laterally constricted; 42: 0->1, radial condyle (capitellum) of humerus: strongly bulbous, rounded, and extends moderately to far proximally along the ventral face and 47:0->1, processus medialis of the humerus lies in a plane slightly distal to that of the caput.

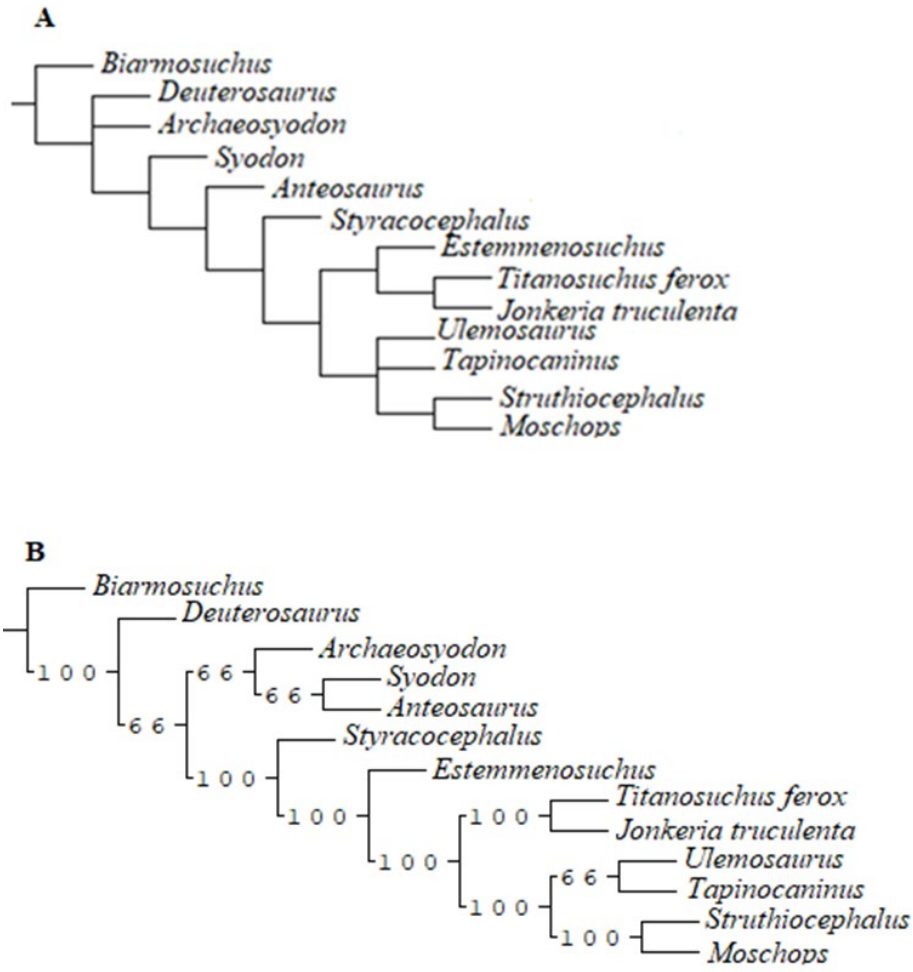

Fig. 5. Results of the phylogenetic analysis. **A.** Strict consensus (equal weight) tree of six most parsimonious trees. **B.** Majority rule consensus of three most parsimonious trees with implied weights (K=3). Number of the nodes indicates proportion of fundamental trees where the group is represented (66 indicate that the group is recovered in two of the three most parsimonious trees).

The following are synapomorphies of *Estemmenosuchus* plus Titanosuchidae, 15:1->0, dorsal margin of the maxilla gently rounded, with no overhang on lacrimal; 21:1->2, shape of dorsal surface of parietal surrounding parietal foramen forms a well-defined chimney; 32:1->2, lower canine passes anterior and external to upper canine; 34:1->0, number of upper (maxillary) postcanines twelve or greater; 45:1->0, lateral margin of the choana formed by less than a third of the palatine.

A second analysis, which used implied weighting, resulted in three most parsimonious trees with a score of 14.243 and the majority rule consensus is show in figure 5B. Some important differences between the implied weighting and strict consensus are highlighted. Titanosuchidae (*Jonkeria* and *Titanosuchus*) is the sister taxa of Tapinocephalidae and the Russian *Estemmenosuchus* is the sister to them. Another interesting result is the recovery of Anteosauridae as monophyletic in the majority rule tree (recovered in two of the three most parsimonious trees). Synapomorphies of Titanosuchidae and Tapinocephalidae are: 8:0->2, incisor morphology with well-developed lingual heel; 9:1->2, dentition on palatine absent; 10:0->1, dentition on palatal ramus of pterygoid absent; 11:0->1, dentition on transverse process of pterygoid absent. Finally, the synapomorphies for Anteosauridae are 7:1->2, canine curvature strong; 16:0->1, ventral margin of maxilla highly convex; 17:0->1, shape of postorbital bar with strong anteroventral curvature, temporal fenestra undercuts orbit.

Tapinocephalia consists of all taxa more closely related to *Tapinocephalus* than *Anteosaurus* (whose counterpart, with the opposite definition, is Anteosauria). Thus, titanosuchids are tapinocephalians (as are estemmenosuchids and styracocephalids in this topology).

5.4 Discussion

Estemmenosuchus and titanosuchids (*Jonkeria* and *Titanosuchus*) share several dental features not seen in other dinocephalians (e.g., the lower postcanine teeth are inset from the lateral margin of the dentary, and the upper postcanines are continuous with the incisors medial to the canine) (Rubidge and Sidor, 2001). Tapinocephalians more derived than the titanosuchians form the Tapinocephalidae.Tapinocephalids carry even further the specializations toward herbivory displayed in the titanosuchians (Rubidge and Sidor, 2001). Although titanosuchians retain a

prominent canine tooth (as is present in anteosaurians and more primitive tapinocephalians), the incisors have a large talon and a prominent crushing heel on their lingual surface. The upper incisors intermesh with the lowers in such a way that when the jaws occlude, the heels meet to form a crushing surface, used to grind plant material. In tapinocephalids, however, the postcanines as well as the incisors have a lingual heel, and inter-digitation of the entire dentition occurs instead of just the anterior teeth. The basal form *Tapinocaninus* has canine teeth in both the upper and lower jaws, a feature that is lost in all other tapinocephalids (Rubidge and Sidor, 2001, Neumann, 2020).

The family Styracocephalidae (*Styracocephalus*) is recovered as the sister-group to the clade formed by *Estemmenosuchus*, Titanosuchidae (*Titanosuchus ferox* and *Jonkeria truculenta*) and Tapinocephalidae (*Tapinocaninus*, *Ulemosaurus*, *Struthiocephalus* and *Moschops*). This occurs in spite of the apparent close relationship of *Styracocephalus* to the Tapinocephalidae suggested by the talon-and-heel morphology of the postcanines and great degree of cranial pachyostosis (Fraser-King *et al*. 2019). The sister group relationship between Styracocephalidae, Estemmenosuchidae, Titanosuchidae and Tapinocephalidae was first mooted by Rubidge and van den Heever (1997) and confirmed by Fraser-King *et al*. 2019.

Of the tapinocephalid taxa used, the analyses show *Tapinocaninus* and *Ulemosaurus* respectively as the most basal tapinocephalid genera and *Tapinocaninus* + *Ulemosaurus and Struthiocephalus* + *Moschops* are sister taxa equally derived with respect to one another. This work has for the first time enabled testing of the the phylogenetic placement of the two valid titanosuchid genera in relation to other middle Permian dinocephalians. In the past, either

Titanosuchidae was used as a family in the analysis (Rubidge and van den Heever, 1997) or only *Jonkeria* was used in the analysis (Fraser-King *et al*. 2019, Neumann, 2020). Kammerer (2011) in his taxonomic revision of Anteosauridae, did not include the family Titanosuchidae in his phylogenetic analysis.

CHAPTER 6: STRATIGRAPHIC DISTRIBUTION OF TITANOSUCHIDS

This chapter describes the stratigraphic ranges of the two valid titanosuchid species, *Titanosuchus ferox* and *Jonkeria truculenta* from the Beaufort Group. Day (2013b) undertook a comprehensive study on middle Permian tetrapod biodiversity change as reflected in the record of the *Eodicynodon*, *Tapinocephalus* and *Pristerognathus* Assemblage Zones of the Beaufort Group. To achieve this Day (2013b) subdivided the outcrop area of the Lower Beaufort Group into nine sectors namely: Beaufort West, Fraserburg, Grahamstown, Jansenville, Laingsburg, Leeu-Gamka, Merweville, Sutherland, and Victoria West sectors (Fig. 6.1). Titanosuchid dinocephalians are known only from the Beaufort West, Laingsburg, Leeu-Gamka, Merweville, and Sutherland sectors.

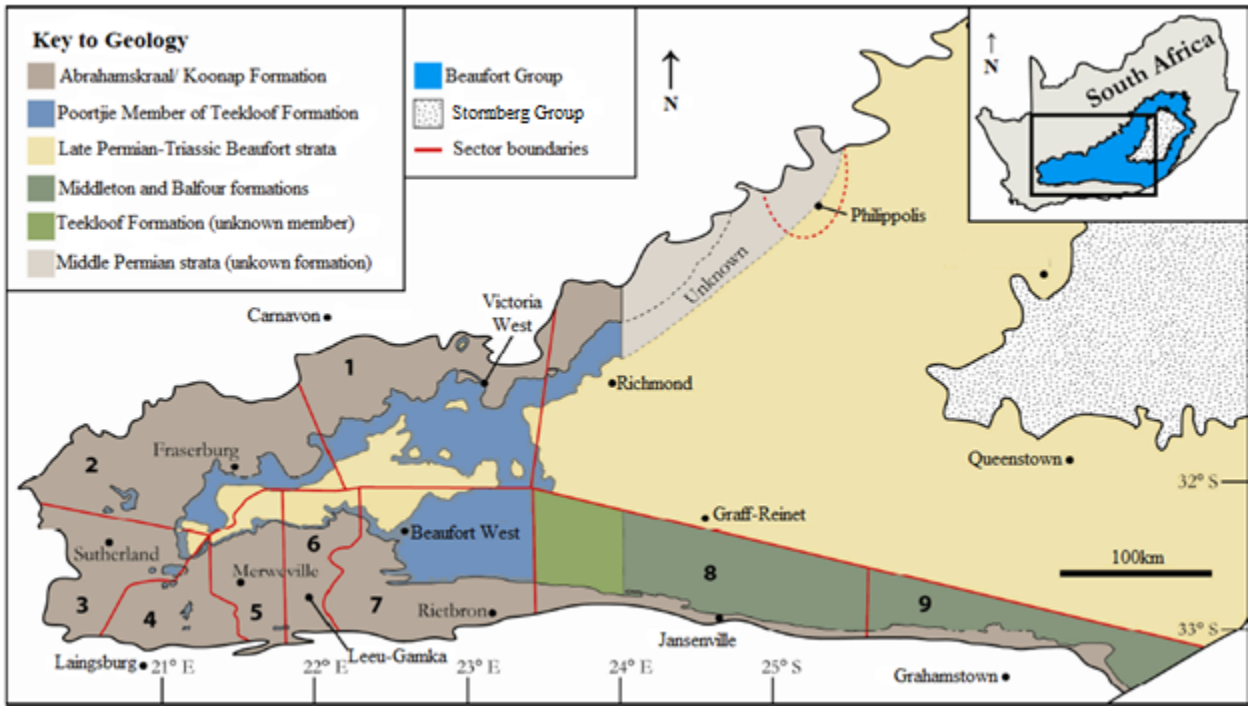

Fig. 6.1. Map showing the sectors used in the calculation of specimen stratigraphic positions. 1 = Victoria West, 2 = Fraserburg, 3 = Sutherland, 4 =Laingsburg, 5 = Merweville, 6 = Leeu-Gamka, 7 = Beaufort West, 8 = Jansenville, 9 = Grahamstown (Day, 2013b).

Up till now the stratigraphic range of the Titanosuchidae has not been precisely determined; Smith and Keyser (1995a) considered that the stratigraphic range of *Titanosuchus* extended throughout the *Tapinocephalus* Assemblage Zone. To solve this, the current study presents the stratigraphic ranges of 15 positively identified *Titanosuchus ferox* specimens, 25 *Jonkeria truculenta* specimens and one indeterminate Titanosuchid specimen using the sectors of Day (2013b). The complete list of identifiable titanosuchid specimens with their updated taxonomic assignment from the Karoo Basin of South Africa is presented in Appendix F and the stratigraphic ranges of both species are shown in Figure 6.2.

6.1 Stratigraphic Range of *Titanosuchus ferox*

6.1.1 Range in the Beaufort West sector (the most easterly occurrence)

The stratigraphically lowest *Titanosuchus ferox* specimens in this sector are SAM-PK-11448 and SAM-PK- 11491 from the farm Mynhardtskraal 311, Beaufort West, in the Prince Albert district, which can be constrained to a stratigraphic interval 2050–2100 m above the base of the Abrahamskraal Formation in this sector. This falls within the middle Moordenaars Member. Two specimens, SAM-PK- 772 and SAM-PK- 773, from Seekoegat, Zeekoegat 22, Prince Albert are not well constrained but they fall within the Moordenaars Member.

The range of *Titanosuchus ferox* is therefore between 2000–2100 m above the base of the Abrahamskraal Formation in this sector (Day, 2013b), equivalent to the middle Moordenaars Member.

6.1.2 Occurrence in the Laingsburg sector

Only one specimen of *Titanosuchus ferox,* SAM-PK-11938, is known from this sector, occurring in the lower Moordenaars Member.

6.1.3 Range in the Leeu-Gamka sector

The stratigraphic constraints on specimens of *Titanosuchus ferox* from the Leeu-Gamka sector are poor and the specimen with the stratigraphically lowest position is SAM-PK-5001, from the farm Sevenfontein 5, in the Prince Albert district. This specimen occurs in the lower Moordernaars Member of the Abrahamskraal Formation. The stratigraphically highest specimen is SAM-PK- 11881from the farm Bloukrans 31, Prince Albert district, which occurs in the middle - upper Moordenaars Member. Specimens SAM-PK- 11299, from Boesmansrivier, Bushmans River 312, Beaufort West, SAM-PK- 11989, from Koedoeskop, Leeuwkraal 309, Beaufort West, and specimens NHMUK 49367, NHMUK 49368, NHMUK 49369 and NHMUK 49370 (holotype of *Titanosuchus ferox*), all from Klein Koedoeskop 310, Beaufort West fall within the middle Moordenaars Member. The stratigraphic range of *Titanosuchus ferox* in the Leeu-Gamka sector is therefore constrained to a stratigraphic interval 2100–2468 m above the base of the Abrahamskraal Formation in this sector, equivalent to the lower to middle-upper Moodenaars Member.

6.1.4 Occurence in the Merweville sector

Titanosuchus ferox specimens from this sector are much better constrained stratigraphically and occur in a narrower stratigraphic interval (50m). Of the stratigraphically lowest specimens, the best constrained are SAM-PK-9162 and SAMPK-9163 from the farm Wakkerstroom, Moordenaarskraal Noord 64, in the Beaufort West district. These occur within the stratigraphic interval 2150–2200 m above the base of the Abrahamskraal Formation, and this falls within the lower Moordenaars Member in this sector.

6.1.5 Overall stratigraphic range

The stratigraphically lowest specimens are four specimens (SAM-PK- 5001, SAM-PK-9127, SAM-PK-9163, SAM-PK-11938), which occur in the lower Moordenaars Member of the Abrahamskraal Formation. The stratigraphically highest specimen identified as *Titanosuchus* is SAM-PK-11881 from the Leeu-Gamka sector, which is constrained to occur in the middle- upper Moordenaars Member. This indicates a stratigraphic range for *Titanosuchus ferox* between 2170 m and 2485m above the base of the Abrahamskraal Formation.

6.2. Stratigraphic range of *Jonkeria*

Previously the stratigraphic range of the genus *Jonkeria* was broadly constrained within the *Tapinocephalus* Assemblage Zone (Smith and Keyser 1995a). This review now constrains *Jonkeria truculenta* as follows:

6.2.1 Range in the Beaufort West sector

The stratigraphic range of *Jonkeria truculenta* in the Beaufort West sector is well constrained to the uppermost Abrahamskraal Formation by three specimens (AMNH 5608, AMNH 5634, and SAM-PK- 9348) that fall within the middle-upper Moordenaars Member (Appendix F; Fig. 6.2).

6.2.2 Occurrence in the Laingsburg sector

Only one specimen of *Jonkeria truculenta* (SAM-PK- 12030) is known from the Laingsburg sector, recovered from the lower Moodenaars member.

6.2.3 Range in the Leeu-Gamka sector

Most of the *Jonkeria truculenta* specimens come from this sector and the stratigraphically lowest specimens are SAM-PK- 11573, SAM-PK- 11574, and SAM-PK- 11575 recovered from Klein Koedoeskop 310, Beaufort West and constrained to the middle Moordenaars Member. Also

constrained in the middle Moordernaars Member is specimen FMNHUC 1511 from the farm Stinkfontein 7, Beaufort West. Eight specimens (AMNH 5620, AMNH 5633, SAM-PK- 738, SAM-PK- 3433, SAM-PK- 4343, SAM-PK-5014, SAM-PK- 9149, and TM 212) cannot be accurately constrained since the strata they come from can only be identified as Moordenaars Member of the Abrahamskraal Formation (Appendix F).

The stratigraphically highest specimens are AMNH 5577, SAM-PK-9002, SAM-PK- 9006, and MB.R 983 all collected from strata that correspond to the middle-upper Moordenaars Member of the Abrahamskraal Formation.

6.2.4 Range in the Merweville sector

In this sector, all the specimens of *Jonkeria truculenta* can be constrained to the lower Moordenaars Member of the Abrahamskraal Formation. These are SAM-PK- 9145 and SAM-PK- 9147 from the farm Zeekoeivlei, Zeekoevalley 282, Beaufort West, SAM-PK- 11884 from the farm Skroefpaal, Scruif Paal 2, Prince Albert, and SAM-PK- 11979 from Kruisvallei, Van der Byls Kraal 265, Beaufort West. As such, the certain range of *Jonkeria* in the Merweville sector corresponds to the stratigraphic interval 2150–2350 m above the base of the Abrahamskraal Formation, in the lower Moordenaars Member.

6.2.5 Overall stratigraphic range

Jonkeria truculenta and *Titanosuchus ferox* have very similar stratigraphic ranges. The lowest specimens of *Jonkeria truculenta* are found in the Laingsburg and Merweville sectors where they are constrained within the lower Moordenaars Member of the Abrahamskraal Fromation, within the stratigraphic interval 2150- 2350m above the base of the Abrahamskraal Formation.

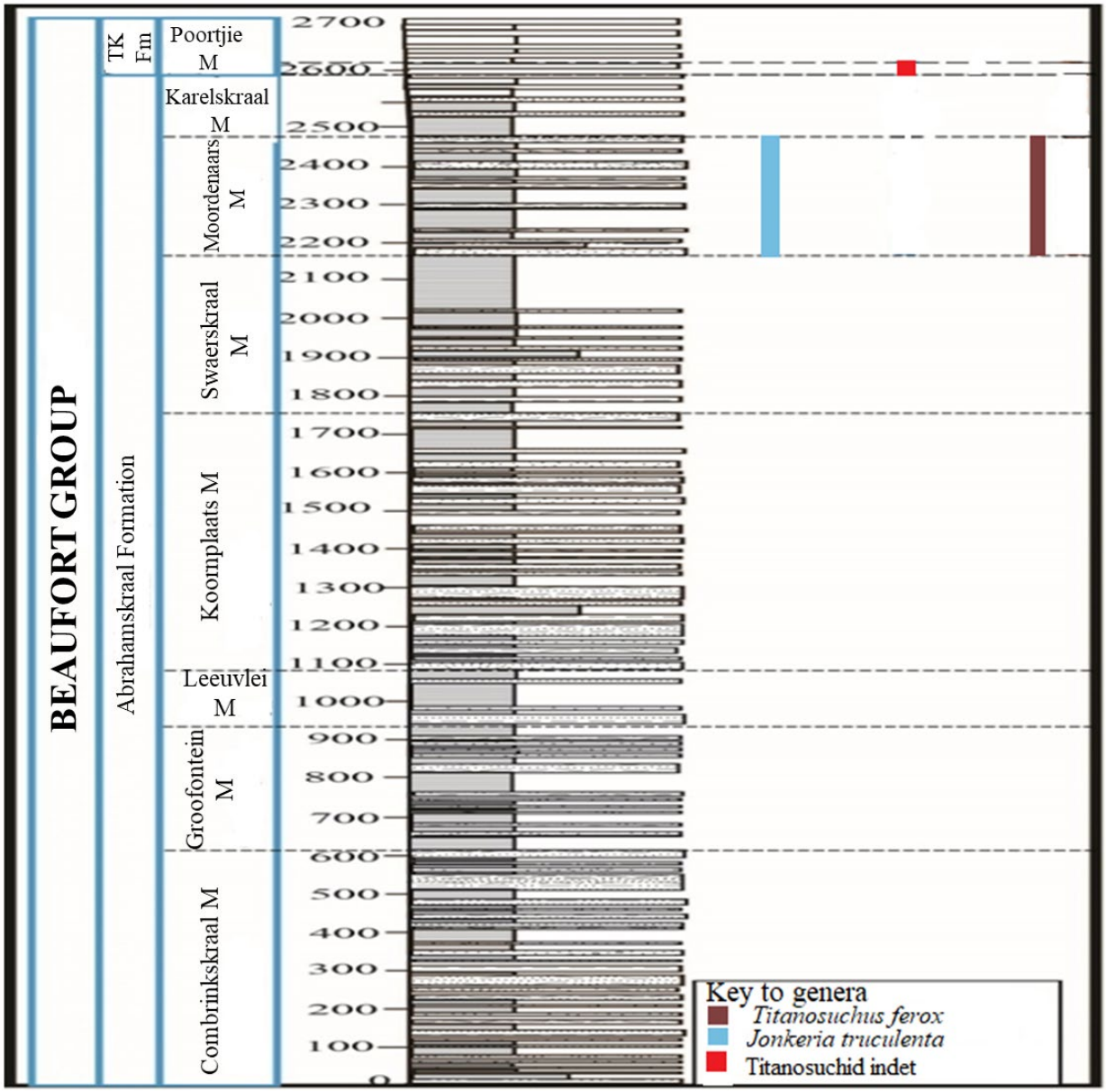

Fig. 6.2. Composite stratigraphic ranges of Titanosuchid genera in the Middle Permian Beaufort Group.

TK Fm = Teekloof Formation

The stratigraphically highest specimens are AMNH 5577 from Rietfontein 56, Prince Albert, SAM-PK-9348 from Mierfontein 318, Beaufort West, SAM-PK- 9002, SAM-PK- 9006 both from Klein Koedoeskop 310, Beaufort West, & MB.R 983 from Springfontein 305, Beaufort West. They are all constrained in the middle-upper Moordenaars Member of the Abrahamskraal

Formation. The certain stratigraphic range of *Jonkeria truculenta* is therefore constrained to an interval 2100–2480 m above the base of the Abrahamskraal Formation at its thickest point, equivalent to the lower to upper Moordenaars Member of the Abrahamskraal Formation. The genus *Jonkeria* (*Jonkeria truculenta*) also mirrors its sister genus *Titanosuchus* (*Titanosuchus ferox*) in its distribution throughout its range, with both genera constrained throughout the Moordenaars Member (Fig. 6.2).

It is worth noting that the lowermost stratigraphic occurrence of both *Titanosuchus* and *Jonkeria* is from the lower Moordenaars Member in the Merweville sector, and the highest occurrences from the mid-upper Moordenaars member are from the Leeu-Gamka and Beaufort West sectors towards the east. This study has demonstrated that the stratigraphic ranges of both *Jonkeria* and *Titanosuchus* are confined to the Moordenaars Member of the Abrahamskraaal Formation. However, a single specimen a fragmentary skull BP/1/7168 (Fig. 6.3), has been provisionally identified as an inderterminate titanosuchid, since it is too framentary to determine the genus nor species, occurs 18m above the base of the Poortjie Member of the Teekloof Formation in the Sutherland sector, where no other titanosuchid specimens have yet been found. This specimen is thus of great significance as it indicates that dinocephalians in general and titanosuchids in particular are present in the Poortjie Member as has also been demonstrated by the presence of the tapinocephalid *Criocephalosaurus* (Day *et al*. 2015).

The question arises as to why no titanosuchids have been recorded from the Karelskraal member of the Abrahamskraal Formation of the Beaufort and this should be an important target for further investigation and fieldwork. This study has however demonstrated that the stratigraphic ranges of both J*onkeria* and *Titanosuchus* are restricted to the uppermost Abrahamskraal Formation and that they are important biostratigraphic indicator taxa in the Karoo Basin of South

Africa. Another important investigation for future research is to determine whether titanosuchids occur in the Fraserburg, Victoria West, Jansenville and Grahamstown (Makanda) sectors of the basin where relatively little fossil prospecting has been undertaken in the *Tapinocephalus* Assemblage Zone.

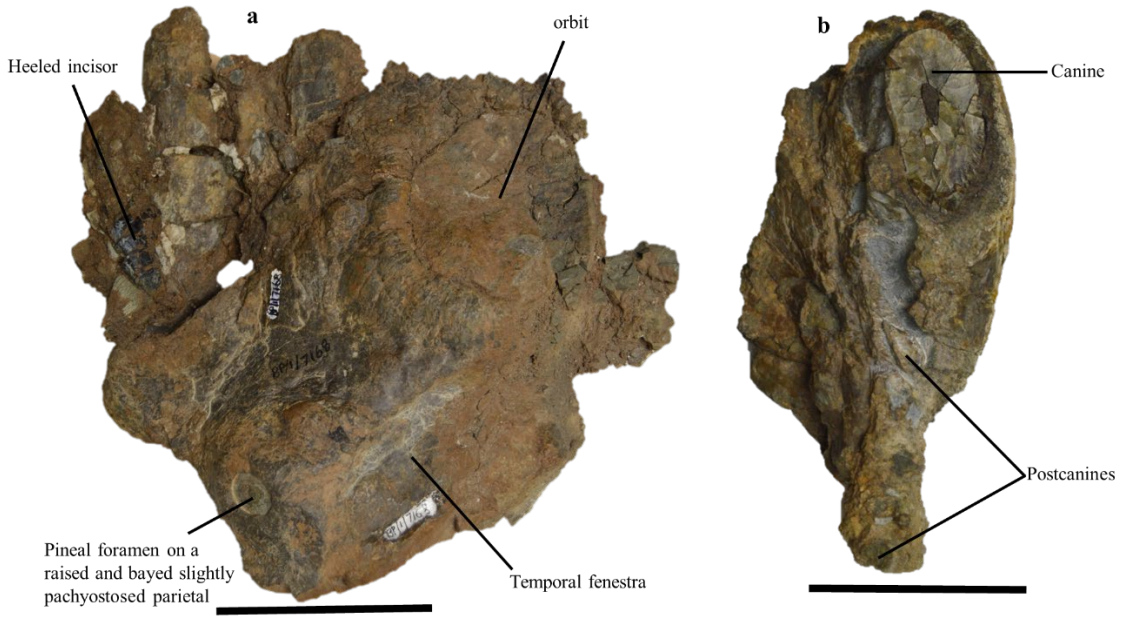

Fig. 6.3. Fragmentary titanosuchid indet skull from the Poortjie Member on farm Ou Tuin, Sutherland disrtrict, South Africa**,** showing the following titanosuchid characters **a**. dorsal view of the skull fragment with a heeled incisor (displaced and in the left orbit); **b.** maxillary fragment with a large canine and a series of postcanines. Scale bars represent 10cm.

CHAPTER 7: DISCUSSION & CONCLUSION

The South African Main Karoo continental succession hosts the most time extensive middle Permian to middle Jurassic record of fossil tetrapods. It is also one of the most significant regions for the study of the middle Permian diversity changes and end-Guadalupian extinction (Day *et al*. 2015a). For this reason, numerous researchers have recently been involved in sorting out of the taxonomy of the tetrapods from the middle Permian of South Africa to understand tetrapod biodiversity and biodiversity changes in the terrestrial realm during the middle Permian.

The middle Permian *Eodicynodon* and *Tapinocephalus* assemblage zones represent the lithologically thickest and longest ranging of the vertebrate-bearing biozones of the South African Beaufort Group, but the fauna of this zone is relatively poorly known compared with that in the Upper Permian and Lower Triassic. In recent years targeted stratigraphic palaeontological collecting and taxonomic work has greatly improved understanding of the taxonomy and biology of Karoo middle Permian tetrapod fauna as well as knowledge of the stratigraphic distribution of the taxa.

7.1 Karoo middle Permian biostratigraphy

Determining the stratigraphic provenance of specimens in the lower portion of the Beaufort Group is complicated by the folded nature of strata of the Abrahamskraal Formation in the south of the Karoo Basin as a result of the Cape Orogenic event (Hälbich, 1983; Cole, 1992; Veevers *et al*. 1994; Catuneanu *et al*. 2005; Rubidge, 2005).

A further problem is that historic specimens in museum collections lack good stratigraphic provenance data. Recently however Day (2013b) provided a detailed synopsis of the

stratigraphic ranges of fossil tetrapod genera in the Abrahamskraal Formation. This ambitious study utilized the GIS database of georeferenced Beaufort Group tetrapod fossils (Nicolas, 2007), combined with long-term targeted stratigraphic fossil collecting, refined stratigraphic mapping, and the systematic measurement of stratigraphic sections in the Abrahamskraal and lower Teekloof formations by the researchers at the Evolutionary Studies Institute at the University of the Witwatersrand. This has resulted in recognition of the *Eodicynodon* and *Tapinocephalus* assemblage zones as the two middle Permian biozones of the Karoo Supergroup, as well as the subdivision of the latter Assemblage Zone into a lower *Eosimops-Glanosuchus Subzone* and an overlying *Diictodon-Styracocephalus* Subzone (Rubidge and Day 2020; Day and Rubidge 2020). These ranges have been correlated with lithostratigraphic members of the Abrahamskraal Formation, some of which have been radiometrically dated using TIMS (Day *et al*. 2015; Day *et al*. in press; Rubidge *et al*. 2013)

Titanosuchids, which are endemic to the South African Karoo Basin, shared the middle Permian terrestrial ecosystems with a host of other tetrapods, including temnospondyls, parareptiles, varanopids and other therapsids such as gorgonopsians, biarmosuchians, therocephalians and anomodonts as well as other members of the dinocephalian clade including anteosaurids, styracocephalids and tapinocephalids. The majority of fossils from the *Tapinocephalus* Assemblage Zone come from the *Diictodon* - *Styracocephalus* Subzone with the following relative abundance of the constituent taxa: 32% Dinocephalia, 31% Dicynodontia, 16% Therocephalia, 16% Pareiasauria, 2% Gorgonopsia, 1% *Eunotosaurus,* 1% Temnospondyli, <1% non-dicynodont Anomodontia, <1% Varanopidae, <1% Biarmosuchia, <1% Millerettidae, and <1% Captorhinidae (Day and Rubidge, 2020). However, a good taxonomic framework is

essential for a reliable biostratigraphic correlation. Below is a brief synopsis showing current understanding of tetrapod taxonomic diversity and the stratigraphic and geographic distribution of the different taxa.

7.2 Middle Permian Tetrapod Taxonomy

Temnospondyli

On cranial evidence Marsicano *et al*. (2017) determined that the *Tapinocephalus* Assemblage Zone is host to only two rhinesuchid species; *Rhinesuchus whaitsi* (Broom, 1908) and *Rhinesuchoides tenuiceps* (Olson and Broom, 1937). Cisneros *et al*. (2020) attributed two different sets of small trackways from the Moordenaars Member of the Abrahamskraal Formation to a small adult temnospondyl or microsaur, and possibly a juvenile rhinesuchid or unknown amphibian.

Rhinesuchidae appear to be endemic to Gondwana and have been recorded in Permian rocks of Brazil, India, Malawi and South Africa (Barbarena *et al*. 1985; Damiani and Rubidge, 2003). The relatively high diversity of rhinesuchids in the Permian of the South African Karoo combined with the wide diversity of Triassic stereospondyls in the Karoo supports the hypothesis that the initial radiation of the Stereospondyli occurred in Gondwana (Yates and Warren, 2000, Warren *et al*. 2000), and more specifically in southern Africa (Damiani and Rubidge, 2003).

The biostratigraphic range of *Rhinesuchus whaitsi* and *Rhinesuchoides tenuiceps* spans the entire *Tapinocephalus* Assemblage Zone (Damiani, 2004) with *Rhinesuchus whaitsi* extending right up to the *Daptocephalus* Assemblage Zone (Viglietti, 2020).

Parareptilia

Recent work recognized only three valid pareiasaurian species from the *Tapinocephalus* Assemblage Zone (*Nochesaurus alexanderi*, *Embrithosaurus schwarzi* and *Bradysaurus seeleyi*) (Van den Brandt, 2020; Van den Brandt *et al*. 2019; 2021). These are the oldest and most basal pareiasaurs, and comprise, the newly created clade Bradysauria, and occur only in the upper *Tapinocephalus* Assemblage Zone (Van den Brandt, 2020).

Eunotosaurus has a restricted stratigraphic range from the upper Koornplaats Member of the Abrahamskraal Formation to the Poortjie Member of the overlying Teekloof Formation. (Day and Rubidge, 2020) and until its recent mention from Malawi (Schoch and Sues, 2020), *Eunotosaurus* was known exclusively from the Karoo of South Africa. Recent morphological histological and embryological research supports a sister-group relationship of *Eunotosaurus* with turtles (Lyson *et al*. 2013, 2016).

The recent discovery of a second and more complete specimen of the parareptile *Broomia perplexa* in the *Tapinocephalus* Assemblage Zone provides new evidence that it is indeed a millerettid and phylogenetic analysis demonstrates that *Broomia* and *Eunotosaurus* are more closely related to the late Permian Millerettiids than to each other (Cisneros *et al*. 2008).

Basal Synapsida

Basal synapsids (‘pelycosaurs’) were the most conspicuous and numerous land vertebrates of Late Carboniferous and Early Permian faunas but were extremely rare members of the succeeding therapsid-dominated faunas (Reisz 1986), but they are recorded together with middle Permian therapsid faunas of Russia and South Africa (Botha-Brink and Modesto, 2009; Anderson and Reisz, 2004). In South Africa they are represented by the varanopids *Heleosaurus*

scholtzi (Reisz and Modesto, 2007; Botha-Brink and Modesto, 2007), and *Elliotsmithia* (Reisz *et al*., 1998) which is closely related to the Russian *Mesenosaurus* and the American *Mycterosaurus* (Modesto *et al*. 2001). Recently, Spindler *et al*. (2018) recognized three varanopid genera from the Karoo (*Elliotsmithia, Heleosaurus, Microvaranops)* and placed them in the monophyletic group the Afrothyra.

Therapsida

Biarmosuchia – This clade is considered the most primitive post-sphenacodont synapsid group (Hopson and Barghusen, 1986). The Capitanian-aged bullacephalids *Bullacephalus* (Rubidge and Kitching, 2003) and *Pachydectes* (Rubidge *et al*. 2006) from the *Tapinocephalus* Assemblage Zone are amongst the oldest biarmosuchians from the South African Karoo Supergroup (Day *et al*. 2016), apart from *Hipposaurus* which comprises two species, *H. boonstrai* and *H. brinki* (Sigoneau-Russell, 1989). This genus is currently under taxonomic review (Rubidge pers comm).

Recently middle Permian burnetiamorphs have been discovered in the Mid-Zambezi Basin of Zambia (Sidor, 2015; Whitney and Sidor, 2016; Day *et al*. 2016). Kammerer and Sidor (2021) recently described the most complete of the new mid-Zambezi Basin burnetiamorphs, recognizing it as a burnetiid.

Gorgonopsia - Gorgonopsia have a very low species diversity in the *Tapinocephalus* Assemblage Zone and are currently considered to be represented by only *Eriphostoma microdon* (Kammerer *et al*. 2015).

Therocephalia - In the *Eodicynodon*, *Tapinocephalus* and lower *Endothiodon* assemblage zones

therocephalians were an important component of the tetrapod fauna, with medium to large forms that were subordinate only to the dinocephalian *Anteosaurus* as coeval predators (Abdala *et al*., 2014). Middle Permian therocephalians belong almost exclusively to one of two families: Lycosuchidae and Scylacosauridae (van den Heever, 1987; 1994).

Anomodontia - In recent years, several new basal anomodont genera have been discovered from the *Eodicynodon* and *Tapinocephalus* assemblage zones including *Patranomodon* (Rubidge and Hopson, 1990; Rubidge and Hopson, 1996) and *Anomocephalus* (Modesto *et al*. 1999). The latter was considered the most basal anomodont until the re-description of the Chinese genus *Biseridens* (Liu *et al*. 2010). The dromasaurs *Galepus, Galechirus and Galeops,* have recently been shown to be from the *Tapinocephalus* Assemblage Zone (Day, 2013a). These three genera previously constituted the Dromasauria, which was of uncertain taxonomic affinity. Currently it is considered that the non-dicynodont anomodonts do not form a clade (Angielczyk, 2004; Fröbisch, 2007; Kammerer *et al*. 2011; Modesto and Rubidge, 2000, Modesto *et al.* 1999) but these taxa form a grade leading up to Dicynodontia.

Dicynodonts were the most abundant therapsids during the middle Permian and as such have proven useful in biostratigraphic subdivision of the Abrahamskraal Formation. This is because, of all the therapsid taxa, the dicynodonts are probably the best understood owing to many recent publications on their taxonomy (e.g. King and Rubidge, 1993; Angielczyk and Sullivan, 2008; Kammerer, *et al*. 2011; Angielczyk and Rubidge, 2012). Using dicyndonts, the Abrahamskraal Formation is biostratigraphically subdivided into the *Eodicynodon* Assemblage Zone (Rubidge and Day, 2020) and the overlying *Eosimops*-*Glanosuchus* and *Diictodon*-*Styracocephalus*

subzones of the *Tapinocephalus* Assemblage Zone (Day and Rubidge, 2020).

Several dicynodont species with postcanine teeth, *Eodicynodon oosthuizeni* (Rubidge, 1990a, b), *Pristerodon mckayi*, *Emydops arctatus*, *Robertia broomiana* (King and Rubidge, 1993) and *Eosimops newtoni* (Angielczyk and Rubidge, 2012) were previously known from the Abrahamskraal Formation. Recently several new species have been described, including *Lanthanostegus mohoii* (Modesto *et al*. 2002, Modesto and Rubidge, 2003; Rubidge *et al*. 2021), *Colobodectes cluveri* (Modesto *et al*. 2003; Angielczyk and Rubidge, 2009) and, *Prosictodon dubei* (Angielczyk and Rubidge, 2010). *Prosictodon* ranges between the base of the Moordenaars Member of the Abrahamskraal Formation and the base of the Poortjie Member (Day, 2013b). *Chelydontops altidentalis* has recently been synonymized with *Brachyprosopus broomi* (Angielczyk *et al*. 2016) and the range of the genus extends from the lower *Tapinocephalus* Assemblage Zone up to the Karelskraal Member (Day and Rubidge, 2020).

Diictodon feliceps, the only dicynodont from the Abrahamskraal Formation without postcanine teeth, is the most abundant dicynodont in this Formation where it occurs toward the top. It has a stratigraphic range extending from the Koornplaas Member (Day and Rubidge, 2020) and survives until the end of the Permian where it was a victim of the Permo-Triassic mass extinction (Kitching, 1995; Smith and Keyser, 1995a; Smith and Ward, 2001).

The middle Permian dicynodont *Abajudon kaayai,* known from the lowermost fossiliferous horizon of the Ruhuhu Formation in Tanzania (Angielczyk *et al*. 2014b) and the lower Madumabisa Mudstone in the Mid-Zambezi Basin of Zambia where it co-occurs with

dinocephalians (Sidor *et al*. 2014), has not yet been recovered from the Abrahamskraal Formation.

Dinocephalia - Anteosauridae are, known from Laurasia (Russia and China) and Gondwana (Africa and South America) in the middle Permian (Kammerer, 2011, Cisneros *et al*. 2012). Only two genera are, currently recognized from the Karoo, *Australosyodon* and *Anteosaurus* (Kammerer, 2011).

The family Styracocephalidae is represented by a single species *Styracocephalus platyrhynchus,* known only from the Moordenaars Member of the Abrahamskraal Formation (*Diictodon-Styracocephalus* Subzone of the *Tapinocephalus* Assemblage Zone) (Day and Rubidge, 2020). Because, *Styracocephalus* is, known from a reasonably complete but squashed skull with a lower jaw (SAM-PK-8936) and some fragmentary skull roof specimens, its taxonomic affinities have been uncertain (Rubidge and van den Heever, 1997), but the recent discovery of a more complete and undistorted specimen (BP/1/7141) justifies the position of the family within the Dinocephalia (Fraser-King *et al*. 2019).

Of the 23 holotypes of short-snouted tapinocephalid taxa, Neumann (2020) recently recognized only nine genera (species) as valid. These are *Tapinocaninus pamelae, Ulemosaurus svijagensis, Riebeeckosaurus longirostris, Agnosaurus pienaari, Moschognathus whaitsi, Criocephalosaurus vanderbyli, Moschops capensis, Tapinocephalus atherstonei,* and *Mormosaurus seeleyi*. Neumann (2020) undertook the first cladistic analysis of short snouted tapinocephalids and confirmed the finding of Rubidge (1990) that *Tapinocaninus* is the most basal tapinocephalid. Currently the taxonomy of the long-snouted tapinocephalids is under review (Kammerer and

Neumann pers comm). To complete the review of the taxonomy of the dinocephalians from the Karoo Supergroup this thesis recognizes *Jonkeria truculenta* and *Titanosuchus ferox,* which are endemic to South Africa, as the only valid titanosuchid species and their stratigraphic range is restricted to the Moordenaars Member of the Abrahamskraal Formation.

7.3 Conclusions and perspectives

The above chapters have presented the middle Permian tetrapod biodiversity of the South African Karoo Supergroup and provided an update of the current understanding of the taxonomy of these animals, however, it is evident that detailed taxonomic analysis of the Titanosuchidae has lagged. This study has demonstrated that because of the fragmentary nature of the 115 catalogued titanosuchid specimens in museum collections, only 42 are identifiable to species level. Previous research on the limb bones of Titanosuchidae revealed that there are two morphs (based on the morphology of the humerus) representing two species, *Jonkeria truculenta* and *Titanosuchus ferox* (Boonstra, 1969; Kammerer, 2009). It was thus necessary to determine whether these are the only differences between the two species.

The holotype skull of *Titanosuchus ferox* is too fragmentary to compare with that of *Jonkeria truculenta.* Until now, there is no well preserved *Titanosuchus ferox* skull material associated with the *Titanoschus ferox* postcranial (humeral) morph and it is thus not possible to provide a diagnostic cranial description of the skull of *Titanosuchus*. The *Jonkeria* postcranial morph is associated with some well-preserved skulls and this study thus presents the first detailed cranial description of *Jonkeria* including a comparative study of all *Jonkeria* holotypes which were described on cranial material. This study revealed that the differences between the holotype

skulls of different *Jonkeria* species are either the result of deformation or are related to the stage of ontogenetic development. Accordingly, all the *Jonkeria* species previously described from cranial material (*Jonkeria vanderbyli*, *Jonkeria ingens*, *Jonkeria haughtoni* and *Jonkeria boonstrai*) are now considered junior synonyms of *Jonkeria truculenta*.

Allometric analysis of titanosuchids demonstrated a growth series of *Jonkeria truculenta* as has recently been achieved for the anteosaurid *Anteosaurus magnificus* (Kruger *et al*. 2017) and tapinocephalid *Moschops capensis* (Neumann, 2020). Instead of the different *Jonkeria* skulls representing different species, they have now been demonstated to represent the different growth series of the same species *Jonkeria truculenta*.

Various people have worked on the lithostratigaphy of the Abrahamskraal Formation and several arenaceous and argillageous packages have been recognized (Steer, 1980; Le Roux, 1985; Loock *et al*. 1994; Cole and Wipplinger, 2001; Day and Rubidge, 2014; Jirah and Rubidge, 2014). The difficulty and stratigraphic challenge is in recognising and correlating these packages throughout the large expanse of the lower Beaufort, particularly in the areas affected by the folding caused by the Cape Orogenesis. Thus, to better understand the stratigraphy of the lower Beaufort, a refined biostratigraphic scheme is necessary. Day (2013); Day and Rubidge (2020) did a mammoth task in understanding the ranges of the different taxa of the *Tapinocephalus* Assemblage Zone. However, up till now, because of the lack of taxonomic resolution of the tetrapod taxa, the stratigraphic range of the titanosuchid genera has been unsure, but now that the taxonomy has been addressed with this research, as illustrated in the discussion above, the taxonomy of the tetrapod fauna from the Abrahamskraal Formation thus far has largely been resolved. Also, the stratigraphic range of *Jonkeria* and *Titanosuchus* is restricted to the

Moordenaars Member in the upper Abrahamskraal Formation within the *Diictodon-Styracocephalus* Subzone of the *Tapinocephalus* Assemblage Zone (Day and Rubidge, 2020).

This research is part of a major project aimed at determining middle Permian tetrapod biodiversity changes in the terrestrial realm and contributes to both a taxonomic revision of Titanosuchid taxa and a refined biostratigraphy of these middle Permian large herbivores. Titanosuchid dinocephalians, just like other dinocephalian families, apart from being the earliest large therapsids, were a major component of the middle Permian terrestrial ecosystems and went extinct at the end of the Capitanian stage of the middle Permian, becoming one of the first therapsid lineages to face extinction. Dinocephalians constituted about 31 % of the fauna in the *Diictodon-Styracocephalus* Subzone (Day and Rubidge, 2020) and comprise an anteosaurid (*Anteosaurus magnificus*), a styracocephalid (*Styracocephalus platyrhynchus*), titanosuchids (*Titanosuchus ferox* and *Jonkeria truculenta*) and tapinocephalids (*Tapinocephalus atherstonei Mormosaurus seeleyi, Moschops capensis, Moschognathus whaitsi, Riebeeckosaurus longirostris, Agnosaurus pienaari, Criocephalosaurus vanderbyli, Struthiocephalus whaitsi* and *Strutionops intermedius*) (Day and Rubidge, 2020).

The recent discovery of middle Permian tetrapod assemblages in Tanzania and Zambia (Simon *et al*. 2010; Sidor *et al*. 2014) raises the question of whether the region's tetrapod communities in the middle Permian were similarly uniform. At a broad scale, such uniformity seems likely: the presence of tapinocephalids, dicynodonts, and temnospondyls in the Ruhuhu Formation and the occurrence of anteosaurids, tapinocephalids, temnospondyls, burnetiids, gorgonopsians, and dicynodonts in the Madumabisa Mudstone Formation (Sidor *et al*. 2014) are reminiscent of the faunas of the *Eodicynodon* and *Tapinocephalus* assemblage zones in South Africa.

Day *et al*., (2015a) provided TIMS dates for different stratigraphic horizons of the *Tapinocephalus* Assemblage Zone and demonstrated that the age of the Moordenaars Member falls between 260.2ma (for the upper Karelskraal) and 262ma (lower Swaerskraal). Thus, the range of titanosuchids, which are restricted to the Moordenaars Member, is less than 2 million years. The problem comes in explaining the long titanosuchid ghost lineage of more than four million years, which was demonstrated in Chapter 5, and also, the recent discovery of an indeterminate titanosuchid in the lower Poortjie Member, creates a challenge to find titanosuchids in the Karelskraal Member, the uppermost lithostratigraphic member of the Abrahamskraal Formation. To solve the enigma that titanosuchids are known only from the South African Karoo and have a long ghost lineage will require more intensive searching in the middle Permian continental rocks of South Africa and other Pangean countries.

REFERENCES

Abdala, F, and Giannini, N.P. 2000. Gomphodont cynodonts of the chan˜ares formation: the analysis of an ontogenetic sequence. *Journal of Vertebrate Paleontology,* 20 (3):501–506.

Abdala, F, Kammerer, C.F, Day, M.O, Jirah, S, and Rubidge, B.S. 2014. Adult morphology of the therocephalian *Simorhinella baini* from the middle Permian of South Africa and the taxonomy, paleobiogeography, and temporal distribution of the Lycosuchidae. *Journal of Paleontology*, 88(6), 2014, p. 1139–1153.

Acuña, F, Sidorkewicj, N.S, Popp, A.I, and Casanave, E.B. 2017. A geometric morphometric study of sex differences in the scapula, humerus and ulna of *Chaetophractus villosus* (Xenarthra, Dasypodidae). Iheringia*, Série Zoologia*, 107: 1-12. DOI: 10.1590/1678-4766e2017010.

Alexander, R. McN. 1985. Body support, scaling and allometry; pp. 27–37 in M. Hildebrand and D. B. Wake (eds.). *Functional Vertebrate Morphology*. The Belknap Press of Harvard University Press Cambridge, Massachusetts.

Anderson, J.M, and Cruickshank, A. R.I. 1978. The biostratigraphy of the Permian and the Triassic. Part 5. A review of the classification and distribution of Permo-Triassic tetrapods. *Palaeontologia africana*. 21, 15- 44.

Anderson, J.S, and Reisz, R.R. 2004. *Pyozia mesenensis*, a new, small varanopid (Synapsida, Eupelycosauria) from Russia: "Pelycosaur" diversity in the middle Permian. Journal of Vertebrate Paleontology 24: 173-179.

Angielczyk, K. D. 2004. Phylogenetic evidence for and implications of a dual origin of propaliny in anomodont therapsids (Synapsida). *Paleobiology* 30: 268-296.

Angielczyk, K.D, Huertas, S, Smith, R.H.M, Tabor, N.J, Sidor, C.A, Steyer, J-S, Tsuji, L.A, and Gostling, N.G. 2014b. New dicynodonts (Therapsida, Anomodontia) and updated tetrapod stratigraphy of the Permian Ruhuhu Formation (Songea Group, Ruhuhu Basin) of southern Tanzania, *Journal of Vertebrate Paleontology*, 34:6, 1408-1426, DOI: 10.1080/02724634.2014.880448.

Angielczyk, K. D., and C. F. Kammerer. 2018. Non-mammalian synapsids: the deep roots of the mammalian family tree. Chapter 5 (pp. 117-198) in Asher, R., and F. Zachos (eds.) Handbook of Zoology: Mammalia. Berlin, DeGruyter.

Angielczyk, K.D, Rubidge, B.S, Day, M.O, and Lin, F. 2016. A reevaluation of *Brachyprosopus broomi* and *Chelydontops altidentalis*, dicynodonts (Therapsida, Anomodontia) from the middle Permian Tapinocephalus Assemblage Zone of the Karoo Basin, South Africa, *Journal of Vertebrate Paleontology*, 36:2, e1078342, DOI: 10.1080/02724634.2016.1078342.

Angielczyk, K.D, and Rubidge, B.S. 2010. A new pylaecephalid dicynodont (Therapsida, Anomodontia) from the *Tapinocephalus* Assemblage Zone, Karoo Basin, middle Permian of South Africa, *Journal of Vertebrate Paleontology*, 30:5, 1396-1409, DOI: 10.1080/02724634.2010.501447.

Angielczyk, K. D, and Rubidge, B. S. 2013. Skeletal Morphology, Phylogenetic Relationships and Stratigraphic Range of *Eosimops Newtoni* Broom, 1921, a Pylaecephalid Dicynodont

(Therapsida, Anomodontia) from the middle Permian of South Africa. *Journal of Systematic Palaeontology* 11, 191–231. doi:10.1080/14772019.2011.623723.

Angielczyk, K.D, and Sullivan, C. 2008. *Diictodon feliceps* (Owen, 1876), a dicynodont (Therapsida, Anomodontia) species with a Pangaean distribution. *Journal of Vertebrate Paleontology*, 28:3, 788-802, DOI: 10.1671/0272-4634(2008)28[788: DFOADT] 2.0. CO; 2.

Barbolini, N, Smith, R.M.H, Tabor, N.J, Sidor, C.A and Angielczyk, K.D. 2016. Resolving the age of Madumabisa fossil vertebrates: palynological evidence from the mid-Zambezi Basin of Zambia. *Palaeogeography, Palaeoclimatology, Palaeoecology* 457:117–128.

Benoit, J, Manger, P.R, Fernandez, V, and Rubidge, B.S. 2016. Cranial bosses of *Choerosaurus dejageri* (Therapsida, Therocephalia): earliest evidence of cranial display structures in Eutheriodonts. *PLOS ONE* 11:e0161457.

Bhat, M.S, Shelton, C.D, and Chinsamy, A. 2021. Bone histology of the graviportal dinocephalian therapsid Jonkeria from the middle Permian Tapinocephalus Assemblage Zone of the Karoo Basin of South Africa. *Acta Palaeontologica Polonica* 66.4: 705-721.

Boonstra, L.D. 1936a. The cranial morphology of some titanosuchid dinocephalians. *Bulletin of the American Museum of Natural History,* 72: 99-116.

Boonstra, L.D. 1946. Report on some reptilian fossils from Gunyankas's Kraal, Busi Valley. *Procedings and Transactions of the Rhodesian Science Association,* 41: 46-49.

Boonstra, L.D. 1953a. A suggested clarification of the taxonomic status of the South African tiatnosuchians. *Annals of the South African Museum,* 42: 19-28.

Boonstra, L.D. 1953b. The cranial morphology and taxonomy of the tapinocephalid genus *Struthiocephalus. Annals of the South African Museum,* 42: 32-53.

Boonstra, L.D. 1954a. The cranial structure of the titanosuchian: Anteosaurus. *Annals of the South African Museum,* 42: 108-148.

Boonstra, L. D. 1954c. The smallest tanosuchid yet discovered from the Karoo. *Annals of the South African Museum*, 42: 149-156.

Boonstra, L.D. 1955a. *Struthiocephalellus*: a new dinocephalian. *Annals of the South African Museum,* 42: 180-184.

Boonstra, L.D. 1955b. The girdles and limbs of the South African Deinocephalia. *Annals of the South African Museum*, 42(3): 185-326.

Boonstra, L.D. 1957. The moschopid skulls in the South African Museum. *Annals of the South African Museum,* 44: 15-38.

Boonstra, L.D. 1962. The dentition of the titanosuchian dinocephalians. *Annals of the South African Museum,* 46: 57-112.

Boonstra, L.D. 1963a. Early dichotomies in the therapsids. *South African Journal of Science,* 59: 176-194.

Boonstra, L.D. 1963b. Diversity within the South African Dinocephalia. *Suid-Afrikaanse Tydskrif vir Wetenskap,* 59: 196-206.

Boonstra, L.D. 1968. The braincase, basicranial axis and median septum in the Dinocephalia. *Annals of the South African Museum,* 50(10): 195-270.

Boonstra, L.D. 1969. The fauna of the *Tapinocephalus* Zone. *Annals of the South African Museum*, 56(1): 1-73.

Boonstra, L.D. 1971. The early Therapsids. *Annals of the South African Museum,* 59: 17-46.

Boonstra, L.D. 1972. Discard the names Theriodontia and Anomodontia: a new classification of the Therapsida. *Annals of the South African Museum,* 59: 315-338.

Boos, A.D. S, Kammerer, C.F, Schultz, C.L, and Paes Neto, V.D. 2015. A tapinocephalid dinocephalian (Synapsida, Therapsida) from the Rio do Rasto Formation (Paraná Basin, Brazil): taxonomic, ontogenetic, and biostratigraphic considerations. *Journal of South American Earth Sciences*, 63: 375-384.

Botha-Brink, J, and Modesto, S.P. 2009. Anatomy and relationships of the middle Permian varanopid *Heleosaurus scholtzi* based on a social aggregation from the Karoo Basin of South Africa. *Journal of Vertebrate Paleontology* 29: 389-400.

Botha-Brink, J, and Modesto, S.P. 2007. A mixed-age classed 'pelycosaur' aggregation from South Africa: earliest evidence of parental care in amniotes? *Proceedings of the Royal Society B* 274, 2829–2834 doi:10.1098/rspb.2007.0803.

Broom, R. 1903c. On the classification of the theriodonts and their allies. *Report of the South African. Association of Advancement of Science*. 1, 286-295.

Broom, R. 1904. Notice of a new fossil (*Scapanodon duplessisi*) from the lower Karroo beds of Prince Albert. *Records of the Albany Museum,* 1: 182-183.

Broom, R. 1905a. On the use of the term Anomodontia. *Records of the Albany Museum,* 1: 266-269.

Broom, R. 1905b. Notice of some new fossil reptiles from the Karroo Beds of South Africa. *Records of the Albany Museum*, 1: 331-337.

Broom, R. 1910. A comparison of the Permian reptiles of North America with those of South Africa. *Bulletin of the American Museum of Natural History,* 28: 197-234.

Broom, R. 1911. On some new South African Permian reptiles. *Procceedings of the Zoological Society of London,* 81(4): 1073-1082.

Broom, R. 1912. On some fossil reptiles from the Permian and Triassic beds of South Africa. *Proceedings of the Zoological Society of London,* 82(4): 859-876.

Broom, R. 1913. A revision of the reptiles of the Karroo. *Annals of the South African Museum,* 7(6): 361-366.

Broom, R. 1914b. On the origin of mammals. *Philosophical Transactions of the Royal Society, B*, 206: 1-48.

Broom, R. 1915. Catalogue of the types and figured specimens of fossil vertebrates in the American Museum of Natural History. II. Permian, Triassic and Jurassic reptiles of South Africa. *Bulletin of the American Museum of the Natural History,* 25 (2): 105-164.

Broom, R. 1923. On the structure of the skull in the carnivorous dinocephalian reptiles. *Proceedings of the Zoological Society of London,* 93(4): 661-684.

Broom, R. 1929. On the carnivorous mammal-like reptiles of the family Titanosuchidae. *Annals of the Transvaal Museum*, 13: 9- 36.

Broom, R. 1932. *The mammal-like reptiles of South Africa and the origin of mammals*. H.F. & Witherby, London, xvi + 376 pp.

Broom, R. 1937. A further contribution to our knowledge of the fossil reptiles from the Karroo. *Proceedings of the Zoological Society of London, B,* 107 (3): 299-318.

Cassini, G.H, Flores, D.A, and Vizcaíno, S.F. 2015. Postnatal ontogenetic scaling of pampas deer (*Ozotoceros bezoarticus celer*: Cervidae) cranial morphology. *Mammalia* 79:69–79.

Catuneanu, O, Hancox, P.J, and Rubidge, B.S. 1998. Reciprocal flexural behavior andcontrasting stratigraphies: a new basin development model for the Karoo retro-arc foreland system, South Africa. *Basin Research*, 10, 417–439.

Cheng, Z. W, and Ji, S. 1996. First record of a primitive anteosaurid dinocephalian from the Upper Permian of Gansu, China. *Vertebrata PalAsiatica*, 34: 123–134.

Cheng, Z. W, and Li, J. L. 1997. A new genus of primitive dinocephalian- the third report on Late Permian Dashankou lower tetrapod fauna. *Vertebrate Palasiatica,* 34: 123-134.

Cheng, Y.N, Holmes, R, Wu, X.C, and Alfonso, N. 2009. Sexual dimorphism and life history of Keichosaurus hui (Reptilia: Sauropterygia). *Journal of Vertebrate Paleontology,* 29: 401–408.

Chinnery, B. 2004. Morphometric analysis of evolutionary trends in the ceratopsian postcranial skeleton. *Journal of Vertebrate Paleontology,* 24: 591–609.

Cisneros, J.C, Day, M.O, Groenewald, J, and Rubidge, B.S. 2020. Small footprints expand middle Permian amphibian diversity in the South African Karoo. *Plaios*, 2020, v. 35, 1–11. DOI: http://dx.doi.org/10.2110/palo.2018.098

Cisneros, J.C, Abdala, F, Atayman-Güven, S, Rubidge, B.S, Şengör, A.M.C, and Schultz, C.L. 2012. Canivorous dinocephalian from the middle Permian of Brazil and tetrapod

dispersal in Pangea. *Proceedings of the National Academy of Sciences*, 109 (5): 1584-1588.

Cisneros, J.C, Rubidge, B.S, Mason, R, and Dube, C. 2008. Analysis of millerettid parareptile relationships in the light of new material of *Broomia perplexa* Watson, 1914, from the Permian of South Africa, *Journal of Systematic Palaeontology*, 6:4, 453-462, doi: 10.1017/S147720190800254X.

Cole, D.I. 1992. Evolution and development of the Karoo Basin. In: De Wit, M.J.,Ransome, I.G.D. (Eds.), Inversion Tectonics of the Cape Fold Belt, Karoo and Cretaceous Basins of Southern Africa. *Balkema*, Rotterdam, pp. 87–99.

Cole, D.I, Wipplinger, P.E. 2001. Sedimentology and Molybdenum Potential of theBeaufort Group in the main Karoo Basin South Africa. *Memoirs for the Council of Geoscience, South Africa*, 80, 225pp

Cope, E.D. 1878. Descriptions of extinct Batrachia and Reptilia from the Permian Formation of Texas. *Proceedings of the American Philosophical Society,* 17(101): 505-530.

Cope, E.D. 1880. Contribution to the history of the vertebrata of the Permian Formation of Texas. *Proceedings of the American Philosophical Society,* 19(107): 38-58.

Damiani, R.J. 2004. Temnospondyls from the Beaufort Group (Karoo Basin) of South Africa and their biostratigraphy. *Gondwana Reasearch*, V.7, No. 1, pp. 165-173.

Day, M. O. 2013a. Historical review charting the fossils of the Great Karoo: a history of tetrapod biostratigraphy in the Lower Beaufort Group, South Africa. *Palaeontologica africana,* 48: 41-47.

Day, M.O. 2013b. Middle Permian continental biodiversity changes as reflected in the Beaufort Group of South Africa: a bio- and lithostratigraphic review of the *Eodicynodon*, *Tapinocephalus* and *Pristerognathus* Assemblage Zones.Unpublished Ph.D thesis, University of the Witwatersrand, Johannesburg, 1 -387.

Day, M.O, and Rubidge, B.S. 2014. A brief lithostratigraphic review of the Abrahamskraal and Koonap formations of the Beaufort Group, South Africa: Towards a basin-wide stratigraphic scheme for the middle Permian Karoo. *Journal of African Earth Sciences*, 100, 227-242.

Day, M.O, Benson, R.B.J, Kammerer, C. F, and Rubidge, B.S. 2018. Evolutionary rates of mid-Permian tetrapods from South Africa and the role of temporal resolution in turnover reconstruction. *Paleobiology*, 44(3), 2018, pp. 347–367. DOI: 10.1017/pab.2018.17.

Day, M.O, Rubidge, B.S, and Abdala, F. 2016. A new mid-Permian burnetiamorph therapsid from the Main Karoo Basin of South Africa and a phylogenetic review of Burnetiamorpha. *Acta Palaeontologica Polonica* 61 (4): 701–719.

Day, M.O, Ramezani, J, Bowring, S.A, Sadler, P.M, Erwin, D.H, Abdala, F, and Rubidge, B.S. 2015a. When and how did the terrestrial mid-Permian mass extinction occur? Evidence from the tetrapod record of the Karoo Basin, South Africa. *Proceedings of the Royal Society* B 282, 20150834.

Day, M. O, Güven, S, Abdala, F, Jirah, S, Rubidge, B, and Almond, J. 2015b. Youngest dinocephalian fossils extend the *Tapinocephalus* Zone, Karoo Basin, South Africa. *South African Journal of Science,* 111 (3-4): 1-5.

Day, M. O, and Rubidge, B. S. 2020. Biostratigraphy of the *Tapinocephalus* Assemblage Zone (Beaufort Group, Karoo Supergroup), South Africa. South African journal of Geology, 123 (2): 149-164. https://doi.org/10.25131/sajg.123.0012.

Duhamel, A, Benoit, J, Day, M.O, Rubidge, B, and Fernandez, V. 2021. Computed Tomography elucidates ontogeny within the basal therapsid clade Biarmosuchia. PeerJ 9:e11866 DOI 10.7717/peerj.11866.

Emerson, S. B, and Bramble, D.M. 1993. Scaling, allometry and skull design; pp. 384–416 in J. Hanken and B. K. Hall (eds.). *The Skull*. Volume 3. University of Chicago Press, Chicago and London.

Estes, R. 1961. Cranial anatomy of the cynodont reptile Thrinaxodon liorhinus. *Bulletin of the Museum of Comparative Zoology,* 125:165–180. Evans HE. 1993. Miller's anatomy of the dog. 3rd Edition. Philadelphia: W.B. Saunders Company.

Flessa, K.W, and Jablonski, D. 1983. Extinction is here to stay. *Paleobiology* 9: 315-321.

Fourie, H, and Rubidge, B. S. 2009. The postcranial skeleton of the basal therocephalian *Glanosuchus macrops* (Scylacosauridae) and comparison of morphological and phylogenetic trends amongst the Theriodontia. *Palaeontologia Africana*, 44: 27-40.

Fraser-King, S.W, Benoit, J, Day, M.O, and Rubidge, B.S. 2019. Cranial morphology and phylogenetic relationship of the enigmatic dinocephalian Styracocephalus platyrhynchus from the Karoo Supergroup, South Africa. *Palaeontologia Africana,* 54: 14-29.

Fröbisch, J. 2007. The cranial anatomy of *Kombuisia frerensis* Hotton (Synapsida, Dicynodontia) and a new phylogeny of anomodont therapsids. *Zoological Journal of the Linnean Society* 150, 117–144.

Gates, T.A, Organ, C, and Zanno, L.E. 2016. Bony cranial ornamentation linked to rapid evolution of gigantic theropod dinosaurs. *Nature Communications* 7:1–10.

Goloboff, P.A, Farris, J. and Nixon, K. 2008. TNT, a Free Program for Phylogenetic Analysis. *Cladistics*, 24: 774-786.

Goloboff, P. and Catalano, S.A. 2016. TNT version 1.5, including a full implementation of phylogenetic morphometrics. *Cladistics,* 32(3): 221-238.

Gregory, W.K. 1926. The skeleton of *Moschops capensis* Broom, a dinocephalian reptile from the Permian of South Africa. *Bulletin American Museum National History,* 56: 179-251.

Gregory, W.K, and Broom, R. 1926. The skeleton of *Moschops capensis* Broom: a Dinocephalian reptile from the Permian of South Africa. New York: *The American Museum of Natural History*.

Grine, F.E. 1997. Dinocephalians are not anomodonts. *Journal of Vertebrate Paleontology,* 17(1): 177-183.

Güven, S, Day. M.O, Almond, J. E, Abdala, F, and Rubidge, B.S. 2012. First tapinocephalid from the *Pristerognathus* Assemblage Zone (Karoo Supergroup, South Africa), including new information on *Criocephalosaurus* (Therapsida: Dinocephalia) - Palaeontological Society of Southern Africa, 16th Biennial Conference, Cape Town, September 5-8. *Palaeontologia africana,* 47:37.

Hälbich, I.W. 1983. A tectonogenesis of the Cape Fold Belt (CFB). In: Söhnge, A.P.G.,Hälbich, I.W. (Eds.),Geodynamics of the Cape Fold Belt, vol. 12. *Geological Society of South Africa*, pp. 165–175.

Hammer, Ø, and Harper, D.A.T. 2006. *Paleontological Data Analysis*, 351 pp. Blackwell Publishing, Oxford.

Hammer, Ø, Harper, D.A.T, and Ryan, P.D. 2001. PAST: paleontological statistics software package for education and data analysis. *Palaeontologia Electronica* 4, 9.

Haughton, S.H. 1915a. On a new dinocephalian from the Gouph. *Annals of the South African Museum,* 12: 52-54.

Haughton, S. H. 1915b. On a new type of Dinocephalia (*Moschosaurus longiceps*). *Annals of the South African Museum,* 12: 78-81.

Haughton, S.H. 1919. A review of the reptilian fauna of the Karroo system of South Africa. *Transactions of the Geological Society of South Africa (The South African Journal of Geology),* 22: 1-25.

Haughton, S.H, and Brink, A.S. 1954. A bibliographical list of Reptilia from Karro beds of Africa. *Palaeontologia africana*, 2: 1-187.

Hopson, J. A, and Barghusen, H. R. 1986. An analysis of therapsid relationships. In *The Ecology and Biology of the Mammal-Like Reptiles,* ed. N. Hotton, P. D. MacLean, J.J. Roth & E.C. Roth., pp. 83- 106. Smithsonian Institution Press, Washington, D.C.

International Commission on Zoological Nomenclature. 1999. *International Code of Zoological Nomenclature.* 4th Edition. The International Trust for Zoological Nomenclature, London, 306 p.

Ivakhnenko, M. F. 1995. Primitive Late Permian dinocephalian titanosuchids of Eastern Europe. *Paleontological Journal*, 29: 120–129.

Ivakhnenko, M.F. 2003. Eotherapsids from the East European Placket. (Late Permian). *Paleontological Journal,* 37: 339-465.

Ivakhnenko, M.F. 2008. Cranial morphology and evolution of Permian Dinomorpha (Eotherapsida) of Eastern Europe. *Paleontological Journal,* 42: 859-995.

Ivakhnenko, M.F, Golubev, V.K, Gubin, Yu. M, Kalandadze, N.N, Novikov, I.V, Sennikov, A.G, and Rautian, A.S. 1997. Permian and Triassic tetrapods of Eastern Europe. *Trudy Paleontologicheskogo Instituta Akademiya Nauk SSSR,* 268: 1-216 [in Russian].

Jablonski, D. 1986. Causes and consequences of mass extinctions: a comparative approach. In *Dynamics of Extinction*, Elliott D.K (ed.). Wiley & Sons: New York: 183-229.

Janensch, W. 1959. Eine *Jonkeria* aus der Karru-Formation des Kaplandes. *Paläontologische Zeitschrift,* 33: 22-49.

Jirah, S, and Rubidge, B.S. 2014. Refined stratigraphy of the middle Permian Abrahamskraal Formation (Beaufort Group) in the southern Karoo Basin. *Journal of African Earth Sciences* 100: 121–135.

Kammerer, C. F. 2009. *Cranial disparity in the non-mammalian Synapsida.* PhD Thesis. University of Chicago, Chicago, xi+ 649p.

Kammerer, C.F. 2011. Systematics of the Anteosauria (Therapsida: Dinocephalia). *Journal of Systematic Palaeontology,* 9(2): 261-304.

Kammerer, C.F, Angielczyk, K.D, and Fröbisch, J. 2011: A comprehensive taxonomic revision of *Dicynodon* (Therapsida, Anomodontia) and its implications for dicynodont phylogeny, biogeography, and biostratigraphy. *Journal of Vertebrate Paleontology* 31, 1–158.

Kammerer, C.F, and Sidor, C.A. 2021. A new burnetiid from the middle Permian of Zambia and a reanalysis of burnetiamorph relationships. *Papers in Palaeontology*, Vol. 7, Part 3, pp. 1261–1295

Kemp, T.S. 1982. *Mammal like Reptiles and the origin of Mammals.* Academic Press, London, xiv+364p.

Kemp, T.S. 2005. The origin and evolution of mammals. Oxford University Press, Oxford, x+331p.

Keyser, A.W., and Smith, R.M.H. 1978. Vertebrate biozonation of the Beaufort Group with special reference to the Western Karoo Basin. Annals Geological Survey South Africa, 12, 1-36.

King, G.M. 1988. Anomodontia. In Handbuch der Paläoherpetologie, Teil 17C, ed. P. Wellnhofer. Gustav Fischer-Verlag, Stuttgart, x + 174 p.

King, G.M, and Rubidge, B.S. 1993. A taxonomic revision of small dicynodonts with postcanine teeth. *Zoological Journal of the Linnean Society* 107, 131–154.

Kitching, J.W. 1995. Biostratigraphy of the *Dicynodon* Assemblage Zone. In Rubidge, B. S. (ed.), Biostratigraphy of the Beaufort Group (Karoo Supergroup). Council for Geoscience, Pretoria. 40–45.

Kraaijeveld, K, Kraaijeveld-Smit, F.J, and Komdeur, J. 2007. The evolution of mutual ornamentation. *Animal Behaviour* 74:657–677.

Kruger, A, Rubidge, B. S, and Abdala, F. 2017. A juvenile specimen of *Anteosaurus magnificus* Watson, 1921 (Therapsida: Dinocephalia) from the South African Karoo, and its implications for understanding dinocephalian ontogeny. *Journal of Systematic Palaeontology*, 16 (2): 139–158, http://dx.doi.org/10.1080/14772019.2016.1276106.

Kulik, Z.T, and Sidor, C.A. 2019. The original boneheads: histologic analysis of the pachyostotic skull roof in Permian burnetiamorphs (Therapsida: Biarmosuchia). *Journal of Anatomy* 235(1):151–166.

Kutorga, S.S. 1838. *Beitrag zur Kenntnissder organischen Überreste des Kupfersandsteins am Westlichen Ablange des Urals.* Gretsch, St. Petersburg, 38 p.

Lande, R. 1980. Sexual dimorphism, sexual selection, and adaptation in polygenic characters. *Evolution* 34(2):292–305.

Langer, M.C. 2000. The first dinocephalians in South America: Late Permian (Rio do Rosto Formation) of the Paran basin, Brazil. *Neues Jahrbuch für Geologie und Paläontology Abhandlungen,* 215 (1): 69-95.

Lee, M.S.Y. 1997a. A taxonomic revision of pareiasaurian reptiles: implications for Permian terrestrial palaeoecology. Modern Geology 21: 231–298.

Lepper, J., Raath, M.A., and Rubidge, B.S. 2000. Adiverse dinocephalian fauna from Zimbabwe. *South African Journal of Science,* 96: 403-405.

Le Roux, J.P. 1985. Palaeochannels and uranium mineralization in the main Karoo Basin of South Africa. Unpublished Ph.D. Thesis, University of Port Elizabeth.250pp.

Liu, J. 2013. Osteology, ontogeny, and phylogenetic position of *Sinophoneus yumensis* (Therapsida, Dinocephalia) from the middle Permian Dashankou Fauna of China. *Journal of Vertebrate Paleontology,* 33(6): 1394-1407.

Liu, J, Rubidge, B.S, and Li, J. 2010. A new specimen of *Biseridens qilianicus* indicates its phylogenetic position as the most basal anomodont. *Proceedings of the Royal Society B* 277, 285–292. Doi:10.1098/rspb.2009.0883.

Loock, J.C, Brynard, H.G, Heard, R.G, Kitching, J.W, and Rubidge, B.S. 1994. The stratigraphy of the lower Beaufort Group in an area north of Laingsburg, SouthAfrica. *Journal of African Earth Sciences*, 18 (3), 185–195.

Lydekker, R. 1889. Part III- Palaeozoology. Vertebrata. In *A manual of Palaeontology for the use of students.Volume 2,* (ed). Nicolson, H. A. and R. Lydekker. William Blackwood and Sons. Edinburg and London. pp. 889-1624.

Lydekker, R. 1890. *Catalogue of the fossil Reptilia and Amphibia in the British Museum. Part IV. Containing the orders Anomodontia, Ecaudata, Caudata, and Labyrinthodontia; and Supplement.* London. xxiii + 295p.

Lyson, T, Rubidge, B. S, Scheyer, T. M, Queiroz, K. DE, Schachner, E. R, Smith, R. M. H, Botha-Brink, J, and Bever, G. S. 2016. Fossorial origin of the turtle shell. *Current Biology*, 26, 1887–1894.

Lyson, T, Scheyer, T. M, Hsiang, A.Y, and Gauthier, J. A. 2013. Evolutionary origin of the turtle shell. *Current Biology*, 23, 1113–1119.

Maddison, W.P, and Maddison, D.R. 2018. MESQUITE: A modular system for evolutionary analysis. Version 3.51 http://www.mequiteproject.org.

Maho, S, Gee, B.M, and Reisz, R.R. 2019. A new varanopid synapsid from the early Permian of Oklahoma and the evolutionary stasis in this clade. *Royal Society open science*. 6: 191297. http://dx.doi.org/10.1098/rsos.191297.

Marsicano, C.A, Latimer, E, Rubidge, B.S, and Smith, R.M.H. 2017. The Rhinesuchidae and early history of the Stereospondyli (Amphibia: Temnospondyli) at the end of the Palaeozoic. *Zoological Journal of the Linnean Society*, 2017, 181, 357–384.

Modesto, S. P, Rubidge, B. S, De Klerk, W.J, and Welman, J. A., 2001. Dinocephalian therapsid fauna on the Ecca-Beaufort contact in Eastern Cape Province, South Africa. *South African Journal of Science*, 97: 161-163.

Modesto, S. P, Sidor, C.A, Rubidge, B.S, and J. Welman, J. 2001. A second varanopseid skull from the Upper Permian of South Africa: implications for Late Permian 'pelycosaur' evolution. *Lethaia* 34:249–259.

Modesto, S, and Rubidge, B.S. 2000. A basal anomodont therapsid from the lower Beaufort Group, Upper Permian of South Africa, *Journal of Vertebrate Paleontology*, 20:3, 515-521.

Modesto, S, Rubidge, B.S, and Welman, J. 1999. The most basal anomodont therapsid and the primacy of Gondwana in the evolution of the anomodonts. *Proceedings of the Royal Society of London*. *Series B*: *Biological Sciences*, 266, 331-337.

Munyikwa, D. 2001. Cranial morphology of a primitive dinocephalian from the Madumabisa mudstone formation, Zimbabwe. MSc thesis, University of the Witswatersrand, Johannesburg, 75p.

Neumann, S. 2020. Taxonomic revision of the tapinocephalid dinocephalian subfamilies Moschopinae, Tapinocephalinae and Reibeeckosaurinae – the key to understanding middle Permian tetrapod biodiversity. Unpublished PhD thesis, University of the Witwatersrand, Johannesburg, 408pp.

Nicholas, M.V.M. 2007. Tetrapod biodiversity through the Permo-Triassic Beaufort Group (Karoo Supergroup) of South Africa. PhD thesis, University of the Witwatersrand, Johannesburg, 668 p.

Nopcsa, F. 1928a. The genera of Reptiles. *Palaeobiologica* 1:163-188.

Olroyd, S.L, Sidor, C.A, and Angielczyk, K.D. 2017. New materials of the enigmatic dicynodont *Abajudon kaayai* (Therapsida, Anomodontia) from the lower Madumabisa Mudstone Formation, middle Permian of Zambia, *Journal of Vertebrate Paleontology*, 37:6, e1403442, DOI: 10.1080/02724634.2017.1403442.

Olson, E.C. 1962. Late Permian terrestrial vertebrates, U.S.A. and U.S.S.R. *Transaction of the American Philosophical Society,* 52(2): 1-224.

Orlov, J. A. 1958. Les Dinocéphales carnassiers de la fauna d'Isheevo (Titanosuchia). *Trudy Paleontologicheskogo Instituta Akademiya Nauk SSSR,* 72:1-114.

Osborn, H.F. 1903. On the primary division of the Reptilia into two-subclasses, Synapsidae and Diapsida. *Science, New Series,* 17(424): 275-276.

Owen, R. 1876. Descriptive and illustrated catalogue of the fossil reptilia of South Africa in the collection of the British Museum. London. *Order of Trustees*. pp. xii+88p. lxx plates

Owen, R. 1879. Description of fragmentary indications of a huge kind of theriodont reptile (*Titanosuchus ferox* Ow) from Beaufort West, Gouph Tract, Cape of Good Hope. *Quarterly journal of the Geological Society of London*, 35: 189-198.

Pearson, M.R, Benson, R.B.J, Upchurch, P, Fröbisch, J, and Kammerer, C.F. 2013. Reconstructing the diversity of early terrestrial herbivorous tetrapods. *Palaeogeography, Palaeoclimatology, Palaeocology,* 372: 42-49.

Radinsky, L. B. 1981a. Evolution of the skull shape in carnivores. 1. Representative modern carnivores. *Biological Journal of the Linnean Society,* 15: 369–388.

Radinsky, L. B. 1981b. Evolution of the skull shape in carnivores. 2. Additional modern carnivores. *Biological Journal of the Linnean Society*, 16: 337–355.

Reisz, R.R. 1986. Pelycosauria. In Wellnhofer, P. (ed.): *Handbuch Der Palaoherpetologie*, volume 17A, 1–102.Gustav Fischer Verlag, Stuttgart.

Reisz, R. R, Dilkes, D. W, and Berman, D. S. 1998. Anatomy and relationships of *Elliotsmithia longiceps* Broom, a small synapsid (Eupelycosauria: Varanopseidae) from the Late Permian of South Africa. Journal of Vertebrate Paleontology, 18, 602–611.

Reisz, R. R, and Modesto, S. P. 2007. *Heleosaurus scholtzi* from the Permian of South Africa: a varanopid synapsid, not a diapsid reptile. *Journal of Vertebrate Paleontology* 27 (3): 734-739.

Reisz, R.R, and Sues H-D. 2000) *Evolution of Herbivory in Terrestrial Vertebrates*, (ed) Sues H-D (Cambridge Univ Press, Cambridge, UK), pp 9-41.

Rey, K, Day, M.O, Amiot, R., Fourel, F, Luyt, J, Van den Brandt, M.J, Lécuyer, C. and Rubidge, B.S. 2020. Oxygen isotopes and ecological inferences of Permian (Guadalupian) tetrapods from the main Karoo Basin of South Africa. *Palaeogeography, Palaeoclimatology, Palaeoecology*, 538, 109485.

Romano, M. 2017. Long bone scaling of caseid synapsids: a combined morphometric and cladistic approach. *Lethaia*, 1-16 doi: 10.1111/let.12207.

Romano, M, and Citton, P. 2015. Reliability of digit length impression as a character of tetrapod ichnotaxobase: considerations from the Carboniferous-Permian ichnogenus Ichniotherium. *Geological Journal,* 50: 827–838.

Romano, M, and Citton, P. 2016. Crouching theropod at the seaside. Matching footprints with metatarsal impressions and theropod authopods: a morphometric approach. *Geological Magazine*. https://doi.org/10.1017/S0016756816000546

Romer, A. 1966. Vertebrate Paleontology. *The University of Chicago Press*. Chicago and London. ix + 468 p.

Romer, A. S, and Price, L. I. 1940. Review of the Pelycosauria. Geological Society of America, Special Paper 28, 1-538.

Rossouw, P. J. and De Villiers, J. 1953. The Geology of the Merweville area, Cape Province: An Explanation of sheet 198 (Merweville). 80. Geological Survey of South Africa, Pretoria.

Rubidge, B.S. 2005. Re-uniting lost continents— fossil reptiles from the ancient Karoo and their wanterlust. 27th Du Toit Memorial Lecture. *South African Journal of Geology, 108,* 135-172.

Rubidge, B. S. 1995. Biostratigraphy of the *Eodicynodon* Assemblage Zone. In: Rubidge, B.S. (ed). *Biostratigraphy of the Beaufort Group (Karoo Supergroup). SACS Biostratigrphic Series, Council for Geosciences,* Pretoria, South Africa, 1: 3-7.

Rubidge, B. S. 1994. *Australosyodon*, the first primitive anteosaurid dinocephalian from the Upper Permian of Gondwana. *Palaeontology*, 37: 579–594.

Rubidge, B.S. 1991. A new primitive dinocephalian mammal-like reptile (therapsid) fauna from Russia. *South African Journal of Science*, 34: 547-559.

Rubidge, B. S. 1990a. A new vertebrate biozone at the base of the Beaufort Group. Palaeontologia Africana, 27, 17–20. Rubidge, B. S. 1990b. The cranial morphology of a new species of the genus *Eodicynodon* (Therapsida, Dicynodontia). Navorsinge van die Nasionale Museum, Bloemfontein, 7, 29–41.

Rubidge, B.S, Day, M.O, and Benoit, J. 2021. New Specimen of the Enigmatic Dicynodont *Lanthanostegus mohoii* (Therapsida, Anomodontia) from the Southwestern Karoo Basin of South Africa, and its Implications for middle Permian Biostratigraphy. *Earth Science*. 9: 668143. Doi: 10.3389/feart.2021.668143.

Rubidge, B. S, and Day, M. O. 2020. Biostratigraphy of the *Eodicynodon* Assemblage Zone (Beaufort Group, Karoo Supergroup), South Africa. South African Journal of Geology 123, 141–148. doi:10.25131/sajg.123.0010.

Rubidge, B.S, Govender, R, and Romano, M. 2019. The postcranial skeleton of the basal tapinocephalid dinocephalian *Tapinocaninus pamelae* (Synapsida: Therapsida) from the South African Karoo Supergroup, 17(20): 1767-1789.

Rubidge, B.S, and Kitching, J.W. 2003. A new burnetiamorph (Therapsida: Biarmosuchia) from the Lower Beaufort Group of South Africa. Palaeontology, 46, 199-210.

Rubidge, B.S, and Sidor, C. A. 2001. Evolutionary patterns among Permo-Triassic therapsids. *Annual Reviews of Ecology and Systematics,* 32: 449-480.

Rubidge, B.S, Sidor, C.A, and Modesto, S.P. 2006. A New Burnetiamorph (Therapsida: Biarmosuchia) from the middle Permian of South Africa. *Journal of Paleontology*, 80, 740-749.

Rubidge, B.S, and van den Heever., J.A., 1997. Morphology and systematic position of the dinocephalian *Styracocephalus platyrhynchus. Lethaia,* 30: 157-168.

Rubidge, B. S, and Hopson, J. A. 1996. A primitive anomodont therapsid fom the base of the Beaufort Group (Upper Permian) of South Africa. *Zoological Journal of the Linnean Society*, 117: I 15- 139.

Rubidge, B. S, and Hopson, J. A. 1990. A new anomodont therapsid from South Africa and its bearing on the ancestry of Dicynodontia. *South African Journal of Science*, 86: 43-45.

Schoch, R.R, and Sues, H-D. 2019. The origin of the turtle body plan: Evidence from fossils and embryos. *Palaeontology*, 63, (3), 2020, pp. 375–393.

Seeley, H.G. 1888a. On the nature and limits of reptilian character in mammalian teeth. *Proceedings of the Royal Society of London,* 44 (266-272): 129-141.

Seeley, H.G. 1892a. Researches on the structure, organization, and classification of the fossil Reptilia.VIII. Further observations on *Pareiasaurus*. *Philosophical Transactions of the Royal Society of London B,* 183: 311-370.

Sennikov, A.G. 1996. Evolution of the Permian and Triassic tetrapod communities of eastern Europe. *Palaeogeography Palaeoclimatology Palaeoecology* 120: 331-351

Sidor, C.A. 2000. *Evolutionary trends and relationssships within Synapsida.* PhD thesis (in two volumes). University of Chicago. Chicago. xiv + 370 p.

Sidor, C. A, Angielczyk, K.D, Smith, R. M.H, Goulding, A. K, Nesbitt, S.J, Peecook, B.R, Steyer, J. S, and Tolan, S. 2014. Tapinocephalids (Therapsida, Dinocephalia) from the Permian Madumabisa Mudstone Formation (Lower Karoo, Mid-Zambezi Basin) of southern Zambia. *Journal of Vertebrate Paleontology*, 34(4): 980-986.

Sigogneau-Russell, D. 1989. Theriodontia I: *Encyclopedia of Palaeoherpetology* Part 17B. Gustav Fisher, Stuttgart, 127pp.

Simon, R.V, Sidor, C.A, Angielczyk, K.D, and Smith, R. M.H. 2010. First record of a tapinocephalid (Therapsida: Deinocephalia) from the Ruhuhu Formation (Songea Group) of southern Tanzania. *Journal of Vertebrate Paleontology*, 30 (4): 1289-1293.

Simpson, G. G, Roe, A, and Lewontin, R.C. 1960. *Quantitative Zoology*. Harcourt, Brace and World, Inc., 440 pp.

Smith, K.K. 1992. The evolution of the mammalian pharynx. *Zoological Journal of the Linnean Society* (1992), 104: 313-349.

Smith, R.M.H, and Keyser, A. W. 1995. Biostratigraphy of the *Tapinocephalus* Assemblage Zone. In: *Biostratigraphy of the Beauferot Group (Karoo Supergroup),* (ed). Rubidge, B.S., pp. 8-12. South African Committee for Stratigraphy Biostratigraphic Series 1.

Smith, R.M.H, and Ward, P.D. 2001: Pattern of vertebrate extinctions across an event bed at the Permian-Triassic boundary in the Karoo Basin of South Africa. *Geology* 29, 1147–1150.

Smith, R.M.H, Rubidge, B.S, and Van Der Walt, M. 2012. Therapsid biodiversity patterns and paleoenvironments of the Karoo Basin, South Africa. In *Forerunners of Mammals: Radiation, Histology, Biology.* (ed). Chinsamy-Turan A., pp.30-62. Indiana University Press.

Stear, W.M. l980. The sedimentary environment of the Beaufort Group Uranium province in the vicinity of Beaufort West, South Africa. Unpublished Ph.D.Thesis, University of Port Elizabeth, South Africa. 188pp.

Frederik Spindler, F, Werneburg, R, Schneider, J.W, Luthardt, L, Annacker, V, and Rößler, R. 2018. First arboreal 'pelycosaurs' (Synapsida: Varanopidae) from the early Permian Chemnitz Fossil Lagerstätte, SE Germany, with a review of varanopid phylogeny. *Paläontologische Gesellschaft* 92:315–364. Doi.org/10.1007/s12542-018-0405-9.

Tchudinov, P.K. 1983. Early therapsids. *Trudy Paleontologischeskogo Institute, Akademia Nauk SSSR,* 202: 1-227. [in Russian]

Tchudinov, P. K. 1968. A new dinocephalian from the Cisuralian Region (Reptilia, Therapsida; Upper Permian). *Postilla*. 121: 1-20.

Twelvetrees, W.H. 1882. On some reptilian teeth from the Upper Permian cupriferous sandstones of Kargalinsk, near Orenburg, Russia. *Geological Magazine,* 9 (8): 337-410.

Van Den Brandt, M.J. 2020. Cranial and postcranial anatomy of middle Permian pareiasaurs. Unpublished PhD thesis, University of the Witwatersrand, Johannesburg, 563pp

Van Den Brandt, M.J, Rubidge, B.S, Benoit, J, and Abdala, F. 2021. Cranial morphology of the middle Permian pareiasaur *Nochelesaurus alexanderi* from the Karoo Basin of South Africa. *Earth and Environmental Science Transactions of the Royal Society of Edinburgh*, 112, 29 –49, 2021.

Van Den Brandt, M. J, Abdala, F, and Rubidge, B. S. 2019. Cranial morphology and phylogenetic relationships of the middle Permian pareiasaur *Embrithosaurus schwarzi* from the Karoo Basin of South Africa. *Zoological Journal of the Linnean society*. 1-40 doi.org/10.1093/zoolinnean/zlz064.

Van Den Heever, J. A. 1994. The cranial anatomy of the early Therocephalia (Amniota: Therapsida). *Annals of the University of Stellenbosch* 1:1-59.

Van Den Heever, J.A. 1987. The comparative and functional cranial morphology of the early Therocephalia (Amniota: Therapsida). Unpublished Ph.D. thesis, University of Stellenbosch, Stellenbosch, 576pp.

Van Der Walt, M, Day, M.O, Rubidge, B.S, Cooper, A. K, and Netterber, I. 2011. A new GIS-based biozone map of the Beaufort Group (Karoo Supergroup), South Africa. *Palaeontologia africana*, 45: 1-5.

Van Heerden, J. 1972. Interspecific variation and growth changes in the cynodont reptile Thrinaxodon liorhinus. *Navorsinge van die Nasionale Museum Bloemfontein*, 2:307–347.

Van Hoepen, E. C. N. 1916. A new Karroo reptile. *Annals of the Transvaal Museum*, 5: (3, suppl. 3).

Veevers, J.J, Cole, D.I, and Cowan, E.J. 1994. Southern Africa: Karoo basin and Cape Fold Belt. In: Veevers, J.J., Powell, C.McA. (eds.), Permian–Triassic Pangean Basins and Fold belts along the Panthalassan Margin of Gondwanaland, vol. 184. *The Geological Society of America*, Boulder, Colorado, Memoir, pp. 223–279.

Watson, D.M.S. 1914. The Deinocephalia, an order of mammal-like reptiles. *Proceedings of the Zoological Society of London,* 84 (3): 749-786.

Watson, D. M.S, and Romer, A.S. 1956. A classification of Therapsid reptiles. *Bulletin of the Museum of Comparative Zoology,* 114: 35-89.

Whitney, M.R, and Sidor, C.A. 2019. Histological and developmental insights into the herbivorous dentition of tapinocephalid therapsids. *Plos One*. https://doi.org/10.1371/journal.pone.0223860.

Whitney, M. R, and Sidor, C.A. 2016. A new therapsid from the Permian Madumabisa Mudstone Formation (Mid-Zambezi Basin) of southern Zambia. Journal of Vertebrate Paleontology doi: 10.1080/02724634.2016.1150767.

Appendix A. Fossils used in this study.

Specimens	Material	Locality	Last ID: as per King, 1988	Current ID
TM 212	Skull, right mandible, right tibia	Abrahamskraal, Prince Albert, South Africa	***Jonkeria truculenta***	***Jonkeria truculenta***
AMNH 5620	Skull without lower jaw	Jan Willemsfontein, Prince Albert, South Africa	***Jonkeria vanderbyli***	***Jonkeria truculenta***
UC 1511	Skull, lower jaw, and fragmentary postcranial elements	Stinkfontein 7, Beaufort West, South Africa	*Jonkeria*. sp (FMNH database)	*Jonkeria truculenta*
MB.R. 983	Imperfect skull and partial lower jaw	Springfontein, Beaufort West, South Africa	***Jonkeria boonstrai***	***Jonkeria truculenta***
SAM-PK-12030	Incomplete skull with right mandibular ramus	Bosluiskraal, Dikbome 53, Laingsburg, South Africa	*Jonkeria truculenta*	*Jonkeria truculenta*
SAM-PK-11884	Skull and lower jaw	Skroefpaal, Prince Albert, South Africa	*Jonkeria vanderbyli*	*Jonkeria truculenta*
SAM-PK- 4343	Skull without lower jaw, humeri, ulna, femur, fibula	Welgemoed, Leeu-Gamka, Prince Albert, South Africa	***Jonkeria haughtoni***	***Jonkeria truculenta***
AMNH 5608	Imperfect skull	Kookfontein, Prince Albert, South Africa	*Jonkeria ingens*	*Jonkeria truculenta*
AMNH 5634	Imperfect skull	Kookfontein, Prince Albert, South Africa	***Jonkeria ingens***	***Jonkeria truculenta***
AMNH 5633	Right mandibular ramus	Abrahamskraal, Prince Albert, South Africa	*Jonkeria truculenta*	*Jonkeria truculenta*
ROZ.B96	Imperfect skull and lower jaw	Zwartskraal, Prince Albert, South Africa	*Jonkeria haughtoni* (Roy Ousthuzien catalogue)	*Jonkeria truculenta*
BMNH 49367a, b, c: BMNH 49868-70	Fragmentary jaw and some "associated post-crania"	Klein Koedoeskop 310, Beaufort West, South Africa	***Titanosuchus ferox***	***Titanosuchus ferox***
BP/1/7380	Cranial fragments, humerus, distal femur	Puntkraal, Sutherland, South Africa	*Titanosuchus ferox* (ESI catalogue)	*Titanosuchus ferox*
SAM-PK- 9004	Pelvis lacking ischia, distal tw0• thirds of ulna	Klein Koedoeskop, Beaufort West South Africa	**Jonkeria koupensis**	***Titanosuchidae insertae sedis***
SAM-PK- 3433	Humerus	Jan Willemsfontein, Prince Albert, South Africa	*Jonkeria ingens*	*Jonkeria truculenta*
SAM-PK- 5014	Deformed left humerus, deformed left ulna, and left radius, left femur, left tibia and left fibula	Abrahamskraal, Prince Albert, South Africa	***Jonkeria rossouwi***	***Jonkeria truculenta***

SAM-PK- 9002	Ulna	Klein Koedoes Kop,Beaufort West, S.A	*Jonkeria haughtoni*	*Jonkeria truculenta*
SAM-PK- 9006	Proximal humerus	Klein Koedoeskop, Beaufort West, South Africa	*Jonkeria ingens*	*Jonkeria truculenta*
SAM-PK- 9145	Radius	Zeekoeivlei, Beaufort West, South Africa	*Jonkeria haughtoni*	*Jonkeria truculenta*
SAM-PK- 9147	Ulna	Zeekoeivlei, Beaufort West, South Africa	*Jonkeria haughtoni*	*Jonkeria trucuclenta*
SAM-PK- 9149	Right humerus	Saairivier, Prince Albert, South Africa	***Jonkeria parvus***	***Jonkeria truculenta***
SAM-PK- 9348	Incomplete and distorted humerus	Mierfontein 318, Beaufort West, South Africa	*Jonkeria ingens*	*Jonkeria truculenta*
SAM-PK- 11463	Ulna	Koedoeskop, Beaufort West, South Africa	*Jonkeria haughtoni*	*Jonkeria truculenta*
SAM-PK- 11994	Humerus with good distal end	Welgemoed, Prince Albert, South Africa	*Jonkeria ingens*	*Jonkeria truculenta*
SAM-PK- 12005	Humerus	Wolwefontein, Prince Albert, South Africa	*Jonkeria parva*	*Jonkeria truculenta*
SAM-PK- 738	Humerus	Jan Willemsfontein, Prince Albert, South Africa	*Titanosuchus ferox*	*Titanosuchus ferox*
SAM-PK- 739	Femur	Beaufort West district, South Africa	*Titanosuchus ferox*	*Titanosuchus ferox*
SAM-PK- 772	Humerus	Seekoegat, Prince Albert, South Africa	*Titanosuchus ferox*	*Titanosuchus ferox*
SAM-PK- 773	Humerus	Seekoegat, Prince Albert, South Africa	*Titanosuchus ferox*	*Titanosuchus ferox*
SAM-PK- 5001	Humerus, femur	Sewefontein, Prince Albert, South Africa	*Titanosuchus ferox*	*Titanosuchus ferox*
SAM-PK- 9127	Lower jaw fragment, femur and fibula	Voelfontein, Prince Albert, South Africa	*Titanosuchus ferox*	*Titanosuchus ferox*
SAM-PK- 9163	Ulna, fibula	Wakkerstroom, Prince Albert, South Africa	*Titanosuchus ferox*	*Titanosuchus ferox*
SAM-PK- 11299	Radius, tibia	Boesmansrivier, Beaufort West, South Africa	*Titanosuchus ferox*	*Titanosuchus ferox*
SAM-PK- 11881	Humerus	Blaauwkranz, Prince Albert, South Africa	*Titanosuchus ferox*	*Titanosuchus ferox*
SAM-PK- 11488	Fibula, tibia	Mynhardtskraal, Beaufort West, South Africa	*Titanosuchus ferox*	*Titanosuchus ferox*
SAM-PK- 11938	Tibia	Steenboksfontein, Laingsburg, South Africa	*Titanosuchus ferox*	*Titanosuchus ferox*

SAM-PK-11491	Femur	Mynhardtskraal, Beaufort West, South Africa	*Titanosuchus ferox*	*Titanosuchus ferox*
SAM-PK-11578	Humerus	Aasvoelbos, Beaufort West, South Africa	*Titanosuchus ferox*	*Titanosuchus ferox*
SAM-PK-11881	Humerus	Blaauwkranz, Prince Albert, South Africa	*Titanosuchus ferox*	*Titanosuchus ferox*
SAM-PK-11989	Fibula	Koedoeskop, Beaufort West, South Africa	*Titanosuchus ferox*	*Titanosuchus ferox*
BP/I/7168	Imperfect skull and postcranial fragments	Puntkraal portion of Uitvlug 90, Sutherland, South Africa	Titanosuchid indet (ESI catalogue)	Titanosuchid indet

Appendix B. Cranial measurements (mm) used for allometric analysis

Specimen	TM 212	SAM-PK-12030	MB.R.983	AMNH 5633	AMNH 5634	AMNH 5608	AMNH 5620	SAM-PK-11884	SAM-PK-4343	FMNHUC 1511
1	525		660		520*	610*	650*	640	590	680
2	330	315	400			390*	400*	431	420	390
3	58		75*				86	95	75	95
4	100					130*	113*	158	114	125
5	151		138			83	83	80	92*	103
6	34		73			70	42	35	40	38
7	161	240*	250				210	217	235	248
8	280		420*				310*	244*	480	
9	75		160					138	140	140
10	119*				140	140*	130*	124	133	140
11	55					63	47	44		55
12	43						54	48		48
13	167						195	224		225
14	440		515				540	530		610
15	90		90				120*	94		105
16	119*				140	140*	130*	124	133	140
17	410	520		565*			195	590		560
18	55	91	109	110		63	47	78		100
19	43	170		115			54	151*		183
20	222		197		280	300	240	171*	197	310

Key

1. Total skull length (until occipital condyle)
2. Snout length
   to tip of snout
3. Orbital length (antero-posterior)
   foramen to edge of occipital condyle
4. Interorbital width
   of snout
5. Intertemporal width (at level of pineal foramen)
   mandible
6. Width of postorbital bar
7. Width of snout (at level of canine)
   eminence)
8. Greatest width of the skull (at level of squamosals)
9. Temporal opening diameter (antero-poterior)
10. Pterygoid process width
11. Width of jugal below eye orbit
12. Inter-nostril width
13. Occiput height
14. Distance from anterior margin of pineal foramen to tip of snout
15. Distance from posterior margin of pineal foramen to occipital condyle
16. Distance from lateral flanges of pterygoid to tip of snout
17. Length of the lower jaw from articular to tip of the jaw
18. Height of the dentary at symphysis
19. Height of the lower jaw at the coronoid eminence
20. Width of occiput between squamosals

Appendix C. Limb bone dataset for Principal component analysis.

? means the measurement is unsure because the bone is broken or weathered.

Humerus

Taxa	Specimen	Length(mm)	Proximal width (mm)	Distal width (mm)	Shaft width (mm)
Titanosuchus ferox	SAM-PK-11881	620	310	300	125
Titanosuchus ferox	SAM-PK-5001	490	?	274	?
Titanosuchus ferox	BMNH 49369	580	310	305	126
Titanosuchus ferox	BP/I/7380	400	280	?	120
Jonkeria truculenta	SAM-PK-4343	455	324	305	167
Jonkeria truculenta	AMNH 5577	450	360	320	120
Jonkeria truculenta	SAM-PK-738	490	350	?	138
Jonkeria truculenta	SAM-PK-3433	506	370	310	?
Jonkeria truculenta	SAM-PK-9149	312	222	252	78
Jonkeria truculenta	SAM-PK-5014	378	330	262	122
Tapinocephalus atherstonei	SAM-PK-5007	610	314	273	115
Tapinocaninus pamelae	NMQR 2987	440	291	241	88
Dimetrodon booneorum	FMNHUC75	118	48	63	13
Dimetrodon booneorum	FMNHUC247	134	49	76	18
Dimetrodon limbatus	FMNHUC841	172	89	121	29
Dimetrodon limbatus	FMNHUC843	163	85	103	22
Dimetrodon loomisi	FMNHUC149	188	85	95	21
Dimetrodon loomisi	FMNHUC421	190	90	95	24

Femur

Taxa	Specimen	Length(mm)	Proximal width (mm)	Distal width (mm)	Shaft width (mm)
Titanosuchus ferox	BMNH 49368	620	?	?	132
Titanosuchus ferox	SAM-PK-739	570	?	235	151
Titanosuchus ferox	SAM-PK-5001	560	310	280	159
Titanosuchus ferox	SAM-PK-9127	570	310	300	144
Titanosuchus ferox	SAM-PK-11491	500	325	235	145
Jonkeria truculenta	SAM-PK-5014	504	280	228	156
Riebeeckosaurus longirostris	SAM-PK-9167	375	170	141	88
Moschops sp.	SAM-PK-12041	377	167	173	103
Tapinocaninus pamelae	NMQR 2987	440	154	153	85
Dimetrodon booneorum	FMNHUC120	150	40	45	18
Dimetrodon booneorum	FMNHUC131	143	40	43	18

Dimetrodon limbatus	FMNHUC857-A	204	73	75	33
Dimetrodon limbatus	FMNHUC857-B	200	59	63	26
Dimetrodon natalis	FMNHUC823-A	125	37	39	17
Dimetrodon natalis	FMNHUC823-B	122	36	37	17

Ulna

Taxa	Specimen	Length(mm)	Proximal width (mm)	Distal width (mm)	Shaft width (mm)
Jonkeria truculenta	SAM-PK-4343	402	222	?	113
Jonkeria truculenta	AMNH 5577	?	190	?	?
Jonkeria truculenta	SAM-PK-9147	360	175	126	93
Titanosuchus ferox	SAM-PK-9163	375	198	131	108
Jonkeria truculenta	SAM-PK-9002	350	180	?	110
Moschops capensis	SAM-PK-11292	162	116	91	66
Struthiocephalus whaitsi	SAM-PK-11939	201	110	65	58
Tapinocaninus pamelae	NMQR 2987	216	141	70	72
Dimetrodon booneorum	FMNHUC819	142	47	32	16
Dimetrodon grandis	NM8365 Romer & Price	205	74	46	27
Dimetrodon limbatus	WM819 Romer & Price	146	47	28	15
Dimetrodon loomisi	FMNHUC142	169	53	39	19
Dimetrodon loomisi	FMNHUC584	169	46	28	15

Radius

Taxa	Specimen	Length(mm)	Proximal width (mm)	Distal width (mm)	Shaft width (mm)
Titanosuchus ferox	SAM-PK-11299	290	164	148	75
Jonkeria truculenta	SAM-PK-9145	310	166	162	80
Jonkeria truculenta	SAM-PK-5014	312	154	131	70
Dimetrodon booneorum	FMNHUC819	148	35	35	20
Dimetrodon limbatus	FMNHUC91	165	46	44	20
Dimetrodon natalis	FMNHUC53	105	22	21	11
Dimetrodon natalis	FMNHUC92	116	23	25	12

Fibula

Taxa	Specimen	Length (mm)	Proximal width (mm)	Distal width (mm)	Shaft width (mm)
Titanosuchus ferox	SAM-PK-9127	245	138	152	?
Titanosuchus ferox	SAM-PK-9163	330	139	125	65
Titanosuchus ferox	SAM-PK-11488	330	141	123	?
Titanosuchus ferox	SAM-PK-11989	297	147	128	71

Jonkeria truculenta	SAM-PK-4343	296	?	?	56
Jonkeria truculenta	SAM-PK-5014	330	127	102	52
Moschops capensis	SAM-PK-11978	233	87	117	47
Moschops capensis	SAM-PK-K318	251	82	98	46
Tapinocaninus pamelae	NMQR 2987	263	85	67	31
Dimetrodon booneorum	FMNHUC68	123	24	25	9
Dimetrodon gigashomogens	MCZ 1283 Romer and Price	211	42	58	16
Dimetrodon limbatus	UM Ivd Romer and Price	155	33	38	13
Dimetrodon loomisi	FMNHUC424	180	37	36	11
Dimetrodon milleri	MCZ 1365 Romer and Price	129	22	25	8
Dimetrodon natalis	MCZ 1443 Romer and Price	85	15	17	6

Tibia

Taxa	**Specimen**	**Length (mm)**	**Proximal width (mm)**	**Distal width (mm)**	**Shaft width (mm)**
Titanosuchus ferox	SAM-PK-11299	320	180	152	87
Titanosuchus ferox	SAM-PK-11488	370	200	154	92
Titanosuchus ferox	SAM-PK-11938	290	165	160	100
Jonkeria truculenta	TM 212	248	128	105	77
Jonkeria truculenta	SAM-PK-5014	300	154	148	79
Moschops capensis	SAM-PK-11977	248	133	96	54
Moschops capensis	SAM-PK-11978	196	131	75	58
Tapinocaninus pamelae	NMQR 2987	228	122	78	55
Dimetrodon booneorum	FMNHUC126	103	39	21	10
Dimetrodon booneorum	FMNHUC61	115	38	23	10
Dimetrodon limbatus	FMNHUC69	138	47	26	16
Dimetrodon limbatus	FMNHUC305-A	162	62	37	18
Dimetrodon natalis	FMNHUC822-A	122	47	26	13
Dimetrodon natalis	FMNHUC822-B	80	26	15	7

Appendix D. Morphological character list for phylogenetic analysis.

The number preceding the character definition corresponds to that of the columns in the data matrix. H&B: Hopson and Barghusen (1986); Ka: Kammerer (2011); Ki: King (1988); R&H: Rubidge and van den Heever (1997); S: Sidor (2000); FBDR: Fraser-King *et al*., (2019); Neu: Guven-Neumann (2020). Citations with an asterisk denote that the character definition has been modified or character state(s) have been added/deleted. Coding of characters is based on personal observation supplemented by references.

1. Vomer ventral surface: flat to convex (0), lateral ridges and median trough (1) (FBDR: 31; Ka*10). Non-mammalian therapsds show a great diversity in vomerine morphology, some with median ridges and others with median troughs (Sidor 2000). *Jonkeria* specimens exhibit a unique vomerine morphology in which the paired vomer are flat elongate straplike rods with a shallow midline trough with bifurcated anterior ends

2. Location of external naris: terminal (0), nonterminal (1) (Ka: 6; S: 8). The presence of a nonterminal external naris has been considered a dinocephalian synapomorphy (Hopson 1991; Grine 1997; Sidor 2000). In most anteosaurs (but not *Archaeosyodon*), the premaxilla is dorsoventrally expanded, such that the distance between the premaxillary margin and the external naris is greater than the height of the naris. Under this definition, *Sinophoneus* is considered to possess a nonterminal naris (Kammerer, 2011). A nonterminal naris is also present in *Jonkeria* and most tapinocephalians, with the primitive condition present in *Estemmenosuchus*.

3. Dorsal profile of snout: oblique convex (0), near straight and flat (1) (FBDR: 1). *Jonkeria* specimens have an almost straight to a flat dorsal snout profile while other dinocephalian families seem to have an oblique convex condition for this character.

4. Posterior extent of the nasal process of premaxilla: less than half preorbital length (0), half of the preorbital length (1), more than half the preorbital length (2), close to the nasal posterior end (3). (FBDR*: 4; H&B*: 1.2.7; S*:4.1; Gu: 3). In all the *Jonkeria* specimens the premaxilla forms an inter-nasal process which tappers posteriorly forming a contact with the frontals thereby occupying more than half the pre-orbital length. In *Styracocephalus* the premaxilla is less than half the pre-orbital length while in tapinocephalids (*Ulemosaurus*, *Tapinocaninus* and *Moschops*), anteosaurs and *Estemmenosuchus* it seems to be half of the preorbital length.

5. Position of jaw articulation: close to the posterior border of the temporal fossa (0), in the center of the temporal fossa (1), at the anterior border of the temporal fossa (2), at the anterior border of the postorbital bar (3), under the orbit (4) (H&B*:2.15.1; Ka*: 35; Ki*: C.1; R&H*:25; Neu: 45). A terminal posterior position for the suspensorium is primitive for therapsids in general, including dinocephalians (Kammerer, 2011). In some tapinocephalia the suspensorium has been rotated forward (extremely so in

tapinocephalids than in *Jonkeria*) and the anteosaurs *Anteosaurus* and *Titanophoneus* (Kammerer, 2011).

6. Postcanine morphology: laterally compressed and pointed (0), bulbous at base of crown (1), laterally compressed and leaf-shaped (2) (H&B*: 2.12.2 and 2.15.3; R&H: 2; Neu: 56).

7. Canine curvature: moderate (0), straight or weak (1), strong (2). (Ka*:4, Neu: 54). The canine in *Jonkeria* specimens where it is preserved (ROZ . B96, SAM-PK- 4343, SAM-PK- 12030) is strongly recurved but slightly less than in the anteosaurs *Microsyodon*, *Archaeosyodon*, and *Syodon*.

8. Incisor morphology: without lingual heel (0), with weakly developed lingual heel (1), with well-developed lingual heel (2) (FBDR: 59; H & B: 1.5.3; R& H: 1; Ki*: C.1; Neu: 51). *Jonkeria* just like tapinocephalids are characterized by incisor teeth with a well developed lingual heel.

9. Dentition on palatine: broadly distributed (0), restricted to small area (1), absent (2) (FBDR*: 35; R&H*:17; S*:4.45; Neu: 35). One of the features that distinguish titanosuchids (*Jonkeria* and *Titanosuchus*) from basal tapinocephalids and anteosaurs is the absence of palatine dendition in the former Family.

10. Dentition on palatal ramus of pterygoid: present (0), absent (1) (Ka: 13; S*: 51). The palatal ramus of the pterygoid in dinocephalians forms a ridge oriented anterolaterally from the midpoint of the transverse processes and in contact with the palatine boss. In *Archaeosyodon*, *Australosyodon* and *Estemmenosuchus*, this ridge is covered with numerous teeth, but other anteosaurs like *Syodon* and *Titanophoneus adamanteus*, have only a single tooth while titanosuchids *Jonkeria* and *Titanosuchus* just like the anteosaurs, *Anteosaurus* and *Titanophoneus potens* have no teeth on the palatal ramus of the pterygoid.

11. Dentition on transverse process of pterygoid: present (0), absent (1) (Ka: 14; R&H*: 16; S*: 52). A primitive condition in therapsids is the presence of numerous teeth on the ventral surface of the transverse processes of the pterygoids. These teeth have been lost to varying degrees in several therapsid groups, including anteosaurs (Kammerer, 2011) and completely in titanosuchids (*Jonkeria* and *Titanosuchus*).

12. Quadrate rami of pterygoids intimately appressed, bifurcating the anterior margin of the basisphenoid: absent (0), present (1) (Ka: 17). Basal therapsids and tapinocephalians (which includes *Jonkeria* and *Titanosuchus*), exhibit an anterior ramus of the basisphenoid which separates the two quadrate rami of the pterygoids. In anteosaurs, however, the quadrate rami remain closely appressed, bifurcating the anterior margin of the basisphenoid (Kammerer, 2011).

13. Snout proportions: height greater than width (0), height equal to width (1), height less than width (2) (FBDR: 2; Ka*: 21; Neu: 7). *Jonkeria* just like *Estemmenosuchus, Biarmosuchus* and the anteosaurs *Archeosyodon* and *Syodon*, and the tapinocephalids *Moschops*, *Ulemosaurus* and *Tapinocaninus* have snouts with a height equal to width while the tapinocephalid *Struthiocephalus* the snout height is less than the width. *Styracocephalus* on the other hand exhibits snout height greater than the width (Fraser-King *et al*., 2019).

14. Temporal fenestra relative to orbit: smaller than orbit (0), larger than orbit (1) (FBDR: 11). All *Jonkeria* specimens (except the juvenile TM 212) and anteosaurs *Anteosaurus*, *Archaeosyodon* and *Syodon* exhibit a larger temporal fenestra relative to the orbit just like *Estemmenosuchus*, tapinocephalids *Tapinocaninus*, and *Ulemosaurus* and *Struthiocephalus* while *Moschops* has smaller temporal fenestra relative to orbits

15. Dorsal margin of maxilla: gently rounded, with no overhang on lacrimal (0), with dorsoposterior process partly overhanging upper margin of lacrimal (1). (Ka: 19). In *Jonkeria* just like in *Biarmosuchus*, and the anteosaurs *Microsyodon* and *Archaeosyodon*, the dorsal sutural border of the maxilla is a bit rounded whereas in other anteosaurs, the posterior dorsal border of the maxilla has a prominent process contacting the prefrontal and overhanging the anterior edge of the lacrimal (Kammerer, 2011).

16. Ventral margin of maxilla: sub-horizontal (0), highly convex (1). (S*: 4.10; Neu: 15). *Jonkeria* just like tapinocephalids (*Tapinocaninus*, *Ulemosaurus*, *Struthiocephalus* and *Moschops*), *Estemmenosuchus*, *Deuterosaurus* exhibits a suhorizontal ventral margin of the maxilla unlike in anteosaurs.

17. Shape of postorbital bar: gently curved (0), strong anteroventral curvature, temporal fenestra undercuts orbit (1). (Ka: 28). The temporal fenestra and the orbit are separated by an almost straight postorbital bar in titanosuchids (*Jonkeria* and *Titanosuchus*) as is the case in most therapsids, leading to a condition where the anterior margin of the temporal fenestra is located posterior to the orbit in lateral view. In anteosaurs, however, the postorbital bar curves anteroventrally, such that the temporal fenestra undercuts the orbit in lateral view (Kammerer, 2011).

18. Pachyostosis of skull: absent (0), pachyostosis present but restricted to orbital and temporal rims (1), entire dorsal surface of skull heavily pachyostosed (2). (Ka: 30). All tapinocephalids and the giant anteosaurs *Titanophoneus* and *Anteosaurus* are extremely pachyostosed in the orbital and temporal regions. In titanosuchids (*Jonkeria* and *Titanosuchus*) the sulls are pachyostosed around the orbit, temporal rim and parietal while other anteosaurs such as *Syodon*, *Notosyodon* and *Sinophoneus*, however, their skulls are weakly pachyostosed around the orbit and temporal or not pachyostosed at all as in *Archaeosyodon*.

19. Antorbital region: long (0), short (1). (Neu: 6). *Jonkeria* just like the tapinocephalid *Struthiocephalus* have very long antorbital region (snouts). Other tapinocephalids have relatively shorter snouts just like is the case with anteosaurids.

20. Shape of dorsal surface of nasals: flat (0), with median boss (1). (FBDR*: 1; S*: 4.15; Neu: 8). Styracocephalids just like biarmosuchians have dorsal surface of nasals that exhibit a median boss while *Jonkeria* skulls have a flat condition for this character.

21. Shape of dorsal surface of parietal surrounding parietal foramen: flat (0), low and diffuse swelling (1), forms well-defined chimney (2). (FBDR: 17). *Jonkeria* just like the tapinocephalid *Struthiocephalus*, estemmenosuchid *Estemmenosuchus*, anteosaurid *Syodon* and biarmosuchus all have a swollen parietal region forming a well defined chimney surrounding the pineal foramen. Some tapinocephalids such as *Tapinocaninus*, *Ulemosaurus* and *Moschops* and the anteosaurids *Anteosaurus* and *Archaeosyodon* have low and diffuse dorsal surface of the the parietal.

22. Boss above postorbital bar: absent (0), present (1). (FBDR: 15). One of the distinguishing characters between anteosaurids, estemmenosuchids and titanosuchids is presence of a boss above the postorbital bar in the former two families, a feature which lacks in titanosuchids.

23. Intertemporal breadth: narrow (0), broad (1). (FBDR*: 18; H&B*:1.4.1; S*: 4.35; Neu: 37). *Jonkeria* skulls just like those of the Styracocephalidae, tapinocephalids *Struthiocephalus* and *Moschops* and Estemmenosuchidae have a broad intertemporal breadth. Anteosaurs (*Archaeosyodon*, *Syodon* and *Anteosaurus*) on the other hand have a narrow condition for this character.

24. Anterior extension of anterior ramus of squamosal: stops under temporal fenestra (0), beyond the anterior margin of the temporal fenestra (1). (FBDR: 21). In all *Jonkeria* skulls the anterior ramus of the squamosal extends beyond the anterior margin of the temporal fenestra while this condition varies among tapinocephalid and anteosaurid species.

25. Tabular: contacts paroccipital process of opisthotic (0), restricted dorsally (1). (FBDR: 25). *Jonkeria* skulls just like those of anteosaurids, and the tapinocephalid *Struthiocephalus*, the tabular contacts the paroccipital process of the opisthotic. In other tapinocephalids (*Tapinocaninus*, *Ulemosaurus* and *Moschops*), the tabular is restricted dorsally.

26. Length of vomerine process of premaxilla: short (0), long, extending posteriorly and forming part of the medial margin of the inner choana (1), absent in ventral view so that vomer abuts body of premaxilla (2). (FBDR: 27).

27. Forward rotation of occiput: none (0), moderate (1), pronounced (2). (FBDR*: 42; H&B*: 2.15.1; S*:4.55; Neu: 41). For *Jonkeria truculenta* just like in *Moschops*, *Ulemosaurus* and *Tapinocaninus* and in *Estemmenosuchus*, the forward rotation of the occiput is more pronounced. In the anteosaurids, the forward rotation of the occiput is moderate.

28. Parietal raised and laterally bayed: absent (0), present (1). This character distinguishes titanosuchids (*Jonkeria* and *Titanosuchus*) with raised and laterally bayed parietals, from other dinocephalian families except some tapinocephalids such as *Avenantia kruisvleiensis* and *Struthiocephalus,* which also have a similar condition.

29. Incisor heels: absent (0), present (1). (FBDR: 59; H & B: 1.5.3; R& H:1; Ki*: C.1; Neu: 51). Titanosuchids just like tapinocephalids have well defined incisor heels, which act as a crushing surface in the oral processing of food.

30. Lower canine: fits into choana (0), fits into fossa roofed by premaxilla and maxilla (1), passes anterior and external to upper canine (2) (FBDR: 62). In titanosuchids just like in *Estemmenosuchus*, the lower canine passes anterior and external to the upper canine while in anteosaurids, the lower canine fits into a fossa roofed by the maxilla and premaxilla.

31. Upper and lower canines: without heels (0), small heels present (1) (FBDR: 63; H&B*: 2.18.2; S*:4.86; Neu: 52). Titanosuchid (*Jonkeria*) canines (both lower and upper) are oval without any heels.

32. Number of upper (maxillary) postcanines: twelve or greater (0), fewer than twelve (1) (FBDR*:65). Titanosuchids have more maxillay postcanines varying from twelve and more.

33. Snout dorsal profile anteriorly: gradually sloping towards the tip (0), steep slope (1), evenly convex (2) (FBDR*: 1; S*: 4.15; Neu: 8). The Jonkeria truculenta snout profile anteriorly gradually slopes towards the tip. This condition is similar in *Moschops*, *Struthiocephalus*, *Ulemosaurus*, *Tapinocaninus*, *Estemmenosuchus* and the anteosaurid *Archaeosyodon*. In *Styracocephalus* and anteosaurids *Anteosaurus* and *Syodon*, the snout dorsal profile is evenly convex.

34. Squamosal lateral surface: not thickened (0), swollen and round (1), slender with longitudinal depression close to anteroventral border (2) (FBDR*: 19; S*: 4.32; Neu: 21). The squamosal is not, thickened in titanosuchids just like in *Styracocephalus*. The condition is swollen and round for this feature in the tapinocephalids, *Moschops*, *Ulemosaurus* and *Tapinocaninus* and the anteosaurids *Anteosaurus* and *Syodon*.

35. Anteroventral slope of the occiput: absent (0), weak (1), moderate (2), strong (3) (FBDR*: 42; H&B*: 2.15.1; S*:4.55). Titanosuchids just like *Estemmenosuchus* and the

anteosaurid *Syodon* have a moderate anteroventral slope of the occiput. *Moschops* has a very strong slope while *Anteosaurus* has a weak slope.

36. Ventral margin of the quadrate ramus of the pterygoid: narrow and slender (0), broad and thickened (1) (Neu: 43). *Jonkeria truculenta* has a narrow and slender ventral margin of the quadrate ramus of the pterygoid. In *Styracocephalus,* this feature is broad and thickened.

37. Anteroventral slope of dentary symphysis: absent (0), moderate slope (1), strong slope (2) (Neu: 46). The anteroventral slope of the dentary symphysis of *Jonkeria truculenta* is moderately steep just like in *Estemmenosuchus*, *Styracocephalus Anteosaurus,* and *Sydon.* This feature is very steep in *Moschops*, *Struthiocephalus* and *Tapinocaninus*.

38. Maxillary dentition decreases in size posteriorly: absent (0), present (1) (H&B*: 2.17.1; S*: 4.83; Neu: 50). Tapinocephalids and titanosuchids have maxillary dentition that decreases in size posteriorly while this feature is absent in anteosaurids.

39. Size of upper canine with respect to incisors: smaller (0), as large (1), larger (2) (S*:4.80; Neu: 53). Titanosuchids (*Jonkeria* and *Titanosuchus*) just like in the styracocephalid, *Styracocephalus* and anteosaurids and biarmosuchians have a very large canine relative to the insisors. *Tapinocaninus* and *Ulemosaurus* have canines, which are almost of an equal size with the incisors.

40. Canine morphology: lingually flat (0), lingually forms small ridge like heel (1), incisiform (2) (FBDR: 63; H&B*: 2.18.2; S*:4.86). Titanosuchid canines are lingually flat just like in other dinocephalian families that have canines. Basal tapinocephalids *Tapinocaninus* and *Ulemosaurus* have canines that form a small ridge like keel.

41. Epicondyle foramina of the humerus: both entepicondylar and ectepicondylar foramina present (0), only entepicondylar foramen present (1). Both *Jonkeria* and *Titanosuchus* humeri have both ect- and ent- epicondylar foramina which is what distinguishes titanosuchids from other dinocephalian families, except the tapinocephalid *Moschops* which also has both foramina present.

42. Radial condyle (capitellum) of humerus: strongly bulbous, rounded, and extends moderately to far proximally along the ventral face (0), more distally positioned (1). Titanosuchids (*Jonkeria* and *Titanosuchus*) have very strongly bulbous and rounded radial condyles, which extend moderately to far proximally along the ventral face of the humerus while those of tapinocephalids and anteosaurids are, more distally positioned.

43. Lateral margin of the choana formed by the palatine: less than a third (0), more than a third (1) (FBDR: 33). *Jonkeria truculenta* just like in the tapinocephalid, *Struthiocephalus* and the anteosaurid, *Anteosaurus* have the palatine forming less than a third of the lateral margin of the choana and the situation seems different in the other

tapinocephalids such as *Moschops*, *Ulemosaurus* and *Tapinocaninus* and the aneosaurids, *Archaeosyodon* and *Syodon*.

44. Position of transverse flange of pterygoid: under posterior half of orbit (0), under anterior half of orbit (1), preorbital (2) (FBDR: 38). *Jonkeria truculenta* just like the tapinocephalids, *Moschops*, *Struthiocephalus*, *Ulemosaurus* and *Tapinocaninus* and the styaracocephalid *Styracocephalus* and the estemmenosuchid, *Estemmenosuchus* and the anteosaurid, *Anteosaurus* have the transverse flange of the pterygoid positioned pre-orbital while that of *Syodon* and *Archaeosyodon* just like in the deuteosaurid *Deuterosaurus* are, positioned under the anterior half of the orbit.

45. Basisphenoid: with a ventral groove (0), with a weak ventral ridge (1), with a strong ventral ridge (2). *Jonkeria truculenta* has a strong ventral ridge on the basishenoid while tapinocephalid basisphenoids have a weak ventral ridge and anteosaurids on the other hand have a ventral groove instead.

46. Squamosal contribution to the occipital surface: narrow (0), broad (1) (Gu: 40). Some tapinocephalids (*Moschops* and *Struthiocephalus*) and anteosaurids (*Archaeosyodon*, *Syodon* and *Anteosaurus*) seem to have a narrow squamosal contribution to the occipital face while other tapinocephalids (*Tapinocaninus* and *Ulemosaurus*), just like the titanosuchid *Jonkeria truculenta* and the styracocephalid, *Styracocephalus* have a broad contribution of the squamosal to the occipital surface.

47. Processus medialis of the humerus: lies in about the same plane as the caput (0), lies slightly in a plane distal to that of the caput (1), lies more (greatly) in a plane distal to that of the caput (2). The processus medialis lies in about the same plane as the caput in Tapinocephalia and Anteosauria but in the Titanosuchia the processus medialis lies in a plane much distally of that of the caput.

48. Proximal and distal expansions of the humerus: smaller (0), larger (1). *Jonkeria truculenta* is distinguishable from *Titanosuchus ferox* by its greatly expanded proximal and distal ends relative to the shaft. *Titanosuchus ferox* on the other hand has less expanded ends.

Appendix E. Data matrix used in the phylogenetic analysis

	1	1111111112	2222222223	3333333334	44444444
Taxon	1234567890	1234567890	1234567890	1234567890	12345678
Biarmosuchus	0000000000	0010000010	200000100?	0100100020	??1100??
Archaeosyodon	1000012010	0111011000	1000011?01	0100100020	??0100??
Syodon	1100012011	1111111110	2000021001	1121211020	??010?0?
Anteosaurus	1110012001	1101111200	1011021001	0121101020	??1200??
Deuterosaurus	1010021011	1101000110	10?0??100?	0110100020	???1????
Estemmenosuchus	1002121000	0011000201	2110?22012	00012?1?20	??02???0
Styracocephalus	1100111010	0100100101	11111?101?	0120111120	??1211??
Jonkeria truculenta	0112120221	1111000100	2111012112	1000201120	00022121
Titanosuchus ferox	?????202??	??????????	????????1?	0???????20	00????10
Tapinocaninus	1102221221	1011000210	1101122011	0101202111	11121101
Ulemosaurus	1102222221	1011100210	1101122011	1101200111	0?12110?
Struthiocephalus	1113421201	1021100200	2110011111?	??02002102	11021?0
Moschops	1103421221	1010100110	1111122012	1101312102	01121000

Appendix F. All the observed and identified Titanosuchid specimens and their stratigraphic positions.

Specimen Number	Collection	Higher Taxon	Family or Clade	Genus	Species	Source of ID	Sector (Day, 2013)	Locality	Centroid	Stratigraphic position
AMNH 5577	AMNH	Dinocephalia	Titanosuchidae	*Jonkeria*	*truculenta*	Jirah 2021	Leeu-Gamka	Rietfontein 56, Prince Albert	Y	mid-upper Moordenaars
AMNH 5608	AMNH	Dinocephalia	Titanosuchidae	*Jonkeria*	*truculenta*	Kammerer 2015; Jirah 2021	Beaufort West	Kookfontein, Antjiefontein 14, Prince Albert	Y	mid-upper Moordenaars
AMNH 5620	AMNH	Dinocephalia	Titanosuchidae	*Jonkeria*	*truculenta*	Kammerer 2015; Jirah 2021	Leeu-Gamka	Jan Willems Fontein, Prince Albert	Y	Moordenaars
AMNH 5633	AMNH	Dinocephalia	Titanosuchidae	*Jonkeria*	*truculenta*	Kammerer 2015; Jirah 2021	Leeu-Gamka	Abrahamskraal 29, Prince Albert	Y	Moordenaars
AMNH 5634	AMNH	Dinocephalia	Titanosuchidae	*Jonkeria*	*truculenta*	Kammerer 2015; Jirah 2021	Beaufort West	Kookfontein, Antjiefontein 14, Prince Albert	Y	mid-upper Moordenaars
BP/I/7168	BPI (ESI)	Dinocephalia	Titanosuchidae			Jirah; Day, Rubidge, 2021	Sutherland	Ou Tuin, Sutherland	N	lower Poortjie
SAM-PK-000738	SAM	Dinocephalia	Titanosuchidae	*Jonkeria*	*truculenta*	Sifelani Jirah 2021	Leeu-Gamka	Abrahamskraal, Prince Albert	Y	Moordenaars
SAM-PK-000772	SAM	Dinocephalia	Titanosuchidae	*Titanosuchus*	*ferox*	Sifelani Jirah 2021	Beaufort West	Seekoegat, Zeekoegat 22, Prince Albert	Y	Probably Moordenaars
SAM-PK-000773	SAM	Dinocephalia	Titanosuchidae	*Titanosuchus*	*ferox*	Sifelani Jirah 2021	Beaufort West	Seekoegat, Zeekoegat 22, Prince Albert	Y	Probably Moordenaars
SAM-PK-003433	SAM	Dinocephalia	Titanosuchidae	*Jonkeria*	*truculenta*	Sifelani Jirah 2021	Leeu-Gamka	Jan Willemsfontein, Jan Willems Fontein 32, Prince Albert	Y	Moordenaars
SAM-PK-004343	SAM	Dinocephalia	Titanosuchidae	*Jonkeria*	*truculenta*	Kammerer 2015; Jirah 2021	Leeu-Gamka	Welgemoed, Veldmans River 9, Prince Albert	Y	Moordenaars
SAM-PK-005001	SAM	Dinocephalia	Titanosuchidae	*Titanosuchus*	*ferox*	Kammerer 2015; Jirah 2021	Leeu-Gamka	Sewefontein, Sevenfontein 5, Prince Albert	Y	lower Moordenaars
SAM-PK-005014	SAM	Dinocephalia	Titanosuchidae	*Jonkeria*	*truculenta*	Kammerer 2015; Jirah 2021	Leeu-Gamka	Abrahamskraal 29, Prince Albert	Y	Moordenaars
SAM-PK-009002	SAM	Dinocephalia	Titanosuchidae	*Jonkeria*	*truculenta*	Jirah 2021	Leeu-Gamka	Klein Koedoeskop	Y	mid-upper Moordenaars

								310, Beaufort West		
SAM-PK-009006	SAM	Dinocephalia	Titanosuchidae	*Jonkeria*	*truculenta*	Jirah 2021	Leeu-Gamka	Klein Koedoeskop 310, Beaufort West	Y	mid-upper Moordenaars
SAM-PK-009079	SAM	Dinocephalia	Titanosuchidae	*Jonkeria*	*truculenta*	Jirah 2021	Leeu-Gamka	Rietkuil 307, Beaufort West	Y	mid Moordenaars
SAM-PK-009127	SAM	Dinocephalia	Titanosuchidae	*Titanosuchus*	*ferox*	Kammerer 2015; Jirah 2021	Merweville	Voelfontein, Vogelfontein 1, Prince Albert	Y	lower Moordenaars
SAM-PK-009145	SAM	Dinocephalia	Titanosuchidae	*Jonkeria*	*truculenta*	Jirah 2021	Merweville	Zeekoeivlei, Zeekoevalley 282, Beaufort West	Y	lower Moordenaars
SAM-PK-009147	SAM	Dinocephalia	Titanosuchidae	*Jonkeria*	*truculenta*	Jirah 2021	Merweville	Zeekoeivlei, Zeekoevalley 282, Beaufort West	Y	lower Moordenaars
SAM-PK-009149	SAM	Dinocephalia	Titanosuchidae	*Jonkeria*	*truculenta*	Kammerer 2015; Jirah 2021	Leeu-Gamka	Saairivier, Jan Willems Fontein 32, Prince Albert	Y	Moordenaars
SAM-PK-009163	SAM	Dinocephalia	Titanosuchidae	*Titanosuchus*	*ferox*	Sifelani Jirah 2021	Merweville	Wakkerstroom, Moordenaarskraal Noord 64, Beaufort West	Y	lower Moordenaars
SAM-PK-009348	SAM	Dinocephalia	titanosuchidae	*Jonkeria*	*truculenta*	Sifelani Jirah 2021	Beaufort West	Mierfontein 318, Beaufort West	Y	mid-upper Moordenaars
SAM-PK-011299	SAM	Dinocephalia	Titanosuchidae	*Titanosuchus*	*ferox*	Sifelani Jirah 2021	Leeu-Gamka	Boesmansrivier, Bushmans River 312, Beaufort West	Y	mid Moordenaars
SAM-PK-011488	SAM	Dinocephalia	Titanosuchidae	*Titanosuchus*	*ferox*	Sifelani Jirah 2021	Beaufort West	Mynhardtskraal 311, Beaufort West	Y	mid Moordenaars
SAM-PK-011491	SAM	Dinocephalia	Titanosuchidae	*Titanosuchus*	*ferox*	Sifelani Jirah 2021	Beaufort West	Mynhardtskraal 311, Beaufort West	Y	mid Moordenaars
SAM-PK-011573	SAM	Dinocephalia	Titanosuchidae	*Jonkeria*	*truculenta*	Sifelani Jirah 2021	Leeu-Gamka	Klein Koedoeskop 310, Beaufort West	Y	mid Moordenaars
SAM-PK-011574	SAM	Dinocephalia	Titanosuchidae	*Jonkeria*	*truculenta*	Sifelani Jirah 2021	Leeu-Gamka	Klein Koedoeskop 310, Beaufort West	Y	mid Moordenaars
SAM-PK-011575	SAM	Dinocephalia	Titanosuchidae	*Jonkeria*	*truculenta*	Sifelani Jirah 2021	Leeu-Gamka	Klein Koedoeskop 310, Beaufort West	Y	mid Moordenaars
SAM-PK-011881	SAM	Dinocephalia	Titanosuchidae	*Titanosuchus*	*ferox*	Sifelani Jirah 2021	Leeu-Gamka	Bloukrans 31, Prince Albert	Y	mid-upper Moordenaars
SAM-PK-011884	SAM	Dinocephalia	Titanosuchidae	*Jonkeria*	*truculenta*	Sifelani Jirah 2021	Merweville	Skroefpaal, Scruif Paal 2, Prince Albert	Y	lower Moordenaars

SAM-PK-011938	SAM	Dinocephalia	Titanosuchidae	*Titanosuchus*	*ferox*	Sifelani Jirah 2021	Laingsburg	Steenboksfontein, Schoppel Maay Kraal 54, Laingsburg	Y	lower Moordenaars
SAM-PK-011979	SAM	Dinocephalia	Titanosuchidae	*Jonkeria*	*truculenta*	Sifelani Jirah 2021	Merweville	Kruisvallei, Van der Byls Kraal 265, Beaufort West	Y	lower Moordenaars
SAM-PK-011989	SAM	Dinocephalia	Titanosuchidae	*Titanosuchus*	*ferox*	Sifelani Jirah 2021	Leeu-Gamka	Koedoeskop, Leeuwkraal 309, Beaufort West	Y	mid-upper Moordenaars
SAM-PK-012030	SAM	Dinocephalia	Titanosuchidae	*Jonkeria*	*truculenta*	Kammerer 2015; Jirah 2019	Laingsburg	Bosluiskraal, Dikbome 53, Laingsburg	Y	lower Moordenaars
TM 212	TM (DMNH)	Dinocephalia	Titanosuchidae	*Jonkeria*	*truculenta*	Kammerer 2015; Jirah 2021	Leeu-Gamka	Abrahamskraal 29, Prince Albert	Y	Moordenaars
MB.R 983	MFN (MB)	Dinocephalia	Titanosuchidae	*Jonkeria*	*truculenta*	Jirah 2021	Leeu-Gamka	Springfontein, Springfontein 305, Beaufort West	Y	mid-upper Moordenaars
OR 49367	NHM UK	Dinocephalia	Titanosuchidae	*Titanosuchus*	*ferox*	Jirah 2021	Leeu-Gamka	Klein Koedoeskop 310, Beaufort West	Y	mid Moordenaars
OR 49368	NHM UK	Dinocephalia	Titanosuchidae	*Titanosuchus*	*ferox*	Jirah 2021	Leeu-Gamka	Klein Koedoeskop 310, Beaufort West	Y	mid Moordenaars
OR 49369	NHM UK	Dinocephalia	Titanosuchidae	*Titanosuchus*	*ferox*	Jirah 2021	Leeu-Gamka	Klein Koedoeskop 310, Beaufort West	Y	mid Moordenaars
OR 49370	NHM UK	Dinocephalia	Titanosuchidae	*Titanosuchus*	*ferox*	Jirah 2021	Leeu-Gamka	Klein Koedoeskop 310, Beaufort West	Y	mid Moordenaars
UC1511	FMNH	Dinocephalia	Titanosuchidae	*Jonkeria*	*truculenta*	Jirah 2021	Leeu-Gamka	Stinkfontein 7, Beaufort West	Y	mid Moordenaars